

UNDERDRAIN DESIGN AND OPERATIONAL CONDITIONS IN SAND MEDIA FILTERS USING RECLAIMED EFFLUENTS IN DRIP IRRIGATION SYSTEMS

Carles Solé Torres

Per citar o enllaçar aquest document:
Para citar o enlazar este documento:
Use this url to cite or link to this publication:
<http://hdl.handle.net/10803/669332>



<http://creativecommons.org/licenses/by-nc-nd/4.0/deed.ca>

Aquesta obra està subjecta a una llicència Creative Commons Reconeixement-
NoComercial-SenseObraDerivada

Esta obra está bajo una licencia Creative Commons Reconocimiento-NoComercial-
SinObraDerivada

This work is licensed under a Creative Commons Attribution-NonCommercial-
NoDerivatives licence



Doctoral Thesis

**UNDERDRAIN DESIGN AND OPERATIONAL
CONDITIONS IN SAND MEDIA FILTERS USING
RECLAIMED EFFLUENTS IN DRIP IRRIGATION
SYSTEMS**

Carles Solé Torres

2020



Doctoral Thesis

**UNDERDRAIN DESIGN AND OPERATIONAL CONDITIONS
IN SAND MEDIA FILTERS USING RECLAIMED EFFLUENTS
IN DRIP IRRIGATION SYSTEMS**

Carles Solé Torres

2020

Doctoral program in Technology

Thesis supervisors:

Jaume Puig Bargués

Gerard Arbat Pujolràs

Miquel Duran Ros

Report submitted to apply for the title of doctor for the University of Girona

THESIS SUPERVISION CERTIFICATE

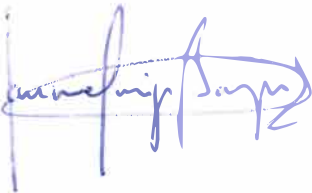
JAUME PUIG BARGUÉS, GERARD ARBAT PUJOLRÀS and MIQUEL DURAN ROS

Professors of the Department of Chemical, Agricultural Engineering and Agrifood Technology of the University of Girona.

DECLARE:

That the work entitled “UNDERDRAIN DESIGN AND OPERATIONAL CONDITIONS IN SAND MEDIA FILTERS USING RECLAIMED EFFLUENTS IN DRIP IRRIGATION SYSTEMS”, presented by the Master in Agronomic Engineering Carles Solé Torres to obtain the title of doctor, has been carried out under my supervision and meets the requirements to qualify for International mention.

And for the record and to have the appropriate effects, we sign this document.




Dr. Jaume Puig Bargués

Thesis supervisor



Dr. Gerard Arbat Pujolràs

Thesis supervisor



Dr. Miquel Duran Ros

Thesis supervisor



Carles Solé Torres

Doctoral student

Girona, February 4th, 2020.

Carles Solé Torres was the recipient of a predoctoral scholarship (IFUdG2016/72) from the University of Girona. The experiment was financed by the Spanish ministry of Economy and Competiveness through grant AGL2015-63750-R.

ACKNOWLEDGMENTS

As Benjamin Franklin said: “an investment in education pays its best interest”. So I would really like to thank all the persons and institutions who have made this educational investment possible. In the first place, to Jaume Puig Bargués, Gerard Arbat and Miquel Duran, for the values and knowledge given, not only in concepts but at field level. For their enthusiasm, patience and orientation in all aspects of the thesis and all good times during this three years.

Also to all my colleagues of the Irrigation Engineering and Management research group, who have collaborate in aspects of the thesis and in its day-to-day: Paco, Xevi, Lluís, Pitu, Cristina, Joan, Jaume i Sílvia. It has been a pleasure to have carried out the thesis in this good team. Also to the staff of University of Girona, especially to Laboratory and Informatics Sections.

To Ester, Carles, Pere and Javi for their help and willing attitude, and the municipality of Celrà, to let us carry out the experiment in the WWTP of this municipality. Also to Carles Girgas of Industrial Ginés, Dani and Xevi, to their continuous helps in setting up the experiment.

À Nassim et Bruno, pour m’avoir accueilli au G-EAU de Montpellier. Ça a été une merveilleuse expérience, dans le sens professionnel et personnel. Cette ville et l’ambiance de l’IRSTEA m’a séduit. Merci aussi à tous les collègues que j’ai connu là, et qui ont fait partie de cette aventure.

To my father who helped me doing field measurements and maintenance, moral support and life perspective. To my mother who cheers me up and prepares me restorative meals, and has made my way easier. To my sister, who shares with me her energy and (sometimes) listens to me, and well, to my brother-in-law, just because otherwise my sister will get mad at me and will not read the thesis. To my family in general, which, given the number, I would need two appendices to thank all of them.

Finally, to the other part of the family: my friends, especially Martí, Andreu, Adrià and Guille, also to Carla. To Nit Puche who has made a video of the thesis. It is a shame I haven’t won an Oscar. Thank you all to have walked in when the rest walked out.

THESIS STRUCTURE

The present doctoral thesis is presented as a compendium of three published scientific articles. These articles are presented separately as chapters, preceded by an introduction as Chapter 1, the objectives as Chapter 2, then the three articles as Chapters 3, 4 and 5, followed by the general discussion as Chapter 6, conclusions as Chapter 7 and bibliography as Chapter 8.

Journal articles presented in the thesis:

1. Solé-Torres, C., Puig-Bargués, J., Duran-Ros, M., Arbat, G., Pujol, J., Ramírez de Cartagena, F., 2019. Effect of underdrain design, media height and filtration velocity on the performance of microirrigation sand filters using reclaimed effluents. *Biosystems Engineering*, 187, 292-304.

Biosystems Engineering journal insights according to JCR in 2018:

- Impact factor: 2.983
- First quartile (ranks 7 of 56) of Agriculture, Multidisciplinary category.

2. Solé-Torres, C., Puig-Bargués, J., Duran-Ros, M., Arbat, G., Pujol, J., Ramírez de Cartagena, F., 2019. Effect of different sand filter underdrain designs on emitter clogging using reclaimed effluents. *Agricultural Water Management*, 223, 105683.

Agricultural Water Management journal insights according to JCR in 2018:

- Impact factor: 3.542
- First quartile (ranks 9 of 89) of Agronomy category.

3. Solé-Torres, C., Duran-Ros, M., Arbat, G., Pujol, J., Ramírez de Cartagena, F., Puig-Bargués, J., 2019. Assessment of field water uniformity distribution in a microirrigation system using a SCADA system. *Water*, 11 (7), 1346.

Water journal insights according to JCR in 2018:

- Impact factor: 2.524
- Second quartile (ranks 29 of 91) of Water Resources category.

THESIS STRUCTURE

The present doctoral thesis is presented as a compendium of three published scientific articles. These articles are presented separately as chapters, preceded by an introduction as Chapter 1, the objectives as Chapter 2, then the three articles as Chapters 3, 4 and 5, followed by the general discussion as Chapter 6, conclusions as Chapter 7 and bibliography as Chapter 8.

Journal articles presented in the thesis:

1. Solé-Torres, C., Puig-Bargués, J., Duran-Ros, M., Arbat, G., Pujol, J., Ramírez de Cartagena, F., 2019. Effect of underdrain design, media height and filtration velocity on the performance of microirrigation sand filters using reclaimed effluents. *Biosystems Engineering*, 187, 292-304.

Biosystems Engineering journal insights according to JCR in 2018:

- Impact factor: 2.983
- First quartile (ranks 7 of 56) of Agriculture, Multidisciplinary category.

2. Solé-Torres, C., Puig-Bargués, J., Duran-Ros, M., Arbat, G., Pujol, J., Ramírez de Cartagena, F., 2019. Effect of different sand filter underdrain designs on emitter clogging using reclaimed effluents. *Agricultural Water Management*, 223, 105683.

Agricultural Water Management journal insights according to JCR in 2018:

- Impact factor: 3.542
- First quartile (ranks 9 of 89) of Agronomy category.

3. Solé-Torres, C., Duran-Ros, M., Arbat, G., Pujol, J., Ramírez de Cartagena, F., Puig-Bargués, J., 2019. Assessment of field water uniformity distribution in a microirrigation system using a SCADA system. *Water*, 11 (7), 1346.

Water journal insights according to JCR in 2018:

- Impact factor: 2.524
- Second quartile (ranks 29 of 91) of Water Resources category.

Communications derived from the doctoral thesis and presented in scientific conferences:

- Solé-Torres, C., Puig-Bargués, J., Duran-Ros, M., Arbat, G., Pujol, J., Ramírez de Cartagena, F., 2019. Efecto de la altura de medio filtrante y la velocidad de filtración en el comportamiento de distintos modelos de filtro de arena en instalaciones de riego por goteo con aguas regeneradas. X Congreso Ibérico de Agroingeniería. Huesca, 3 – 6 de septiembre, 2019.
- Solé-Torres, C., Puig-Bargués, J., Duran-Ros, M., Arbat, G., Pujol, J., Ramírez de Cartagena, F., 2019. Efecto de diferentes diseños de drenajes de filtros de arena en la obturación de goteros utilizando aguas residuales regeneradas. X Congreso Ibérico de Agroingeniería. Huesca, 3 – 6 de septiembre, 2019.

Scientific stages in other research institutions:

- UMR G-EAU (Gestion de l'Eau, Acteurs, Usages) à l'IRTSEA de Montpellier (France), during 96 days, from April 29th to August 3rd 2019, in the frame of determining particle retention in sand media filters using Optical Coherence Tomography (OCT) technique.

Other derived works:

- Winner of the contest "Thesis in 4 minutes" at the University of Girona, and finalist of the Catalan Universities final phase. Barcelona, June 6th 2018.
Video available on youtube:
https://www.youtube.com/watch?v=UfF_DDvjTC0&t=3s

Communications derived from the doctoral thesis and presented in scientific conferences:

- Solé-Torres, C., Puig-Bargués, J., Duran-Ros, M., Arbat, G., Pujol, J., Ramírez de Cartagena, F., 2019. Efecto de la altura de medio filtrante y la velocidad de filtración en el comportamiento de distintos modelos de filtro de arena en instalaciones de riego por goteo con aguas regeneradas. X Congreso Ibérico de Agroingeniería. Huesca, 3 – 6 de septiembre, 2019.
- Solé-Torres, C., Puig-Bargués, J., Duran-Ros, M., Arbat, G., Pujol, J., Ramírez de Cartagena, F., 2019. Efecto de diferentes diseños de drenajes de filtros de arena en la obturación de goteros utilizando aguas residuales regeneradas. X Congreso Ibérico de Agroingeniería. Huesca, 3 – 6 de septiembre, 2019.

Scientific stages in other research institutions:

- UMR G-EAU (Gestion de l'Eau, Acteurs, Usages) à l'IRTSEA de Montpellier (France), during 96 days, from April 29th to August 3rd 2019, in the frame of determining particle retention in sand media filters using Optical Coherence Tomography (OCT) technique.

Other derived works:

- Winner of the contest "Thesis in 4 minutes" at the University of Girona, and finalist of the Catalan Universities final phase. Barcelona, June 6th 2018.
Video available on youtube:
https://www.youtube.com/watch?v=UfF_DDvjTC0&t=3s

INDEX OF TABLES

<i>Table 1.1. World's irrigated and microirrigated area, and its area percentage for developed and developing countries. Source: ICID: (2013, 2019).....</i>	<i>10</i>
<i>Table 6.1. Pressure loss percentage (%) of the different filter designs for the different sections and operational conditions, at the beginning of the cycle, 1/3, 2/3, end of the cycle and mean value.....</i>	<i>88</i>
<i>Table 6.2. Graded sections depending on the percentage of head loss s for different filtration operating conditions and time of the cycle for the three filters tested.....</i>	<i>90</i>
<i>Table 6.3. Number of cycles, mean filtered volume per cycle (m³), maximum and minimum filtration volume per cycle (m³) and filtered volume distribution for each filter design regarding operational conditions.....</i>	<i>91</i>
<i>Table 6.4. General experiment conditions, filter designs and operational conditions and turbidity removal efficiencies in different published studies using sand filters with effluents....</i>	<i>98</i>
<i>Table 6.5. DU_{iq} for each irrigation subunit computed with different emitter samples and number of completely clogged emitters at the three different irrigation accumulated times.....</i>	<i>103</i>
<i>Table 6.6. Root mean square error (RMSE) between DU_{iq} obtained using all emitter discharges regarding DU_{iq} computed following the different procedures.....</i>	<i>104</i>

INDEX OF FIGURES

<i>Figure 1.1. Water distribution on Planet Earth. Source: own elaboration from data provided by Postel (1992).</i>	3
<i>Figure 1.2. Hydrologic cycle. Source: UNESCO (2017).</i>	4
<i>Figure 1.3. Hydric resources and population distribution by continent. Source: Own elaboration from FAO (2019a).</i>	4
<i>Figure 1.4. World's high quality water consumption depending on its use and region development. Source: own elaboration from UNESCO (2018).</i>	6
<i>Figure 1.5. Volume of reclaimed water reused by sector in Catalonia. Source: own elaboration from ACA (2018).</i>	7
<i>Figure 1.6. Diagram of a microirrigation system. Source: Kansas State University (2019).</i>	9
<i>Figure 1.7. Evolution of the irrigated surface in Spain according to the irrigation technique from 2007 to 2018. Source: MAPAMA (2018).</i>	11
<i>Figure 1.8. Screen filter diagram. Source: Kansas State University (2019).</i>	12
<i>Figure 1.9. Disc filter diagram. Source: Kansas State University (2019).</i>	13
<i>Figure 1.10. Media filter diagram. Source: Kansas State University (2019).</i>	14
<i>Figure 1.11. Backwashing media filter diagram. Source: Kansas State University (2019).</i>	16
<i>Figure 1.12. Arm collector underdrain design. A) Single slotted piece, B) Arm formed by pieces, C) Arm collector design. Source: Bové (2018).</i>	18
<i>Figure 1.13. Inserted domes underdrain design. A) Dome, B) Dome interior design, C) Inserted dome underdrain. Source: Bové (2018).</i>	19
<i>Figure 1.14. Scaled laboratory sand filter with the new designed underdrain and its isometric view (B). Source: Bové et al. (2017).</i>	21
<i>Figure 1.15. Adapted new underdrain design following the dimensions of the underdrain proposed by Bové et al., 2017. A) Media used as underdrain, B) Underdrain design assembled. Source: Own elaboration.</i>	22
<i>Figure 1.16. Location of the emitters used for DU_{iq} determination for the different methodologies.</i>	25
<i>Figure 1.17. SCADA diagram used in a microirrigation system using effluents. The SCADA system consist of a computer, operational and measurement instruments and automats to connect both of them.</i>	28
<i>Figure 1.18. Evolution of water and energy demand per hectare for irrigation in Spain. Source: own elaboration from Corominas (2010) and MAPAMA (2018).</i>	29
<i>Figure 6.1. Pressure transducers (1-6) across the filters and head loss sections.</i>	81
<i>Figure 6.2. Pressure profiles throughout the vertical axis along the three different designs for the two media heights, at filtration velocity of 30 m/h (a) and 60 m/h (b).</i>	82
<i>Figure 6.3. Average pressure loss across the whole filter regarding filtration velocity for different underdrain designs and conditions tested</i>	83

<i>Figure 6.4. Average pressure (kPa) values for each operational condition of the different pressure transducers across the filter at the beginning, 1/3, 2/3 and at the end of the filtration cycles, for the porous media underdrain filter.</i>	<i>85</i>
<i>Figure 6.5. Average pressure (kPa) values for each operational condition of the different pressure transducers across the filter at the beginning, 1/3, 2/3 and at the end of the filtration cycles, for the dome underdrain filter.</i>	<i>86</i>
<i>Figure 6.6. Average pressure (kPa) values for each operational condition of the different pressure transducers across the filter at the beginning, 1/3, 2/3 and at the end of the filtration cycles, for the arm collector underdrain filter.</i>	<i>87</i>
<i>Figure 6.7. Head loss (kPa) regarding filtered volume (m³) for the three different filters designs and two filtration velocities under 0.2 m media height</i>	<i>93</i>
<i>Figure 6.8. Head loss (kPa) regarding filtered volume (m³) for the three different filters designs and two filtration velocities under 0.3 m media height</i>	<i>94</i>
<i>Figure 6.9. Debris deposition of the firsts centimetres (dotted line) on the first media layer after 250 h of filtration with 0.3 m and 30 m/h for porous media design.....</i>	<i>96</i>
<i>Figure 6.10. Inside views of last location emitters protected by the different filter designs at the end of the experiment.</i>	<i>101</i>
<i>Figure 6.11. Frequency of the discharges of all the emitters for all irrigation subunits at different measuring times and normal plot adjustments</i>	<i>102</i>

LIST OF SYMBOLS AND ABBREVIATIONS

C/N: ratio of the mass of carbon to the mass of nitrogen (dimensionless)

CE: electrical conductivity (dS/m)

CFD: computational fluid dynamics

CV: manufacturer variation coefficient (dimensionless)

d_e : effective diameter, size opening which will pass 10% by dry weight of a representative sample of the media material (mm)

DO: dissolved oxygen (mg/l)

DU: distribution uniformity (dimensionless)

DU_q : flow distribution uniformity (dimensionless)

DU_p : pressure distribution uniformity (dimensionless)

FNU: formazin nephelometric units (dimensionless)

k: constant depending on the kind of emitter, flow and pressure (dimensionless)

P: pressure (MPa)

p_a : mean pressure of all location in an irrigation system (kPa)

p_{25} : mean pressure of the 25% of locations with the lowest pressure in an irrigation system (kPa)

q: emitter flow rate (l/h)

q_a : mean flow of all emitter in an irrigation system (l/h)

q_{25} : mean flow of the 25% of emitters with the lowest flow in an irrigation system (l/h)

RMSE: root mean square error (same parameter units, in this case emitter discharge: l/h)

SCADA: supervisory control and data acquisition

TSS: total suspended solids (mg/l)

UC_s : uniformity coefficient, ratio of the size opening which will pass 60% of the sand to the size opening which will pass 10% (dimensionless)

x: emitter discharge exponent (dimensionless)

Δh : pressure loss (kPa)

TABLE OF CONTENTS

ACKNOWLEDGMENTS	ix
THESIS STRUCTURE.....	xi
INDEX OF TABLES.....	xiii
INDEX OF FIGURES.....	xiv
LIST OF SYMBOLS AND ABBREVIATIONS	xvii
TABLE OF CONTENTS.....	xix
SUMMARY	xxi
RESUM	xxiii
RESUMEN	xxv
1. INTRODUCTION	1
1.1. WATER: AN ESSENTIAL NATURAL RESOURCE	3
1.1.1. Water distribution.....	3
1.1.2. Water management: availability and consumption.....	5
1.2. IRRIGATION WITH RECLAIMED EFFLUENT	8
1.3. IRRIGATION SYSTEMS.....	9
1.4. MICROIRRIGATION	9
1.4.1 Microirrigation system components	9
1.4.2. Microirrigation actual condition	10
1.4.3. Advantages and disadvantages of microirrigation.....	11
1.5. FILTRATION.....	12
1.5.1. Screen filters.....	12
1.5.2. Disc filters	13
1.5.3. Media filters	14
1.6. EMITTERS.....	23
1.7. DISTRIBUTION UNIFORMITY	24
1.8. OPERATION AND MAINTENANCE FOR REDUCING EMITTER CLOGGING	26
1.9. PROCEDURE AND DURATION OF MICROIRRIGATION EXPERIMENTS	27
1.10. MONITORING AND CONTROL OF MICROIRRIGATION SYSTEMS.....	28
1.11. ENERGY CONSUMPTION OF MICROIRRIGATION SYSTEMS.....	29
2. OBJECTIVES.....	31
3. EFFECT OF THE UNDERDRAIN DESIGN, MEDIA HEIGHT AND FILTRATION VELOCITY ON THE PERFORMANCE OF MICROIRRIGATION SAND FILTERS USING RECLAIMED EFFLUENTS.	35

4. EFFECT OF DIFFERENT SAND FILTER UNDERDRAIN DESIGNS ON EMITTER CLOGGING USING RECLAIMED EFFLUENTS.	51
5. ASSESSMENT OF FIELD WATER UNIFORMITY DISTRIBUTION IN A MICROIRRIGATION SYSTEM USING A SCADA SYSTEM.	63
6. GENERAL DISCUSSION.....	79
6.1. FILTER PERFORMANCE	81
6.1.1. Pressure loss across the filters	81
6.1.2. Pressure loss throughout sections and filtration cycles.....	84
6.1.3. Pressure loss evolution regarding the filtered volume	91
6.1.4. Effect of filtration and operational conditions on effluent quality.....	95
6.2. EMITTER PERFORMANCE	99
6.3. IMPLICATIONS FOR IRRIGATION UNIFORMITY ASSESSMENT	101
6.3.1. Emitter discharge distribution.....	102
6.3.2. Distribution uniformity assessment	102
7. CONCLUSIONS	105
7.1. FUTURE PROSPECTIONS	108
8. REFERENCES	109

SUMMARY

At present, agriculture is the human activity which requires more volume of water. Given the importance and scarcity of this resource, the efficient use of water has become a priority. On one hand, if possible, it is necessary to use irrigation systems such as microirrigation that use water more efficiently. On the other hand, treated wastewater reuse by agriculture helps to have the necessary water at the same time that it allows to release water of higher quality for other uses. In this sense, microirrigation is the safest system to apply reclaimed effluents. However, its main problem is emitter clogging, which can negatively affect crop yields and system maintenance. In order to avoid emitter clogging, the use of filters is compulsory. Those filters that work better with effluents are sand filters, although, due to their pressure requirements, concentrate most of the energy demand of drip irrigation systems.

This thesis determines the effect of three types of sand filters with different drainage designs (arm collector, inserted domes and porous media), two media height (0.2 and 0.3 m) and two filtration velocities (30 and 60 m/h) in the quality of filtered water, the pressure loss in the filters, the energy consumption of the system and emitter clogging. So, for each filter design, each of the four operating conditions studied (two media heights and two filtration velocities) was tested for 250 h, so the experiment had a total duration of 1000 h for each filtration unit. Silica sand with an effective diameter of 0.48 mm and a coefficient of uniformity of 1.73 was used as filter media. Every filtration unit was associated with an irrigation subunit, each one with four laterals 90 m long, and 226 integrated and pressure-compensating emitters in each lateral, with a nominal emitter discharge of 2.3 l/h. The experimental setup had different sensors, instruments and a Supervision, Control and Data Acquisition (SCADA) system which allowed the monitoring and management of the system, as well as data acquisition of water volumes, water quality, pressures and energy consumption at different parts of the installation. The effluent used came from a secondary treatment of the Wastewater Treatment Plant (WWTP) of the municipality of Celrà (Girona).

Operational conditions affected pressure loss in the different filters tested, being higher with filtration velocities of 60 m/h. The porous media design presented less pressure loss for all conditions tested, except for 0.3 m media height and 30 m/h, in where the domes underdrain design performed better. Pressure loss percentage was higher in the media than in the underdrain for all filter designs and conditions analyzed. On the other hand, porous media design filtered more water per energy consumption unit (8.4 m³/kWh) than domes underdrain design (8.31 m³/kWh) and the arm collector design (8.17 m³/kWh).

Regarding turbidity removal efficiency, there was a triple interaction between filter design, media height and filtration velocity. Porous media design presented a turbidity removal significantly higher for all operational conditions, except for 0.3 media height and filtration velocity of 30 m/h, where it was the dome underdrain design the best (47.74 vs. 39.19%). Higher turbidity removals were observed at 30 m/h than at 60 m/h. However, this pattern was not that clear between media heights.

The interactions between filter design and experimental time, filter design and emitter location, and time and emitter location significantly affect emitter clogging. There was a significant reduction of emitter discharge over time for each design. This reduction was lower with arm collector design (7.6% at 500 h and of 9.6% at 1000 h), while it was 8.76 and 8.06% in porous media design and 12.35 and 11.29% in domes designs, at 500 h and 1000 h respectively. For

each filter design, significant differences were observed in emitter discharges, but only at the last locations (last 1.2 m for porous media and domes design and 0.8 m for arm collector). After 500 h, the last three emitters in the dripline had significantly less emitter discharge than the rest of the lateral, while after 1000 h these happened for four last positions. Besides, at the end of the test, there were found 10 completely clogged emitters in the porous media subunit, 8 in the domes subunit and 6 in the arm collector subunit.

SCADA system was used to assess pressure and flow distribution uniformity throughout the experiment. The estimated SCADA DU_{lq} presented a good correlation with real DU_{lq} , showing that it is a good tool not only to calculate this parameter, but for managing and monitoring irrigation systems. Finally, different methods for assessing flow distribution uniformity (DU_{lq}) could be compared, being the one proposed by Juana et al. (2007), which was derived from Merriam and Keller (1978) methodology, the one that presented better similarity to real DU_{lq} , especially when there are clogged emitters.

RESUM

En l'actualitat, l'agricultura és l'activitat humana que requereix més quantitat d'aigua. Davant la importància i escassetat d'aquest recurs, l'ús eficient de l'aigua s'ha convertit en una prioritat. D'una banda i si és possible, es fa necessària la utilització de sistemes de reg com el reg per degoteig que empren de forma més eficient l'aigua. D'altra banda, la reutilització d'aigües residuals tractades per l'ús agrícola ajuda a disposar de l'aigua necessària per a reg al mateix temps que permet alliberar aigües de major qualitat per a altres usos. En aquest sentit, el reg per degoteig és el sistema més segur per aplicar aigües regenerades. No obstant això, el seu principal problema és l'obtenció dels degoters, que pot afectar negativament al rendiment dels cultius i al maneig de la instal·lació. Per intentar evitar les obtencions, resulta imprescindible instal·lar filtres. Els que millor funcionen amb aquest tipus d'aigües són els filtres de sorra, encara que, degut a la pressió que requereixen, concentren la major part de demanda d'energia dels sistemes de reg per degoteig.

En la present tesi es determina l'efecte de tres tipus de filtres de sorra amb diferents dissenys de drenatge (de braços col·lectors, de crepines inserides i de medi porós), l'alçada del medi filtrant (0.2 i 0.3 m) i la velocitat de filtració (30 i 60 m/h) en la qualitat de l'aigua filtrada, la caiguda de pressió en els filtres, el consum energètic del sistema i l'obtenció dels degoters. D'aquesta manera, per a cada disseny del filtre, cadascuna de les quatre condicions operatives estudiades (dues alçades de llit filtrant i dues velocitats de filtració) es va assajar durant 250 h, per la qual cosa l'assaig va tenir una durada total de 1000 h per cada unitat de filtració. Es va utilitzar sorra sílicia com a medi filtrant, amb un diàmetre efectiu de 0.48 mm i un coeficient d'uniformitat de 1.73. Cada unitat de filtració tenia associada una subunitat de reg, amb quatre laterals de 90 m de llarg, i 226 degoters integrats i autocompensants a cada lateral, amb un cabal nominal de 2.3 l/h. El dispositiu experimental disposava de diferents sensors i un sistema de Supervisió, Control i Adquisició de Dades (SCADA), que permetia la gestió i monitorització del sistema, així com l'emmagatzematge de dades de volums d'aigua, qualitat d'aquesta, pressions i consums energètics en diferents punts de la instal·lació. Per a l'assaig es va fer servir aigua residual regenerada procedent del tractament secundari de la estació depuradora (EDAR) del municipi de Celrà (Girona).

Les condicions operatives van afectar a la pèrdua de pressió en els diferents filtres, essent més elevades amb velocitats de 60 m/h. Va ser el disseny de medi porós el que va presentar menys pèrdua de pressió per a totes les condicions operatives, excepte amb 0.3 m i 30 m/h, combinació en la qual el filtre de crepines va ser el que en va presentar menys. El percentatge de pèrdua de pressió fou més gran en el medi filtrant que en el drenatge per a cada filtre i condició assajada. D'altra banda, el filtre de medi porós va filtrar significativament més volum d'aigua per unitat d'energia consumida (8.4 m³/kWh) que el filtre de crepines inserides (8.31 m³/kWh) i que el filtre de braços col·lectors (8.17 m³/kWh).

Pel que fa a la reducció de terbolesa, hi va haver una interacció triple entre els factors de disseny del filtre, alçada de llit filtrant i velocitat de filtració. El filtre de drenatge de medi porós va presentar una reducció de terbolesa significativament major per a totes les condicions operatives, excepte per a l'alçada de 0.3 m i la velocitat de filtració de 30 m/h, on va ser el filtre de crepines inserides (47.74 respecte 39.19%). Es van observar reduccions de terbolesa més elevades a 30 m/h que a 60 m/h. Tanmateix, no es va observar un patró tant clar entre les dues alçades de llit filtrant.

Respecte a l'obturació dels degoters, es van detectar interaccions entre disseny del filtre i temps d'assaig, disseny del filtre i posició dels degoters, i entre temps d'assaig i posició dels degoters. Va haver-hi una reducció significativa del cabal al llarg del temps d'assaig per a cada disseny. Aquesta reducció va ser menor en el cas del filtre de braços col·lectors (del 7.6% a les 500 h i del 9.6% a les 1000 h), mentre que va ser del 8.76 i 8.06% en el filtre de medi porós i del 12.35 i 11.29% en el de crepines inserides, a les 500 i 1000 h respectivament. Per a cada disseny del filtre, es van observar diferències significatives en els cabals, però només per als emissors del final del lateral (últims 1.2 m per als filtres de medi porós i cúpules inserides i 0.8 m per al de braços col·lectors). Transcorregudes 500 h d'assaig, els tres últims degoters van emetre significativament menor cabal que la resta, mentre que passades 1000 h foren els quatre últims. Així mateix, al final de l'assaig, es van trobar 10 degoters completament obturats en els degoters protegits pel filtre de medi porós, 8 amb el de crepines inserides i 6 amb el de braços col·lectors.

El sistema SCADA va permetre mesurar la uniformitat de distribució tant de pressió com de cabals de la instal·lació durant tot l'assaig. Pel que fa a l'estimació de la DU_{iq} , es va obtenir una bona correlació amb la DU_{iq} real, amb la qual cosa es va demostrar que resulta una bona eina tan per el càlcul d'aquest paràmetre com per a la gestió i monitorització dels sistemes de reg en temps real. Finalment, es van poder comparar diferents mètodes de càlcul d'uniformitat de distribució de cabals (DU_{iq}), essent el proposat per Juana et al. (2007), que de fet és una modificació de la metodologia de Merriam i Keller (1978), el que va presentar més similitud amb la DU_{iq} real, especialment quan hi ha degoters obturats.

RESUMEN

En la actualidad, la agricultura es la actividad humana que requiere más volúmenes de agua dulce. Ante la importancia y escasez de este recurso, el uso eficiente del agua se ha convertido en una prioridad. Por un lado, y cuando resulte posible, es necesario el uso de sistemas de riego como el riego por goteo que utilicen de forma más eficiente el agua. Por otro lado, la reutilización de aguas residuales para el uso agrícola ayuda a disponer del agua necesaria al mismo tiempo que permite liberar aguas de mejor calidad para otros usos. Ambos conceptos se plantean como una estrategia frente a los retos que concierne la utilización de dicho recurso.

En este sentido, los sistemas de riego por goteo son los más seguros para aplicar aguas regeneradas. Sin embargo, el principal problema de este sistema cuando se utilizan aguas regeneradas son las obturaciones de los goteros, que puede afectar negativamente al rendimiento de los cultivos y al manejo de la instalación. Para paliar las obturaciones, se hace imprescindible instalar filtros. Los que mejor funcionan con este tipo de aguas son los de matriz granular, como los filtros de arena, aunque es este elemento donde se concentra la mayor demanda energética de los sistemas de riego por goteo, a nivel de caída de presión.

En la presente tesis se determina como afectan tres filtros con distintos diseños de drenaje (de brazos colectores, de crepinas insertadas y de medio poroso), la altura del lecho filtrante (0.2 y 0.3 m) y la velocidad de filtración (30 m/h y 60 m/h) en la calidad del agua filtrada, la caída de presión en el filtro, el consumo energético del sistema y en la obturación de los goteros. Así, para cada diseño de filtro, se estudiaron cuatro condiciones operativas (dos alturas de lecho con dos velocidades de filtración). Cada condición operativa se ensayó durante 250 h, por lo que el ensayo tuvo una duración total de 1000 h para cada unidad de filtración. El medio filtrante utilizado consistió en arena silíceo con un diámetro efectivo de 0.48 mm y un coeficiente de uniformidad de 1.73. Cada unidad de filtración tenía asociada una subunidad de riego, que consistía en cuatro laterales de 90 m de largo y 226 emisores cada uno. Se utilizaron emisores comerciales integrados y autocompensantes, con un caudal nominal de 2.3 l/h. El dispositivo experimental disponía de distintos sensores y un sistema de supervisión, control y adquisición de datos (SCADA), que permitía la gestión y monitorización del sistema, y almacenaba datos de volúmenes de agua, calidad de ésta, presiones y consumo energético en distintos puntos de la instalación. Para el ensayo se utilizó agua residual regenerada procedente del tratamiento secundario de la estación depuradora (EDAR) del municipio de Celrà (Girona).

Por lo que a la calidad del agua se refiere, se observó que la reducción de turbidez en el proceso de filtración se ve afectada por la velocidad de filtración, siendo significativamente ($p < 0.05$) mayor con 30 m/h (34.2%) que con 60 m/h (11.3%), y por el diseño del filtro, siendo el diseño de medio poroso el que redujo más la turbidez (26.3%) respecto el diseño de crepinas insertadas (18.5%) y el de brazos colectores (13.4%).

Las condiciones operativas afectaron a la pérdida de presión en los distintos filtros, siendo éstas más elevadas con velocidades de filtraciones de 60 m/h. Fue el diseño de medio poroso el que presentó menos pérdida de presión para todas las condiciones excepto con 0.3 m y 30 m/h, que fue el diseño de crepinas insertadas. El porcentaje de pérdida de presión fue mayor en el lecho filtrante que en el drenaje para cada filtro y condición testada. Por otro lado, el filtro de drenaje con medio poroso filtró significativamente más volumen de agua por unidad de energía consumida (8,4 m³/kWh) que el filtro de crepinas insertadas (8,31 m³/kWh) y que el filtro de brazos colectores (8,17 m³/kWh).

En la reducción de turbidez, se observó una interacción triple entre los factores de diseño del filtro, altura de lecho filtrante y velocidad de filtración. El filtro con drenaje de medio poroso presentó una reducción de turbidez significativamente mayor para todas las condiciones operativas, exceptuando la altura de 0.3 m y velocidad de filtración de 30 m/h, donde fue el filtro de crepinas insertadas (47.74 respecto 39.19%). Se detectaron reducciones de turbidez más elevadas a 30 m/h que a 60 m/h. Sin embargo, no se observó un patrón tan claro entre las dos alturas de lecho filtrante. Respecto a la obturación de los goteros, se produjo una reducción del caudal medido en los goteros a lo largo del ensayo, siendo del 8% a las 500 h y del 11% a las 1000 h. El tipo de filtro tuvo un efecto significativo a las 1000 h, siendo los goteros del diseño de brazos colectores los que obtuvieron un caudal significativamente superior. Las diferencias de caudal atribuidas a la posición del gotero se observaron a partir de las 500 h, siendo significativamente inferiores en los últimos 5 m del lateral. Al final del ensayo, se encontraron 10 goteros completamente obturados en los goteros protegidos por el filtro de medio poroso, 8 con el de crepinas insertadas y 6 con el de brazos colectores.

El sistema SCADA permitió medir la uniformidad de distribución de presión y caudales de la instalación de riego durante todo el ensayo. En lo que a la DU_{iq} se refiere, el sistema SCADA obtuvo una buena correlación con la DU_{iq} real, con lo que se demostró que resulta una buena herramienta tanto para el cálculo de este parámetro como para la gestión y monitorización de los sistemas de riego en tiempo real. Finalmente, se pudieron comparar distintos métodos de cálculo de uniformidad de distribución de caudales (DU_{iq}), siendo el propuesto por Juana et al. (2007), que de hecho es una modificación de la metodología de Merriam y Keller (1978), el que presentó más similitud con la DU_{iq} real, especialmente cuando existen goteros obturados.

1. INTRODUCTION

1. INTRODUCTION

1.1. WATER: AN ESSENTIAL NATURAL RESOURCE

1.1.1. Water distribution

The Earth is known as “the Blue Planet” since more than 70% of its surface is covered by water, besides the parts of the emerged surface in where there are rivers, lakes and glaciers. Water was the origin of life and it is the base of all alive form, as it represents more than 80 % of the body of almost all living creatures. Water is also indispensable for all the ecosystems, and for humans it is the main natural resource on Earth (Saladié and Oliveras, 2010).

More than 97% of the water on Earth is seawater, 2.6% is locked in icecaps and glaciers or lies too far underground to exploit it (Postel, 1992) (Figure 1.1), but a small fraction (less than 0.4%) is renewed and made fresh by nature’s solar-powered water cycle (Jackson et al., 2001). Thus, although water is an essential resource, only a small proportion of Earth’s water can be directly used for humankind.

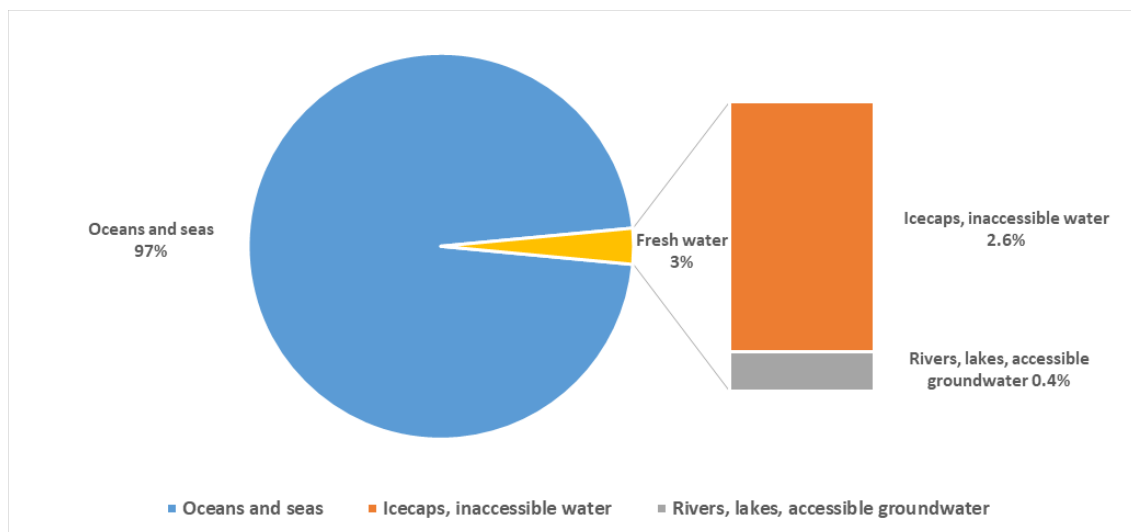


Figure 1.1. Water distribution on Planet Earth. Source: own elaboration from Postel (1992).

The amount of Earth’s water is constant and it only varies its state and distribution. However, there is a constant supply of this resource thanks to the hydrologic cycle (Figure 1.2). For this reason, water can be considered as a natural recyclable resource, although, due to its irregular distribution along the Earth, in some places of the planet it is considered scarce.

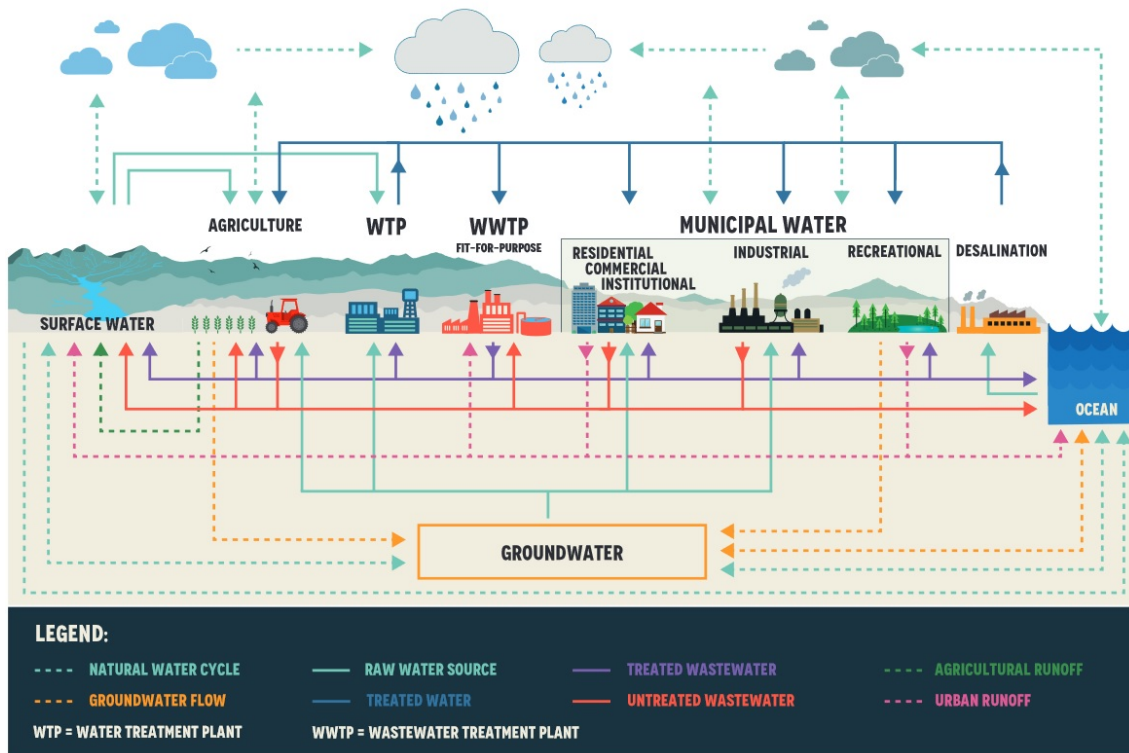


Figure 1.2. Hydrologic cycle. Source: UNESCO (2017).

There are variations both in space and time as rain, evaporation and water movement across the continents is concerned. Among all the variables the differences are mainly due to geological factors, and the unequal distribution of emerged land among the two hemispheres. Besides, local factors such as orography and soil characteristics play also an important role. Globally, while America and Oceania have higher percentages of hydric resources than their population, Asia, Europe and Africa have not (Figure 1.3) (FAO, 2019a).

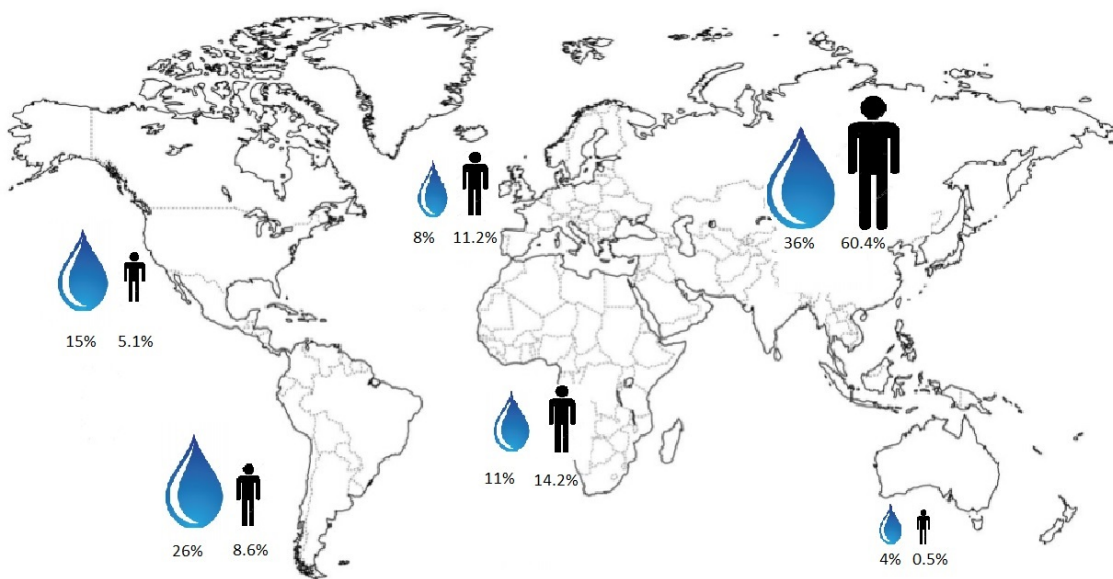


Figure 1.3. Hydric resources and population distribution by continent. Source: own elaboration from FAO (2019a).

In addition to spatial variability, temporal variability also affects the availability of water resources. Thus, variability in available water in function of the season of the year and the water demand can affect the normal supply in a given period, causing droughts of different severity and duration. These droughts are mainly caused by the decrease in precipitation in a region, by climatic factors such as global warming, but also by the consumption of water by human activity (Martin-Vide, 2004; Cortesi et al., 2012).

These differences confirm the unequal availability of water across Earth, with areas with a positive balance and areas with a negative one, being of great importance, for example, in the Mediterranean climate (Cramer et al., 2018; Greve et al., 2018). The fact that a specific amount of water could be enough to satisfy human needs will depend on consume and socioeconomic activities the humans of these areas carry out.

In addition to the aforementioned factors, a reduction of fresh water reservoirs due to climate change should be taken into account. Some predictions show a greater irregularity in rain distribution and intensity, which will increase surface runoff and reduce availability (Saladié and Oliveras, 2010).

1.1.2. Water management: availability and consumption

The small amount of available fresh water on Earth can be affected by the human activity. Water use can be consumptive or non-consumptive. According to FAO (2019b), “consumptive water use is the part of water withdrawn from its source for use in a specific sector (for example, for agricultural, industrial or municipal purposes) that will not become available for reuse because of evaporation, transpiration, incorporation into products, drainage directly to the sea or evaporation areas, or removal in other ways from freshwater resources”. Conversely, non-consumptive water use is when water is only utilized as a conveyance, landscape element (e.g. touristic, recreational and sportive) or energy source.

This last decade, Earth’s total water consumption has increased by a factor of 6.5 compared to the beginning of the 20th century and it is expected a continuous increase in water consumption next decades, due to an increase of World’s population (Sánchez, 2008; Saladié and Oliveras, 2010).

Agricultural use consumes more water than urban and industrial water use, specifically for agricultural irrigation, although there exist differences among the development level of the zones (Figure 1.4).

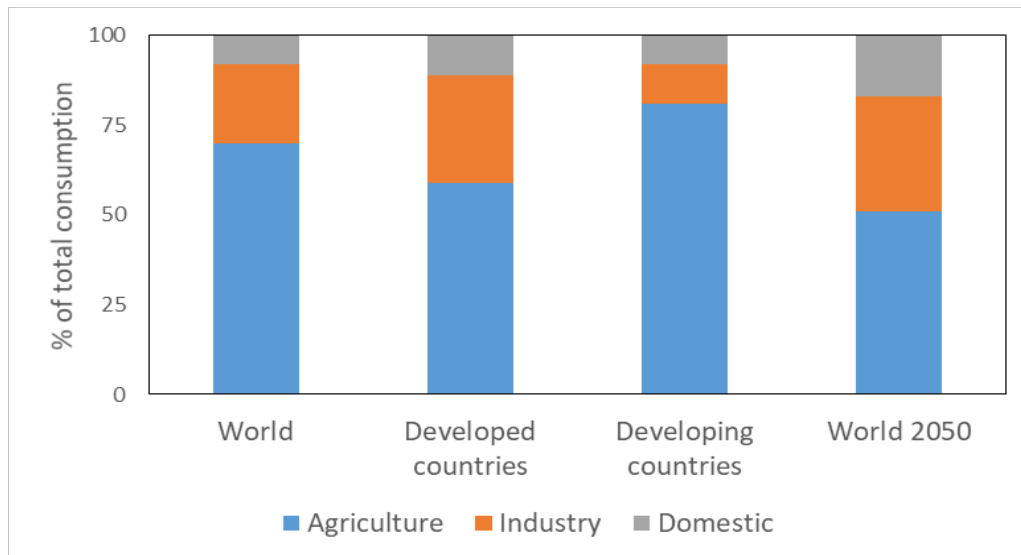


Figure 1.4. World's high quality water consumption depending on its use and region development. Source: own elaboration from UNESCO (2018).

According to projections for 2050 shown in Figure 1.4, agricultural water consumption will still be the highest. As World's population is estimated to increase (UN, 2017) this means that there will be a growth in food demand, which must be satisfied with more efficient use of water since water used by agriculture would be reduced by 27% (UNESCO, 2018).

An increasing demand of water and a potential risk of contaminating it, makes it necessary a proper and integrated hydrologic management, which has to be based in water savings and its depuration and regeneration, as water use depends not only of its accessibility and its availability, but of its quality.

Water pollution can be reduced throughout water treatment in wastewater treatment plants (WWTP), in where after a series of processes, water can go back to the original source or being reused. In developed countries treated water quality is good enough so that the impact to the ecosystems might be minimal when reused or returned to the environment (Van Puijenbroek et al., 2015).

Under conditions of increasing water scarcity, it is a challenge to satisfy the irrigation water demand, conserve water and improve its efficiency use through better water management and policy reforms (Lazarova et al., 2011). To deal with water stress, many strategies will need to be implemented during the forthcoming decades. In that sense, wastewater irrigation might be one of the most important strategies to carry on, as wastewaters of municipal and industrial origin can be used to irrigate a wide variety of crops and landscapes across the world (Hamilton et al., 2007). Recycling practices are expected to provide sustainable, low-energy and cost-effective options to improve water availability based on criteria of quality and recycling capacity (Ait Mouheb et al., 2018).

In the European Union (EU), more than 40,000 million m³ were treated in 2018, but only one billion were reused, which accounts for approximately 2.4% of the treated urban wastewater effluents, although EU potential is much higher, estimated in the order of 6 billion m³ (six times the current volume). Particular cases are Malta and Cyprus which reuse more than 60 and 90% of their wastewater respectively, while Greece or Italy reused between 5 and 12% of their effluents, clearly indicating a huge potential for further uptake (European Commission, 2019).

In 2017, Spain reused 10.7% of its wastewater, although Mediterranean regions such as Balearic Islands, Murcia and Valencian Community (45, 50 and 59%, respectively). In this country, reused wastewater was employed mainly in agriculture (62%), parklands such as golf courses (20%) and industry (7%) (García de Rentería et al., 2018).

At local level, Figure 1.5 shows the volume of reclaimed water reused and the sector that uses it in Catalonia, in the north-eastern region of Spain, in the Mediterranean shore. There was a decrease of the volume of reclaimed water reused from 2007 to 2017. Due to the economic crisis that hit the country in 2008, some WWTP were closed or tertiary treatments stopped, especially those designed for environmentally purposes. Nevertheless, the volume of reclaimed water in 2017 was higher than in the six previous years, and has increased year after year: in 2013 1.3 hm³ were reused while in 2017 were 4.8 hm³. The maximum amount of reused wastewater was in 2007 and 2008 coinciding with a severe drought which affected this area, while the following years were wetter. This fact points out the feasibility of reusing wastewater during water scarcity periods. However, in the same period, the average amount of reclaimed wastewater used in agriculture in Catalonia represented only 6%, in front of the 60% used for environmentally purposes, and far from 60% of reclaimed wastewater used in agriculture in Spain.

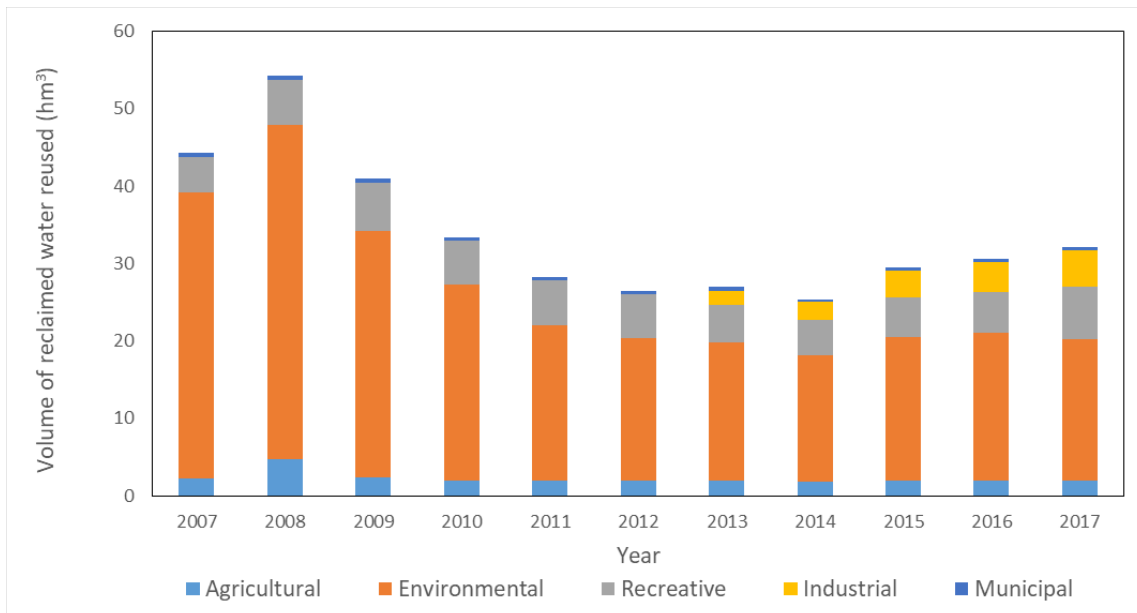


Figure 1.5. Volume of reclaimed water reused by sector in Catalonia. Source: own elaboration from ACA (2018).

1.2. IRRIGATION WITH RECLAIMED EFFLUENT

Reclaimed wastewater can be used in those cases which do not require drinking water quality standards, such as agricultural and landscape irrigation, industrial uses and non-potable urban uses (Sala and Serra, 2004), releasing high quality water for other uses (Kiziloglu et al., 2008; Lazarova et al., 2011). Wastewater reuse should gain wider acceptance in the near future (Bahri, 2009).

Moreover, in agriculture, the use of wastewater can provide nutrients which can be assimilated by crops, decreasing the fertilization cost and compensating the investment cost of the wastewater irrigation system (Trooien and Hills, 2007). In that sense, some studies have pointed out an increase of the productivity and yield of some crops (e.g. celery, eggplant, lettuce, maize and sorghum) due to the effluent content of fertilizers (Kiziloglu et al., 2008; Cirelli et al., 2012; Tripathi et al., 2016). In addition to this, the metabolism activity of soil microorganisms increases when sewage effluents are used for irrigation (Gonçalves et al., 2007). Finally, the use of effluents reduce wastewater discharge to the environment, particularly to sensitive coastal, lacustrine and riverline systems (Aronino et al., 2009; Li et al., 2019a). In that sense, these advantages would be an interesting aspect to consider in the use of the drip irrigation systems in the study area of this experiment, since it is a land with high agricultural activity, in addition to reducing the discharge of effluents to Ter river, which is the nearby river where they are discharged currently.

However, on the other hand, irrigation using effluents presents some disadvantages since it could raise sanitary problems, such as risk of viral and bacterial infections for both farmers and crops (Pereira et al., 2002; Kouamé et al., 2017) and also might lead to contamination for different chemical compounds, such as heavy metals, although in urban treated wastewater effluents, the concentration of heavy metals is smaller (Hamilton et al., 2007). In addition, emerging contaminants including antibiotics can pollute the water used for food production (Müller et al., 2007), and some crops can uptake and accumulate them (Sallach et al., 2018; Picó et al., 2019). Moreover water eutrophication (Sala and Mujeriego, 2001; Canna-Michaelidou and Christodoulidou, 2008) and leaching nutrients and other solutes poses one of the greatest threats to groundwater health (Haruta et al., 2008), like groundwater nitrate contamination (Nejatjahromi et al., 2019). Eventually, in cases with a high C/N ratio, soil micro-fauna would be increased which leads to pores-clogging problems in the soil matrix due to significant decrease of the soil hydraulic conductivity (Magesan et al., 2000; Magesan, 2001).

To minimize such environmental problems, there exist regulations to guarantee a safe reuse of wastewater in irrigation and other uses. Those regulations should take into account social, economic and environmental concerns (Ait-Mouheb et al., 2018), and should make a wiser use of the precautionary principle (Molle et al., 2012).

In Spain, the Royal Decree 1620/2007 regulates the use of wastewater for different uses depending its quality. In that sense, it establishes maximum admissible values (of intestinal nematodes, *Escherichia coli*, suspended solids, turbidity and other contaminants) for different wastewater uses (e.g. urban gardens, golf course, agricultural irrigation, industrial use). In agricultural irrigation, quality admissible values vary depending if the irrigation technique allows wastewater contact with the edible fruit, and if this is to be consumed fresh or industrially processed.

1.3. IRRIGATION SYSTEMS

Irrigation is the procedure by which it is applied water to a crop, helping its optimal development. There are three main irrigation techniques: surface irrigation, sprinkler irrigation and microirrigation.

In surface irrigation, water moves thanks to gravity, and the ground needs to be as flat as possible in order to optimize water use efficiency, although sometimes it requires some slope. In sprinkler irrigation, water is driven by pipes and it is applied to the crop by means of artificial rain. This technique remains limited when using wastewater, as the risk of pathogen aerosol dispersion it entails, as several studies have highlighted (Molle et al., 2016; Tomas et al., 2019). Lastly, microirrigation consists of maintaining a correct and constant soil humidity level by the slow application of water by surface drip, subsurface drip, bubbler or microsprinkler systems, which are placed close to the root system of the plant.

Water and food production sectors are forcing to the optimization of the irrigation systems to reach acceptable trade-offs, both at global and local scale (Belaud et al., 2019).

1.4. MICROIRRIGATION

1.4.1 Microirrigation system components

Microirrigation is the slow application of water on, above, or below the soil by surface drip, subsurface drip, bubbler, and microsprinkler systems (Ayars et al., 2007). A microirrigation system (Figure 1.6) consists of a pumping and filtration system, a main and submain lines and laterals, in where water is applied. The filtration system protects the installation for clogging, and the pumping system provides the irrigation water at the needed pressure for the installation. A microirrigation system can also have a chemical tank and a pump, to inject fertilizers or chlorine, and a control and monitoring system for managing irrigation events. Drip irrigation is a particular case of microirrigation where water is applied drop by drop. This last technique is the one used in the current experiment.

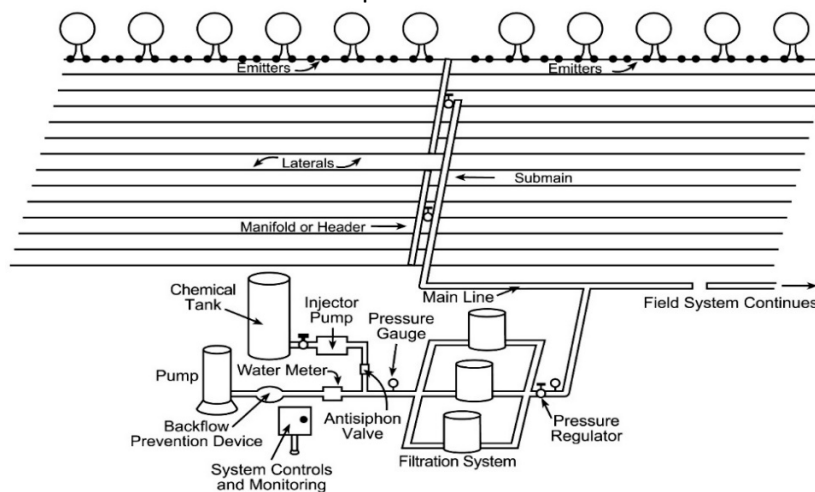


Figure 1.6. Diagram of a microirrigation system. Source: Kansas State University (2019).

1.4.2. Microirrigation actual condition

In front of the water scarcity scenario and the need of increasing agricultural production, a significant number of farmers have decided to change their irrigation system to microirrigation (Daccache et al., 2014; Tarjuelo et al., 2015). Thus, the world surface with this system increased by 31% between 1990 and 2012, while irrigated surface increased by 21% in the same period (FAO, 2019b). Table 1.1 shows the increase of irrigated area, microirrigated area and its share in irrigated area from 2013 to 2019, especially for developing countries, which points out the growth of this technique in the last years.

Table 1.1. World's irrigated and microirrigated area, and its area percentage for developed and developing countries. Source: ICID (2013, 2019).

Countries	Total irrigated area (Mha)			Microirrigation area (Mha)			Microirrigation share (%)		
	2013	2019	Δ%	2013	2019	Δ%	2013	2019	Δ%
Developed countries	43.0	44.4	3.2	4.3	5.1	18.6	10.0	11.5	15.0
Developing countries	174.2	183.9	5.6	6.5	10.8	66.2	3.7	5.9	59.5
Total	219.4	228.9	4.3	10.8	15.9	47.2	13.7	17.4	27.0

Spain is one of the countries in which this tendency has been clearly shown, increasing irrigated surface without incrementing water demand. In this sense, while agricultural irrigated surface increased from 3.4 Mha in 2002 to 3.7 Mha in 2017, demand in water decreased from 15.8 km³ in 2002 to 14.9 km³ in 2016 (MAPAMA, 2018). The explanation lies in the adoption of microirrigation, which in 2017 were used in about 51% of the irrigated surface in Spain (Figure 1.7). The decrease in the use of traditional irrigation techniques based on surface irrigation and the corresponding rural exodus that has occurred in recent decades (González-Díaz et al., 2019; Viñas, 2019) have also contributed to the percentage increase in the use of microirrigation. This irrigation technique grows every year on an ongoing basis, to the detriment of surface irrigation.

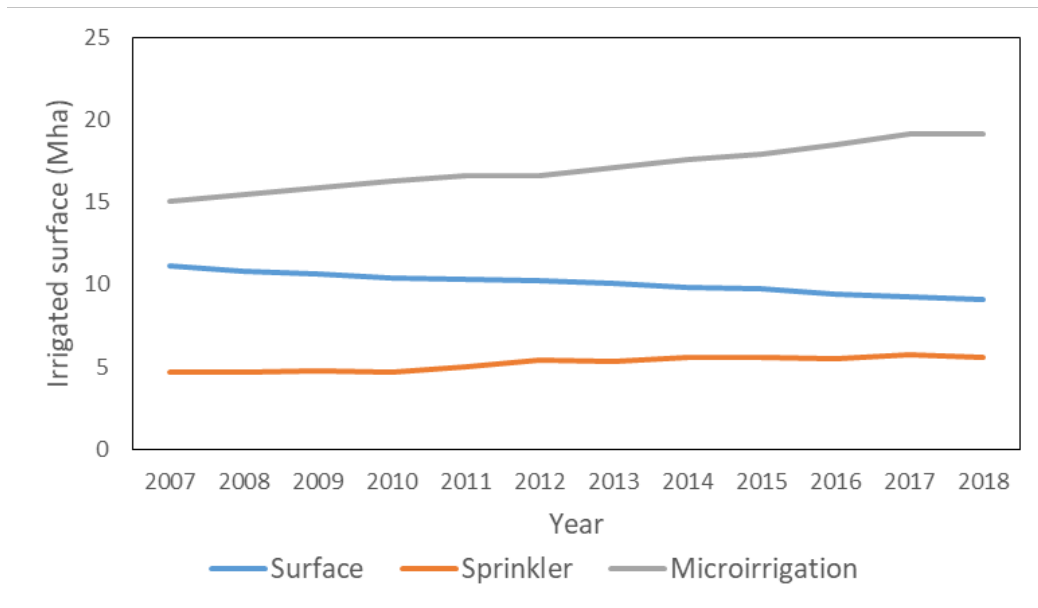


Figure 1.7. Evolution of the irrigated surface in Spain according to the irrigation technique from 2007 to 2018. Source: MAPAMA (2018).

1.4.3. Advantages and disadvantages of microirrigation

Microirrigation, and particularly drip irrigation, is the technique which offers the most environmental advantages and minor sanitary risks using wastewater effluents (Bucks et al., 1979), because, by the way it applies water, it minimises the contamination risk of the crops, it uses low flow rates and it has relatively low pressure requirements. Besides, it can irrigate surfaces of different forms and areas, with high slopes, and it avoids aerosols drift contamination (Gushiken, 1995; Trooien et al., 2000). On the other hand, microirrigation is the method with the best efficiency of the use of water (Ayars et al., 2007).

A major problem about microirrigation, and particularly to drip irrigation systems, is emitter clogging (Bucks et al., 1979; Adin and Sacks, 1987; Ravina et al., 1997; Trooien and Hills, 2007) which can affect seriously water distribution and, consequently, reduces crop yields (Tajrishy et al., 1994) and the life expectancy of laterals and increases their reposition. In particular crops, especially those with high economic value, economic losses due to clogging can be severe (Nakayama et al., 2007). Microirrigation has also important installation and maintenance costs, being necessary trained staff for its proper management (Trooien and Hills, 2007).

Emitter clogging is directly related with irrigation water quality. On one hand, physical clogging, mainly due to suspended solids, can plug completely the emitters and laterals. Some solid particles such as clay and silt are too small to be retained by the filter and can agglomerate themselves, favouring deposition and resulting in clogging (Bounoua, 2010). On the other hand, chemical phenomena can occur such as incrustation of dissolved matter, which in saturated concentration, precipitate and stick to the pipes and emitters. But the main phenomena using wastewater effluents is the biofilm formation on the pipe and emitter walls (Adin, 2002). This phenomenon can be favoured by the two previous ones, because the accumulated sediments in the system are the substrate which allow microbiologic growth (Song et al., 2017). A correct design, installation and maintenance of the microirrigation system can minimize these

problems but, unfortunately, not always these measures are completely successful (Nakayama et al., 2007). Several authors have studied how biofilm and chemical precipitation, which are the most common clogging risks when reclaimed effluents are reused, affect emitter performance (Gamri et al., 2014; Green et al., 2018; Zhou et al., 2018; Lequette et al., 2019).

1.5. FILTRATION

A correct filtration process is essential for a good performance of a microirrigation system, since it prevents emitter clogging caused by organic and inorganic particles (Ayars et al., 2007), especially when using wastewater because it increases the risk of emitter clogging due to its solid particles, chemical substances and microorganisms load (Trooien and Hills, 2007). Some solid separation techniques (such as inverse osmosis, ultrafiltration or microfiltration) suppose a high energetic cost so the choices for filtrating water in microirrigation systems are reduced to three types of filters: screen, disc and media filters.

1.5.1. Screen filters

Screen filter makes water to pass through a mesh so particles can be retained in it (Figure 1.8). The screens may be made of steel, plastic or synthetic cloth and they are easy to operate (Abbot, 1985). The trapped particles will be greater than the mesh free space. Therefore, solid retention takes place in the mesh surface which leads to the mesh clogging. To restore the initial filter conditions, a backwashing must be carried out for releasing the retained particles.

There are some self-cleaning designs which provide a tangential flow inside the filter that sweeps along the retained particles when debris is accumulated (Nakayama et al., 2007), but these designs have the problem that the velocity on the screen surface has to be relatively high, which compress organic particles and retention efficiency is reduced (Puig-Bargués, 2003). Some modern screen filters incorporate a suction system which clean retained particles while operating. If they do not have a self-cleaning system, two screen filters are needed, so one can operate normally while the other is backwashed.



Figure 1.8. Screen filter diagram. Source: Kansas State University (2019).

1.5.2. Disc filters

Disc filters use a series of grooved plastic or plastic-coated metal discs to form a filtering device when clamped together (Figure 1.9). When these discs are stacked tightly together, they form a cylindrical filtering body, which resembles a deep tubular screen (Nakayama et al., 2007). These filters have more surface area than screen filters of similar sizes and like screen filters must be cleaned periodically (Capra and Scicolone, 2004; Wilén et al., 2016). To carry out backwashing, filtered water is pumped in the opposite direction, so discs loosen and release particles stuck in them (Figure 1.9). This means that filtration process is intermittent due to interruptions needed for cleaning the discs. In order to maintain the filtration process continuous two disc filters working together are necessary, so when one filter is backwashed, the other one can work properly.

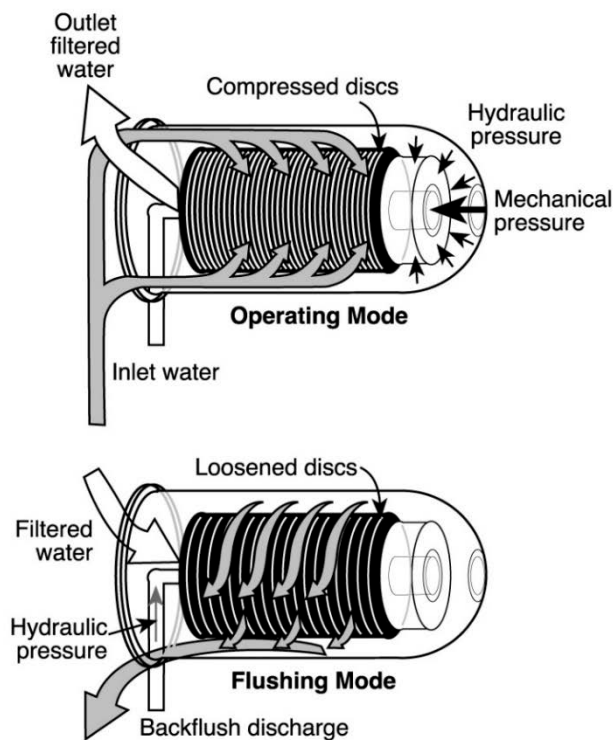


Figure 1.9. Disc filter diagram. Source: Kansas State University (2019).

1.5.3. Media filters

Media filters consist in a closed tank filled with a filtering media (Figure 1.10). The media lies above a bracket, which separates the filter inlet and outlet. Below the bracket there is the drainage, which lets the water flow but not the media. Media filters present the best efficiency in solid suspension and turbidity removal and, for this reason, are considered the standard for emitter protection (Trooien and Hills, 2007), especially when wastewater is used (Tajrishy et al., 1994; Puig-Bargués et al., 2005a; Capra and Scicolone, 2007; Duran-Ros et al., 2009a). Nevertheless, media filters are more expensive than the screen and disc filters (Pujol et al., 2011) and a good performance require experienced and trained staff (Capra and Scicolone, 2007). In some scenarios, filtration with a combination of sand and disk filter would be most appropriate strategy against emitter clogging using wastewater (Tripathi et al., 2014). In this case, the combination of the two filters could result in a better emitter discharge exponent, a reasonably good coefficient of variation, uniformity coefficient and distribution uniformity.

1.5.3.1. Operation

Media inside the tank forms a column, and water comes from above and pass through the media. Water circulation must be the most uniform possible, to avoid preferential water corridors. To achieve that, a deflector should be installed at filter inlet or the discharge pipe points to the top of the filter and the filter wall becomes the deflector. Although deflectors contribute little to head loss, they do have an effect on media bed deformation, because if they do not perform properly, preferential water passages can appear. In that sense, using a vertical wind tunnel, it has been visualized the importance of this element in the correct water distribution in the filter interior (Dos Santos et al., 2013; Mesquita et al., 2019).

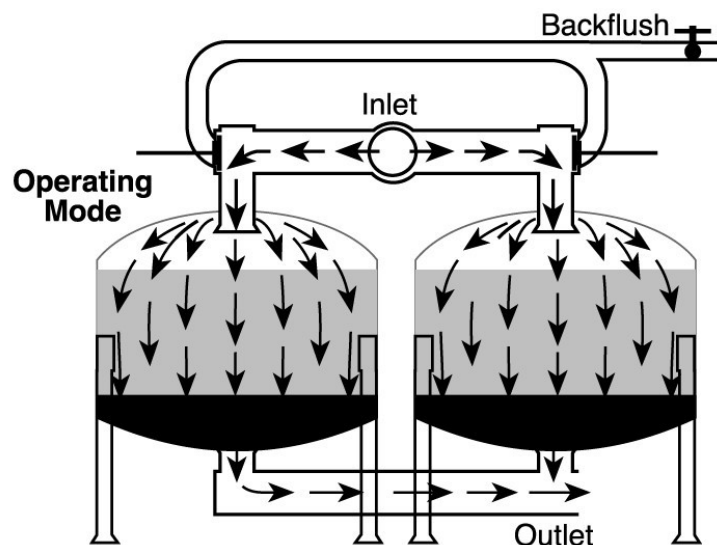


Figure 1.10. Media filter diagram. Source: Kansas State University (2019).

The most common material used in media filters is silica sand (Nakayama et al., 2007). However, other materials present good hydraulic properties for filtration similar to silica sand, such as recycled glass, and gradually, there start to appear studies about the behavior of this material in media filters used for microirrigation systems. Although both silica sand and recycled glass present asymmetries in their geometry, Bové et al. (2015a) found that recycled glass presented more sharp and angular features that gave lower sphericity and higher porosity than silica sand. Consequently, in an experiment carried out by the same authors comparing both filtration media, head loss was lower using silica sand. On the other side, recycled glass has the advantage of reutilization of a residue (Rutledge and Gagnon, 2002; Hu and Gagnon, 2006; Horan and Lowe, 2007; Soyer et al., 2010); thus reducing the energy utilisation in the life cycle assessment (Diotto et al., 2014) and avoids the exhaustion of a natural and finite resource, such as sand.

1.5.3.2. Filtration mechanism

Basically, the grains of the media form an interconnected porous package, and the water flow which goes through this structure loses pressure, being the flow direction always the same to pressure gradient. In spite of the flow inertia, water trajectory inside granular media is difficult to predict because channels formed are full of bends and each time that a grain of the filtration bed is intercepted, an unpredictable change of direction is produced (Mesquita et al., 2017).

There are three mechanisms for suspended solid retention (Pizarro, 1987). The first one is that if the minimum dimension of the particle is higher than the porous overture, the particle gets stuck (like it would do in a mesh), and a debris between the interface fluid/media is formed. The other two are less evident. On one hand, suspended particles can be settled on the grain surface, that is, sedimentation above the media grains. This is due to flow velocity, which tends to be zero in media surface, being no dragging phenomena when velocity is zero (Valdés and Santamaria, 2007). On the other hand, there are attraction phenomena between suspended particles and media grains explained by different electric charge, known as the Van der Waals forces (Petrucci, 2007; Vigneswaran and Kwon, 2015).

These last two mechanisms explain solid retention in depth and the effect of water turbidity removal. The main retention zone lies in the superior part of the filtration bed (Ojha and Graham, 1994), where particles are accumulated forming a layer of grain media and sediments which contributes to accumulate more sediments and, at the same time, head loss increases. Moreover, when using high filtration velocities, turbidity removal tend to happen in the first filtration layers, being the media height not as important as filtration velocity.

The thickness of the media filtration only influences to a specific value, called critical thickness. Higher values of thickness do not increase quality in filtration, and can cause inefficiency of the backwashing process (Pizarro, 1987; Rodrigo et al., 1997). However, it must be taken into account that the active zone, that is the zone of the filtration media which is capable of retaining solids, is delimited by the proximity of the drainage. In the surrounding areas of the draining elements, a curvature of the flow is produced, which implies a loss of passing surface, velocity increases and a dragging of the solids sediments is generated (Bové et al., 2017). Because of that, it is recommended that the media column has a minimum height of 30 cm beyond the drainage (Burt, 2010).

Grain size and media height are two factors which affect filtration performance in sand filters. For the characterization of the sand media particles, sand effective diameter (d_e , which is the size opening which will pass 10% by dry weight of a representative sample of the media material) and uniformity coefficient (UC_s , ratio of the size opening which will pass 60% of the sand to the size opening which will pass 10%) are usually used. Another factor which affects filtration performance is filtration velocity, which has been studied by several authors (Mesquita et al., 2012; Wu et al., 2015; de Deus et al., 2016).

1.5.3.4. Filter backwashing

Backwashing consists in cleaning the filters by reversing the direction of the water flow through the filtration media lifting it up to allow solids and particles to flow outside the filter (Abbott, 1985). Once the filtration media is clogged of solids, initial conditions must be restored. This is achieved thanks to backwashing: water flow goes through the media in the opposite direction of filtration trajectory (Figure 1.11). The backwashing flow must be much higher than the filtration flow, considering that it is desirable to surpass the superficial velocity that cause the fluidization of the filtration bed, facilitating the separation of the suspended solids retained between the media grains.

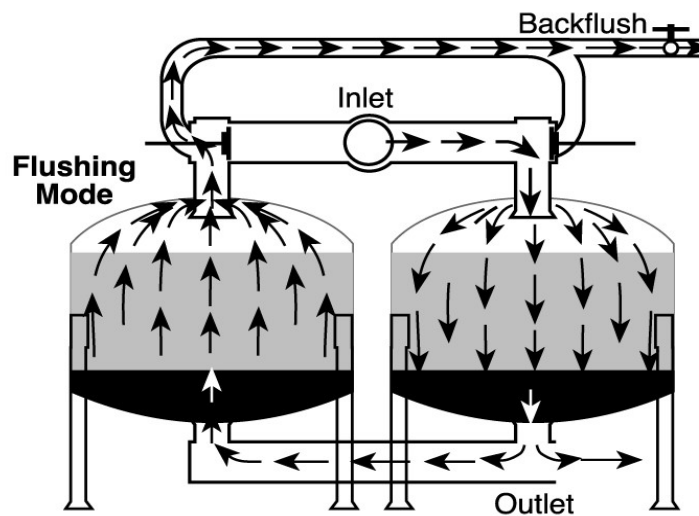


Figure 1.11. Backwashing media filter diagram. Source: Kansas State University (2019).

Usually, in media filters backwashing can be manual or automatic, on a set time interval or at specific pressure drop, to control automatic backwashing, setting a pressure loss is normally used (Ayars and Phene, 2007), although different values are recommended. Thus, Haman et al. (1994) set the backwashing between values of 20 – 55 kPa for clean media filters and depending on the media size and the flow rate, but Burt and Styles (2000) suggest cleaning the filters when the pressure loss is between the range 35 to 55 kPa; Ravina et al. (1992) recommend backwashing when head loss reaches 50 kPa, while Sawa and Frenken (2002) recommend 70 kPa. One of the advantages of automatic filter backwashing systems is that it eliminates sudden changes in water quality which can create problems if a filter is washed only at regular intervals

(Haman et al., 1994) and avoids the contact between the effluent and the irrigator (Capra and Scicolone, 2004).

Filters should be backwashed frequently (Pitts et al., 1990, Burt and Styles, 2007), and it is highly recommended to conduct several initial backwashings when new sand media are used and to divert the initial backwashing water (Elbana et al., 2012). However, inadequate sand filter backwashing intervals and durations cause poor performance in drip irrigation systems (Enciso-Medina et al., 2011).

Underdrain design also affects backwashing cleaning process, which could also be related to turbidity removal efficiency as the filter underdrains are essential to guarantee a homogeneous particle removal during backwashing (Mesquita, 2014). Cylindrical and pyramidal dome underdrains prevent the absence of flow in some regions of the media bed during backwashing, avoiding the expansion of the media bed and its cleaning, but underdrains designs with more effective filtration area such as the sphere-dome proposed by Mesquita (2014) achieved better backwash performance and reduced head loss.

The time span that an effluent of degraded water quality passes through a filter immediately after being backwashed is called filter ripening. Amirtharajah (1985) showed that more than 90% of the particles passing through a well-operating filter did so during the ripening period. Thus, filter ripening is a period during which emitter clogging is likely to occur as filter protection is not as effective as it should be. This ripening period has been studied in depth. Scientists have focused primarily on effluent turbidity (Amirtharajah, 1985; Amburgey and Amirtharajah, 2005) and on particle size distribution (Darby and Lawler, 1990) as principal indicators of filter ripening, while Elbana et al., (2012) concluded that the ripening period is 15 min for sand filter in microirrigation systems.

1.5.3.5. Underdrain designs

The main purpose of the underdrain is to let water pass but not the media, and to support the filtration bed. In pressurized filters, the underdrain is designed with metal or plastic distributed so that it occupies the most part of the filter surface. Mainly, there exist several types of underdrains in sand media filters (Burt, 2010; Mesquita et al., 2012).

One type of commercial underdrain consists in a series of nozzles which are placed together in tubes, in a star formation, forming an arm collector. These elements have slots which let the water pass but not the media (Figure 1.12).

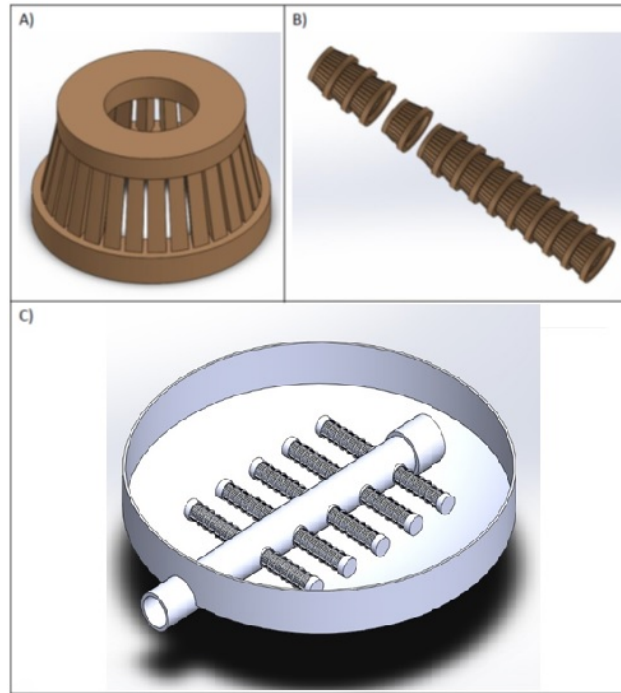


Figure 1.12. Arm collector underdrain design. A) Single slotted piece, B) Arm formed by pieces, C) Arm collector design. Source: Bové (2018).

As the underdrain arms separate, the distance between them increases, which is why in some cases, when the filters have a high diameter, a second underdrain is installed, in an alternated position with the first one.

This type of underdrain presents some performance problems, because flow uniformity in the media close to the nozzles can be low. Due to the length of the underdrain arms and the thin slots, the pressure loss is important. Moreover, the media situated below the underdrain does not perform correctly, since there is no flow activity in this part of the media. For this reason this area is not backwashed properly when backwashing is produced (Mesquita, 2014).

Another underdrain in pressurised media filters consist in a series of nozzles inserted in the underdrain base. Nozzles are formed of a dome with slots placed above a collector and a bottom cover which gives a water tightness to the whole element (Figure 1.13).



Figure 1.13. Inserted domes underdrain design. A) Dome, B) Dome interior design, C) Inserted dome underdrain.
Source: Bové (2018).

Domes are distributed to the underdrain base, so unlike the previous design, no media is placed underneath the underdrain. These designs help backwashing, so all the media column is mobilised when counter-current water is applied. However, the thickness of slots and collector is really narrow which produces an important head loss (Bové et al., 2015b).

Due to its geometry, sand filters generate an important head loss which does not contribute to improve water quality. Arbat et al. (2011) using computational fluid dynamics found that head loss between the bottom of media bed and the surrounding area of the dome underdrain was a 35% of the total filter pressure loss. Mesquita et al. (2012), in an experimental study that analysed the effect of internal auxiliary elements, such as the underdrain and the diffuser plate, greatly affected the pressure drop. Arbat et al. (2013), in an experimental study with a scaled commercial sand filter testing different sand media depths, showed that most of the pressure drop occurs at the bottom of the sand column and in the nozzle. Moreover, these authors developed an analytical model to predict pressure drop in sand filters taking into account the effect of underdrain, which improved the pressure drop predicted by Ergun equation and showed the importance of the underdrain geometry. On the other hand, Dos Santos et al. (2013) experimentally confirmed the importance of the underdrain design in the flow-line trajectories.

Bové et al. (2015b) and Pujol et al. (2016) showed that by modifying the position of the slots above the underdrain element, a reduction greater than 20% of the filter energy consumption was achieved, as the nozzle shape highly influenced the overall pressure drop.

So far, two different components of the total pressure drop in media filters can be distinguished: that produced by the filter media, necessary for filtration process, and that produced by the filter components themselves, the design of which could be important to reduce energy requirements and optimize energy efficiency in sand filters.

Bové et al. (2015b) identified three different strategies to reduce pressure drop in the underdrain and therefore energy consumption: using a large particle size at the bottom of the

filtering medium around the underdrain, since this would reduce the pressure drop caused by the porous material in contact with the nozzle; placing some of the slots at the top of the nozzle thereby intercepting the stream lines from the porous medium perpendicularly and facilitating the outflow; increasing the cross-sectional area of the duct located at the outlet of the nozzle, which is responsible for most of the pressure drop. Because of these researches, a new underdrain was proposed, which could reduce the pressure drop of the entire filter by some 35%. On one hand, the section between the underdrain outlet and the water chamber at the bottom of the filter should be enlarged for reducing flow velocity across the underdrain and thereby reducing the pressure drop. On the other hand, the underdrain could be covered with granular medium with a greater size and therefore higher hydraulic conductivity than that of the filtration column for achieving a lower pressure loss. All the aforementioned improvements have been the basis of the Spanish utility model U201530629 (Bové et al., 2015c).

Although several authors have studied the influence of underdrain design on pressure loss (Mesquita et al., 2012; Bové et al., 2015b; Pujol et al., 2016), none of them has analyzed how filter design affect to emitter clogging.

A scaled laboratory sand filter with the new underdrain design (Figure 1.14) was studied by Bové et al. (2017). Laboratory tests confirmed that the new underdrain reduced pressure loss regarding different previous underdrains designs tested by the same authors (Bové et al. 2015b). The pressure drop across the filter was 20% smaller when the filter worked at low filtration surface velocities (<0.01 m/s) and 45% at the high filtration surface velocities (>0.02 m/s) under filtration with granular bed of silica sand of grain size between 0.63 and 0.75 mm and a height of 300 mm.

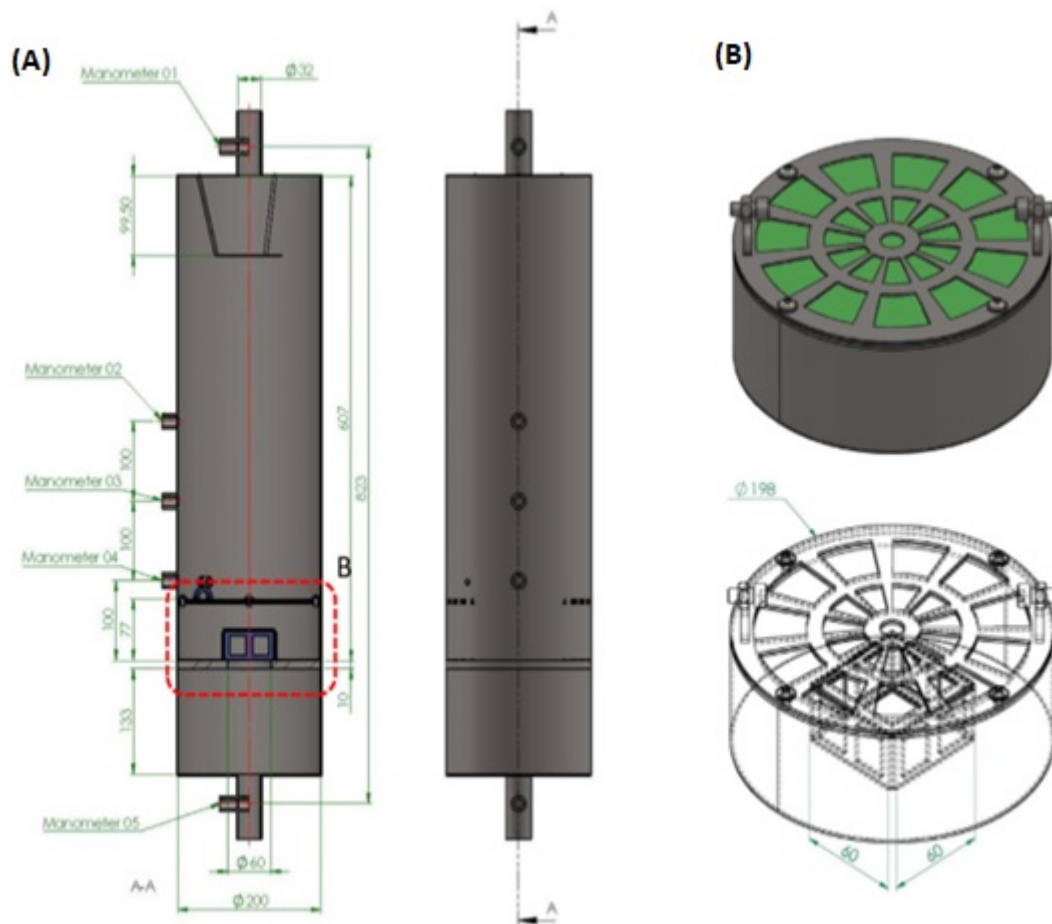


Figure 1.14. Scaled laboratory sand filter with the new designed underdrain (A) and its isometric view (B). Source: Bové et al. (2017).

However, in the same study Bové et al. (2017) also concluded that further research was warranted for analysing the effect of the new underdrain on particle removal efficiency and on the overall microirrigation system pressure loss. In that sense, a prototype of this underdrain was built to be tested in field conditions following the dimensions of the one used in Bové et al. (2017) (Figure 1.15). In that sense, the mentioned prototype underdrain was tested in the experiments for this thesis, among the other two types of commercial underdrains (arm collector and domes), since, as discussed at the beginning of this chapter, media filters are the ones that work best when using effluents, and silica sand used as filtration media as it is the most common media used.

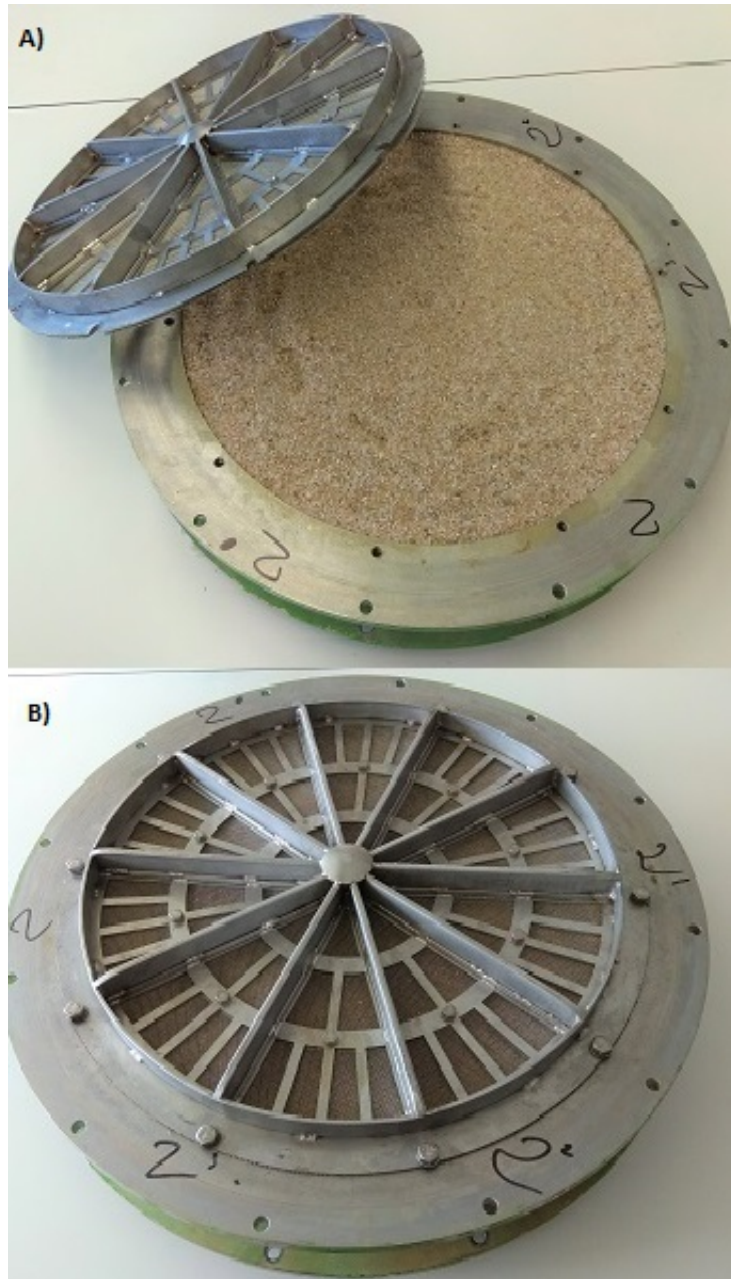


Figure 1.15. Adapted new underdrain design following the dimensions of the underdrain proposed by Bové et al. 2017. A) Media used as underdrain, B) Underdrain design assembled.

1.6. EMITTERS

Emitter clogging depends upon quality of water, dripper type, emitter design, filtration methods and environmental conditions (e.g. temperature). The extent of dripper clogging was studied by many researchers (Taylor et al., 1995; Puig-Bargués et al., 2005b; Capra and Scicolone 2007; Yavuz et al., 2010; Niu et al., 2013; Katz et al., 2014), agreeing that emitter design is a key factor that affect emitter clogging. Many types of emitters have been studied for a long time, such as labyrinth inserted (Taylor et al., 1995) and integrated (Trooien et al., 2000) emitters, or inserted orifice (Ravina et al., 1992; El-Berry et al., 2003; Capra and Scicolone, 2007); but the use of pressure compensating (Puig-Bargués et al., 2010a; Pei et al., 2014) and integrated (Pei et al., 2014) emitters reduce emitter clogging and uniformity problems. Capra and Scicolone (2007) noticed that labyrinthine emitters were more prone to clogging and Ravina et al. (1992) and Trooien et al. (2000) observed a tendency in emitters with high flow to clog less, while integrated emitters were also more clogging resistant (El-Berry et al., 2003). Additionally, partial clogging emitter is a progressive fact and more frequent than total clogging (Ravina et al., 1992; Rowan, 2004). Pei et al. (2014) suggested the use of pressure-compensating flat emitters and cusp-shaped saw-tooth non-pressure-compensating emitters with short flow when reclaimed water is used in drip irrigation. On the other hand, most common working pressure among experiments is 100 kPa, although studies like Dehghanisanij et al. (2004) tested higher working pressures (150 kPa).

When it comes to emitter clogging, emitter location is an important factor. Last locations at the end of the lateral are more prone to clog (Trooien et al., 2000; Duran-Ros et al., 2009a; Puig-Bargués et al., 2010a; Oliver et al., 2014) which can be attributed to a reduction of the flow rate at the end of the lateral (Shannon et al., 1982) and a greater concentration of particles (Wu et al., 2015). Different lateral length have been tested, highlighting short lateral length of 3.7 m (Rowan, 2004) and 400 m (Schischa et al., 1997), as well as different separations between emitters. Lavanholi et al. (2018) defined a methodology to evaluate dripper sensitivity to clogging due to solid particles, taking into account hydraulic emitter design. Besides, some studies have studied the influence of hydrodynamics on labyrinth-channel drippers (Al-Muhammad et al., 2018) and its impact on clay particle deposition and biofilm development (Ait-Mouheb et al., 2019). Cararo et al. (2006) also pointed out that having short discharge channels and membranes for self-cleaning were interesting features to avoid clogging.

The recovery of clogged emitters due to pressure variations or deformation of organic particles has also been observed (Ravina et al., 1992; Duran-Ros et al., 2009a). On the other hand, Feng et al. (2018) highlighted a randomness on emitter clogging.

There are several studies that compare the effect of different filters in emitter clogging when using reclaimed effluent (Ravina et al., 1992; Capra and Scicolone, 2004; Duran-Ros et al., 2009a; Tripathi et al., 2014).

1.7. DISTRIBUTION UNIFORMITY

Emitters allow that water leaves drop by drop. Emitter discharge follows the equation:

$$q = k \cdot P^x$$

where q : flow rate (l/h); k : constant depending on the kind of emitter, flow and pressure (dimensionless); P : pressure (MPa); and x : discharge emitter exponent (dimensionless).

One of the most commonly used parameter when designing and evaluating a drip irrigation system is distribution uniformity (DU) (Barragán et al., 2006). DU expresses the variation of the emitter discharge of the irrigation system, which mainly depends on the hydraulic design, the coefficient of manufacturing variation and emitter clogging (Barragán et al., 2006; Wu et al., 2007). DU shows the efficiency of a drip irrigation system because, in fact, it measures the non-uniform pattern of emitter flow of a drip irrigation system (Wu et al., 2007).

Flow distribution uniformity (DU_{lq}) and pressure distribution uniformity (DU_{lp}) are two of the indices most useful for the design and assessment of drip irrigation systems (Barragán et al., 2006). When these parameters are used for evaluation, they allow to know if there are important differences in the crop watering application and allow to determine their causes (Wu et al., 2007).

Both DU_{lq} and DU_{lp} depend basically of the hydraulic design, the variation coefficient of fabrication and emitter clogging (Barragán et al., 2006), as well as other parameters such as topography, pipe size and emitter spacing. DU_{lq} is a good indicator for emitter clogging when the system is well designed and the manufacturer's coefficient of variation is low, and it is particularly interesting when water with a high clogging potential are used, such as reclaimed effluents (Bucks et al., 1979; Ravina et al., 1992).

DU_{lq} is defined as:

$$DU_{lq} = \frac{q_{25}}{q_a} \cdot 100$$

where DU_{lq} : flow distribution uniformity (%); q_{25} : mean flow of the 25% of emitters with the lowest flow (l/h); and q_a : mean flow of all emitters (l/h).

On the other hand, DU_{lp} is defined as:

$$DU_{lp} = \left(\frac{p_{25}}{p_a} \right)^x \cdot 100$$

where DU_{lp} : pressure distribution uniformity (%); p_{25} : mean pressure of the 25% of locations with the lowest pressure (kPa); p_a : mean pressure of all locations (kPa); and x : emitter discharge exponent (dimensionless).

Several methods have been developed to determine system uniformity such as Merriam and Keller (1978), which was also adopted by the Food and Agriculture Organization of the United Nations FAO (Vermeiren and Jobling, 1986) and the ITRC of California Polytechnic State University method (Burt, 2004).

The Merriam and Keller (1978) method selects four locations of a secondary branch, one at the beginning, another at the end and the other two between the two previous ones and located at the same distance. From each lateral, it calculates the mean of the flow discharge of two contiguous emitters, each pair located at the beginning, 1/3, 2/3 and end of the length of the lateral. This way, from 32 volume measurements, 16 emitter discharge flows are obtained to calculate DU_{lq} . Juana et al. (2007) pointed out that, on one hand, no reason is given for the recommendation to calculate the mean of the pair of emitters and, on the other hand, from a statistical point of view, the selected locations do not represent the average flow discharge of all emitters or their variance. Besides, another problem of this method is that by measuring the discharge of the last two emitters or measuring it in previous positions can significantly affect the DU_{lq} , since the last emitters are more prone to clogging (Ravina et al., 1992; Trooien et al., 2000; Puig-Bargués et al., 2010a; Wu et al., 2015). However, Merriam and Keller method does not specify which exact emitter locations should be evaluated, although the use of extreme locations provide useful information on head losses in laterals and submain. Following a similar methodology, Juana et al. (2007) proposed taking 4 different lateral positions depending on a shape factor of rectangular and trapezoidal irrigation subunits.

Another method to evaluate DU_{lq} is the developed by the Irrigation Training & Research Center (ITRC) of the California Polytechnic State University (Burt, 2004), which selects three locations and a total of 60 emitters. The first location is composed of 16 contiguous emitters at the beginning of a lateral close to the water source. Is in those locations where the cleanest emitters are expected to be found. The second location, also composed of 16 contiguous emitters, is in the middle of a lateral near the middle of a field. The third location, composed of 28 emitters, is at the end of the dripline at the end of the most distant manifold, which is expected to be the dirtiest part. It must be noted that there are no differences in pressure between the selected emitters of each location. This method also needs more pressure measurements and uses different location of the selected emitters. Figure 1.16 shows the location of the emitters used for computing DU_{lq} with the different methodologies.

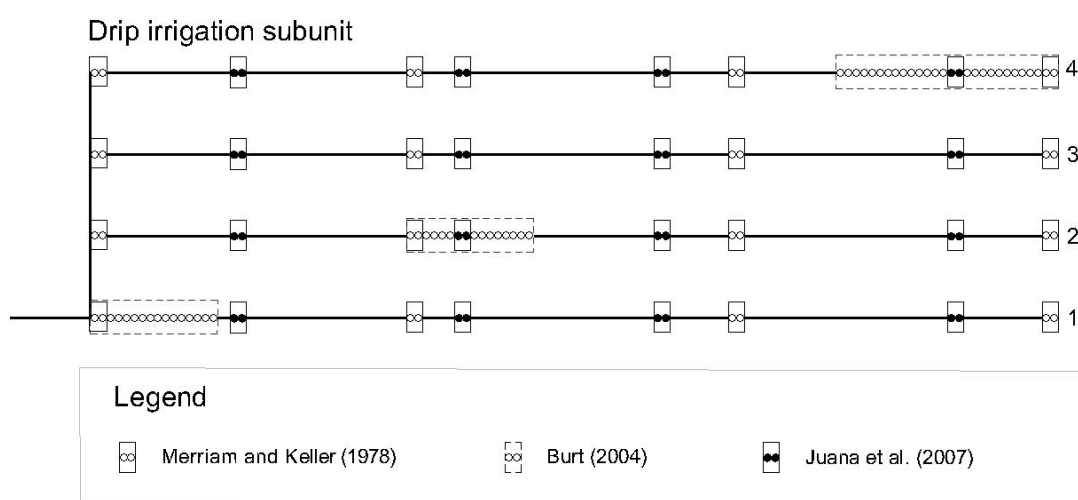


Figure 1.16. Location of the emitters used for DU_{lq} determination for the different methodologies.

Finally, Bralts and Kesner (1983) proposed to select a random 18-sample set assuming a normal distribution of flow rates, although random selection of emitters is more laborious than fixed locations approaches, and pressure measurements at disperse points is not always a practical issue (Juana et al., 2007). The approach of Bralts and Kesner (1983) was adopted by the ASABE in a former standard. More emitter discharge measurements or the measurements of all emitter flow discharges would be more representative for the calculation of the DU_{lq} , but in real field conditions, it may be impractical (Wu et al., 2007) and would represent more time and labour costs.

1.8. OPERATION AND MAINTENANCE FOR REDUCING EMITTER CLOGGING

Appropriate operation and maintenance of microirrigation systems can reduce clogging. Thus, lateral flushing is considered an indispensable maintenance practice for avoiding emitter clogging (Nakayama et al., 1978; Taylor et al., 1995; Pei et al., 2014), as it reduces sediment deposition within driplines (Puig-Bargués et al., 2010b; Li et al., 2018a; Li et al., 2019b) as well as biofilm formation (Li et al., 2015; Li et al., 2019b). To achieve the best effectiveness of a microirrigation system, it should be designed so that it can be flushed properly. In some cases, flushing can control emitter clogging to about half in magnitude (Tripathi et al., 2014). Flushing must be done at a suitable velocity to dislodge and transport the accumulated sediments (Pitts et al., 1990; Adin and Sacks, 1991; Ravina et al., 1992; Nakayama et al., 2007; Puig-Bargués et al., 2010b; Li et al., 2018a). A minimum flow velocity of 0.3 m/s is needed for flushing the lateral lines as recommended by the standard ASABE EP-450.1 (ASAE Standards, 2003). However, a flushing velocity not smaller than 0.5 m/s is suggested to assure that all particles are removed (Hills and Brenes, 2001). Li et al. (2018a) recommended a velocity of 0.6 m/s and short flushing intervals. Flushing frequency and duration has also an impact on emitter clogging control (Puig-Bargués et al., 2010a; 2010b; Feng et al., 2017; Li et al., 2019b). Flushing is advisable whatever the frequency (Puig-Bargués et al., 2010a; 2010b) but Feng et al. (2017) recommended to flush the laterals with freshwater at the end of each irrigation event and Li et al. (2019b) every five irrigation events.

Some authors advise to apply chlorination (Pei et al., 2014) or some acid product to reduce pH to decrease bacterial growth and prevent biological clogging (Hills and Brennes, 2001; Dehghanisani et al., 2005; Cararo et al., 2006) as the strong oxidation of chlorine inhibits the reproduction and growth of microorganisms and the formation of biofilms (Li et al., 2010) as well as, if combined with acidification, the precipitation of solid particles in the drip emitters (Hao et al., 2018). Free chlorine levels between 1.5-2.5 mg/l at the end of the laterals effectively reduced emitter clogging (Li et al., 2010; Song et al., 2017). Finally, filtration, as previously discussed, can also be considered an operational and maintenance practice.

1.9. PROCEDURE AND DURATION OF MICROIRRIGATION EXPERIMENTS

Distribution uniformity should be assessed throughout the irrigation life cycle. In that sense, the procedures and sampling timing of the experiments carried out for assessing distribution uniformity in a microirrigation system are diverse. Methodology and sampling frequency for the uniformity distribution assessment varies from one study to another. For example, Puig-Bargués (2005b) determined irrigation uniformity every 50 h, using Vermeiren and Jobling methodology, while Ravina et al. (1997) took measures from five emitters from the beginning and five from the end one time every 500 h, as well as the continue measurements of the flow rate and pressure values in the irrigation laterals. Relating to sampling timing, some authors took measures every 15 days in a 24 months test period (Nakayama et al., 1978) while others measured emitter discharge daily, which represented a measuring frequency of 4-6 h during the 60 h period test (Capra and Scicolone, 2007).

Other authors measured the effect of drip irrigation frequency on emitter clogging using reclaimed water, with irrigation frequencies of once every 2 days, 6, 8 and 16 days in a 540 h test period, and observed that emitter clogging degrees increased with shorter drip irrigation interval, mainly due to the effects of drip irrigation frequencies on the comprehensive biofilm growth and detachment inside emitters (Zhou et al., 2015).

The test working time of filtration studies vary substantially, as much the length of the irrigation test as the daily regime hours. In relation with the total test working hours, the most common duration is between 100 and 400 h. For example, Li et al. (2012) tested a total of 216 h, while Capra and Scicolone (2007) tested a daily working regime of 4-6h/day and a total of 60 h, the same duration than Li et al. (2018a). Tarchitzky et al. (2013) tested emitter discharge during a 7 month irrigation season, and Adin and Sachs (1987) did a 24 h/day regime with a total of 2880 h. Recent studies lasted around 540 h (Pei et al., 2014; Zhou et al., 2015), 700 h (Li et al., 2015) or 1260 h (Green et al. 2018).

There is a reduction of emitter discharge throughout irrigation time which has been widely observed by several authors (Ravina et al., 1992; Duran-Ros et al., 2009a; Tripathi et al., 2014; Wu et al., 2015; Pei et al., 2014), although emitter discharge values and its pattern throughout time varies from one study to another. For example, in an experiment that lasted 540 h (Pei et al., 2014), the relative average emitter discharge reduced 4.1-13.1% during the first period (0-204 h) but reduced 37.5-67.3% at the end of the experiment (204-540 h) for pressure-compensating emitters, while Wu et al. (2015) observed major emitter discharge reductions in first testing stages (from 0 to 150 h) compared to reductions in final testing stages (from 150 to 300 h).

1.10. MONITORING AND CONTROL OF MICROIRRIGATION SYSTEMS

Specific problems in pumping, head losses in filters and pipes or emitter clogging in drip irrigation affect working conditions of microirrigation systems. These problems can be worsened when wastewater is used, and in these cases, due to variability of effluent characteristics, a continuous control is essential to assess filter and clogging processes. The implementation of monitoring and control systems allows detecting clogging in the first stages of development (Ravina, 2002).

Monitoring is the automation of the surveillance processes, giving the operator the needed mechanisms for alert, as well as the interaction between the process itself and evolving registers, with the aim of facilitating the detection of uncommon situations and their diagnose through the continuous surveillance of the performance variables (Corominas et al., 2010). Thanks to the monitoring and control of a microirrigation systems, the operation of the system can be carried out with the maximum efficiency (Mareels et al., 2005). To achieve the correct operation, various sensors can be used in real time for obtaining values of flow rates, volumes, pressures, water quality, soil humidity and weather measurements (Ayars and Phene, 2007). All of these applications contribute to have a precision irrigation, which saves water, energy and money (Madramootoo and Morrison, 2013). Initially, some of these data was used to scheduling irrigation (Goldhamer and Fereres, 2004; Casadesús et al., 2012; González-Perea et al., 2017) and later used to improve microirrigation systems designs (Morillo et al., 2015).

One of the approaches used to control and monitoring microirrigation systems is the SCADA (Supervisory Control and Data Acquisition), which is a software application with access to field data throughout digital communication with the instruments it activate, and a high level graphic interface with the user (Domingo et al., 2003). In that sense, a SCADA system consists of a computer with high information process capacity and a unity control with an operational system in real time. These two mechanisms need to be connected to each other and to the automatons and measurement instruments (Domingo et al., 2003) (Figure 1.17).

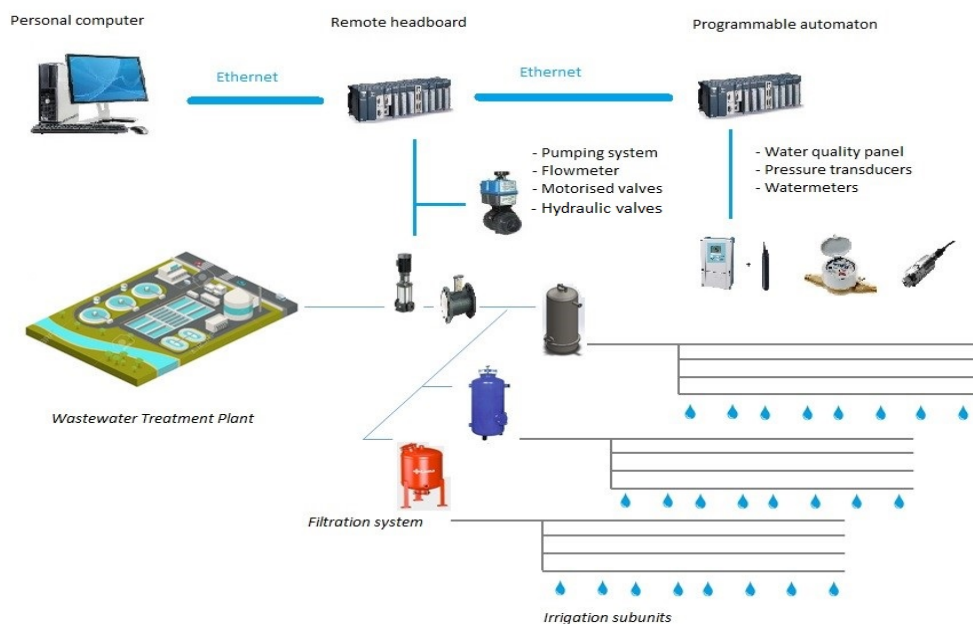


Figure 1.17. SCADA diagram used in a microirrigation system using effluents. The SCADA system consist of a computer, operational and measurement instruments and automatons to connect both of them.

Some SCADA systems have been developed for irrigation canal automation (Burt, 2005; Rijo, 2008, Rijo and Arranja, 2010), for irrigation scheduling and for precisely manage the whole microirrigation system (Ayars and Phene, 2007; Fernández-Pacheco et al., 2014; Li et al., 2018b). In microirrigation systems, the implementation of SCADA systems has showed that it is a useful tool for assessing the microirrigation system performance, thanks to quicker detection equipment failures and anomalies, and the obtaining of data at regular intervals during long periods of time, which allow high information of irrigation behaviour (Duran-Ros et al., 2008). SCADA systems has also a great capacity to adapt to changing necessities, such as incorporate an irrigation automation system based on soil water content. However, the use of SCADA systems for assessing microirrigation system performance has not yet been widely explored due to its high investment cost, conversely, they are widely used in industry.

1.11. ENERGY CONSUMPTION OF MICROIRRIGATION SYSTEMS

One of the constraints of microirrigation is the increase of energy consumption that entails (Burt et al., 2011; Corominas, 2010). Although energy needs for irrigation represent a small fraction of the total energy consumption by human activities, energy has become an important issue for the irrigation sector and a critical factor for food security (Belaud et al., 2019). Even though the adoption of pressurized irrigation systems has decreased irrigation water consumption, energy demand has increased. In that sense, in pressurized irrigation systems, water and energy are interdependent, and in semi-arid regions energy needs have reached values as high as 0.95 – 1.55 kWh/m³ (Soto-García et al., 2013).

Figure 1.18 shows the water and energy demand per hectare in Spain from 1950 to 2014. As it can be seen, water demand has been reduced by 49 % but, conversely, energy demand has been increased by 655 %, which leads to a reduction of economic benefits for farmers (Pardo et al., 2013).

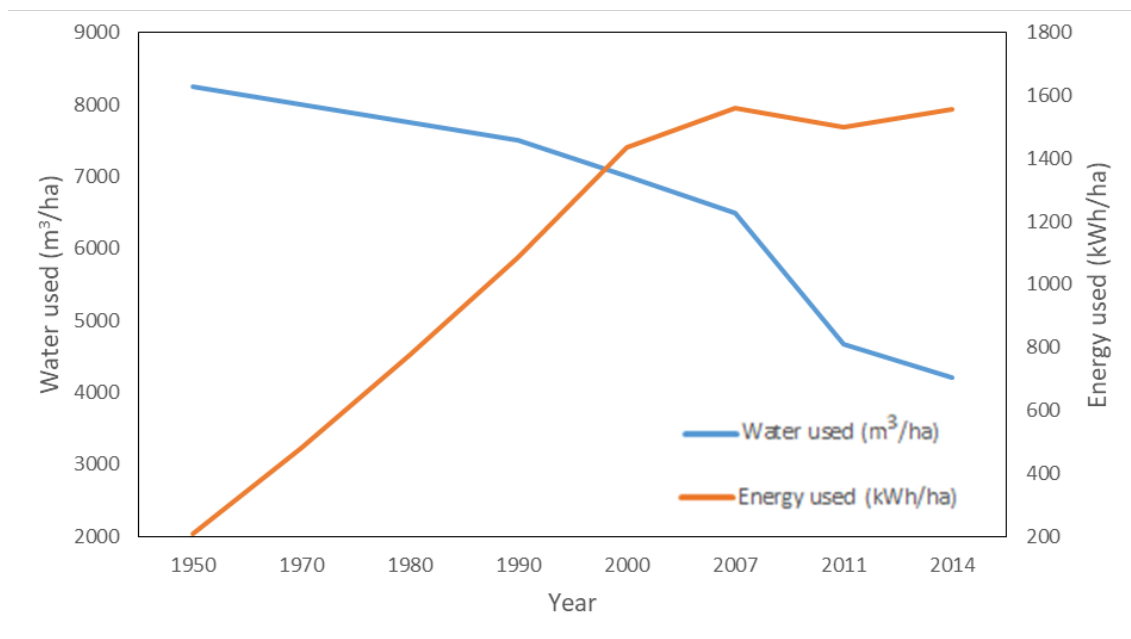


Figure 1.18. Evolution of water and energy demand per hectare for irrigation in Spain. Source: own elaboration from Corominas (2010) and MAPAMA (2018).

Among the pressurized irrigation systems, microirrigation is the one with less energy requirements with an average energy requirements of 0.18 kWh/m³ in comparison of 0.23 kWh/m³ for sprinkler irrigation. For instance, for treating wastewater is needed an average value of 0.5 kWh/m³ (Corominas, 2010).

Several studies have been carried out in order to reduce energy consumption in pressurized irrigation systems (Carrillo-Cobo et al., 2014; Tarjuelo et al., 2015). Different alternatives have been analyzed, including methods for sectoring irrigation networks (Jiménez-Bello et al., 2015), changes from scheduled to on-demand irrigation (Rodríguez-Díaz et al., 2009), selection of new pumping equipment (Fernández-García et al., 2014), changes in the diameter of water sprinklers (Moreno et al., 2010) or the dual use of irrigation networks delivering water and producing renewable energy beyond biofuel production (Belaud et al., 2019). For the aforementioned reasons, reducing energy consumption is a challenge as important as reducing water consumption (Hardy and Garrido, 2012). In fact, Spain is the first Mediterranean country in energy demand for irrigation, with values over 774 GWh (Daccache et al., 2014).

Some alternatives to renewable energy sources, like the use of photovoltaic panels in irrigation systems have been carried out (Senol, 2012; Carrillo-Cobo et al., 2014; Chandel et al., 2015; Reza et al., 2016; Méridia-García et al., 2019) given its environmental benefits associated (Wettstein et al., 2018). Picazo et al. (2018) studied the use of photovoltaic panels in different irrigation scheduled programmes and the costs linked to energy, highlighting the potential savings in conventional electrical energy (e.g. coal, fuel or nuclear), but concluding that investments for purchasing equipment at present make this alternative difficult.

In a microirrigation system, one of the major energy demander is filtration. Pressure demand in filtration is higher than the pressure demand in the emitters. The tendency is to use low pressure drippers, but energy consumption in filtration has not been modified substantially. In that sense, and as an example, in California emitters usually work at a pressure between 41 and 82 kPa, but the average pressure in the discharge of the pumping systems of the microirrigation areas increases to 310 kPa (Burt et al., 2011). Moreover, filter backwashing requires even higher pressures, due to backwashing is more efficient under higher pressures (Duran-Ros et al., 2009b). With these data in mind, Burt et al., (2011) realised that improvements in the filter designs should reduce pressure demand and, consequently, energy consumption. As filtration energy consumption is linked to pressure loss, reducing pressure requirements will mean savings in energy. Is for that reason that improvements in the filter design, such as the underdrain, should result in a decrease of energy demand (Bové et al., 2015b).

2. OBJECTIVES

2. OBJECTIVES

The general objective of this doctoral thesis is to determine the effect of operational conditions related to media height and filtration velocity and three different sand media filters on water quality, pressure loss across the filters, energy consumption and emitter clogging when using a reclaimed effluent.

To reach the general objective, the following specific objectives were formulated:

1. Analyze the performance of three different sand filter designs using reclaimed effluents under four different combinations of media height and velocity regarding:

- 1.1. The water quality.

- 1.2. The pressure loss, filtered volume and energy consumption.

- 1.3. The emitter clogging.

2. Analyze the field water distribution uniformity in a drip irrigation system through:

- 2.1. Comparison of different procedures for assessing water distribution uniformity.

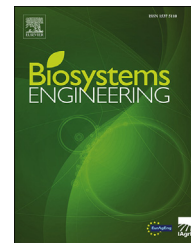
- 2.2. Development of a methodology for assessing irrigation distribution uniformity using a SCADA system.

As the experimental setup consisted of a filtration bank and irrigation subunits controlled and supervised by a SCADA system, different aspects could be studied. In the first place, at the filtration bank, the effect of three different designs and four operational conditions in water quality, head loss and energy consumption, are studied in chapter 3. Besides, the analyses of the irrigation subunits of each filtration unit allowed studying emitter clogging and its effect with the underdrain designs, are shown in chapter 4. Finally, field and SCADA data and observations allowed comparing and proposing different methods for assessing distribution uniformity, are analysed in chapter 5. Thus, each specific aspect of the experiment is collected in an independent chapter, which, put together, study the general approaches of a drip irrigation system using effluents and are discussed in chapter 6.

3. EFFECT OF THE UNDERDRAIN DESIGN, MEDIA HEIGHT AND FILTRATION VELOCITY ON THE PERFORMANCE OF MICROIRRIGATION SAND FILTERS USING RECLAIMED EFFLUENTS.

Available online at www.sciencedirect.com

ScienceDirect

journal homepage: www.elsevier.com/locate/issn/15375110

Research Paper

Effect of underdrain design, media height and filtration velocity on the performance of microirrigation sand filters using reclaimed effluents



Carles Solé-Torres, Jaume Puig-Bargués*, Miquel Duran-Ros, Gerard Arbat, Joan Pujol, Francisco Ramírez de Cartagena

Department of Chemical and Agricultural Engineering and Technology, University of Girona, Carrer Maria Aurèlia Capmany, 61, 17003, Girona, Catalonia, Spain

ARTICLE INFO

Article history:

Received 11 March 2019

Received in revised form

21 September 2019

Accepted 24 September 2019

Keywords:

Drip irrigation

Filtration efficiency

Filtered volume

Electricity consumption

Clogging

Sand filters are commonly used in microirrigation systems to prevent emitter clogging, especially when wastewater is used. However, little is known about the operating conditions required to guarantee a good filtration and a low energy consumption. For this reason, three sand filters with different drainage designs (collector arms, inserted domes and porous medium) using reclaimed effluents were analysed when operating with two sand media heights (0.20 and 0.30 m) and two filtration velocities (30 and 60 m h⁻¹). Each one of these four different operating conditions (combination of two sand media heights and filtration velocities) was tested for 250 h. Filtered and backwashed volumes, energy consumption during filtration and backwashing, inlet and outlet filter pressures, and water quality parameters at filter inlet and outlet were recorded using a supervisory control and data acquisition system. Results showed that porous media underdrain design presented higher turbidity removal efficiencies for most of the tested conditions (38.53, 33.63 and 10.51% at 0.20 m/30 m h⁻¹, 0.20 m/60 m h⁻¹ and 0.30 m/60 m h⁻¹, turbidity removal, with sand media height/filtration velocity, respectively) and dome underdrain only at 0.30 m/60 m h⁻¹ (47.74%). Porous media underdrain also filtered more water volume per electrical energy unit (8.30 m³ kWh⁻¹) than domes and arm collector underdrain (8.18 and 8.07 m³ kWh⁻¹, respectively). In general, filtration velocities of 30 m h⁻¹ showed higher turbidity removals and filtered more water volume per electrical energy unit than 60 m h⁻¹. Media height did not show a clear effect, but smaller media heights did allow energy and material saving.

© 2019 IAGrE. Published by Elsevier Ltd. All rights reserved.

* Corresponding author. Fax: +34 972 41 83 99.

E-mail address: jaume.puig@udg.edu (J. Puig-Bargués).<https://doi.org/10.1016/j.biosystemseng.2019.09.012>

1537-5110/© 2019 IAGrE. Published by Elsevier Ltd. All rights reserved.

Nomenclature

d_e	Effective diameter, mm
E	Removal efficiency, %
EE_f	Electrical energy consumption during filtration process, kWh
EE_b	Electrical energy consumption during backwashing process, kWh
F	Glass microfibre filter weight, mg
F_f	FNU Glass microfiber filter weight after water sample being filtered, mg Formazin nephelometric unit, dimensionless
N_i	Inlet turbidity or dissolved oxygen, FNU or mg l ⁻¹ respectively
N_o	Outlet turbidity or dissolved oxygen, FNU or mg l ⁻¹ respectively
R_m	Retained mass in a filtration cycle, g
SS	Suspended solids, mg l ⁻¹
SS_i	Filter inlet suspended solids, mg l ⁻¹
SS_o	Filter outlet suspended solids, mg l ⁻¹
UC_s	Uniformity coefficient, dimensionless
V	Reclaimed effluent volume sample, l
V_{eec}	Filtered volume per electrical energy consumption unit, m ³ kWh ⁻¹
V_f	Filtration volume in a filtration cycle, m ³
ρ_b	Filtration media bulk density, kg m ⁻³
ρ_r	Real filtration media density, kg m ⁻³
ε	Media porosity, dimensionless

1. Introduction

The use of reclaimed wastewater in agriculture can alleviate water scarcity (Asano, Burton, & Leverenz, 2007). The best irrigation technique for using wastewater from the points of view public health and the environment is microirrigation (World Health Organization, 2006), although it has a high risk of emitter clogging (Trooien & Hills, 2007). To prevent emitter clogging, filtration is required but it does not completely avoid it (Nakayama, Boman, & Pitts, 2007). In microirrigation systems, sand filters offer a better form of protection (Trooien & Hills, 2007) especially when reclaimed effluents are used, since they remove suspended solids efficiently (Puig-Bargués, Barragán, & Ramírez de Cartagena, 2005) and consequently reduce emitter clogging (Capra & Scicolone, 2007; Duran-Ros, Puig-Bargués, Arbat, Barragán, & Ramírez de Cartagena, 2009a). Filtration, and especially filter backwashing, requires higher pressures than the other microirrigation system components. So, filters have an important role to play in the energy consumption of drip irrigation systems (Bové et al., 2015a), which should be optimised due to the increased costs of energy resources (Tarjuelo et al., 2015). However, most of the energy consumption optimization studies have been carried out mainly at irrigation district level (e.g. Jiménez-Bello, Royuela, Manzano, García Prats, & Martínez-Alzamora, 2015; Moreno, del Castillo, Montero, Tarjuelo, & Ballesteros, 2016; Fernández García, Montesinos, Camacho Poyato, & Rodríguez Díaz, 2017; Abadía, Vera, Rocamora, & Puerto,

2018) than at farm level (Soto-García, Martín-Gorrioz, García-Bastida, Alcón, & Martínez-Álvarez, 2013).

Knowledge of the performance of sand media filter is needed for engineers and irrigation practitioners to achieve efficient design and management of their equipment. Burt, Howes, and Freeman (2011) stated that by improving sand filter design, a reduction of energy consumption and an increase of filtration efficiency can be achieved. In addition, sand filter design coupled with emitter location and irrigation time has an effect on emitter clogging (Solé-Torres et al., 2019). In sand media filters pressure loss due to filter design is mainly located in auxiliary elements such as diffuser plate and underdrain, and different configurations of these elements affect pressure drop (Arbat et al., 2011; Mesquita, Testezlaf, & Ramirez, 2012; Mesquita, de Deus, Testezlaf, da Rosa, & Diotto, 2019b). So far, several studies have quantified head loss across the whole filter with dimensional analyses (Duran-Ros, Arbat, Barragán, Ramírez de Cartagena, 2010; Elbana, Ramírez de Cartagena, & Puig-Bargués, 2013) and others have experimentally determined the head loss across sand filters (Arbat et al., 2011). The effect of different underdrain designs on pressure loss has also been widely studied (Bové et al., 2015a; Mesquita et al., 2012; Pujol et al., 2016).

Although the use of sand filters is common in micro-irrigation systems, little is known about what suitable operating conditions are required to ensure good filtration and low energy consumption. Several studies have focused on the influence of different media bed materials and their physical characteristics in filtration process. Silica sand is the most common used material (Nakayama et al., 2007) and the finer the sand the higher the efficiency of the filtration process (Mesquita, de Deus, Testezlaf, & Diotto, 2019a; Wu, Huang, Liu, Yin, & Niu, 2015). For the characterisation of the sand media particles, sand effective diameter (d_e , which is the size opening which will pass 10% by dry weight of a representative sample of the media material) and uniformity coefficient (UC_s , ratio of the size opening which will pass 60% of the sand to the size opening which will pass 10%) are usually used. Nakhla and Farooq (2003) found turbidity removal efficiencies of 33–56% when using d_e of 0.50 mm and 40–62% with d_e of 0.30 mm at turbidity inlet values of 0.20–0.95 FNU, while Duran-Ros et al. (2009a), using effluents with inlet turbidity of 6.76 and 4.08 FNU found removal efficiencies of 57 and 66% when using sand with d_e of 0.40 and 0.27 mm, respectively. Recently, other materials such as crushed recycled glass have been used as media bed (Bové et al., 2015b) although this has still not been widely studied. Nevertheless, although several studies have related the physical characteristics of the media bed and filtration velocities with solid removal characteristics (Mesquita et al., 2019a), there is a lack of information about how media bed height and filtration velocity influence both together filtration performance. Moreover, reducing the media height bed has a positive impact on the environmental costs (Bové et al., 2018).

The objective of this paper is to analyse the effects that operational filtration conditions such as media height and filtration velocity and three different sand filter underdrains (the prototype designed by Bové et al. (2017) and two commercial designs) have on the filtration quality, as well as water and energy consumption.

2. Material and methods

2.1. Experimental setup

The reclaimed effluent used in the experiment came from the wastewater treatment plant (WWTP) of Celrà (Girona, Spain), which treats urban and industrial effluents using an activated sludge process.

In the experimental irrigation system, three different sand filters were used (Fig. 1). The first one (Fig. 1A) was the experimental sand filter built with an underdrain designed by Bové et al. (2017), which consisted of a cylinder that occupied the entire surface of filtration of the filter. This cylinder was confined by two 0.75 mm meshes, one at the top and one at the bottom, and was filled with silica sand sieved to 0.75–0.85 mm grain size, with an equivalent diameter of 0.92 mm, bulk density of 1.508 kg m^{-3} , real density of 2.510 kg m^{-3} and a porosity of 40%. The second one (Fig. 1B) was the sand filter model FA-F2-188 (Regaber, Parets del Vallès, Spain), whose underdrain consisted of 12 pyramidal shaped domes mounted on a manifold and inserted in a back plate. The third one (Fig. 1C) was a sand filter model FA1M (Lama, Sevilla, Spain), whose underdrain consisted of 7 pieces with slots that overlapped each other by forming striated tubes converging in a central tube which worked as a manifold, with a total of 10 striated tubes, 5 tubes on each side of the manifold. Table 1 shows the main characteristics of the different sand filters used.

The sand used as a media bed was silica sand CA-07MS (Sibelco Minerales SA, Bilbao, Spain) with an effective diameter (d_e) of 0.48 mm, a uniformity coefficient (UC_s) of 1.73, real density (ρ_r) of 2454 kg m^{-3} , bulk density (ρ_b) of 1509 kg m^{-3} , and a porosity (ϵ) of 0.39. All these parameters were determined experimentally following the methods described by Bové et al. (2015b).

A multicellular centrifugal pump model CR-15-4 (Grundfos, Bjerringbro, Denmark) governed by a variable frequency drive model FRN-4 (Fuji Electric, Cerdanyola del Vallès, Spain) pumped the reclaimed effluent from the WWTP to the filters, with only one filter operating at a time. The inlet flow was measured with an electromagnetic flowmeter Isomag MS2500 (ISOIL Industria SpA, Cinisello Balsamo, Italy). After being filtered, the reclaimed effluent was conveyed to a drip irrigation subunit. Since the filtrated flow was higher than that needed for the irrigation subunit, a proportional electrohydraulic actuator SKD32 (Siemens, Munich, Germany) operated a three-way valve VXG41 (Siemens, Munich, Germany), so that

Table 1 – Underdrain design and main operation characteristics of the different filters used in the experiment. Data was obtained from manufacturers.

Characteristic	Filter underdrain design		
	Porous media	Domes	Collector arms
Filter nominal diameter (mm)	500	508	500
Filter filtration surface (m^2)	0.1960	0.2026	0.1960
Maximum filtration flow ($\text{m}^3 \text{ h}^{-1}$)	20	18	23
Maximum filtration height (m)	0.70	0.69	0.40
Number of underdrains	1	12	10
Mean slot width (m)	–	4.5×10^{-4}	2.5×10^{-4}
Number of slots by underdrain	–	90	140
Underdrain opening area per underdrain unit (m^2)	7.44×10^{-2}	6.26×10^{-4}	9.11×10^{-4}
Underdrain total opening area (m^2)	0.0744	0.0075	0.0091
Underdrain effective area (ratio of underdrain opening area to filter surface area, %)	37.95	3.71	4.65

the excess flow was brought to a water storage tank of 3000 l Aquablock (Shütz, Selters, Germany) that was used for filter backwashing. All these devices were connected to a supervisory control and data acquisition (SCADA) system previously developed (Duran-Ros, Puig-Bargués, Arbat, Barragán, Ramírez de Cartagena, 2008), which allowed filter scheduling and filter performance data recording every minute.

The parameters measured before filtration were electrical conductivity, using a transmitter LIQUISYS-M CLM253-CD0010 and a sensor CLS21-C1E4A and pH and the temperature, using a transmitter LIQUISYS-M CPM253-MR0010 and a sensor CPS11D-7BA21. The parameters measured before and after filtration were turbidity, using a transmitter LIQUISYS-M CUM253-TU0005 and a sensor CUS31-A2E, and dissolved oxygen using a transmitter LIQUISYS-M COM253-WX0015 and a sensor COS 61-A1F0. All the transmitters and sensors used were made by Endress + Hauser (Gerlingen, Germany). These effluent quality parameters were also recorded every minute by the SCADA system.



Fig. 1 – Different underdrain designs: porous media (A), inserted domes (B) and arm collector (C).

The system had a 200 l deposit of chlorine, which continuously injected chlorine to achieve a concentration of 2 mg l^{-1} into the water after being filtered, using a DosTec AC1/2 membrane pump (ITC, Sta. Perpètua de Mogoda, Spain). When sand filters were backwashed, backwashing water entering the filters was chlorinated to reach a 4 mg l^{-1} chlorine concentration.

Two pressure transducers model TM-01/C (STEP, Barcelona, Spain) measured the pressure at the inlet and outlet of the filter. Filters were automatically backwashed when the total pressure drop across them measured by pressure transducers reached 50 kPa. The backwashing time was 3 min throughout the entire test, and during that time, backwashing water did not reach the irrigation subunit. The backwashing flow was maintained at $3 \text{ m}^3 \text{ h}^{-1}$ more than the nominal filtration flow. The water used for the backwashing, came from the filtered water storage tank (Fig. 2).

2.2. Operational procedure

The experiment lasted 1000 h for each filter, taking place between March and November 2018, except during the month of June where the installation was out of operation to a failure in the turbidity sensors. Whenever possible, six daily irrigation sessions of 4 h each (i.e. two daily sessions of 4 h per filter)

were carried out. In practice, it was attempted to establish irrigation sessions as homogeneous as possible, which was not always possible due to minor failures that prevented the use of a filter for a certain period of time. After these failures were resolved, the operation time of the affected filter was increased to equalise the hours of operation.

Two different filter media heights (0.20 and 0.30 m) and two different filtration velocities (30 and 60 m h^{-1}) for each height were tested, thus each filter ran under four different operating conditions. Media heights were conditioned by the lower height of arm collector filter (0.40 m, Table 1) and the need to carry out the experiment under the same experimental conditions for each filter. So, a maximum and minimum media heights of 0.30 and 0.20 were selected, respectively. Filtration velocities higher than 60 m h^{-1} can cause excessive movement of the sand surface bed (Mesquita et al., 2012) and is usually the maximum filtration velocity recommended for sand media filters used in microirrigation systems (Pizarro, 1996). Thus, 60 m h^{-1} and its half (30 m h^{-1}) were chosen for this study. Each operating condition was the same for each filter, being tested for 250 h each one. Media sand was changed after each operational condition was tested. Filters were backwashed three times at the beginning of the experiment and after every change of the sand media to get rid of the finest particles. The nominal working flow for reaching the

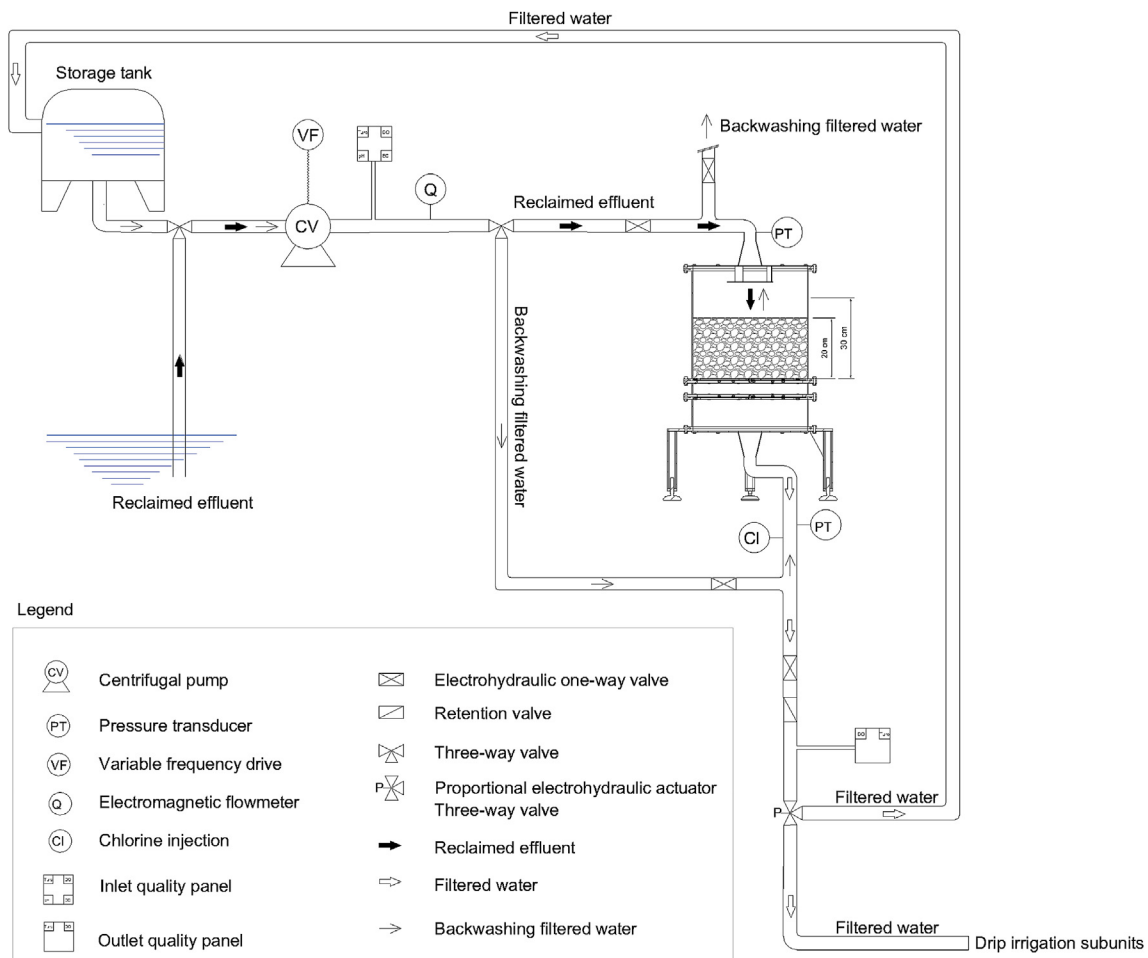


Fig. 2 – Diagram of the experimental system. For simplicity, only one of the three filters is depicted.

filtration velocities of 30 and 60 m h⁻¹ was 6 and 12 m³ h⁻¹, respectively, and for backwashing process 9 and 15 m³ h⁻¹, respectively, controlled by the electromagnetic flowmeter which governed the pump throughout the SCADA. A turbidity inlet alarm was set, with a value of 20 FNU so the system stopped every time the effluent reached this value to prevent valve and installation clogging.

During the experiment, suspended solids (SS) were determined. By doing so, several effluent samples of 1 l were taken, at both filter inlet and outlet, and the turbidity values measured by the sensor noted. The determination of suspended solids of the reclaimed effluent was carried out in the laboratory. Firstly, glass microfibre filters (Ahlstrom, Helsinki, Finland) of 47 mm diameter and 1.2 µm porous size were dried in a natural convection heater Digiteat 190L (Selecta, Abrera, Spain) at 105 °C for 12 h, and after that, the microfibre filters were cooled down in a polycarbonate desiccator (Nalgene, Rochester, NY, USA) with silica gel for 2 h. Once dried and at room temperature, filters were weighed with a scale HM-200 (A&D Instruments Ltd., Tokyo, Japan) with a precision of ±0.01 mg. The next step was to measure 500 ml of the sample with a 500 ml tube, and the glass microfibre filter was placed with the smooth side down in the funnel of the filtration system. The filtration system used was a Magnetic Filter Funnel (Pall Corporation, East Hills, NY, USA) that consisted of a funnel with a capacity of 300 ml and a filter magnetically united. As the sample was 500 ml, it was filtered twice with a vacuum pump SV 1004B (Busch, Maulburg, Germany). Once the sample was filtered, the glass microfibre filters were dried in the heater for 2 h at 105 °C, then cooled down in the desiccator for 2 h and weighed. If the dry residue was not between the values of 5–50 mg, the whole procedure was repeated increasing or decreasing the volume of the sample. Suspended solids were calculated as:

$$SS = \frac{F_f - F}{V} \quad (1)$$

where SS are the suspended solids (mg l⁻¹), F is the glass microfibre weight before being filtered (mg), F_f is the glass microfibre filter weight after being filtered (mg) and V is the volume of the sample (l).

Turbidity and suspended solids were statistically adjusted and it was found that turbidity variability was responsible for 93.02% of suspended solids variability. Residual plots had no structure, which reflected the goodness of the adjustment. The equation that related suspended solids from turbidity with a regression coefficient $R^2 = 0.93$ and $p < 0.01$ was:

$$SS = 1.5332 \times \text{Turbidity} \quad (2)$$

where SS are the suspended solids (mg l⁻¹), and turbidity is expressed in FNU.

On the other hand, the amount of retained mass for each filtration cycle was calculated as:

$$R_m = (SS_i - SS_o) \times V_f \quad (3)$$

where R_m is the retained mass in a filtration cycle (g), SS_i and SS_o are the suspended solids at filter inlet and outlet (mg l⁻¹) during a filtration cycle, and V_f the filtered volume in a filtration cycle (m³).

2.3. Characterisation of inlet reclaimed effluent

The main inlet reclaimed effluent quality parameters for each filter were recorded every minute, as was explained in Section 2.1. Since the filters did not operate simultaneously, it was necessary to assess if effluent characteristics were different during the experiment. Table 2 presents the mean values of the electrical conductivity, dissolved oxygen, pH, temperature, and turbidity values recorded through the 250 h the experiment lasted for each operating condition.

No significant differences ($p > 0.05$) were found in inlet water quality in any parameter for the three different filter underdrain designs under 0.20 m/30 m h⁻¹ and 0.30 m/60 m h⁻¹ conditions, except for temperature under 0.30 m/60 m h⁻¹, where the filter with porous media underdrain worked at significantly higher temperatures (21.46 °C) than the arm collector underdrain filter (19.37 °C). For 0.30 m/30 m h⁻¹, there were also no differences in temperature.

Under 0.20 m/60 m h⁻¹, water electrical conductivity inlet values were significantly ($p < 0.05$) lower for the domes underdrain filter (2.18 dS m⁻¹) than for porous media and arm collector underdrain filters (2.79 and 2.54 dS m⁻¹, respectively); dissolved oxygen values for the domes underdrain were significantly higher (4.27 mg l⁻¹) than with porous media underdrain (3.44 mg l⁻¹) but not than arm collector underdrain (3.93 mg l⁻¹); pH for domes underdrain filter (7.71) was significantly different from the other two filters, and pH for arm collector filter was also significantly different (7.52) from the porous media underdrain filter (7.29). Water temperature for domes and arm collector underdrain filters were significantly higher (24.01 and 25.02 °C, respectively) than that used with porous media underdrain filter (21.03 °C), but turbidity values were significantly lower in these two filters (2.84 and 3.50 FNU, respectively) than for the porous media underdrain filter (5.82 FNU).

With 0.30 m/30 m h⁻¹, water electrical conductivity inlet values were significantly ($p < 0.05$) lower for the experiments carried out with the porous media underdrain filter (1.85 dS m⁻¹) than those with domes and arm collector underdrain filters (2.35 and 2.66 dS m⁻¹, respectively). No differences were found in dissolved oxygen values between porous media and domes underdrains and domes and arm collector underdrains, although porous media had significantly higher values (3.37 mg l⁻¹) than arm collector underdrain (1.97 mg l⁻¹); pH was significantly higher for porous media underdrain (7.71) than with the other two designs. Finally, no significant differences were found among turbidity levels between porous media underdrain and arm collector underdrain, and between arm collector and domes underdrain, but turbidity levels were significantly higher for domes underdrain (7.35 FNU) than for porous media underdrain (4.07 FNU).

Overall, inlet water quality displayed no significant differences when operated at 0.20 m/30 m h⁻¹ and 0.30 m/60 m h⁻¹, but there were different mean groupings for the different monitored quality parameters. This was due to the usual variability found in the composition of reclaimed effluents (Puig-Bargués et al., 2005).

Table 2 – Average \pm standard error of the effluent physical and chemical parameters at filter inlets. Different letters mean that there were significant differences ($p < 0.05$) in the values of each parameter at the different filter inlets.

Media height (m)	Filtration velocity (m h^{-1})	Underdrain design	Electrical conductivity (dS m^{-1})	Dissolved oxygen (mg l^{-1})	pH (–)	Temperature ($^{\circ}\text{C}$)	Turbidity (FNU)
0.20	30	Porous media	2.68 ± 1.24 abc	2.69 ± 0.15 def	7.04 ± 0.02 f	15.29 ± 0.51 g	8.16 ± 0.36 ab
		Domes	2.90 ± 0.79 a	3.07 ± 0.11 cde	7.10 ± 0.02 f	15.31 ± 0.31 g	7.49 ± 0.36 abc
		Arm collector	2.89 ± 0.57 a	2.89 ± 0.09 def	7.07 ± 0.02 f	16.35 ± 0.28 g	8.51 ± 0.42 a
0.20	60	Porous media	2.79 ± 0.40 ab	3.44 ± 0.08 bcd	7.29 ± 0.02 e	21.03 ± 0.40 def	5.82 ± 0.21 cd
		Domes	2.18 ± 0.71 de	4.27 ± 0.11 a	7.71 ± 0.02 a	24.01 ± 0.21 ab	2.84 ± 0.17 e
		Arm collector	2.54 ± 0.29 bc	3.93 ± 0.16 ab	7.52 ± 0.02 b	25.02 ± 0.11 a	3.50 ± 0.30 e
0.30	30	Porous media	1.85 ± 1.49 e	3.37 ± 0.28 bcde	7.71 ± 0.05 a	22.50 ± 0.25 bcd	4.07 ± 1.04 de
		Domes	2.35 ± 0.62 cd	2.66 ± 0.20 ef	7.51 ± 0.02 bc	23.17 ± 0.11 b	7.35 ± 0.91 abc
		Arm collector	2.66 ± 0.42 abc	1.97 ± 0.14 f	7.42 ± 0.01 cd	23.11 ± 0.08 bc	5.91 ± 0.31 cd
0.30	60	Porous media	2.58 ± 0.48 abc	3.23 ± 0.12 bcde	7.39 ± 0.01 de	21.46 ± 0.22 cde	6.29 ± 0.23 bc
		Domes	2.38 ± 0.41 cd	3.45 ± 0.13 bcd	7.44 ± 0.01 bcd	20.04 ± 0.17 ef	5.77 ± 0.17 cd
		Arm collector	2.43 ± 0.49 cd	3.79 ± 0.10 abc	7.38 ± 0.01 de	19.37 ± 0.27 f	5.98 ± 0.24 cd

2.4. Data treatment and statistical analyses

Filter run time, filtration and backwashing flow, filtration and water backwashing volume, filter pressure at filter inlet and outlet, inlet and outlet reclaimed effluent parameters, filtration and backwashing energy consumption and chlorine injection were recorded every minute by a SCADA system previously developed (Duran-Ros, Puig-Bargués, Arbat, Barragán, & Ramírez de Cartagena, 2008) that was then adapted to this experiment.

Filter performance for removing turbidity and dissolved oxygen was assessed through the removal efficiency (E) achieved in the filters, which was calculated as:

$$E = \frac{N_i - N_o}{N_i} \times 100 \quad (4)$$

where N_i and N_o are the values of turbidity and dissolved oxygen at filter inlet and outlet, respectively.

The volume filtered per electrical energy consumption unit, V_{eec} ($\text{m}^3 \text{ kW h}^{-1}$), was calculated as:

$$V_{\text{eec}} = \frac{V_f}{EE_f + EE_b} \quad (5)$$

where V_f is the filtered volume in a filtration cycle (m^3), and EE_f and EE_b were the electrical energy consumed during a filtration cycle and its backwashing, respectively (kWh).

The time elapsed for a filtration cycle started from the end of a backwashing to the beginning of the following backwashing, if the filter operated in filtration mode between these backwashes. Not all the filtration cycles were taken into account for data treatment. Specifically, those cycles were discarded which did not reach a 50 kPa head loss or those for which some recorded data were not valid for the whole cycle (e.g. due to maintenance, calibrating processes, scaled down sensors, lower nominal filtration flow or forced backwashing issues). Cycles with inefficient backwashing were also not computed for statistical treatment, as they cannot release most of the particles retained (Duran-Ros, Puig-Bargués, Arbat, Barragán, & Ramírez de Cartagena, 2009b) and tend to accumulate aggregates of the suspended matter, which has a negative impact on filtrate turbidity and on filter run time

(Cleasby, 1990). Inefficient backwashes were identified as those with head loss thresholds across the filter greater than 40 kPa after being backwashed. The total number of valid cycles, their total experimental time and the average cycle duration are shown in Table 3.

Statistical analyses were carried out using SPSS Statistics 25 software (IBM, New York, USA). For each parameter, the model that was used included as fixed effects the filter underdrain design, media height and filtration velocity. As the inlet reclaimed effluent parameters were not homogeneous (Table 2), inlet turbidity was taken as a covariate in the model when it was significant, as oxygen was taken dissolved as a covariate in the statistical treatment of dissolved oxygen removal. To differentiate the averages that were significantly different with a probability of 0.05 or less, Tukey's pairwise comparison test was used.

3. Results and discussion

3.1. Volume and energy consumption characterization

Table 4 shows the average volumes, electrical energy consumption and retained mass per cycle.

Volumes and electrical energy consumptions depended on operational conditions. Conversely to 0.30 m height, filtered volumes were higher at 60 m h^{-1} with 0.20 m. On average, with 0.30 $\text{m}/60 \text{ m h}^{-1}$ there were more filtration cycles but they were shorter (Table 3). The lowest filtered volume and electricity consumption were with 0.20 $\text{m}/30 \text{ m h}^{-1}$. Backwashing volumes and their electrical energy consumed were higher at 60 m h^{-1} than at 30 m h^{-1} , as backwashed nominal flow was higher (Section 2.2), but no significant differences were observed during backwashing periods within the same filtration velocity. In general, more volume was filtered per energy unit at media heights of 0.20 m ($8.35\text{--}8.70 \text{ m}^3 \text{ kWh}^{-1}$) than at 0.30 m ($7.67\text{--}8.22 \text{ m}^3 \text{ kWh}^{-1}$), except for porous media underdrain design at 30 m h^{-1} , which filtered $8.50 \text{ m}^3 \text{ kWh}^{-1}$. Overall, porous media underdrain presented the highest values of filtered volume per total electrical energy consumption, with the only exception of 0.20 $\text{m}/60 \text{ m h}^{-1}$.

Table 3 – Number of valid cycles and total experimental duration of the different operational condition for each filter and the average \pm standard error of the cycle durations.

Media height (m)	Filtration velocity (m h ⁻¹)	Underdrain design	Number of valid cycles	Total duration (h)	Average cycle duration (min)
0.20	30	Porous media	21	94.58	270.24 \pm 35.81
		Domes	55	206.50	229.44 \pm 29.81
		Arm collector	64	241.80	226.69 \pm 31.50
0.20	60	Porous media	77	222.45	180.36 \pm 15.34
		Domes	42	192.28	274.69 \pm 25.83
		Arm collector	29	126.12	260.93 \pm 39.70
0.30	30	Porous media	10	172.45	1034.70 \pm 222.18
		Domes	36	236.30	393.83 \pm 48.02
		Arm collector	35	212.58	364.43 \pm 38.25
0.30	60	Porous media	75	209.47	167.57 \pm 12.77
		Domes	111	226.47	122.41 \pm 6.99
		Arm collector	84	236.63	169.02 \pm 8.05

Average values obtained were higher than those (5.26–6.25 m³ kWh⁻¹) found by [Soto-García et al. \(2013\)](#) at farm level (i.e. with higher crop area) in south-eastern Spain. Finally, filter with porous media underdrain retained more mass per cycle than the other two filters in all conditions, except for 0.30 m/30 m h⁻¹, when a mass release was observed. In this case, low inlet turbidity values (4.07 FNU) may explain the poor performance of porous media underdrain. Altogether, under the same media heights, lower filtration velocities retained more mass.

3.2. Effect of underdrain design and operational conditions on effluent quality

Dissolved oxygen and turbidity removal efficiencies were calculated using Eq. (4), and retained mass using Eq. (3), and their values were statistically treated as was explained in Section 2.4. Table 5 shows the significance level of the model, fixed factors (underdrain design, media height and filtration velocity) and their interactions. Each interaction will be analysed and discussed in the following sub-sections.

3.2.1. Dissolved oxygen removal

For the dissolved oxygen (DO) removal efficiency, there was a significant effect ($p < 0.01$) on the underdrain design, with the domes design being the one which increased DO (26.75%) more than porous media and arm collector (11.20 and 11.03%, respectively). Media height of 0.30 m also increased significantly DO at filter outlet (28.33%) than 0.20 m (4.30%). In addition, filtration velocity of 30 m h⁻¹ increased more DO (21.53%) than 60 m h⁻¹ (15.06%).

Only the interaction between underdrain design and filtration velocity was significant ($p < 0.05$) for DO removal (Fig. 3). Although under a velocity of 30 m h⁻¹ there were no significant differences among underdrains, the arm collector design presented higher DO increases (28.01%) followed by the domes (18.21%) and porous media (11.08%) underdrains. Conversely, at 60 m h⁻¹ the DO increase at filter outlet was significantly higher for the domes (31.10%) than for porous media (11.22%) and arm collector (-3.52%). For the porous media and domes, there was a significant effect ($p < 0.05$) of velocities, with a higher DO increment at 60 m h⁻¹. On the

contrary, although it was not significant, there was a 112.56% decrease for DO removal efficiency when increasing the velocity from 30 up to 60 m h⁻¹ with the arm collector filter. DO removals were higher than those observed by [Duran-Ros et al. \(2009a\)](#) (0.49% for 2.80 mg l⁻¹ inlet DO and d_e of 0.40 mm) and [Elbana, Ramírez de Cartagena, and Puig-Bargués \(2012\)](#) (3.75% for 4.00 mg l⁻¹ inlet DO and d_e of 0.48 mm), which were obtained in experiments without any chlorination treatment. The main reason for this DO increase was related to chlorination of backwashing water which reduced microbial population ([Li, Chen, Li, Yin, & Zhang, 2010](#)) that consumes oxygen. Greater DO increases observed at higher filtration velocities can be attributed to more frequent backwashing ([Elbana et al., 2012](#)) as cycles were shorter (Table 3). The higher backwashing flow used at 60 m h⁻¹ (see Section 2.2), should increase chlorine contact with sand media, reducing microbial population and thus increasing DO. However, performance of arm collector underdrain filter did not follow this pattern as it had fewer backwashing cycles at 60 m h⁻¹ (113 vs. 152 of porous media underdrain and 153 of domes underdrain).

3.2.2. Turbidity removal and retained mass

For turbidity removal efficiency, there was a significant effect ($p < 0.05$) of the underdrain design, having the porous media the highest removal (26.28%) followed by domes and arm collector (18.53 and 13.45%, respectively). Filtration velocity was also significant, with higher values at 30 m h⁻¹ (34.17%) than at 60 m h⁻¹ (11.27%).

The triple interaction of underdrain design, media height and filtration velocity was significant ($p < 0.05$). Thus, interactions between media height and filtration velocity were studied among each underdrain design (Fig. 4). For the porous media, a velocity of 60 m h⁻¹ significantly ($p < 0.05$) reduced less turbidity than 30 m h⁻¹ for both media heights of 0.20 m (33.63 vs. 38.53%) and 0.30 m (14.82 vs. 39.19%). However, turbidity removals were significantly greater with 0.30 m at 30 m h⁻¹ and with 0.20 m at 60 m h⁻¹. With this last velocity, differences in turbidity removal were more pronounced (33.63% with 0.20 m versus 14.82% with 0.30 m).

For the dome underdrain, with a porous media height of 0.20 m, 30 m h⁻¹ showed higher turbidity removals (31.91%) than with 60 m h⁻¹ (1.04%), although they were not significant

Table 4 – Average ± standard error values of the main volume, energy consumption and mass retention for each experimental condition.

Media height	Filtration velocity	Underdrain design	Filtered volume per filtration cycle	Backwashing volume per filtration cycle	Backwashing per total volume ratio	Electrical consumption per filtration cycle	Electrical consumption per backwashing cycle	Backwashing energy consumption ratio	Filtered volume per total electrical consumption	Retained mass per cycle
(m)	(m h ⁻¹)		(m ³)	(m ³)	(%)	(kWh)	(kWh)	(%)	(m ³ kWh h ⁻¹)	(g)
0.20	30	Porous media	31.04 ± 4.84	0.45 ± 0.003	1.76 ± 0.27	3.14 ± 0.41	0.02 ± 0.001	0.78 ± 0.11	8.70 ± 0.04	180.70 ± 39.97
		Domes	17.51 ± 1.64	0.45 ± 0.003	3.21 ± 0.35	2.07 ± 0.19	0.02 ± 0.001	1.12 ± 0.12	8.35 ± 0.10	88.97 ± 18.85
		Arm collector	15.73 ± 1.02	0.46 ± 0.002	3.54 ± 0.29	1.84 ± 0.12	0.02 ± 0.001	1.17 ± 0.12	8.48 ± 0.03	98.67 ± 13.35
0.20	60	Porous media	36.43 ± 3.30	0.77 ± 0.003	5.14 ± 1.17	4.18 ± 0.39	0.04 ± 0.001	2.94 ± 0.94	8.51 ± 0.10	119.46 ± 17.35
		Domes	54.19 ± 5.26	0.77 ± 0.007	2.37 ± 0.39	6.17 ± 0.60	0.04 ± 0.001	0.96 ± 0.15	8.70 ± 0.07	17.89 ± 12.10
		Arm collector	55.45 ± 8.50	0.77 ± 0.005	3.72 ± 0.71	6.51 ± 1.01	0.04 ± 0.001	2.01 ± 0.43	8.56 ± 0.05	-42.36 ± 13.93
0.30	30	Porous media	92.12 ± 21.53	0.45 ± 0.002	1.76 ± 1.18	10.76 ± 2.50	0.01 ± 0.002	0.40 ± 0.24	8.50 ± 0.05	-60.17 ± 167.60
		Domes	39.82 ± 4.89	0.45 ± 0.002	2.60 ± 0.53	4.81 ± 0.59	0.02 ± 0.001	0.90 ± 0.20	8.22 ± 0.04	142.28 ± 20.41
		Arm collector	37.14 ± 3.95	0.46 ± 0.002	2.23 ± 0.46	4.59 ± 0.49	0.02 ± 0.001	0.85 ± 0.21	8.11 ± 0.13	59.39 ± 13.60
0.30	60	Porous media	33.10 ± 2.57	0.68 ± 0.017	2.97 ± 0.27	4.08 ± 0.32	0.04 ± 0.001	1.40 ± 0.10	8.01 ± 0.10	50.58 ± 8.06
		Domes	24.22 ± 1.40	0.75 ± 0.008	4.14 ± 0.23	3.00 ± 0.17	0.05 ± 0.001	2.15 ± 0.13	7.94 ± 0.04	24.09 ± 4.70
		Arm collector	33.66 ± 1.60	0.76 ± 0.006	2.76 ± 0.17	4.38 ± 0.21	0.04 ± 0.001	1.27 ± 0.08	7.67 ± 0.06	19.72 ± 7.75

Table 5 – Significance level (p-value) of the statistical model and of each factor and interaction for explaining dissolved oxygen and turbidity removal efficiencies and retained mass during the experiment.

	Removal efficiency (%)		Retained mass per cycle (g)
	Dissolved oxygen	Turbidity	
Model	<0.001	<0.001	<0.001
Underdrain design	<0.010	<0.001	<0.001
Media height	<0.010	n.s	<0.001
Filtration velocity	<0.001	<0.001	n.s
Underdrain design x media height	n.s	<0.010	<0.001
Media height x filtration velocity	n.s	<0.001	n.s
Underdrain design x filtration velocity	<0.050	n.s	n.s
Underdrain design x media height x filtration velocity	n.s	<0.001	<0.010
Inlet dissolved oxygen	<0.001	–	–
Inlet turbidity	–	<0.001	<0.001

n.s.: no significant (p > 0.050); -: not included in the model.

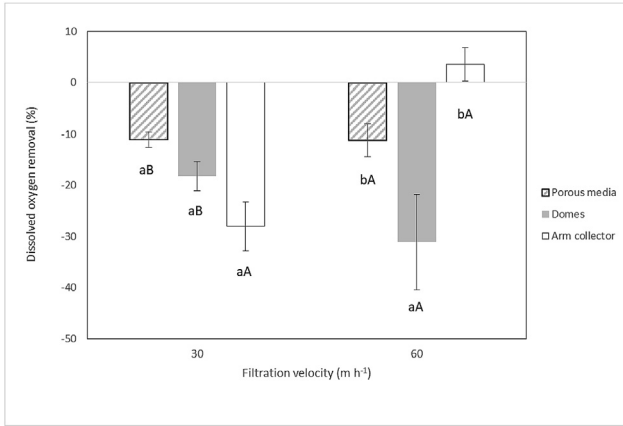


Fig. 3 – Dissolved oxygen removal efficiency and standard error bars (%) for the different underdrain designs at the two filtration velocities. For each filtration velocity, different small letters mean significant differences ($p < 0.05$) among underdrain designs. For each underdrain design, capital letters mean significant differences ($p < 0.05$) between filtration velocities.

due to the high dispersion of inlet turbidity values used as a covariate. With a media height of 0.30 m, 30 m h⁻¹ also achieved significant higher turbidity removals (47.74%) than at 60 m h⁻¹ (10.51%). On the other hand, the 0.30 m media height removed turbidity significantly greater than 0.20 m for both 30 m h⁻¹ (47.74 vs. 31.91%) and 60 m h⁻¹ (10.51 vs. 1.04%).

A significant ($p < 0.05$) interaction between media height and filtration velocity was also observed for the arm collector design. With both 0.20 and 0.3 m, 30 m h⁻¹ had significant higher turbidity removals (35.89% and 16.04%) than with 60 m h⁻¹ (-9.93% and 3.30%). Media height effect was also significant between filtration velocities. With 30 m h⁻¹, 0.20 m height showed significantly higher turbidity removals (35.89%)

than with 0.30 m (16.04%) but, conversely, with 60 m h⁻¹, only the 0.30 m media height removed turbidity (3.30%).

Overall, porous media design presented higher turbidity removals than the other two underdrains in all the operative conditions tested, except for a 0.30 m/30 m h⁻¹, for which the dome underdrain achieved higher removals (47.74% vs. 39.19%). For all the designs, higher filtration velocities (60 m h⁻¹) presented less turbidity removals. However, there was not a clear pattern in media height variations.

Higher solid removals were observed at higher velocities when more loaded water was used (De Deus, Testezlaf, & Mesquita, 2016; Mesquita et al., 2019a). Moreover, at high filtration velocities, solid removal tend to happen in the first filtration layers, with the media height not being as important as filtration velocity. However, at lower filtration rates, this tendency is not so clear (De Deus et al., 2016), as our results also have shown.

Underdrain design also affects backwashing cleaning process as underdrains are essential to guarantee an homogeneous particle removal and reduced head loss during backwashing (Mesquita, 2014). The analysis of backwashing flow depending on the design was not studied in the present paper, but further research is warranted since it is a key factor in filter performance.

The small inlet levels of turbidity of the reclaimed effluent and the small media height bed used in the filters may also explain the small turbidity removals obtained. The media height bed used in the present experiment (see Section 2.2) was between 40 and 60% lower than the heights used by Duran-Ros et al. (2009a) and Elbana et al. (2012). These authors, with similar effluents to those of the present experiment, observed turbidity removals that ranged 57–66%, using sands with d_e of 0.27–0.40 mm and UC_s of 1.81–2.89 and inlet turbidity of 4.08–10.80 FNU. Wu et al. (2015) used similar grain sand sizes obtaining total suspended solid removal efficiencies of 34 and 48% with d_e of 0.45 and 0.41 mm and UC_s of 2.04 and 1.95, respectively. On the other hand, Tripathi,

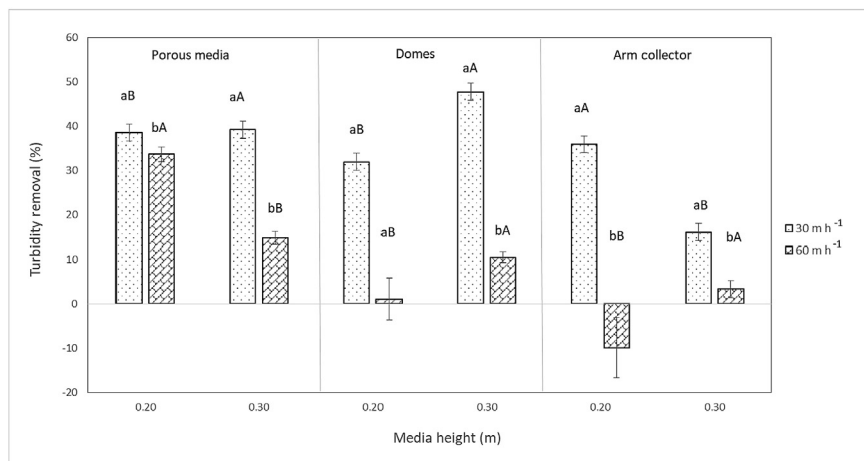


Fig. 4 – Interactions between media height and filtration velocity for each underdrain design in turbidity removal efficiency (%). For each media height and underdrain design, small letters mean significant differences ($p < 0.05$) between filtration velocities. For each filtration velocity and underdrain design, different capital letters mean significant differences ($p < 0.05$) between media heights.

Rajput, and Patel (2014) obtained turbidity reductions of 51% using effluents with inlet 55 FNU. However, in neither of the two other papers were details of the sand filter design and media heights provided.

For the calculated retained mass per cycle (Table 5) there was a significant effect ($p < 0.001$) of the underdrain and media height, being the porous media the design which retained more mass ($81.78 \text{ g cycle}^{-1}$), followed by the dome ($50.11 \text{ g cycle}^{-1}$) and arm collector ($39.38 \text{ g cycle}^{-1}$). In addition, the height of 0.20 m retained greater mass ($78.67 \text{ g cycle}^{-1}$) than 0.30 m ($41.47 \text{ g cycle}^{-1}$) ($p < 0.05$). The triple interaction of underdrain, media height and filtration velocity was also significant and followed the same pattern as in turbidity removal explained above, as total suspended solid is highly correlated with turbidity (Eq. (2)). The effect of underdrain design on retained mass has been previously reported by Burt (2010), who, conversely to our results, found that an arm collector underdrain, which was different from that used in the present study, retained more mass than a screen-domes underdrain. These results highlight the importance of filter design on its performance.

3.3. Effect of filter and operational conditions on water and energy consumption

Filtered volume and filtered water volume per electrical energy consumption unit were also statistically analysed (Table 6). In the following sub-sections, significant interactions for each parameter will be discussed.

3.3.1. Filtered volume per filtration cycle

There was a significant effect ($p < 0.001$) of underdrain and media height on the filtered volume. On average, porous media filtered more volume per cycle (38.41 m^3), followed by the arm collector (33.69 m^3) and dome (31.73 m^3); while with

0.20 m more effluent was filtered (36.42 m^3) than under 0.30 m (32.97 m^3). Double interactions between underdrain and media height, media height and filtration velocity, and underdrain design and filtration velocity were all significant (Table 6).

With a height of 0.20 m, no significant differences among underdrains were found (Fig. 5), but at 0.30 m, the porous media underdrain filtered significantly more ($p < 0.05$) volume (39.35 m^3) than the dome (28.01 m^3), but without significant differences with the arm collector (34.61 m^3). However, for each filter there were no significant differences in filtered volume between both media heights.

The height of 0.20 m (Fig. 6) yielded more filtered volume ($p < 0.05$) at 60 m h^{-1} (49.23 m^3) than at 30 m h^{-1} (18.75 m^3), which appears to be logical because higher filtration velocity was achieved by higher nominal flow. But at 0.30 m, the filtered volume was significantly higher at 30 m h^{-1} (45.13 m^3) than at 60 m h^{-1} (29.57 m^3). This fact could be explained for the low inlet turbidity values obtained when the porous media was tested at $0.30 \text{ m}/30 \text{ m h}^{-1}$ (Table 2), with consequent longer filtration cycles, increasing thus the filtered volume for all the filters, while at 60 m h^{-1} the pressure loss produced

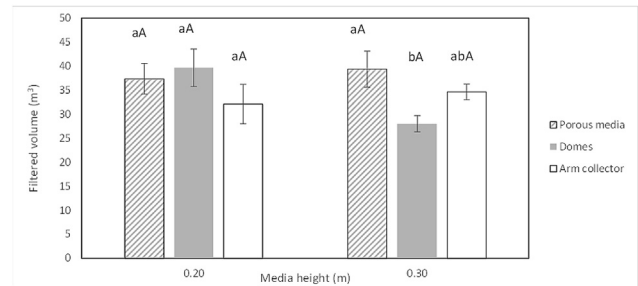


Fig. 5 – Interactions between media heights and underdrain designs for filtered water volume per cycle (m^3). For each media height, small letters mean significant differences ($p < 0.05$) among underdrain designs. For each underdrain design, different capital letters mean significant differences ($p < 0.05$) among media heights.

	Filtered volume per filtration cycle (m^3)	Filtered volume/total electrical consumption ($\text{m}^3 \text{ kW h}^{-1}$)
Model	<0.001	<0.001
Underdrain design	<0.001	<0.050
Media height	<0.001	<0.001
Filtration velocity	n.s	<0.010
Underdrain design x media height	<0.001	n.s
Media height x filtration velocity	<0.001	<0.001
Underdrain design x filtration velocity	<0.001	<0.050
Underdrain design x media height x filtration velocity	n.s	n.s
Inlet turbidity	<0.001	n.s

n.s.: no significant ($p > 0.050$).

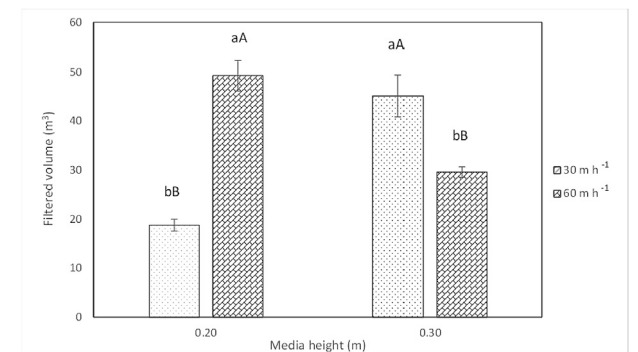


Fig. 6 – Interactions between media heights and filtration velocities for filtered water volume per cycle (m^3). For each media height, small letters mean significant differences ($p < 0.05$) between filtration velocities. For each filtration velocity, different capital letters mean significant differences ($p < 0.05$) between media heights.

across the filter quickly reached the pre-set threshold of 50 kPa, where backwashing was activated.

The porous media design filtered significantly more water at 30 m h⁻¹ (54.94 m³) than the dome and arm collector (30.20 and 24.48 m³, respectively) probably due to the cleaner effluent produced in the WWTP during its use, but at 60 m h⁻¹ both porous media and arm collector filtered significantly more water (35.55 and 40.66 m³, respectively) than the dome design (32.36 m³). All the underdrains presented significant differences of filtered water volume between velocities. However, porous media underdrain filtered more volume at 30 m h⁻¹ (54.94 m³) than at 60 m h⁻¹ (35.55 m³). Conversely, domes and arm collector filtered more water at 60 m h⁻¹ (32.36 m³ and 40.66 m³, respectively) than at 30 m h⁻¹ (30.20 and 24.48 m³, respectively) (Fig. 7).

3.3.2. Filtered volume per total electrical consumption

The ratio between filtered volume and total electrical energy consumption (i.e. considering both filtration and backwashing), which was calculated with Eq. (5), significantly ($p < 0.05$) depended on underdrain, media height and filtration velocity (Table 6). The porous media design filtered more water volume per kWh consumed, followed by the domes and arm collector (8.30, 8.18 and 8.07 m³ kW h⁻¹, respectively). The height of 0.20 m had higher ratios than 0.30 m (8.53 vs. 7.95 m³ kW h⁻¹) as well as velocity of 30 m h⁻¹ regarding 60 m h⁻¹ (8.35 vs. 8.11 m³ kW h⁻¹). Interactions between media height sand filtration velocities as well as between underdrain designs and filtration velocities were found to be significant.

There were no significant differences between filtration velocities at 0.20 m (Fig. 8), with similar values at 60 m h⁻¹ and 30 m h⁻¹ (8.57 and 8.47 m³ kW h⁻¹, respectively). However, with a height of 0.30 m, this ratio was significantly higher at 30 m h⁻¹ than at 60 m h⁻¹ (8.21 vs. 7.87 m³ kW h⁻¹). As was previously discussed in Section 3.3.1, higher ratios at 30 m h⁻¹ than at 60 m h⁻¹ with 0.30 m height could be explained by the longer filtration cycles of porous media underdrain at 0.30 m/30 m h⁻¹ due to the occasional lower inlet turbidity. On the other hand, at 60 m h⁻¹ a faster pressure loss was produced due to higher velocity, with the consequent shorter filtration

cycles and less filtered volume. In that sense, for all the designs, higher ratio values were obtained at 30 m h⁻¹ than at 60 m h⁻¹, although nominal flow was higher at 60 m h⁻¹. The ratio was higher with a height of 0.20 than 0.30 m, as there was more flow resistance due to a greater sand bed thickness in the latter.

At 30 m h⁻¹, porous media underdrain presented a significantly ($p < 0.05$) higher ratio (8.61 m³ kW h⁻¹) than arm collector and domes (8.33 and 8.27 m³ kW h⁻¹, respectively), but at 60 m h⁻¹, both porous media and dome designs (Fig. 9) showed greater ratios (8.25 and 8.14 m³ kW h⁻¹, respectively) than arm collector (7.88 m³ kW h⁻¹).

Results for volume and electrical energy consumption concur with those obtained by Mesquita et al. (2012), in which the effect of three sand filters with different designs on head loss was tested using clean water and different sand sizes, media heights and filtration velocities, being all the factors

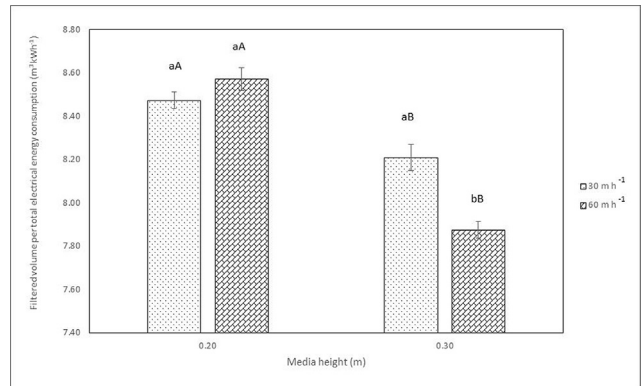


Fig. 8 – Interactions between media heights and filtration velocities for filtered water volume per total energy consumption (m³ kW h⁻¹). For each media height, small letters mean significant differences ($p < 0.05$) between filtration velocities. For each filtration velocity, different capital letters mean significant differences ($p < 0.05$) between media heights.

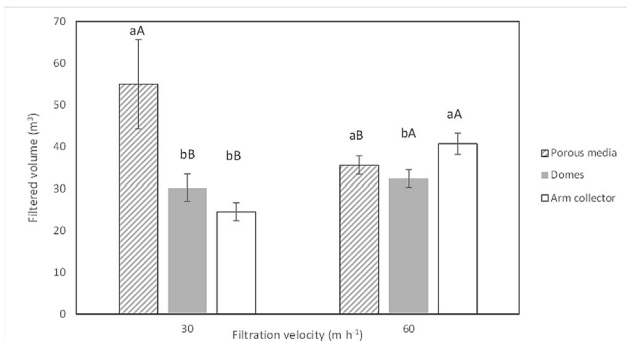


Fig. 7 – Interactions between filtration velocities and underdrain designs for filtered water volume per cycle (m³). For each filtration velocity, small letters mean significant differences ($p < 0.05$) among underdrain designs. For each underdrain design, different capital letters mean significant differences ($p < 0.05$) between filtration velocity.

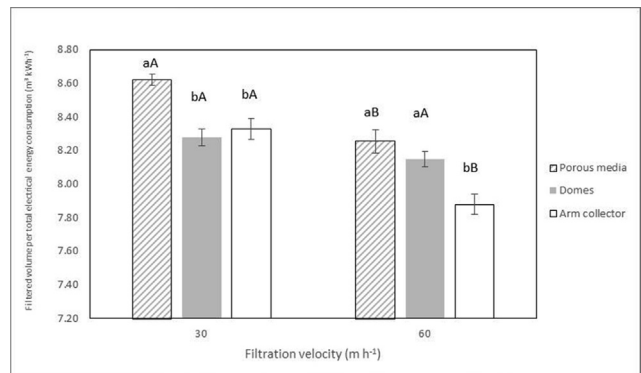


Fig. 9 – Interactions between filtration velocity and underdrain design in filtered water volume per total energy consumption (m³ kW h⁻¹). For each filtration velocity, small letters mean significant differences ($p < 0.05$) among underdrain designs. For each underdrain design, different capital letters mean significant differences ($p < 0.05$) between filtration velocities.

and their interactions significant. Head loss increased proportionally with filtration velocity (Burt, 2010; Mesquita et al., 2012) as well as with deeper sand heights (Mesquita et al., 2012). However, at a low filtration velocity of 20 m h^{-1} , no significant differences were detected with different heights. Two of the underdrains tested by Mesquita et al. (2012) were similar to those used in the present experiment (arm collector and domes) and the former presented higher pressure losses than the latter in almost all conditions tested. Nevertheless, Burt (2010), studying two similar designs (arm collector and dome), did not find that a specific design had a more significant effect in pressure loss.

4. Conclusions

Media height, filtration velocity and the underdrain design affected removal efficiency, filtered volume and electrical energy consumption of sand filters for microirrigation systems using reclaimed effluents in field conditions.

Overall, when using reclaimed effluents with similar characteristics as this experiment in sand media filters, working at a filtration velocity of 30 m h^{-1} instead of 60 m h^{-1} provide higher turbidity removals (34.17 vs. 11.27%), higher mass retention (84.97 vs. 31.56 g cycle^{-1}), longer filtration cycles (289 vs. 178 min) and higher ratio of filtered volume per electrical energy unit (8.35 vs. $8.11 \text{ m}^3 \text{ kW h}^{-1}$).

On the other hand, a porous media underdrain that improves hydraulic performance of the sand media achieved better turbidity removals (26.28% vs. 18.53 and 13.45% of the domes and arm collector underdrains, respectively), more filtered volume per filtration cycle (38.41 vs. 31.73 and 33.69 m^3) and more filtered volume per electrical consumption ratio (8.30 vs. 8.18 and $8.07 \text{ m}^3 \text{ kW h}^{-1}$) than the other two underdrain designs tested under the same operational conditions. The porous media underdrain removes 12.83% more of turbidity with 2.77% less energy consumption regarding the filter that showed the lowest values.

Media height, however, did not follow a clear pattern either in turbidity removal or in filtered volume. As with a 0.20 m lower media height, higher filtered volume per electrical energy unit ratio was observed, thus lower media heights are recommended, considering that additional savings for the smaller amount of media required would be achieved.

Further research is needed for confirming the results with other effluents, media heights, filtration velocities and underdrain designs. The effect of the factors here considered in backwashing efficiency requires also new specific studies.

Conflicts of interest

None declared.

Acknowledgements

The authors would like to express their gratitude to the former Spanish Ministry of Economy and Competitiveness for its

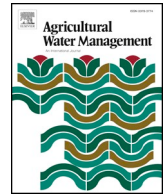
financial support for this experiment through grant AGL2015-63750-R. Carles Solé Torres was the recipient of a predoctoral scholarship (IFUG2016/72) from the University of Girona. The authors would also like to thank the Municipality of Celrà for their help in carrying out this experiment.

REFERENCES

- Abadía, R., Vera, J., Rocamora, C., & Puerto, H. (2018). Generalization of supply energy efficiency in irrigation distribution networks. *Biosystems Engineering*, 175, 146–155.
- Arbat, G., Pujol, T., Puig-Bargués, J., Duran-Ros, M., Barragán, J., Montoro, L., et al. (2011). Using computational fluid dynamics to predict head losses in the auxiliary elements of a microirrigation sand filter. *Transactions of the ASABE*, 54(4), 1367–1376.
- Asano, T., Burton, F. L., & Leverenz, H. L. (2007). *Water reuse: Issues, technologies and applications*. New York, USA: McGraw Hill Inc.
- Bové, J., Arbat, G., Duran-Ros, M., Pujol, T., Velayos, J., Ramírez de Cartagena, F., et al. (2015b). Pressure drop across sand and recycled glass media used in micro irrigation filters. *Biosystems Engineering*, 137, 55–63.
- Bové, J., Arbat, G., Pujol, T., Duran-Ros, M., Ramírez de Cartagena, F., Velayos, J., et al. (2015a). Reducing energy requirements for sand filtration in microirrigation: Improving the underdrain and packing. *Biosystems Engineering*, 140, 67–78.
- Bové, J., Puig-Bargués, J., Arbat, G., Duran-Ros, M., Pujol, T., Pujol, J., et al. (2017). Development of a new underdrain for improving the efficiency of microirrigation sand media filters. *Agricultural Water Management*, 179, 296–305.
- Bové, J., Pujol, J., Arbat, G., Duran-Ros, M., Ramírez de Cartagena, F., & Puig-Bargués, J. (2018). Environmental assessment of underdrain designs for a sand media filter. *Biosystems Engineering*, 167, 126–136.
- Burt, C. (2010). *Hydraulics of commercial sand media filter tank used for agricultural drip irrigation*. San Luis Obispo, CA, USA: Irrigation Training and Research Center. ITCR Report No. R 10001.
- Burt, C., Howes, D. J., & Freeman, B. (2011). *Public interest energy research (PIER) program. Final project report, agriculture water energy efficiency*. San Luis Obispo, CA, USA: California Energy Commission and Irrigation Training and Research Center.
- Capra, A., & Scicolone, B. (2007). Recycling of poor quality urban wastewater by drip irrigation systems. *Journal of Cleaner Production*, 15(16), 1529–1534.
- Cleasby, J. L. (1990). Filtration. In *American water work association water quality and treatment: A handbook of public water supplies* (4th ed.). New York, USA: McGraw-Hill, Inc.
- De Deus, F. P., Testezlaf, R., & Mesquita, M. (2016). Assessment methodology of backwashing in pressurized sand filters. *Revista Brasileira de Engenharia Agrícola e Ambiental*, 20(7), 600–605.
- Duran-Ros, M., Arbat, G., Barragán, J., Ramírez de Cartagena, F., & Puig-Bargués, J. (2010). Assessment of head loss equations developed with dimensional analysis for micro irrigation filters using effluents. *Biosystems Engineering*, 106, 521–526.
- Duran-Ros, M., Puig-Bargués, J., Arbat, G., Barragán, J., & Ramírez de Cartagena, F. (2008). Definition of a SCADA system for a microirrigation network with effluents. *Computers and Electronics in Agriculture*, 64(2), 338–342.
- Duran-Ros, M., Puig-Bargués, J., Arbat, G., Barragán, J., & Ramírez de Cartagena, F. (2009a). Effect of filter, emitter and location on clogging when using effluents. *Agricultural Water Management*, 96(10), 67–79.

- Duran-Ros, M., Puig-Bargués, J., Arbat, G., Barragán, J., & Ramírez de Cartagena, F. (2009b). Performance and backwashing efficiency of disc and screen filters in microirrigation systems. *Biosystems Engineering*, 103(1), 35–42.
- Elbana, M., Ramírez de Cartagena, J., & Puig-Bargués, J. (2012). Effectiveness of sand media filters for removing turbidity and recovering dissolved oxygen from a reclaimed effluent used for micro-irrigation. *Agricultural Water Management*, 111, 27–33.
- Elbana, M., Ramírez de Cartagena, J., & Puig-Bargués, J. (2013). New mathematical model for computing head loss across sand media filter for microirrigation systems. *Irrigation Science*, 31, 343–349.
- Fernández García, I., Montesinos, P., Camacho Poyato, E., & Rodríguez Díaz, J. A. (2017). Optimal design of pressurized irrigation networks to minimize the operational cost under different management scenarios. *Water Resources Management*, 31(6), 1995–2010.
- Jiménez-Bello, M. A., Royuela, A., Manzano, J., García Prats, A., & Martínez-Alzamora, F. (2015). Methodology to improve water and energy use by proper irrigation scheduling in pressurized networks. *Agricultural Water Management*, 149, 91–101.
- Li, J., Chen, L., Li, Y., Yin, J., & Zhang, H. (2010). Effects of chlorination schemes on clogging in drip emitters during application of sewage effluent. *Applied Engineering in Agriculture*, 26(4), 565–578.
- Mesquita, M. (2014). *Desenvolvimento tecnológico de um filtro de areia para irrigação localizada* (Unpublished doctoral dissertation). Campinas, Brazil: Universidade Estadual de Campinas.
- Mesquita, M., de Deus, F. P., Testezlaf, R., da Rosa, L. M., & Diotto, A. V. (2019b). Design and hydrodynamic performance testing of a new pressure sand filter diffuser plate using numerical simulation. *Biosystems Engineering*, 183, 58–69.
- Mesquita, M., de Deus, F. P., Testezlaf, R., & Diotto, A. V. (2019a). Removal efficiency of pressurized sand filters during the filtration process. *Desalination Water Treat*, 161, 132–143.
- Mesquita, M., Testezlaf, R., & Ramirez, J. (2012). The effect of media bed characteristics and internal auxiliary elements on sand filter head loss. *Agricultural Water Management*, 115, 178–185.
- Moreno, M. A., del Castillo, A., Montero, J., Tarjuelo, J. M., & Ballesteros, R. (2016). Optimization of the design of pressurized irrigation systems for irregular shaped plots. *Biosystems Engineering*, 151, 361–373.
- Nakayama, F. S., Boman, B. J., & Pitts, D. J. (2007). Maintenance. In F. R. Lamm, J. E. Ayars, F. S. Nakayama, & F.S. (Eds.), *Microirrigation for crop production. Design, operation, and management* (pp. 389–430). Amsterdam, Netherlands: Elsevier.
- Nakhla, G., & Farooq, S. (2003). Simultaneous nitrification–denitrification in slow sand filters. *Journal of Hazardous Materials*, 96(2–3), 291–303.
- Pizarro, F. (1996). *Riegos localizados de alta frecuencia* (3rd ed.). Madrid, Spain: Mundi Prensa.
- Puig-Bargués, J., Barragán, J., & Ramírez de Cartagena, F. (2005). Filtration of effluents for microirrigation systems. *Transactions of the ASABE*, 48(3), 968–978.
- Pujol, T., Arbat, G., Bové, J., Puig-Bargués, J., Duran-Ros, M., Velayos, J., et al. (2016). Effects of the underdrain design on the pressure drop in sand filters. *Biosystems Engineering*, 150, 1–9.
- Solé-Torres, C., Puig-Bargués, J., Duran-Ros, M., Arbat, G., Pujol, J., & Ramírez de Cartagena, F. (2019). Effect of different sand filter underdrain designs on emitter clogging using reclaimed effluents. *Agricultural Water Management*, 223, 105683.
- Soto-García, M., Martín-Goriz, B., García-Bastida, P. A., Alcón, F., & Martínez-Álvarez, V. (2013). Energy consumption for crop irrigation in a semiarid climate (south-eastern Spain). *Energy*, 55, 1084–1093.
- Tarjuelo, J. M., Rodríguez-Díaz, J. A., Abadía, R., Camacho, E., Rocamora, C., & Moreno, M. A. (2015). Efficient water and energy use in irrigation modernization: Lessons from Spanish case studies. *Agricultural Water Management*, 162, 67–77.
- Tripathi, V. K., Rajput, T. B. S., & Patel, N. (2014). Performance of different filter combinations with surface and subsurface drip irrigation systems for utilizing municipal wastewater. *Irrigation Science*, 32, 379–391.
- Trooien, T. P., & Hills, D. J. (2007). Application of biological effluent. In F. R. Lamm, J. E. Ayars, & F. S. Nakayama (Eds.), *Microirrigation for crop production. Design, operation, and management* (pp. 329–356). Amsterdam, Netherlands: Elsevier (Chapter 9).
- World Health Organization, WHO. (2006). *Guidelines for the safe use of wastewater, excreta and greywater* (Vol. II). Geneva, Switzerland: WHO Press.
- Wu, W. Y., Huang, Y., Liu, H. L., Yin, S. Y., & Niu, Y. (2015). Reclaimed water filtration efficiency and drip irrigation emitter performance with different combinations of sand and disc filters. *Irrigation and Drainage*, 64(3), 362–369.

4. EFFECT OF DIFFERENT SAND FILTER UNDERDRAIN DESIGNS ON
EMITTER CLOGGING USING RECLAIMED EFFLUENTS.



Effect of different sand filter underdrain designs on emitter clogging using reclaimed effluents



Carles Solé-Torres, Jaume Puig-Bargués*, Miquel Duran-Ros, Gerard Arbat, Joan Pujol, Francisco Ramírez de Cartagena

Department of Chemical and Agricultural Engineering and Technology, University of Girona, Carrer Maria Aurèlia Capmany, 61, 17003 Girona, Catalonia, Spain

ARTICLE INFO

Keywords:

Wastewater
Microirrigation
Media filter
Filtration
Plugging

ABSTRACT

Sand media filters are those that achieve a higher retention of organic and inorganic solids, which is why they are usually recommended when reclaimed effluents are used in drip irrigation systems. Sand filters usually differ on the design of their underdrain, where an important pressure drop is produced. However, the effect of the design of sand filter underdrain on emitter clogging has not been widely studied. Three sand media filters with different underdrain designs (collector arms, inserted domes and drainage with porous media) were used for filtering a reclaimed effluent in a surface drip irrigation system. Pressure-compensating emitters with 2.3 l/h nominal emitter discharge were placed every 40 cm in 4 irrigation laterals each measuring 90 m in length. Effluents were chlorinated after being filtered. The filters operated for 1000 h with sand media heights of 20 and 30 cm and filtration velocities of 30 and 60 m/h. At the beginning, after 500 h, and at the end of the experiment the emitter discharge of each one of the 2712 emitters that were installed was experimentally measured under field conditions. On average, there was a statistically significant reduction ($p < 0.05$) on emitter discharge regarding the initial value of 8.03% at 500 h and 10.84% at 1000 h. Emitter clogging was primarily affected by the interactions between underdrain design, emitter location and irrigation time. Differences on emitter discharge due to underdrain design were only observed at 1000 h, showing a significantly higher flow rate ($p < 0.05$) those emitters protected with the filter with a collector arm underdrain, despite the fact that this filter did not achieve the highest turbidity removals. Emitter location had also a significant effect after 500 h of operation, being discharge significantly lower ($p < 0.05$) only in the last 2 m of the laterals, with the minimum values found for the final two drippers. The three filters used in the experiment did not show a significant effect on the percentage of completely clogged emitters, which mainly depended on the interaction between irrigation time and emitter location.

1. Introduction

The use of reclaimed wastewater in agriculture has become a viable, stable and economic alternative to confront the issue of water scarcity on our planet (Asano et al., 2007), because municipal and industrial wastewater may be used for irrigating a large variety of crops (Hamilton et al., 2007), thus releasing water of higher quality for other uses (Lazarova and Asano, 2005).

The best irrigation technique for using wastewater from the public health and environmental points of view is drip irrigation (Bucks et al., 1979; World Health Organization, 2006). However, the main problem using drip irrigation with reclaimed effluents is emitter clogging (Bucks et al., 1979; Ravina et al., 1992). Emitter clogging depends on factors such as wastewater characteristics, emitter type, system operation,

maintenance and filtration (Capra and Scicolone, 2007; Duran-Ros et al., 2009).

As clogging is related to the quality of water used, Bucks et al. (1979) derived a hazard rating depending on the values of different physical, chemical and biological quality parameters. According to Bucks et al. (1979) an irrigation water with suspended solids below 50 mg/l, a pH below 7 and bacterial number smaller than 10,000 cfu/ml should pose a minor clogging hazard. However, Capra and Scicolone (1998) suggest higher clogging hazard thresholds when emitters with higher discharge rates are used. Pressure compensating emitters (Puig-Bargués et al., 2010a; Pei et al., 2015), integrated emitters (Pei et al., 2014) and high discharge emitters (Ravina et al., 1992; Trooien et al., 2000) are more resistant to clogging. Some authors analyzed flow and particle movements within emitter components aiming to suggest

* Corresponding author.

E-mail address: jaume.puig@udg.edu (J. Puig-Bargués).

<https://doi.org/10.1016/j.agwat.2019.105683>

Received 14 February 2019; Received in revised form 18 June 2019; Accepted 19 June 2019

Available online 12 July 2019

0378-3774/ © 2019 Elsevier B.V. All rights reserved.

designs that could prevent clogging development (Wei et al., 2008; Al-Muhammad et al., 2016; Feng et al., 2018b). Clogging could also be reduced with lower irrigation frequencies (Zhou et al., 2015) and lateral flushing (Puig-Bargués et al., 2010a, 2010b; Tripathi et al., 2014; Feng et al., 2017).

Several authors have studied how biofilm and chemical precipitation, which are the most common clogging causes when reclaimed effluents are reused, affect emitter performance (Gamri et al., 2014; Green et al., 2018; Zhou et al., 2018). Chlorination has also resulted in being effective in reducing emitter clogging and it has been widely used to prevent biological clogging (Hills and Brenes, 2001; Dehghanisani et al., 2005; Cararo et al., 2006) as the strong oxidation of chlorine inhibits the reproduction and growth of microorganisms and the formation of biofilms (Li et al., 2010) as well as, if combined with acidification, the precipitation of solid particles in the drip emitters (Hao et al., 2018).

Other authors analyzed the effect of different filter types on emitter clogging when reclaimed effluents were used (Ravina et al., 1992; Capra and Scicolone, 2004; Duran-Ros et al., 2009; Tripathi et al., 2014). There is an agreement that filtration is an essential operation which can prevent emitter clogging (Oron et al., 1979), although it does not avoid it completely (Tajrishy et al., 1994). Sand filters are considered those that offer a better protection for drip irrigation systems (Trooien and Hills, 2007) since they remove efficiently suspended solids (Duran-Ros et al., 2009), organic compounds, phosphorus and microorganisms (Dalahmeh et al., 2012) and consequently prevent emitter clogging (Capra and Scicolone, 2007). In sand media filters the pressure loss is mainly located at filtration media and auxiliary elements such as the underdrain (Arbat et al., 2013). Several authors have studied the influence of underdrain designs on pressure loss (Mesquita et al., 2012; Bové et al., 2015; Pujol et al., 2016), but none of them have analyzed how filter design affects emitter clogging. On the other hand, sand filters have to be periodically backwashed for releasing those particles retained in the media, which increase pressure loss across filtration time. Backwashing is an important procedure for an effective filter performance (Nakayama et al., 2007) but the media cleaning pattern depends on the underdrain design (Burt, 2010). Usually, filter backwashing is carried out at pre-set pressure loss, nevertheless daily backwashing has been also verified to be a good practice for assuring good emitter performance (Enciso-Medina et al., 2011). Even though filter and backwashing operations in drip irrigation systems have been studied (Elbana et al., 2012) there are few studies which try to improve the design and performance of sand media filters. With this in mind, Bové et al. (2017) designed a new underdrain aiming to reduce pressure loss across sand filters for improving both water and energy use efficiency.

The main objective of this study was to analyse the effect of three sand filters with different underdrain designs (the prototype designed by Bové et al. (2017) and two commercial ones) on emitter clogging when a reclaimed effluent is used.

2. Material and methods

2.1. Experimental setup

Reclaimed effluent from the Celrà (Girona, Spain) wastewater treatment plant (WWTP), which treats urban and industrial effluents using a sludge process, was used in the experiment.

The experimental irrigation system consisted of three sand filters with three underdrain different designs (Fig. 1): a sand filter model FA1M (Lama, Sevilla, Spain), a sand filter model FA-F2-188 (Regaber, Parets del Vallès, Spain) and an experimental sand filter built with an underdrain designed by Bové et al. (2017). Table 1 shows the main characteristics of the different sand filters used. The underdrain of the filter model FA1M (Lama, Sevilla, Spain) consisted of 7 parts with slots which overlapped each other forming striated tubes converging in a

central tube which worked as a manifold. This contained a total of 10 striated tubes with 5 tubes on each side of the manifold. In model FA-F2-188 (Regaber, Parets del Vallès, Spain) the underdrain consisted of 12 inserted domes on a back plate. These domes were pyramidally shaped with vertical slots, mounted on a manifold. Finally, the underdrain designed by Bové et al. (2017) consisted of a cylinder that occupied the entire surface of filtration of the filter. This cylinder was confined by two 0.75 mm meshes, one at the top and one at the bottom, and was filled with silica sand sieved to 0.63 – 0.75 mm grain size, with an equivalent diameter of 0.71 mm, bulk density of 1.478 kg/m³, real density of 2.573 kg/m³ and a porosity of 42.2% (Bové et al., 2017).

All the filters were filled with silica sand CA-07MS (Sibelco Minerales SA, Bilbao, Spain) with an effective diameter (D_e , size opening which will pass 10% by dry weight of a representative sample of the filter material) of 0.48 mm and a coefficient of uniformity (ratio of the size opening which will pass 60% of the sand through the size opening which will pass 10% through) of 1.73. Each filter had an irrigation subunit associated, which consisted of four laterals, each with a total length of 90 m (Fig. 2). Each lateral had 226 emitters, so for each emitter location there were 4 replications per subunit. However, for location 226 only there were 3 emitters per subunit.

Commercial integrated and pressure compensating emitters Uniram AS 16010 (Netafim, Tel Aviv, Israel), with 2.31/h of nominal flow discharge, a distance between emitters of 0.4 m, a nominal working pressure of 50–400 kPa and a manufacturing coefficient of variation of 0.03 were used. This emitter was selected since its design improves clogging resistance and its pressure compensation allows to use it in a wide range of topographical conditions.

The reclaimed effluent was pumped from the WWTP to the filters using a multicellular centrifugal pump model CR-15-4 (Grundfos, Bjerringbro, Denmark) governed by a frequency variator model FRN-4 (Fuji Electric, Cerdanyola del Vallès, Spain). The inlet flow was measured with an electromagnetic flowmeter Isomag MS2500 (ISOIL Industria SpA, Cinisello Balsamo, Italy) with a pulse transmitter. The experimental setup allowed that only one filter was operating at a time. After being filtered, the reclaimed effluent was carried to the drip irrigation subunits. Since the filtrated flow was higher than which was needed for the irrigation subunits, a proportional electrohydraulic actuator SKD32 (Siemens, Munich, Germany) operated a three-way valve VXG41 (Siemens, Munich, Germany), so that the excess flow was brought to a water storage tank of 3000 l Aquablock (Shütz, Selters, Germany) that was used for filter backwashing.

A chlorine deposit of 200 l was installed, to continuously inject chlorine for achieving a concentration of 2 ppm in the water after being filtered, using a DosTec AC1/2 membrane pump (ITC, Sta. Perpètua de Mogoda, Spain). When sand filters were backwashed, backwashing water entering the filters was chlorinated to reach a 4 ppm chlorine concentration.

Several effluent quality parameters before and after being filtered were measured and recorded every minute in a supervisory control and data acquisition system (SCADA) previously developed (Duran-Ros et al., 2008). The parameters measured before filtration were the electrical conductivity using a transmitter LIQUISYS-M CLM253-CD0010 and a sensor CLS21-C1E4A, the pH and the temperature using a transmitter LIQUISYS-M CPM253-MR0010 and a sensor CPS11D-7BA21. The parameters measured before and after filtration were turbidity using a transmitter LIQUISYS-M CUM253-TU0005 with a sensor CUS31-A2E and dissolved oxygen with a transmitter LIQUISYS-M COM253-WX0015 and a sensor COS 61-A1F0. All the transmitters and sensors used were manufactured by Endress + Hauser (Gering, Germany).

The filters were washed automatically when the total pressure drop across them measured by pressure transducers reached 50 kPa (Ravina et al., 1992). The backwashing time was 3 min throughout the entire test, and during that time, backwashing water did not reach the laterals. The water used for the backwashing, came from the filtered water



Fig. 1. Different underdrain designs: porous media (A), inserted domes (B) and arm collector (C).

storage tank.

2.2. Operational procedure

The experiment lasted 1000 h for each filter, taking place uninterruptedly between March and November 2018, except for the month of June, where the installation did not work due to a breakdown of turbidity sensors. Whenever possible, six daily irrigation sessions of 4 h each (i.e. two daily sessions of 4 h per filter) were carried out. In practice, it was attempted to establish irrigation sessions as homogeneous as possible, which was not always possible due to small breakdowns that prevented the use of a filter for a certain period of time. When these breakdowns were solved, the operation time of the affected filter was increased to equalize the hours of operation.

During the 1000 h that the experiment lasted, two different media heights were tested (20 and 30 cm), and two different filtration velocities (30 and 60 m/h) for each one, which made a total of four different operating conditions. The operating conditions were the same for each filter with each being tested for 250 h. Working pressure was set to 172 kPa at drip irrigation subunit inlet. No lateral flushing was carried out during the experiment.

2.3. Assessment of filter and emitter performance

Filter performance for removing turbidity and dissolved oxygen was assessed through the removal efficiency (E) achieved in the filters, which was calculated as:

$$E = \frac{N_0 - N}{N_0} \times 100 \quad (1)$$

where N_0 and N are the values of turbidity and dissolved oxygen at filter inlet and outlet, respectively.

Flow discharge for all the emitters of all the laterals (i.e. a total of 2712 emitters) was measured in the experimental field at the beginning, after 500 h and at the end of the experiment (1000 h). The flow of each dripper was collected for 5 min in collection dishes and then transferred to a 500 ml graduated cylinder to measure its discharge. The experimental determination of emitter discharge lasted for about 20 h after the target time (0, 500 and 1000 h) due to the number of emitters being measured. In addition, the percentage of completely clogged emitters (i.e. emitters that had 0 l/h discharge) was also computed at each control time.

Table 1

Underdrain design and main operation characteristics of the different filters used in the experiment. Data was obtained from manufacturers.

Filter underdrain design	Filter nominal diameter (mm)	Filter filtration surface (m ²)	Underdrain opening surface/filter filtration surface (%)	Maximum filtration flow (m ³ /h)	Maximum filter media height (m)	Average initial pressure loss* (kPa)
Porous media	500	0.1960	37.95	20	0.70	27.86
Domes	508	0.2026	3.71	18	0.69	29.89
Collector arms	500	0.1960	4.65	23	0.40	33.94

* experimentally measured and averaged for the different media heights and filtration velocities.

During the emitter discharge measurements, pressure was also determined in four positions on each lateral (at the beginning, one third of the lateral length, two thirds of the lateral length and at the end) using a digital manometer Leo 2 (Keller, Winterthur, Switzerland) with a precision of $\pm 0.07\%$ that was placed at a pressure intake (Ein-tal, Or-Akiva, Israel). Pressure uniformity of pressures (U_{plq}) (Bliesner, 1976) was calculated according to the formula:

$$U_{plq} = \left(\frac{p_{25}}{p^-} \right)^x \times 100 \quad (2)$$

where p_{25} is the average pressure of 25% of the positions with the lowest pressure (kPa), p^- is the average pressure of all the tested positions (kPa) and x is the emitter flow exponent, which was considered 0.05.

At the end of the experiment, emitters from the locations 1, 224, 225 and 226 of the first and second lateral for each irrigation subunit were analysed for visual evidence of clogging. These emitters were cut and opened for external and internal inspection. Pictures were taken with a DMC-FZ150 (Panasonic Corporation, Osaka, Japan) camera.

2.4. Characterization of inlet water

The main water quality parameters for each filter were recorded each minute, as was explained in Section 2.1. Since the filters did not operate simultaneously, it was necessary to assess if effluent characteristics were different during the experiment. Table 2 presents the mean values of the pH, temperature, electrical conductivity, dissolved oxygen and turbidity values recorded through the 1000 h the experiment lasted.

Significant differences ($p < 0.05$) were observed for pH, temperature, electrical conductivity and dissolved oxygen for the reclaimed effluents available at each filter inlet. Reclaimed effluent used during the experiment with the dome underdrain filter had a pH significantly higher ($p < 0.05$) than that for both porous media and arm collector underdrain filters. According to Bucks et al. (1979) classification, there was a moderate chemical clogging hazard regarding the pH for all the filters. Water inlet temperatures when the porous media underdrain was tested were significantly higher ($p < 0.05$) than those for the arm collector underdrain but not for those of the dome underdrain. These differences between temperatures may have helped the formation and growth of biofilms, which are closely related to emitter clogging (Li

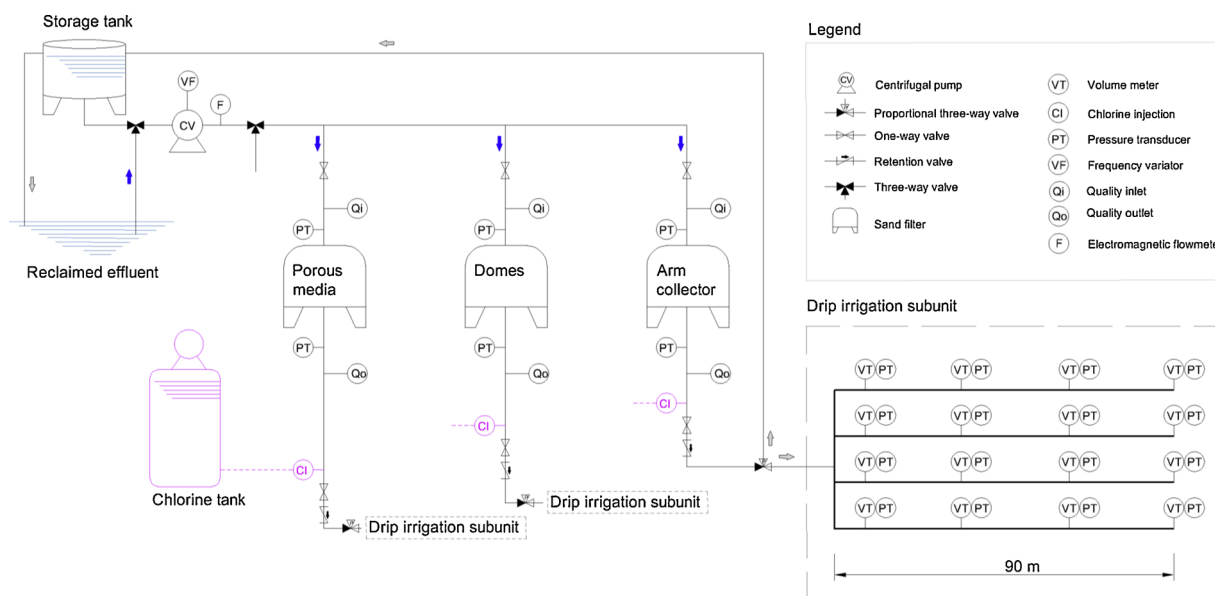


Fig. 2. Diagram of the experimental irrigation system.

et al., 2012; Zhou et al., 2013). Electrical conductivity when porous media and collector arm filters were used was significantly higher ($p < 0.05$) than that with the dome underdrain. Effluent used during the operation of dome underdrain filter had a dissolved oxygen level significantly higher ($p < 0.05$) than those for both porous media and arm collector filters. This means that microorganism levels should be smaller when an inserted dome filter was used. No significant differences were observed in turbidity values in inlet water for any of the tested filters, meaning that the risk of physical clogging was the same. All these variations are due to the usual variability present when reclaimed effluents are treated in the WWTP.

2.5. Statistical analyses

Statistical analyses carried out using SPSS Statistics 25 software (IBM, New York, USA). In order to analyze pressure uniformity, emitter discharge and percentage of completely clogged emitters, an analysis of the variance was carried out. The model that was used included as fixed effects the filter underdrain design, the time of measurement and the position of the emitters (for Uplq it was lateral position) as well as the double interactions between the filter and time, filter and position, and time and position. Triple interactions were initially assessed but, as they were not significant ($p > 0.05$), they were excluded from the final analyses. To differentiate the averages that were significantly different with a probability of 0.05 or less, the Tukey's pairwise comparison test was used.

3. Results and discussion

3.1. Filter performance

Variations caused by the different underdrain designs on the quality

Table 2

Average \pm standard deviation of the effluent physical and chemical parameters at filter inlets. Different letters mean that there were significant differences ($p < 0.05$) in the values of each parameter at the different filter inlets.

Filter underdrain design	pH (-)	Temperature (°C)	EC (ds/m)	DO (mg/l)	Turbidity (FTU)
Porous media	7.33 \pm 0.20 b	20.61 \pm 3.26 a	2.64 \pm 0.46 a	3.27 \pm 0.83 b	6.22 \pm 2.11
Inserted domes	7.43 \pm 0.24 a	20.12 \pm 3.49 ab	2.46 \pm 0.53 b	3.57 \pm 1.02 a	5.82 \pm 3.08
Arm collector	7.31 \pm 0.22 b	19.68 \pm 3.57 b	2.63 \pm 0.44 a	3.28 \pm 1.04 b	6.42 \pm 2.77

Table 3

Average \pm standard deviation of the removal efficiencies of dissolved oxygen and turbidity achieved by the different underdrain design filters, expressed in percentage reductions of the inlet values. Negative values indicate an increase of the parameter. Different letters mean that there were significant differences ($p < 0.05$) in the removal efficiency for a parameter.

Filter underdrain design	Removal efficiency (%)	
	Dissolved oxygen	Turbidity
Porous media	-11.20 \pm 33.84	26.29 \pm 16.50 a
Domes	-6.68 \pm 30.53	18.53 \pm 24.38 b
Arm collector	-11.03 \pm 35.89	13.45 \pm 25.07 b

of the reclaimed effluents were characterized. Table 3 presents the percentages of oxygen and turbidity removals, computed using the Eq. (1), for the different underdrain designs.

The porous media underdrain filter showed turbidity removals of 26.29%, significantly higher ($p < 0.05$) than those reached by dome (18.53%) and arm collector (13.45%) underdrain filters, which were not significantly different from each other. Previous experiments with effluents of the same WWTP and using a dome underdrain sand filter with a filtration media height of 50 cm achieved turbidity removals of 57.57% with an inlet 6.76 FTU (Duran-Ros et al., 2009) and 70.6% with an inlet 9.78 FTU (Elbana et al., 2012). Tripathi et al. (2014) observed turbidity reductions of 51.1% using effluents with inlet 55 FTU. Wu et al. (2015) obtained reduction efficiencies of suspended solids from 11.4 to 48.0% using a sand filter filled with different media with equivalent diameters ranging between 2.1 and 0.45 mm. No details about sand filter design were provided in either of the two previous papers. The smaller turbidity removal observed in the present experiment (19.4% on average) for all of these three underdrain designs may

be due to the smaller inlet levels of turbidity of the effluent used (6.15 FTU on average) and to the reduced height of sand media bed in the filters, which was between 40 and 60% lower than the heights used by Duran-Ros et al. (2009) and Elbana et al. (2012) with a dome underdrain filter. Lower media heights used in the present experiment are explained by the limitation caused by reduced maximum height of arm collector underdrain filter (40 cm) and the need to carry out the experiment under the same experimental conditions for each filter.

The increase of dissolved oxygen achieved by the porous media (11.20%) and arm collector underdrain (11.03%) filters were greater than that observed with the dome underdrain filter (6.68%), although no significant differences were noted between these values. The smaller increases in dissolved oxygen achieved by the dome underdrain filter might be explained by the significantly ($p < 0.05$) higher values of this parameter at this filter inlet (Table 2). Dissolved oxygen increases in the dome underdrain filter were higher than those observed by Duran-Ros et al. (2009) (0.49% for inlet DO values of 2.80 mg/l and working with an effective sand size of 0.40 mm) and Elbana et al. (2012) (3.75% for inlet DO values of 4.00 mg/l and using an effective sand size of 0.48 mm), which were obtained in an experiment without any chlorination treatment. Although DO increase can be attributed to minor imperfections that result in air intrusions (Maestre-Valero and Martínez-Álvarez, 2010), the main reason is related to chlorination of backwashing water which reduced microbial population (Li et al., 2010) that consumes oxygen.

3.2. Pressure distribution across laterals

Table 4 shows the average pressure uniformity coefficient (Uplq) for the 4 driplines placed after each different filter in the three periods where emitter discharge was assessed under field conditions. For all the irrigation subunits, Uplq was above 98% during the whole experiment, so the pressure distribution for the driplines can be considered uniform. Since the emitter manufacturing coefficient of variation was low (3%), discharge reductions can mainly be explained by emitter clogging. However, slightly smaller pressure values were observed on the irrigation subunit after the dome underdrain filter. The reason was a clogged screen located inside the volume meter placed at the beginning of these laterals that was discovered after 800 h. However, since pressure compensating emitters were used, the effect of this smaller pressures on emitter discharge should have been minimum since pressure across the whole lateral was always within the acceptable pressure range for the tested emitter (50–400 kPa).

In order to assess if there were a possible effect of Uplq on results, a statistical treatment was carried out analyzing Uplq of each dripline. No significant ($p > 0.05$) effects were observed either for the different laterals, or for the different assessment times, the position of the four driplines and for any interaction between these factors. These results confirmed that values of Uplq did not have any differential effect on any of the laterals of the experimental setup.

Table 4

Average \pm standard deviation of the pressure distribution coefficients (Uplq) of irrigation subunits of the three different underdrains at the beginning, after 500 h and at the end of the experiment. No significant differences ($p > 0.05$) were found.

Underdrain	Uplq (%)		
	0 h	500 h	1000 h
Porous media	98.99 \pm 0.05	99.02 \pm 0.07	99.23 \pm 0.33
Domes	98.93 \pm 0.06	98.43 \pm 0.55	99.22 \pm 0.04
Arm collector	99.04 \pm 0.04	99.30 \pm 0.04	99.14 \pm 0.15

Table 5

Significance level (P-value) of the statistical model and of each factor and interaction for explaining flow rate variability during the experiment.

	Significance level (P-value)
Model	< 0.001
Time	< 0.001
Emitter location	< 0.001
Underdrain design	< 0.001
Underdrain design x time	< 0.001
Underdrain design x emitter location	< 0.001
Time x emitter location	< 0.001

3.3. Emitter performance

Emitter discharge values were treated statistically and there was (Table 5) a significant effect ($p < 0.05$) of each fixed factor (time, emitter position and filter underdrain design) as well as the interactions of underdrain design and time, underdrain design and emitter location and time and emitter location. Each interaction will be analyzed and discussed in the following sections.

Overall, there was a significant reduction ($p < 0.05$) of emitter discharge, which gradually decreased from an average measured discharge of 2.49 l/h at the beginning of the experiment, to 2.29 l/h at 500 h and 2.22 l/h at 1000 h. Globally, there has been a 10.8% reduction of emitter discharge from the beginning to the end of the experiment. This emitter discharge reduction throughout irrigation time due to clogging incidence has been widely observed (Ravina et al., 1992; Duran-Ros et al., 2009; Tripathi et al., 2014; Wu et al., 2015; Pei et al., 2014).

3.3.1. Effect of the underdrain design and irrigation time

Emitter discharge with regard to filter underdrain design and irrigation time is shown in Fig. 3. There was a significant reduction in emitter discharge over time for all the filter designs. Emitters protected by an arm collector underdrain sand filter showed a discharge reduction of 7.6% at 500 h and 9.6% at 1000 h from the initial value. These discharge diminutions were smaller than those observed for those emitters protected by the porous media and dome underdrain filters (8.76 and 8.06% at 500 h and 12.35 and 11.29% at 1000 h, respectively). Most of discharge rate reductions took place during the first 500 h, compared with those from 500 to 1000 h (3.93% for the porous media, 3.51% for the dome and 2.16% for the arm collector underdrain). Wu et al. (2015) also observed major emitter discharge reductions in first testing stages (from 0 to 150 h) compared to reductions in final testing stages (from 150 to 300 h). However, in an experiment

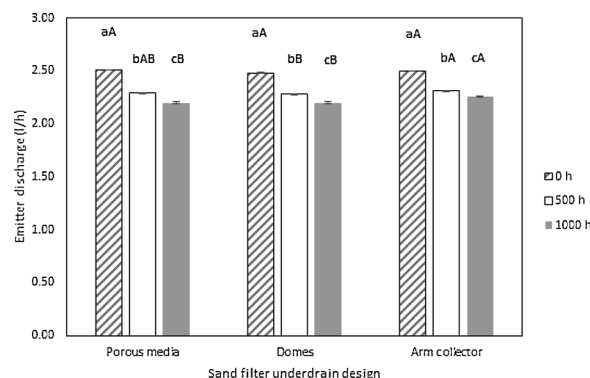


Fig. 3. Average emitter discharge and standard error (l/h) of all the emitters protected by sand filters with different underdrain designs at three measurement times. For each filter underdrain design, different small letters mean significant differences ($p < 0.05$) among times. For each measured time, different capital letters mean significant differences ($p < 0.05$) among filter underdrain designs.

operated for 540 h with pressure-compensating emitters (Pei et al., 2014), the relative average emitter discharge reduced 4.1–13.1% during the first period (0–204 h) but reduced 37.5–67.3% at the end of the experiment (204–540 h).

At the beginning of the experiment, no differences in emitter discharge between underdrain designs were found (Fig. 3). After 500 h, the average discharge of emitters protected by an arm collector design (2.31 l/h) was significantly higher ($p < 0.05$) than with the dome underdrain (2.28 l/h) but not with the porous media design (2.29 l/h). After 1000 h, the average discharge of emitters protected by the arm collector design (2.26 l/h) was significantly higher ($p < 0.05$) than those from both dome and porous media (2.20 l/h) underdrain filters. However, these differences were only about 3% of emitter discharge, on average.

Further research on the hydrodynamics conditions under filtration and, especially, backwashing, since the last has an important effect on filter performance (Burt, 2010; Enciso-Medina et al., 2011), for each underdrain design should be carried out in order to identify different patterns on particle removal that may have an effect on emitter clogging.

3.3.2. Effect of the underdrain design and emitter location

Emitter discharges related to filter underdrain design and emitter location are shown in Fig. 4. For each underdrain sand filter design, significant differences ($p < 0.05$) in emitter discharge were found, but only for emitters placed at the end of each lateral. In addition, slight variations were observed between filter designs. Thus, for both porous media and dome underdrain designs, emitter discharge of the three last emitters (last 1.2 m of the dripline) was significantly ($p < 0.05$) lower than the discharge of emitters located at the first 88.8 m of the lateral, i.e. emitters 1–222. For the arm collector underdrain, the smallest emitter discharge was only observed in the two last emitters (last 0.8 m) regarding emitter discharge of emitters 1–223. For all the underdrain designs, last emitter had clearly the lowest emitter average discharge (1.09 l/h for the porous media, 1.31 l/h for the dome and 1.57 l/h for arm collector designs).

For each emitter position, differences in emitter discharge between underdrain designs were only found in 11 emitters, which accounted for only 5% of the emitters on each dripline. The distribution of these emitters did not follow any pattern since they were emitter number 20, 31, 43, 105, 110, 111, 112, 153, 156, 160 and 217. In 27% of these emitters (emitters number 105, 111 and 112), discharge achieved with porous media underdrain sand filter was significantly higher than with arm collector filter while just the opposite happened with 18% of the emitters (emitters 20 and 217). For another 18% of these emitters (emitters 31 and 110) dome underdrain sand filter achieved more emitter discharge than arm collector but for emitters 156 and 160 the results was exactly the opposite. These differences might be explained by the randomness that is commonly observed in emitter clogging (Feng et al., 2018a).

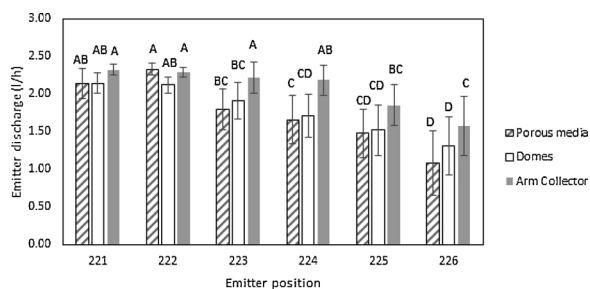


Fig. 4. Average emitter discharge and standard error (l/h) of the last 6 emitters of the lateral for each filter underdrain design. For each underdrain design, different capital letters mean significant differences ($p < 0.05$) among locations.

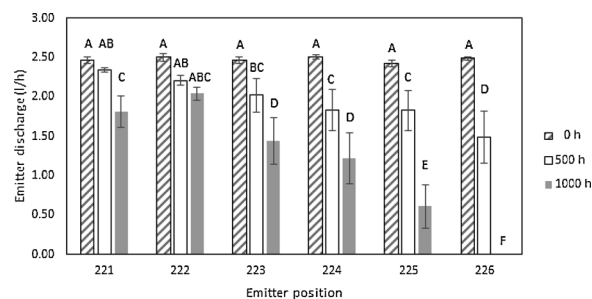


Fig. 5. Emitter discharge averages and standard error (l/h) for the last 6 emitters of the lateral at each measured time. For each measured time, different capital letters mean significant differences ($p < 0.05$) among locations.

3.3.3. Effect of time and emitter location

The interaction between time and location on emitter performance was also significant (Table 5). At the beginning of the experiment, there were no significant differences among locations, although after 500 and 1000 h significant differences ($p < 0.05$) appeared (Fig. 5), with smaller discharges observed in the emitters at the end of the 90 m long driplines. After 500 h, the three last emitters (positions 224, 225 and 226) had significantly lower ($p < 0.05$) discharges than the rest of emitters, with average values of 1.83, 1.83 and 1.49 l/h respectively. After 1000 h, the last four emitters (locations 223, 224, 225 and 226) had a lower discharge ($p < 0.05$) than the 222 previous ones, with values of 1.45, 1.22, 0.61 and 0.00 l/h respectively. This means that all the final emitters were completely clogged at the end of the experiment, whatever the filter was. In addition, the emitter located in position 221 showed also a smaller discharge than that of the previous 220 emitters, with the exception of emitters 213 and 218. After 1000 h, there was a flow discharge reduction in almost all the emitters compared with 500 h emitter flow rates, with this reduction accentuated along the lateral. Greater discharge reductions at the end of laterals have been widely observed by many authors (e.g. Ravina et al., 1992; Ravina et al., 1997; Trooien et al., 2000; Puig-Bargués et al., 2010a; Wu et al., 2015).

Moreover, significant differences ($p < 0.05$) in discharges between different times were found in almost all emitter locations, with the following combinations for emitter discharges: 0 h > 500 h > 1000 h, 0 h > (500 h = 1000 h), 0 h = 500 h = 1000 h, (0 h = 500 h) > 1000 h, and (0 h = 500 h and 500 h = 1000 h) but 0 h > 1000 h. A total of 77.68% of the emitter discharges were significantly higher ($p < 0.05$) at 0 h, but not between 500 h and 1000 h, and 11.61% were significantly different for all the measured times. In 5.80% of the emitters, discharge at 0 h was significantly different from that at 1000 h, but there were neither differences between 0 h and 500 h nor between 500 h and 1000 h. For 4.02% of the emitters, discharge at 0 h and 500 h was significantly higher than at 1000 h. Finally, 0.89% of emitters did not show any significant difference in discharge over time (Table 6).

3.4. Completely clogged emitters

The total number of totally clogged emitters after 500 h was 5 emitters (0.56% of the total) for the laterals protected by the porous media underdrain filter and 2 (0.22% of the total) for the dome underdrain filter. No clogged emitters for the arm collector underdrain filter were found. After 1000 h, the total number of clogged emitters was 10 for the porous media filter (1.13% of the total), 8 for the dome (0.91% of the total) and 6 for the arm collector underdrain filter (0.68% of the total). The emitter protected with dome underdrain in location 223 recovered from total clogging after 500 h to a flow rate of 0.36 l/h after 1000 h. Some authors had observed the recovery of clogged emitters and attributed this fact to a release of the material that plugged the emitter (Ravina et al., 1992; Duran-Ros et al., 2009) due to pressure variations or deformation of organic particles. Although the filter with porous media underdrain had turbidity removals significant higher

Table 6
Gradation and frequency of significant differences ($p < 0.05$) on emitter discharge and their location regarding assessment times.

Gradation regarding assessment times	Frequency of observations (%)	Emitter position (from 1 to 226)
0 h > 500 h > 1000 h	11.61	11, 12, 14, 15, 28, 36, 42, 66, 74, 127, 144, 145, 146, 148, 169, 170, 172, 181, 183, 195, 196, 198, 202, 214, 220, 226
0 h > (500 h = 1000 h)	77.68	Rest of emitters
0 h = 500 h = 1000 h	0.89	75, 216
(0 h = 500 h) > 1000 h	4.02	205, 208, 210, 211, 213, 218, 219, 221, 225.
0 h > 1000 h; 0 = 500 h and 500 = 1000 h	5.80	23, 72, 76, 77, 82, 124, 147, 204, 209, 212, 215, 223, 224

Table 7
Significance level (P-value) of the statistical model and of each factor and interaction for explaining the percentage of completely clogged variability during the experiment.

	Significance level (P-value)
Model	< 0.001
Time	< 0.001
Emitter location	< 0.001
Underdrain design	0.074
Underdrain design x time	0.572
Underdrain design x emitter location	0.994
Time x emitter location	< 0.001

than the other two designs, it presented a higher percentage of completely clogged emitters. A possible explanation could be that other particles such as small sized sand released from the filter might have clogged the emitter, but this was not observed, and it will be discussed on Section. 3.5. Thus, the randomness observed in clogging (Feng et al., 2018a) might also explain this observation.

The percentage of totally clogged emitters for each location was treated statistically, and there was a significant effect of time, emitter location and the interaction of both (Table 7). Either the effect of underdrain sand filter design or its interaction between time and emitter location were found to be significant ($p > 0.05$). These means that the different underdrain designs tested in the present experiment did not explain the percentage of completely clogged emitters. Regarding experiment time, after 500 h of irrigation significant differences ($p < 0.05$) of the percentage of completely clogged emitters among locations were found, with locations 224 and 225 (each one with 16.66% of completely clogged emitters) being significantly different from the rest except emitter number 223 (8.33% of totally clogged emitters) and emitter 226 (22.22% of completely clogged emitters). Completely clogged emitters for location 226 were significantly higher than those observed in locations 1-223. After 1000 h, location 226 had a significantly higher percentage of completely clogged emitters than the rest of emitter locations at this time. Emitter 225 also had a significantly higher percentage of completely clogged emitters (58.33%) than the emitters placed before and emitters 223 and 224 had, at the same time, a higher percentage of totally clogged emitters (25 and 33.33%, respectively) than that observed for the first 222 emitters (Fig. 6).

All the clogged emitters were located at the end of the lateral. Several studies show this same clogging emitter tendency (Trooien et al., 2000; Duran-Ros et al., 2009; Puig-Bargués et al., 2010a; Oliver et al., 2014) which can be attributed to a reduction flow rate at the end of the lateral (Shannon et al., 1982) and a greater concentration of particles (Wu et al., 2015). Despite the fact that reclaimed effluent was chlorinated after being filtered, at the end of laterals emitter discharges were lower (Sections 3.3.2 and 3.3.3) and more emitters became fully clogged. Some qualitative measurements of chlorine at the emitter outlet at the end of the lateral were made using chlorine test strips and, as it may be anticipated, the chlorine level was very low at this point since injection was carried out at a long distance away from the filters. Free chlorine levels between 1.5–2.5 mg/l at the end of the laterals

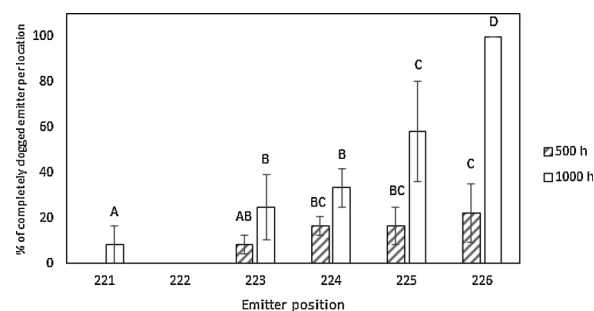


Fig. 6. Percentage of completely clogged emitters (%) per emitter location, after 500 and 1000 testing hours. For each time, different capital letters mean significant differences ($p < 0.05$) among locations.

effectively reduced emitter clogging (Li et al., 2010; Song et al., 2017).

It should be pointed out that no lateral flushing was carried out during the experiment in order to have more clogging incidence. Flushing reduces sediment deposition within driplines (Puig-Bargués et al., 2010b; Li et al., 2018) as well as biofilm formation (Oliver et al., 2014; Li et al., 2015). However, the number of completely clogged emitters was relatively small.

For each emitter location, only significant differences in the percentage of completely clogged emitters (Table 8) were found at position 224 (being the percentage at 1000 h higher than at 0 h but not than at 500 h) and 226 (being the percentage of 1000 h higher than the other two times).

3.5. Emitter observation

Emitters from the beginning and the end of the laterals were taken for observation after 1000 h. While there were not visually appreciable deposits on the emitters placed at the beginning of the laterals (Fig. 7A) for any irrigation subunit, biofilm growth was observed in those emitters located at the end of the laterals, especially at the final position (Fig. 7B), where biofilm covered the total surface of the emitter and the dripline. The amount of deposits increased along the ending locations and it was formed mainly of biofilm and sludge particles. These observations were in accordance with the findings of Ravina et al. (1992); Trooien et al. (2000); Duran-Ros et al. (2009) and Puig-Bargués et al. (2010a). No visual differences in the amount of deposits were observed between irrigation subunits, being the emitter of the last location completely covered in all the samples observed. No sand particles, which might be released from the sand filters, were visually observed in any of the emitters that were cut and opened. On the other hand, the observation of emitter labyrinths of the final locations (Fig. 7C) show an important biofilm growth near the water outlet. Biofilm composition was not analyzed since it was out of the scope of the paper and emitter sampling was carried out under conditions that not allowed to have representative biofilm results for each treatment. However, further research should be undertaken in order to characterize the features of the biofilm formed.

Table 8

Gradation and frequency of significant differences ($p < 0.05$) over assessment time on the percentage of completely clogged emitters (%) for each emitter location.

Gradation regarding assessment times	Frequency of observations (%)	Emitter position (from 1 to 226)
0 h = 500 h = 1000 h	99.12	Rest of emitters
1000 h > 0 h; 0 h = 500 h and 500 h = 1000 h	0.44	224
1000 h > (0 h = 500 h)	0.44	226

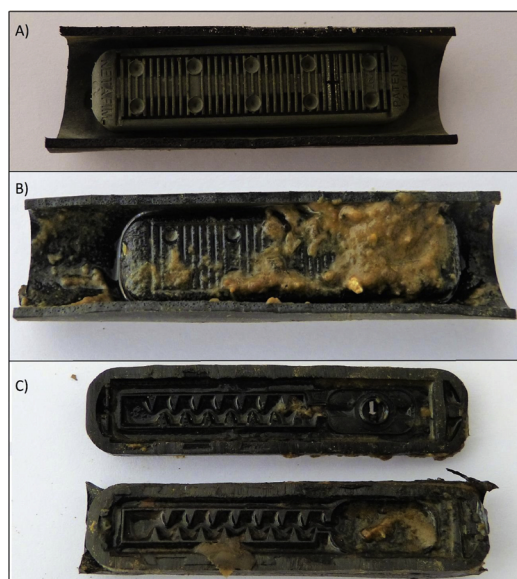


Fig. 7. External views of an emitter protected by the porous media underdrain filter placed at the first location (A) at last location (B), and inside view of the last one (C) after 1000 h of irrigation.

4. Conclusions

The present study was carried out to determine the effect of three different underdrain designs used for sand media filters on emitter clogging when using a chlorinated reclaimed effluent, with an average turbidity of 6.15 FTU and dissolved oxygen of 3.17 mg/l, during 1000 irrigation hours of 90 m length laterals that were not flushed during the whole experiment.

Emitter clogging was affected by the interactions between underdrain design, emitter location and irrigation time. Emitter location had a significant effect only after 500 h of operation, with significant differences among emitter discharge ($p < 0.05$) in the last three emitters (last 1.2 m of the lateral) and after 1000 h for those emitters located at the last 2 m of the laterals. There was also a significant reduction in emitter discharge that ranged from 9.6% to 12.35% depending on the filter design after 1000 h of irrigation. A significantly higher emitter discharge ($p < 0.05$) was observed in those emitters protected by a sand filter with arm collector underdrain, although this filter did not achieve the highest turbidity removals. There was also a location effect on emitter discharge among underdrain designs. The emitter discharge values were significantly lower from the final 4, 3, and 2 emitters when sand filter with a porous media, dome and arm collector underdrains, respectively, were used.

On the other hand, the percentage of completely clogged emitters depended on the interaction between irrigation time and emitter location, without any significant effect of any of the three different sand filter underdrain designs.

Based on the results, a sand filter with an arm collector underdrain design showed less emitter clogging when reclaimed effluent was used, but only after 1000 h of irrigation. For shorter times, clogging protection between the different tested filters was not different. However,

emitter clogging, which is a complex process, depended also on the interaction between irrigation time and emitter location. Further research should be carried out to analyse if different sand filter designs have a specific effect on any of the emitter clogging agents.

Acknowledgements

The authors would like to express their gratitude to the former Spanish Ministry of Economy and Competiveness for its financial support for this experiment through grant AGL2015-63750-R. Carles Solé-Torres was the recipient of a predoctoral scholarship (IFUDG2016/72) from the University of Girona. The authors would also like to thank the Municipality of Celrà for their help in carrying out this experiment.

References




- Al-Muhammad, J., Tomas, S., Anselmet, F., 2016. Modeling a weak turbulent flow in a narrow and wavy channel: case of micro-irrigation. *Irrig. Sci.* 34 (5), 361–377.
- Arbat, G., Pujol, T., Puig-Bargués, J., Duran-Ros, M., Montoro, L., Barragán, J., 2013. An experimental and analytical study to analyse hydraulic behaviour of nozzle-type underdrains in porous media filters. *Agric. Water Manage.* 126, 64–74.
- Asano, T., Burton, F.L., Leverenz, H.L., 2007. *Water Reuse: Issues, Technologies and Applications*. McGraw Hill Inc., New York.
- Bliesner, R.D., 1976. Field evaluation of trickle irrigation efficiency. in: *Proceedings of Water Management for Irrigation and Drainage ASCE*. pp. 382–393.
- Bové, J., Arbat, G., Pujol, T., Duran-Ros, M., Ramírez de Cartagena, F., Velayos, J., Puig-Bargués, J., 2015. Reducing energy requirements for sand filtration in microirrigation: improving the underdrain and packing. *Biosyst. Eng.* 140, 67–78. <https://doi.org/10.1016/j.biosystemseng.2015.09.008>.
- Bové, J., Puig-Bargués, J., Arbat, G., Duran-Ros, M., Pujol, T., Pujol, J., Ramírez de Cartagena, F., 2017. Development of a new underdrain for improving the efficiency of microirrigation sand media filters. *Agric. Water Manage.* 179, 296–305.
- Bucks, D.A., Nakayama, F.S., Gilbert, R.G., 1979. Trickle irrigation water quality and preventive maintenance. *Agric. Water Manage.* 2 (2), 149–162.
- Burt, C.M., 2010. *Hydraulics of Commercial Sand Media Filter Tanks Used for Agricultural Drip Irrigation*. Irrigation Training & Research Center, California Polytechnic State University, San Luis Obispo, California.
- Capra, A., Scicolone, B., 1998. Water quality and distribution uniformity in drip/trickle irrigation systems. *J. Agric. Engng. Res.* 70, 355–365.
- Capra, A., Scicolone, B., 2004. Emitter and filter tests for wastewater reuse by drip irrigation. *Agric. Water Manage.* 68, 135–149.
- Capra, A., Scicolone, B., 2007. Recycling of poor quality urban wastewater by drip irrigation systems. *J. Clean. Prod.* 15 (16), 1529–1534.
- Cararo, D.C., Botrel, T.A., Hills, D.J., Leverenz, H.L., 2006. Analysis of clogging in drip emitters during wastewater irrigation. *Appl. Eng. Agric.* 22 (2), 251–257.
- Dalahmeh, S.H., Pell, M., Vinnerås, B., Hylander, L.D., Öborn, I., Jönsson, H., 2012. Efficiency of bark, activated charcoal, foam and sand filters in reducing pollutants from greywater. *Water Air Soil Pollut.* 223, 3657–3671.
- Dehghanisani, H., Yamamoto, T., Ould Ahmad, B., Fujiyama, H.Y., Miyamoto, K., 2005. The effect of chlorine on emitter clogging induced by algae and protozoa and the performance of drip irrigation. *Trans. ASAE* 48 (2), 519–527.
- Duran-Ros, M., Puig-Bargués, J., Arbat, G., Barragán, J., Ramírez de Cartagena, F., 2008. Definition of a SCADA system for a microirrigation network with effluents. *Comput. Electron. Agric.* 64 (2), 338–342.
- Duran-Ros, M., Puig-Bargués, J., Arbat, G., Barragán, J., Ramírez de Cartagena, F., 2009. Effect of filter, emitter and location on clogging when using effluents. *Agric. Water Manage.* 96 (10), 67–79.
- Elbana, M., Ramírez de Cartagena, J., Puig-Bargués, J., 2012. Effectiveness of sand media filters for removing turbidity and recovering dissolved oxygen from a reclaimed effluent used for micro-irrigation. *Agric. Water Manage.* 111, 27–33.
- Enciso-Medina, J., Multer, W.L., Lamm, F.R., 2011. Management, maintenance and water quality effects on the long-term performance of subsurface drip irrigation systems. *Appl. Eng. and Agric.* 27 (6), 969–978.
- Feng, D., Kang, Y., Wan, S., Liu, S., 2017. Lateral flushing regime for managing emitter clogging under drip irrigation with saline groundwater. *Irrig. Sci.* 35, 217–225.
- Feng, J., Li, Y., Liu, Z., Muhammad, T., Wu, R., 2018a. Composite clogging characteristics of emitters in drip irrigation systems. *Irrig. Sci.* <https://doi.org/10.1007/s00271-018-0605-9>.
- Feng, J., Li, Y., Wang, W., Xue, S., 2018b. Effect of optimization forms of flow path on

- emitter hydraulic and anti-clogging performance in drip irrigation system. *Irrig. Sci.* 36 (1), 37–47.
- Gamri, S., Soric, A., Tomas, S., Molle, B., Roche, N., 2014. Biofilm development in micro-irrigation emitters for wastewater reuse. *Irrig. Sci.* 32 (1), 77–85.
- Green, O., Katz, S., Tarchitzky, J., Chen, Y., 2018. Formation and prevention of biofilm and mineral precipitate clogging in drip irrigation systems applying treated wastewater. *Irrig. Sci.* 36 (4–5), 257–270.
- Hamilton, A.J., Stagnitti, F., Xiong, X., Kreidl, S.L., Benke, K.K., Maher, P., 2007. Wastewater irrigation: the state of play. *Vadose Zone J.* 6 (4), 823–840.
- Hao, F.Z., Li, J., Wang, Z., Li, Y.F., 2018. Effect of chlorination and acidification on clogging and biofilm formation in drip emitters applying secondary sewage effluent. *Trans. ASABE* 61 (4), 1351–1363.
- Hills, D.J., Brenes, M.J., 2001. Microirrigation of wastewater effluent using drip tape. *Applied Eng. in Agric.* 17 (3), 303–308.
- Lazarova, V., Asano, T., 2005. Challenges of sustainable irrigation with recycled water. In: Lazarova, V., Bahri, A. (Eds.), *Water Reuse for Irrigation – Agriculture, Landscape and Turf Grass*. CRC Press, Washington D.C., USA.
- Li, J., Chen, L., Li, Y., Yin, J., Zhang, H., 2010. Effects of chlorination schemes on clogging in drip emitters during application of sewage effluent. *Appl. Eng. Agric.* 26 (4), 565–578.
- Li, G.B., Li, Y.K., Xu, T.W., Liu, Y.Z., Jin, H., Yang, P.L., Yan, D.Z., Ren, S.M., 2012. Effects of average velocity on the growth and surface topography of biofilms attached on the reclaimed wastewater drip irrigation system laterals. *Irrig. Sci.* 30, 103–113.
- Li, Y., Song, P., Pei, Y., Feng, J., 2015. Effects of lateral flushing on emitter clogging and biofilm components in drip irrigation systems with reclaimed water. *Irrig.Sci.* 33 (3), 235–245.
- Li, Z., Yu, L., Li, N., Chang, L., Cui, N., 2018. Influence of flushing velocity and flushing frequency on the service life of labyrinth-channel emitters. *Water* 10 (11), 1630.
- Maestre-Valero, J.F., Martínez-Álvarez, V., 2010. Effect of drip irrigation systems on the recovery of dissolved oxygen from hypoxic water. *Agric. Water Manage.* 97 (11), 1806–1812.
- Mesquita, M., Testezlaf, R., Ramirez, J., 2012. The effect of media bed characteristics and internal auxiliary elements on sand filter head loss. *Agric. Water Manage.* 115, 178–185.
- Nakayama, F.S., Boman, B.J., Pitts, D.J., 2007. Maintenance. In: Lamm, F.R., Ayars, J.E., Nakayama, F.S. (Eds.), *Microirrigation for Crop Production. Design, Operation, and Management*. Elsevier, Amsterdam, pp. 389–430.
- Oliver, M.M.H., Hewa, G.A., Pezzaniti, D., 2014. Bio-fouling of subsurface type drip emitters applying reclaimed water under medium soil thermal variation. *Agric. Water Manag.* 133, 12–23.
- Oron, G., Shelef, G., Turzynski, B., 1979. Trickle irrigation using treated wastewaters. *J. Irrig. Drain. Div.* 105 (IR2), 175–186.
- Pei, Y.T., Li, Y.K., Liu, Y.Z., Zhou, B., Shi, Z., Jiang, Y.G., 2014. Eight emitters clogging characteristics and its suitability evaluation under on-site reclaimed water drip irrigation. *Irrig.Sci.* 32 (2), 141–157.
- Puig-Bargués, J., Arbat, G., Elbana, M., Duran-Ros, M., Barragán, J., Ramírez de Cartagena, F., Lamm, F.R., 2010a. Effect of flushing frequency on emitter clogging in microirrigation with effluents. *Agric. Water Manage.* 97, 883–891.
- Puig-Bargués, J., Lamm, F.R., Trooien, T.P., Clark, G.A., 2010b. Effect of dripline flushing on subsurface drip irrigation systems. *Trans. ASABE* 53 (1), 147–155.
- Pujol, T., Arbat, G., Bové, J., Puig-Bargués, J., Duran-Ros, M., Velayos, J., Ramírez de Cartagena, F., 2016. Effects of the underdrain design on the pressure drop in sand filters. *Biosyst. Eng.* 150, 1–9.
- Ravina, I., Paz, E., Sofer, Z., Marcu, A., Shisha, A., Sagi, G., 1992. Control of emitter clogging in drip irrigation with reclaimed wastewater. *Irrig. Sci.* 13 (3), 129–139.
- Shannon, W.M., James, L.G., Basset, D.L., Mih, W.C., 1982. Sediment transport and deposition in trickle irrigation laterals. *Trans ASAE.* 25 (1), 160–164.
- Song, P., Li, Y., Zhou, B., Zhang, Z., Li, J., 2017. Controlling mechanism of chlorination on emitter bio-clogging for drip irrigation using reclaimed water. *Agric. Water Manage.* 184, 36–45.
- Tajrishy, M.A., Hills, D.J., Tchobanoglous, G., 1994. Pretreatment of secondary effluent for drip irrigation. *J. Irrig. Drain. Engrg.* 120 (4), 716–731.
- Tripathi, V.K., Rajput, T.B.S., Patel, N., 2014. Performance of different filter combinations with surface and subsurface drip irrigation systems for utilizing municipal wastewater. *Irrig. Sci.* 32, 379–391.
- Trooien, T.P., Lamm, F.R., Stone, L.R., Alam, M., Rogers, D.H., Clark, G.A., Schlegel, A.J., 2000. Subsurface drip irrigation using livestock wastewater: dripline flow rates. *Appl. Eng. Agric.* 16 (5), 505–508.
- Trooien, T.P., Hills, D.J., 2007. Application of biological effluent. In: Lamm, F.R., Ayars, J.E., Nakayama, F.S. (Eds.), *Microirrigation for Crop Production. Design, Operation, and Management*. Elsevier, Amsterdam, pp. 329–356.
- Wei, Q., Lu, G., Liu, J., Shi, Y., Dong, W., Huang, S., 2008. Evaluations of emitter clogging in drip irrigation by two-phase flow simulations and laboratory experiments. *Comput. Electron. Agric.* 63 (2), 294–303.
- World Health Organization, WHO, 2006. *Guidelines for the Safe Use of Wastewater, Excreta and Greywater, Vol II*. WHO Press, Geneva.
- Wu, W.Y., Huang, Y., Liu, H.L., Yin, S.Y., Niu, Y., 2015. Reclaimed water filtration efficiency and drip irrigation emitter performance with different combinations of sand and disc filters. *Irrig. and Drain.* 64, 362–369.
- Zhou, B., Li, Y.K., Pei, Y.T., 2013. Quantitative relationship between biofilms components and emitter clogging under reclaimed water drip irrigation. *Irrig. Sci.* 31 (6), 1251–1263.
- Zhou, B., Li, Y.K., Yaoza, L., Feipeng, X., 2015. Effect of drip irrigation frequency on emitter clogging using reclaimed water. *Irrig. Sci.* 33, 221–234.
- Zhou, B., Wang, D., Wang, T.Z., Li, Y.K., 2018. Chemical clogging behavior in drip irrigation systems using reclaimed water. *Trans. ASABE* 61 (5), 1667–1675.

5. ASSESSMENT OF FIELD WATER UNIFORMITY DISTRIBUTION IN
A MICROIRRIGATION SYSTEM USING A SCADA SYSTEM.

Article

Assessment of Field Water Uniformity Distribution in a Microirrigation System Using a SCADA System

Carles Solé-Torres, Miquel Duran-Ros, Gerard Arbat , Joan Pujol ,
Francisco Ramírez de Cartagena and Jaume Puig-Bargués * 

Department of Chemical and Agricultural Engineering and Technology, University of Girona,
Carrer Maria Aurèlia Capmany, 61, 17003 Girona, Catalonia, Spain

* Correspondence: jaume.puig@udg.edu; Tel.: +34-972-418-459

Received: 13 June 2019; Accepted: 27 June 2019; Published: 28 June 2019



Abstract: Microirrigation is an efficient irrigation technique, although when wastewater is used the probability of operation problems such as emitter clogging increases. In most of microirrigation systems, control of irrigation performance is manual and sporadic, therefore clogging problems may not be detected at the right time. As it is easier to prevent emitter clogging if it is detected earlier, close monitoring of pressure and flow rates in microirrigation systems is an important way to achieve microirrigation system requirements and accomplish higher irrigation efficiencies. A supervisory control and data acquisition (SCADA) system was used to monitor and control the performance of three microirrigation subunits; each one with four laterals, 90 m long with 226 emitters. The SCADA system monitored the pressure and flow across the irrigation laterals, and distribution uniformity coefficients were determined in real time, as they are indexes commonly used for evaluating drip irrigation systems. Results were compared with those experimentally obtained, showing a good correlation; although the emitter position had an important effect on the computed values. This work shows that a SCADA system can be easily used to continuously assess the pressure and water distribution uniformity without carrying out time-consuming manual field assessments.

Keywords: wastewater; drip irrigation; supervisory control; data acquisition; emitter clogging

1. Introduction

Microirrigation is the slow application of water on, above, or below the soil by surface drip, subsurface drip, bubbler, and microsprinkler systems [1]. Microirrigation has experienced an important growth over the past few decades, especially in developing countries [2] due to the need to save water since it is a technique that allows high irrigation efficiency, from 85 to 95% [1]. Moreover, microirrigation is the most appropriate technique for applying wastewater from both health and environmental points of view [3,4], in addition to being a viable alternative to deal with water scarcity [5], being especially important in areas with water scarcity.

One of the most commonly used parameters when designing and evaluating microirrigation systems is distribution uniformity (DU) [6]. DU expresses the variation of the emitter discharge of the irrigation system, which mainly depends on the hydraulic design, the coefficient of manufacturing variation, and emitter clogging [6,7]. Besides, DU allows detection and assessment of differences in water application and distribution in the crop and determining the causes, being able to reduce them and keep the irrigation system as close as possible to the uniformity system it was designed for [7]. For this reason, a regular evaluation of the irrigation system is also recommended.

Whenever the manufacturer's coefficient of variation (CVm) and the evaluated system installation is adequate, the DU is a good indicator of emitter clogging, which is one of the most common problems

in microirrigation systems. Emitter clogging can have physical, chemical, and biological causes, and can be especially important when low quality water such as wastewater is used [3,8].

One of the most frequent methods to determine the flow distribution uniformity coefficient (DU_{lq}) is that proposed by Merriam and Keller [9], which was also adopted by the Food and Agriculture Organization of the United Nations FAO [10]. The Merriam and Keller [9] method selects four locations of a secondary branch, one at the beginning, another at the end and the other two between the two previous ones and located at the same distance. From each lateral, it calculates the mean of the flow discharge of two contiguous emitters, each pair located at the beginning, 1/3, 2/3, and end of the length of the lateral. This way, from 32 volume measurements, 16 flows are obtained to calculate the DU_{lq} . The procedure and use of this method present some problems. On the one hand, from a statistical point of view, the selected locations do not represent the average flow discharge of all emitters or their variance. On the other hand, no reason is given for the recommendation to calculate the mean of the pair of emitters [11]. Moreover, Merriam and Keller method does not specify the exact emitter locations that should be evaluated. When it comes to end locations, measuring the last two emitters or measuring previous positions can significantly affect the DU_{lq} , since the end emitters are more prone to clogging [8,12,13].

More emitter discharge measurements or the measurements of all emitter flow discharges will be more representative for the calculation of the DU_{lq} ; but in real field conditions, it may be impractical [7] and will require more time and labour costs, as they are very laborious.

Precision irrigation saves water and money, and reduces run-off and energy consumption [14]. Irrigation scheduling using data from soil and plant sensors was the initial target of several precision irrigation studies on drip irrigation [15–17], but it was extended to microirrigation system design [18,19]. Supervisory control and data acquisition systems (SCADA) have been used to precisely manage the microirrigation systems [20,21] as well as the irrigation canal automation [22,23]. However, the use of SCADA systems for assessing microirrigation system performance has not yet been widely explored. Thus, the main objective of this work is to develop a procedure for allowing the usage of a SCADA system for assessing water distribution uniformity in a microirrigation system without manual measurements of emitter discharge under field conditions.

2. Materials and Methods

2.1. Experimental Setup

The experiment was carried out using the effluent produced at the wastewater treatment plant (WWTP) of Celrà (Girona, Spain), which treats the urban and industrial wastewaters using an activated sludge process as the secondary treatment. The treated wastewater was pumped into the experimental irrigation system, which consisted of three different irrigation subunits (called A, B, and C, respectively). Each irrigation subunit had a sand filter that differed in its underdrain design. Thus, in one irrigation unit an experimental sand filter built with a porous media underdrain designed by Bové et al. [24] was used, in another a sand filter model FA-F2-188 (Regaber, Parets del Vallès, Spain) was installed, and the third one had a sand filter model FA1M (Lama, Sevilla, Spain). The three sand filters were filled with silica sand of the same characteristics (effective diameter (D_e , size opening which will pass 10% by dry weight of a representative sample of the filter material) of 0.48 mm and coefficient of uniformity (ratio of the size opening which will pass 60% of the sand through the size opening which will pass 10% through) of 1.73). Each irrigation subunit consisted of four laterals with a total length of 90 m each (Figure 1). Commercially integrated and pressure compensating emitters Uniram AS 16010 (Netafim, Tel Aviv, Israel), with 2.3 L/h of nominal flow discharge, a distance between emitters of 0.4 m, a nominal working pressure of 50–400 kPa, and a manufacturing coefficient of variation of 0.03 were used. Driplines had an outside diameter of 16.2 mm and a wall thickness of 1.0 mm. Each lateral had 226 emitters, so there were 904 emitters per irrigation subunit.

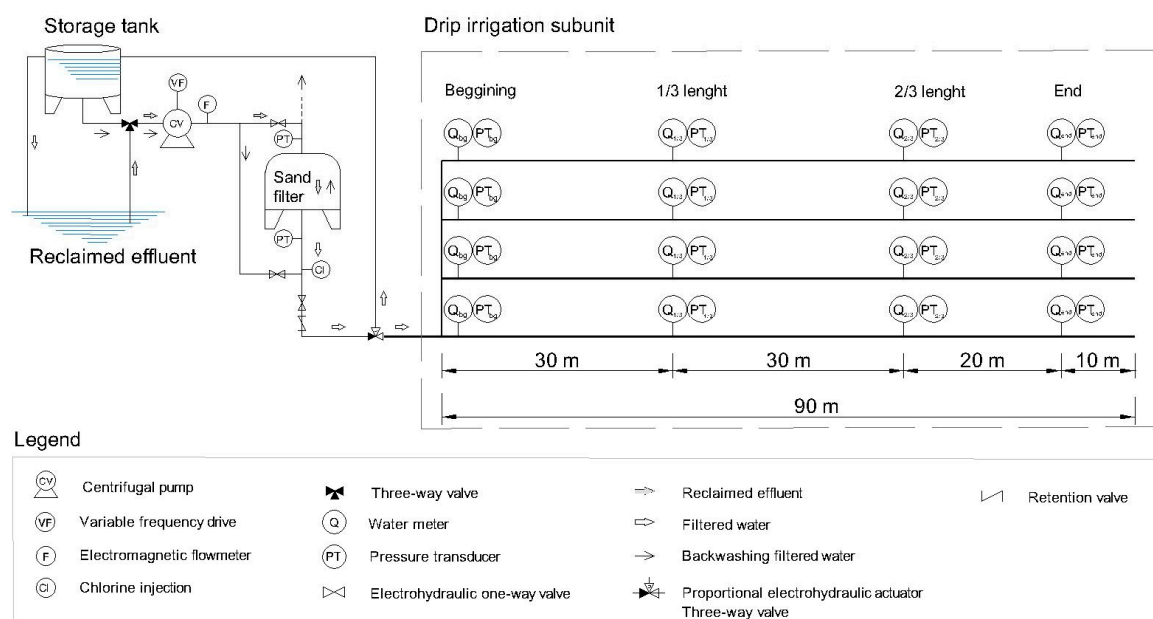


Figure 1. Diagram of the experimental irrigation system. For simplicity, only one out of the three drip irrigation subunits is depicted.

2.2. Monitoring Equipment

A multicellular centrifugal pump model CR-15-4 with a rated flow of 12 m³/h and a rated pressure of 500 kPa (Grundfos, Bjerringbro, Denmark) governed by a variable frequency drive model FRN-4 (Fuji Electric, Cerdanyola del Vallès, Spain) pumped the wastewater from the WWTP to the subunits, with the inlet flow measured by an electromagnetic flowmeter Isomag MS2500 (Isoil Industria SpA, Cinisello Balsamo, Italy). Only one irrigation subunit was operating at a time. Since the filtrated flow was higher than that needed for the irrigation subunits, a proportional electrohydraulic actuator SKD32 (Siemens, Munich, Germany) operated a three-way valve VXG41 (Siemens, Munich, Germany), so that the excess flow was brought to a water storage tank of 3000 L Aquablock (Shütz, Selters, Germany) which was used for filter backwashing. The experimental irrigation system also had a chlorine deposit of 200 L in order to continuously inject chlorine to achieve a concentration of 2 mg/L into the effluent after being filtered, using a DosTec AC1/2 membrane pump (ITC, Sta. Perpètua de Mogoda, Spain), aiming to reduce biofilm growth and, consequently, emitter clogging [25]. When sand filters were backwashed, backwashing water entering the filters was chlorinated to reach a 4 mg/L chlorine concentration. The filters were washed automatically when the total pressure drop across them measured by pressure transducers model TM-01/C (Step S.L., Barcelona, Spain), with a measuring operational range from 0 to 600 kPa and an accuracy of $\leq \pm 0.5\%$ full scale, reached 50 kPa [8]. The backwashing time was 3 min throughout the test, and during that time, backwashing water did not reach the laterals. The water used for the backwashing came from the filtered water storage tank.

Several effluent quality parameters before and after being filtered were measured and recorded. At filter inlet, electrical conductivity was measured with a transmitter LIQUISYS-M CLM253-CD0010 and a sensor CLS21-C1E4A, and pH and temperature using a transmitter LIQUISYS-M CPM253-MR0010 and a sensor CPS11D-7BA21. At both filter inlet and outlet, turbidity was measured using a transmitter LIQUISYS-M CUM253-TU0005 and a sensor CUS31-A2E, and dissolved oxygen using a transmitter LIQUISYS-M COM253-WX0015 and a sensor COS 61-A1F0. All the transmitters and sensors used were made by Endress + Hauser (Gerlingen, Germany).

Each lateral of each irrigation subunit had water meters and pressure transducers at the beginning, 1/3 of the length, 2/3 of the length, and at the end of the lateral; so there were a total of 16 water meters and 16 pressure transducers for each irrigation subunit (Figure 2). The water meters used were model

405S DN15 (Sensus, Raleigh, NC, USA) with an operational range from 0.3 to 3 m³/h and a precision of $\pm 5\%$ full scale installed with an impulse emitter HRI-A1 (Sensus, Raleigh, NC, USA). This allowed the flow to be calculated in real time. Pressure transducers, model TM-01/C (Step S.L., Barcelona, Spain) with a measuring operational range from 0 to 250 kPa and an accuracy of $\pm 0.5\%$ full scale were used. The water meters and pressure transducers located at the end of the lateral were placed 10 m before the dripline distal end (Figure 1) to ensure that the volume measured was high enough to be within the measurement range.



Figure 2. View of the pressure transducers and water meters of the irrigation subunits.

2.3. SCADA System and Components

The SCADA system that was implemented consisted of a personal computer, a programmable automaton, a set of activators and recorders, and a communication network for both of them. All these elements, which allowed measurement of flow and volume, pressure and water quality parameters generated a digital signal or an electric impulse from 4 to 20 mA, which was transformed later to a digital format (16 bits) and stored by a SCADA initially developed by Duran-Ros et al. [26] but was further modified for this experiment.

The personal computer sent data and commands to the programmable automaton and at the same time received data from it. Data were organized, classified, and filed on the computer, which also operated as an interlayer between the user and the installation. The personal computer was an EliteDesk (HP, Palo Alto, CA, USA) with a processor IntelCore I3, with 2.7 GHz and 8 MB de RAM, with an operational system Windows 7 (Microsoft, Redmon, WA, USA). Besides, the computer had the visualization software RSView32 (Rockwell Software, Milwaukee, WI, USA) for the development of human/machine interface.

A programmable automaton, model Compact Logix (Allen-Bradley, Milwaukee, WI, USA) communicated with a remote headboard 1734A (Allen-Bradley, Milwaukee, WI, USA) and accepted orders from the personal computer, to which data were also sent. Communication between devices was via Ethernet (Index protocol) with a 5th category wire. Figure 3 shows the communication network.

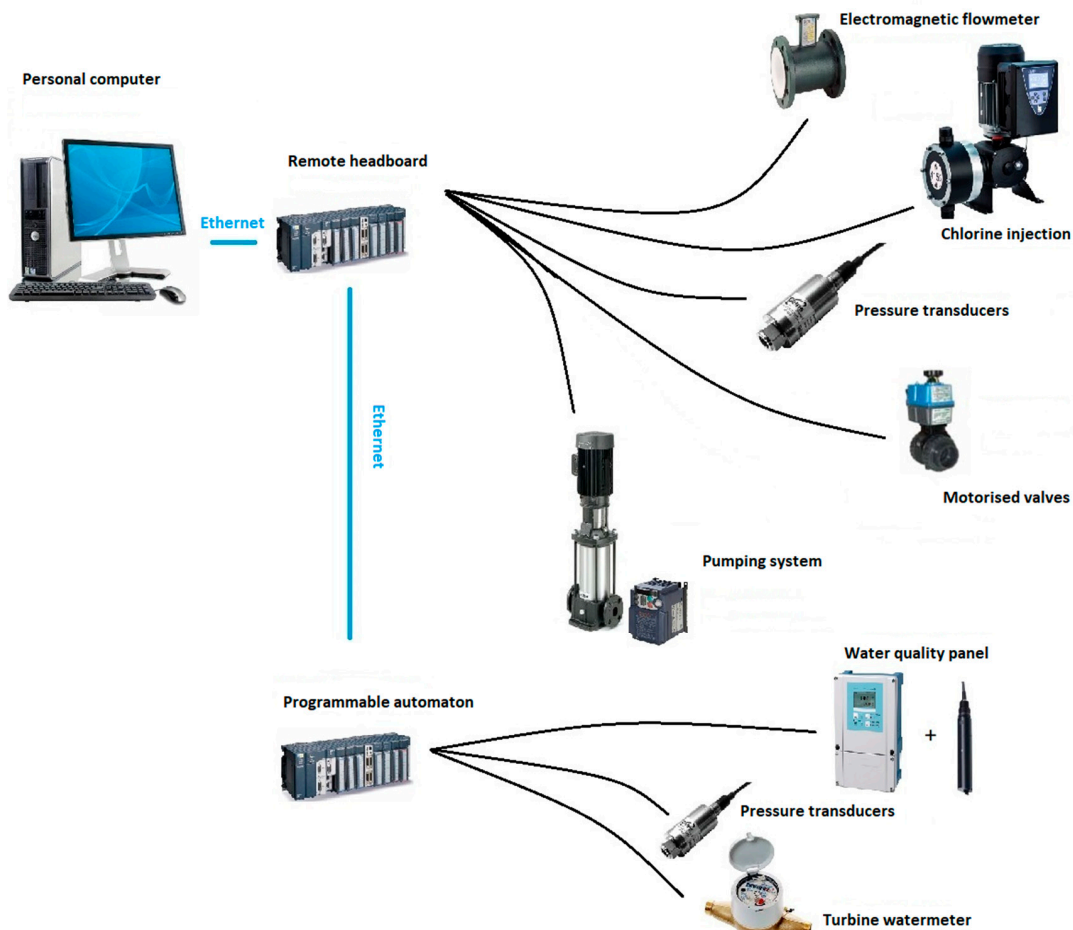


Figure 3. Communication network of the supervisory control and data acquisition (SCADA) system developed.

Programmable automaton consisted of eight modules with electrical source and input and output modules, and commanded the field automatons:

- Two modules 1769-IQ32 (Allen-Bradley, Milwaukee, WI, USA) with 32 digital inputs each having a direct current of 24 V to detect current flow from lateral water meters and pressure transducers.
- One module 1769-OB16 with 16 digital outputs to activate quality panel valves.
- Three modules 1769-IF16C with 16 analogic inputs with a range of measurement from 4 to 20 mA and a 16-bit resolution, connected to lateral water meters and pressure transducers.
- Two modules 1769-IF4I with four analogic inputs with a range of measurement from 4 to 20 mA and a 16-bit resolution, connected to quality panel transmitters.

Remote headboard ruled the bank filtration automatons and was composed of nine modules:

- Two modules 1734-IB8 with eight digital inputs of direct current of 24 V to detect direct current flow from the four washing triggers of the quality panel, emergency stop, water level sensor of the catch basin, and filtered tank and chlorine tank sensor level.
- Three modules 1734-IEOB8 with eight digital outputs to activate motorized valves and pumping system.
- Three modules 1734-IE8C with eight analogic inputs with a measurable range from 4 to 20 mA and a 16-bit resolution and connected to the headboard flowmeter, quality panel water meters, and to the filter pressure transducers.

- One module 1734-OE4C with four analogic outputs with a measurable range from 4 to 20 mA and a 16-bits resolution connected to the variable frequency drive, headboard centrifugal pump, proportional valve, and the chlorine injection system.

For the automatons that needed electricity supply, two alimentation sources were chosen 1606-XLE-80-E (Alley-Bradley, Milwaukee, WI, USA) which gave 80 W power with 24 V of direct current.

Data from the devices were recorded every minute for the duration of the 1000 h experiment, and could be supervised in real time using the developed human/machine interface. It was also possible to access the personal computer of the experimental setup from any device connected to Internet. For making that possible, a modem model E612 (Huawei, Bantian, China) was installed, with a SIM card (Subscriber Identity Module). By the use of the program Escritorio Movistar (TelefónicaS.A., Madrid, Spain) it was possible to connect to the Internet.

The Internet service hired allocated a variable IP (Internet Protocol) direction. To gain remote access and to be able to control the installation, a TeamViewer program with GPL (General Public License) was used.

2.4. Quality of the Wastewater

Using the monitoring equipment and the SCADA system described in Sections 2.3 and 2.4, respectively, the main wastewater quality parameters were recorded each minute. Table 1 shows the mean values of pH, temperature, electrical conductivity, dissolved oxygen, and turbidity during the experiment.

Table 1. Average \pm standard deviation of the main physical and chemical parameters of wastewater before and after being filtered. Different letters mean that there were significant differences ($p < 0.05$) in the values of each parameter.

Subunit	Filter Inlet				Filter Outlet		
	pH (-)	Temperature (°C)	Electrical Conductivity (dS/m)	Dissolved Oxygen (mg/L)	Turbidity (FTU)	Dissolved Oxygen (mg/L)	Turbidity (FTU)
A	7.33 \pm 0.20 b	20.61 \pm 3.26 a	2.64 \pm 0.46 a	3.27 \pm 0.83 b	6.22 \pm 2.11	3.31 \pm 0.82 b	4.46 \pm 1.24 b
B	7.43 \pm 0.24 a	20.12 \pm 3.49 ab	2.46 \pm 0.53 b	3.57 \pm 1.02 a	5.82 \pm 3.08	3.56 \pm 1.04 a	4.18 \pm 1.42 c
C	7.31 \pm 0.22 b	19.68 \pm 3.57 b	2.63 \pm 0.44 a	3.28 \pm 1.04 b	6.42 \pm 2.77	3.25 \pm 0.65 b	4.89 \pm 1.13 a

There were significant differences ($p < 0.05$) for pH, temperature, electrical conductivity, and dissolved oxygen at filter inlets and for dissolved oxygen and turbidity at filter outlet. The variations observed are due to the usual variability in wastewaters. According to Bucks et al. classification [3], the wastewaters pose a moderate chemical clogging hazard and a minor physical clogging hazard.

2.5. Operational Procedure and Data Treatment

The experiment lasted 1000 h for each irrigation subunit, taking place between March and November 2018, and no lateral flushing was carried out during the experiment.

Emitter discharges (observed measures) for all the emitters of all the laterals (i.e., 2712 emitters) were obtained at the beginning, after 500 h and at the end of the experiment (1000 h). In order to measure flow discharge, the volume of each dripper was collected in collection recipients for 5 min and then transferred to a graduated cylinder, with a volume between 100 and 250 mL being collected as recommended by Merriam and Keller [9]. The experimental determination of emitter discharge lasted about 20 h after the target time (0, 500, and 1000 h) due to the number of emitters to be measured. With emitter discharge values for all the emitters in a lateral, the total lateral flow discharge was obtained. In addition, the total water flow at each section of the lateral (Figure 1) was also known.

Following the Merriam and Keller method [9] method, the flow discharge of the two contiguous emitters placed at the beginning, at 1/3, 2/3, and at the end of each lateral length was measured, assuming the mean of the two measurements as representative flow discharge.

Pressure was also determined in these four positions on each lateral during the emitter discharge measurements using a digital manometer Leo 2 (Keller, Winterthur, Switzerland) with a precision of $\pm 0.07\%$ that was placed at a pressure intake (Ein-tal, Or-Akiva, Israel). Distribution uniformity of pressures (DU_{lp}) [27] was calculated according to the formula:

$$DU_{lp} = \left(\frac{p_{25}}{\bar{p}} \right)^x \times 100 \quad (1)$$

where p_{25} is the average pressure of 25% of the positions with the lowest pressure (kPa), \bar{p} is the average pressure of all the tested positions (kPa), and x is the emitter flow exponent, which was considered 0.05.

With all emitter flow discharges, flow distribution uniformity (DU_{lq}) was calculated as:

$$DU_{lq} = \frac{q_{25}}{\bar{q}} \times 100 \quad (2)$$

where, q_{25} is the average flow discharge of 25% of the emitters with the lowest flow discharge (L/h) and \bar{q} is the average flow discharge of all the tested emitters (L/h).

To determine the flow uniformity distribution through the SCADA system, the recorded values during the real measurements of the emitters for each irrigation subunit (at 0 h, 500 h, and 1000 h) were selected. The dripline flow at the beginning, 1/3, and 2/3 lateral length represented the flow of all emitters from the measured point to the end, and the flow at the end represented the flow of the end emitters (last 10 m) (Equation (3)). For that reason, to determine the flow of each lateral stretch, the subsequent measured flow was subtracted from the previous measured flow, following Equations (4)–(6).

$$q_{end} = Q_{end} \quad (3)$$

$$q_{2/3} = Q_{2/3} - Q_{end} \quad (4)$$

$$q_{1/3} = Q_{1/3} - Q_{2/3} \quad (5)$$

$$q_{bg} = Q_{bg} - Q_{1/3} \quad (6)$$

where, Q_{end} is the measured flow at the last water meter (L/h), $Q_{2/3}$ is the measured flow located at 2/3 of the lateral length (L/h), $Q_{1/3}$ is the measured flow located at 1/3 of the lateral length (L/h), Q_{bg} is the measured flow located at the beginning of the lateral (L/h), q_{end} is the estimated flow of the emitters placed at the end of the lateral (L/h), $q_{2/3}$ is the estimated flow of the emitters placed between 2/3 and end water meters (L/h), $q_{1/3}$ is the estimated flow of the emitters placed between locations 1/3 and 2/3 of the lateral (L/h), and q_{bg} is the estimated flow of the emitters placed from the beginning to 1/3 of the lateral (L/h).

Then, the estimated flow for each lateral stretch was divided by the number of emitters in each stretch in order to obtain the average emitter flow discharge for every emitter of each dripline section. So, every lateral had four average emitter discharge values, each of which represented a section, and consequently, every irrigation subunit had sixteen average emitter discharge values. With these values, DU_{lq} for SCADA system was calculated following Equation (2).

Relative flow was also calculated throughout the experiment as:

$$q_r = \frac{q_h}{q_0} \times 100 \quad (7)$$

where, q_r is the relative flow in a precise time (%), q_h is the flow of a precise time (h) (L/h), and q_0 is the initial flow at 0 h (L/h).

The reduction percentage of relative flow (q_r) and DU_{lq} with respect to their initial values was calculated as:

$$\Delta V = \frac{V_0 - V_i}{V_0} \times 100 \tag{8}$$

where, ΔV is the reduction percentage (%), V_0 is the initial value, and V_i is the value that needs to be compared.

Mean separation and regression statistical analyses were carried out using SPSS Statistics 25 software (IBM, NY, USA) with a significance level of 0.05.

3. Results and Discussion

3.1. Pressure Distribution across Laterals

Pressure distribution uniformity (DU_{lp}) values were higher than 98% in all the measurements for all the times (Table 2). Pressure distribution uniformity values meant that the experimental irrigation system was well designed and, since the emitter manufacturing coefficient of variation was low (3%), discharge reductions can mainly be explained by emitter clogging.

Table 2. Pressure distribution coefficients (DU_{lp} , %) of the three irrigation subunits (A, B, and C) at the beginning, after 500 h, and at the end of the experiment measured with the Merriam and Keller [9] and SCADA procedures.

Irrigation Time	0 h			500 h			1000 h			Mean ± Standard Deviation
	A	B	C	A	B	C	A	B	C	
Merriam and Keller (M&K)	98.75	98.66	98.80	98.77	98.27	99.12	99.03	99.04	98.92	98.82 ± 0.26
SCADA	98.94	98.88	98.70	99.00	98.31	99.13	99.13	98.88	98.90	98.88 ± 0.25

Figure 4 shows the regression between DU_{lp} calculated in the field using data from the emitters located at those points suggested by Merriam and Keller [9] and that computed using data from pressure transducers located at different driplines points and recorded by the SCADA system. There was a high regression between both methods, with an $R^2 = 0.93$ and a signification level of $p < 0.01$.

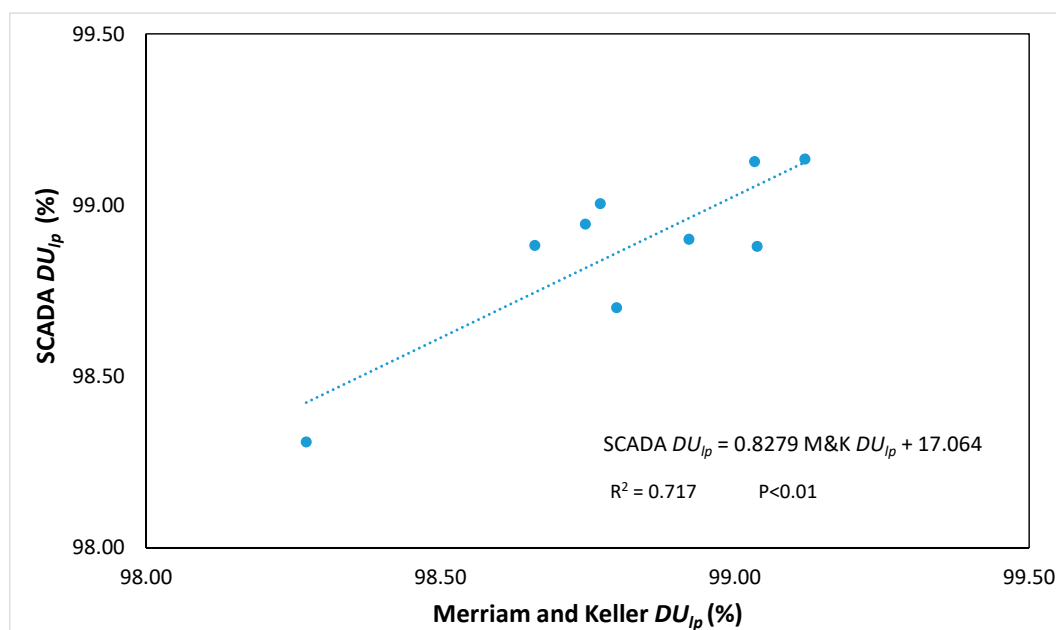


Figure 4. Relationship between observed DU_{lp} (%) following Merriam and Keller procedure and DU_{lp} (%) recorded by the SCADA system at the beginning, after 500 h, and 1000 h of the experiment.

3.2. Measured SCADA Flow Distribution across Laterals

Figure 5 shows the regression between the observed field accumulated emitter discharges and those measured by the SCADA system following the procedure described in Section 2.4. There was a high regression coefficient ($R^2 = 0.99$) between the observed flows and the SCADA flows, with a significance level of $p < 0.001$, which validates that water meter measurements at the dripline and recorded into a SCADA system as a good measurement tool for the real flow of the irrigation subunits for the entire duration of the experiment.

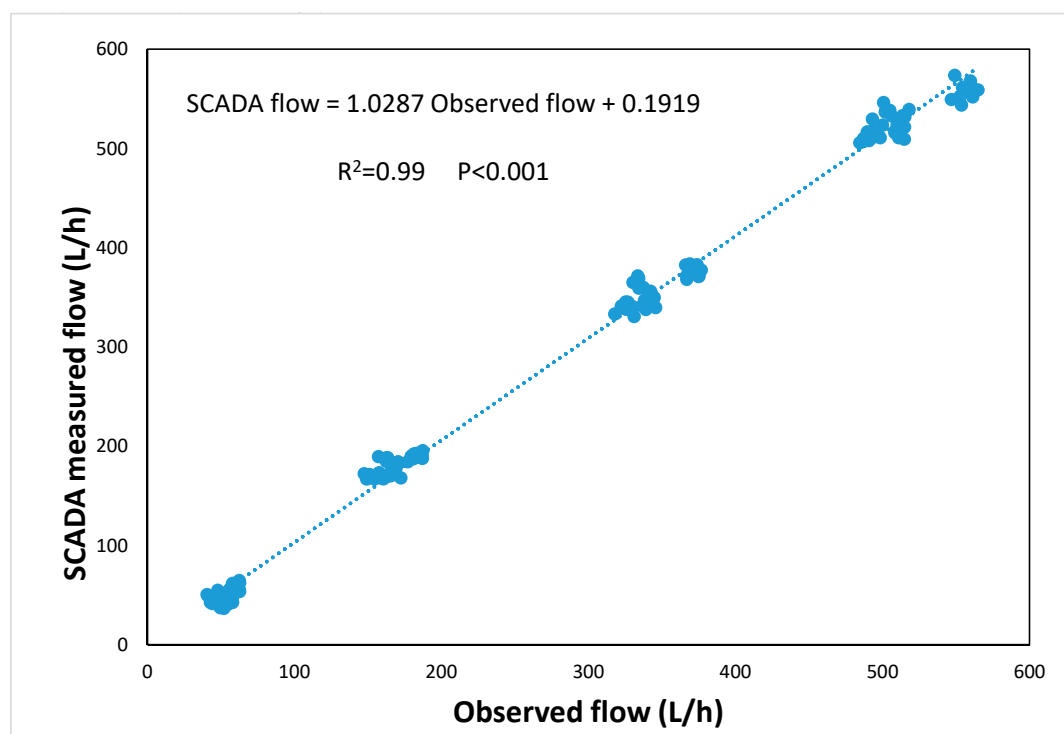


Figure 5. Relationship between the observed flow (L/h) and the measured flow by the SCADA system (L/h) for all water meters at different locations and measuring times.

3.3. Dripline Flow Evolution throughout the Experiment

There was a decrease in the flow that went to the irrigation subunits, for all laterals of all subunits with irrigation time. This flow reduction was due to emitter clogging, which commonly happens when low quality waters such as wastewaters, are used in drip irrigation systems [8,13]. Figure 6 shows the average relative flow (q_r), computed following Equation (7) with data of the four water meters placed at the beginning (Q_{bg}) of each lateral, for each irrigation subunit throughout the experiment. Specific increases in the flow were due to factors such as the switch on and off of the irrigation system, unblocking of the water meters' protective filters, or emitter discharge variations. For all irrigation subunits, there was a decrease in the q_r along the accumulated irrigation time. The flow decrease was more accentuated from the beginning to 500 h for all irrigation subunits. From 500 h to 750 h of the experiment, q_r of the subunit A remained more or less constant, but it decreased slightly during the last 250 h. A similar behavior was observed for subunit B, where q_r suffered small variation from 500 h to 780 h, but then it suddenly decreased until the end of the experiment. On the other hand, subunit C q_r remained constant for almost all the experiment, with a little increase in the end.

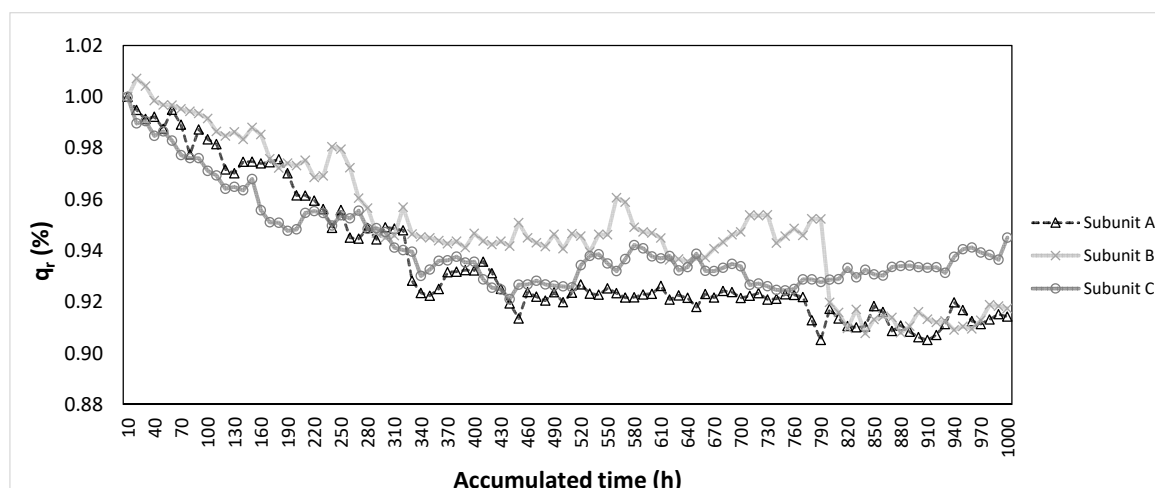


Figure 6. Average relative flow of the four water meters placed at the beginning for each irrigation subunit along the 1000 h experiment.

Variation of DU_{lq} along the experiment can be explained by the flow variation observed in each irrigation subunit. As field DU_{lq} was measured using data of all emitters at the beginning, after 500 h, and 1000 h, the total flow variation with respect to the initial value of the first water meter was measured as well as DU_{lq} was computed using Equation (8) (Table 3). A low correlation between the DU_{lq} variation (ΔDU_{lq}) and q_r variation (Δq_r) of the first water meter was observed, with an $R^2 = 0.34$ but was not significant ($p > 0.05$). Thus, despite the fact that measuring the whole flow entering in a dripline will be the easiest way for measuring DU_{lq} , it is not accurate enough to use it, especially when emitter clogging is observed over time. It will be interesting to carry out further research using water meters located at different positions in order to find out if a correlation exists between the flow variation of specific water meters and the DU_{lq} variation.

Table 3. Relative flow (q_r) and relative flow variation (Δq_r), distribution uniformity coefficient (DU_{lq}) and distribution uniformity coefficient variation (ΔDU_{lq}) at the beginning, after 500, and 1000 h of each irrigation subunit.

Irrigation Subunit	Irrigation Time (h)	q_r	Δq_r	DU_{lq}	ΔDU_{lq}
A	0	1.00	-	95.41	-
	500	0.92	8.02	92.83	2.70
	1000	0.91	8.58	89.18	6.53
B	0	1.00	-	93.97	-
	500	0.94	5.93	93.07	0.96
	1000	0.92	8.26	87.88	6.48
C	0	1.00	-	96.31	-
	500	0.93	7.40	94.84	1.53
	1000	0.94	6.37	91.44	5.06

3.4. Comparison of Different Procedures for DU_{lq} Determination

As Merriam and Keller (M&K) method does not specify which exact emitter location should be used to calculate DU_{lq} , this index was calculated with different alternative emitter locations at the end of the lateral. Thus, DU_{lq} was calculated taking the final two emitters (M&K_{1/2}), the second and third emitters starting from the distal end of the lateral (M&K_{2/3}), the 5th and 6th (M&K_{5/6}), and the 20th and 21th (M&K_{20/21}). The results of the DU_{lq} are shown in Table 4.

Table 4. DU_{lq} calculated for different methods (Merriam and Keller (M&K) observed for all emitters and SCADA) for each irrigation subunit at the beginning, after 500, and 1000 h of the experiment, and its regression significance level with the SCADA method.

Time	DU_{lq} (%)									p -Value of Regression with SCADA Procedure
	0 h			500 h			1000 h			
Subunit	A	B	C	A	B	C	A	B	C	
M&K _{1/2}	95.15	96.28	97.82	41.37	82.55	94.74	28.61	0.00	33.86	<0.05
M&K _{2/3}	94.85	96.06	97.67	66.36	82.13	95.74	46.57	33.55	60.89	<0.01
M&K _{5/6}	96.49	93.60	97.75	95.02	93.14	95.08	85.29	84.81	92.98	<0.01
M&K _{20/21}	95.57	95.47	96.76	92.62	94.40	96.27	90.23	90.46	95.96	<0.001
Observed	95.41	93.97	96.31	92.83	93.07	94.84	89.18	87.88	91.44	<0.01
SCADA	90.54	91.71	95.50	85.35	88.93	96.03	79.26	76.92	94.66	-

Although for the initial stages of the experiment DU_{lq} did not vary much between the methods, after 500 and especially 1000 h these differences were accentuated, due to a different DU_{lq} calculation and the effect of emitter clogging. There was a great variation among the DU_{lq} calculated with different emitter locations following the Merriam and Keller method. Lower DU_{lq} values were obtained for the emitters of final locations (M&K_{1/2} and M&K_{2/3}) than for the emitters located closer to the beginning of the lateral (M&K_{5/6} and M&K_{20/21}), especially after 1000 h to the experiment, when there is more variability of emitter discharge, mainly due to emitter clogging [7,11]. Merriam and Keller method was penalized due to it taking the emitter discharges of the end of the lateral, although these emitter discharges may not be representative of all emitter discharges of the end section, as end locations are more prone to be partially or completely clogged [12] and affect the DU_{lq} calculation (Equation (2)). On the other hand, DU_{lq} obtained with drippers closer to the dripline beginning are higher. This shows which emitter locations should be taken into account when calculating the DU_{lq} according to Merriam and Keller method, in order to be as representative as possible of the emitter discharges of the irrigation subunit. Merriam and Keller DU_{lq} adjust more to the observed DU_{lq} if emitters placed further away from the end are taken into account.

The different DU_{lq} obtained with the Merriam and Keller method were related with DU_{lq} obtained with the SCADA system (Figure 7). For the DU_{lq} taking the last two emitters of the laterals (M&K_{1/2}), the regression coefficient was low ($R^2 = 0.58$), but it increased when other two contiguous emitters were used: $R^2 = 0.68$ for M&K_{2/3}, $R^2 = 0.72$ for M&K_{5/6}, $R^2 = 0.97$ for M&K_{20/21} and $R^2 = 0.69$ for DU_{lq} obtained with all the observed emitter discharges. Although all regressions were statistically significant, the significance level of M&K_{1/2} was lower ($p < 0.05$) than that for M&K_{2/3}, M&K_{5/6}, and Observed ($p < 0.01$). The regression with SCADA values and M&K_{20/21} showed the highest significance level ($p < 0.001$).

Overall, the SCADA DU_{lq} had an acceptable correlation to DU_{lq} measured with all the emitters. A better correlation and better level of significance were observed between SCADA and M&K procedures when this last method took into account the emitters placed closer to the beginning of the lateral. So, DU_{lq} prediction with SCADA system is a good method of calculation that can replace existing methods such as M&K when measured emitters locations are not those at the very end. In addition, this method would allow the DU_{lq} monitoring in real time without needing manual field uniformity assessments, with the time and labour cost savings that entails. The proposed system would allow the possibility of determining more frequent DU_{lq} calculations, having a DU_{lq} control over time, and would also easily allow subsurface drip irrigation DU calculation. On the other hand, the cost of the instruments and sensors have to be taken into account since investment cost is high and cannot be affordable for some farmers.

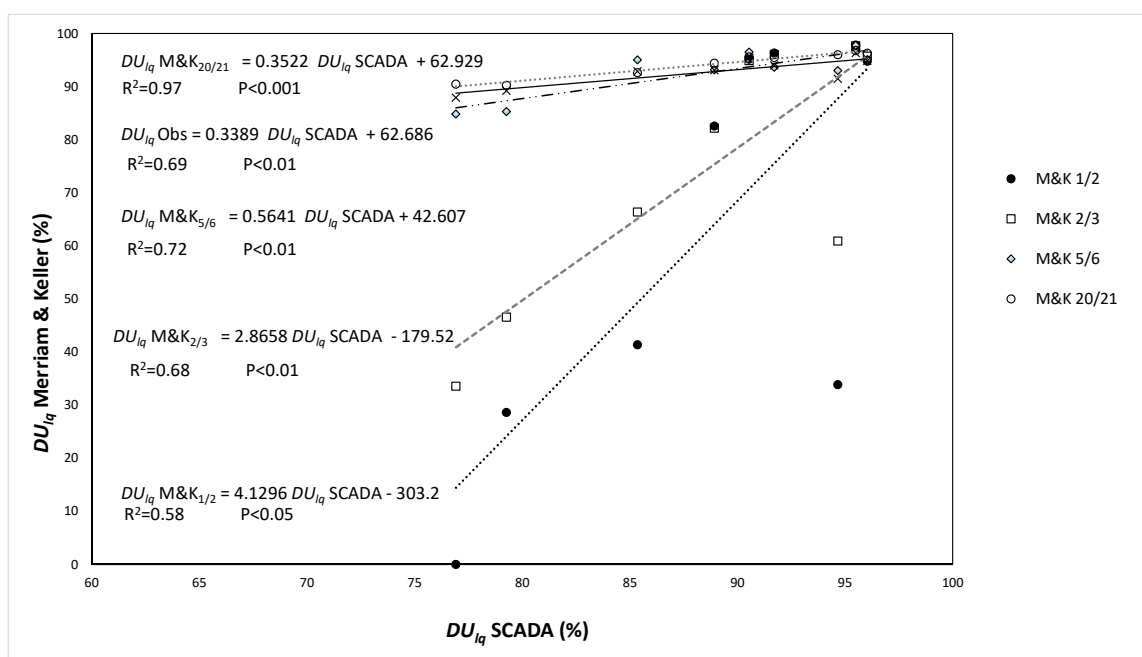


Figure 7. Relationship between DU_{lq} SCADA and DU_{lq} using Merriam and Keller method taking different end emitters, and DU_{lq} for all emitters (Observed).

4. Conclusions

A supervisory control and data acquisition (SCADA) system allowed to accurately measure the water distribution uniformity in a microirrigation system when using wastewater. Distribution uniformity of pressure and emitter discharges experimentally measured in field conditions showed high regression levels ($R^2 = 0.93$ and 0.99 , respectively) with data recorded in the SCADA system from pressure transducers and water meters placed at strategic dripline positions. Therefore, SCADA can be used for measuring both pressure and flow discharge of a microirrigation system, which in addition allows monitoring the performance of the irrigation system. The SCADA system will also allow detection of operation anomalies in real time, shortening the time needed for solving them.

SCADA can be a good tool to calculate flow distribution uniformity (DU_{lq}) of an irrigation system instead of using existing methods such as Merriam and Keller, especially when last emitter locations are not taken into account. Results also showed the incidence of emitter clogging in the DU_{lq} calculation, and indicate which emitter locations should be measured when determining DU_{lq} , in order to be representative of the lateral section. Moreover, SCADA will allow calculating DU_{lq} without the need for annual field measurements, saving labour costs, in spite of its high investment cost.

The proposed method presents automation advantages as it considers indirectly all the irrigation emitters, so DU_{lq} calculation is as affected by emitter clogging as the Merriam and Keller method. In addition, the proposed method also allows evaluating subsurface irrigation installations that will be impossible to evaluate without digging out the laterals.

Author Contributions: Conceptualization, F.R.d.C., M.D.-R., G.A., J.P., and J.P.-B.; methodology, F.R.d.C., M.D.-R., G.A., C.S.-T., and J.P.-B.; formal analysis, C.S.-T., M.D.-R., and J.P.-B.; investigation, C.S.-T. and M.D.-R.; data curation, C.S.-T., M.D.-R., J.P., and J.P.-B.; writing—original draft preparation, C.S.-T., M.D.-R., and J.P.-B.; writing—review and editing, F.R.d.C., G.A., J.P., and J.P.-B.

Funding: This research was funded by the former Spanish Ministry of Economy and Competiveness, grant AGL2015-63750-R. C.S.-T. was the recipient of a predoctoral scholarship (IFUdG2016/72) from the University of Girona.

Acknowledgments: The authors would also like to thank the Municipality of Celrà for their help in carrying out this experiment, and the help provided by Pau Combis and Alfred Solé in the measurements of all emitter discharges for the irrigation subunits.

Conflicts of Interest: The authors declare no conflict of interest.

References

1. Ayars, J.E.; Bucks, D.A.; Lamm, F.R.; Nakayama, F.S. Introduction. In *Microirrigation for Crop Production. Design, Operation and Management*; Lamm, F.R., Ayars, J.E., Nakayama, F.S., Eds.; Elsevier: Amsterdam, The Netherlands, 2007; pp. 1–26.
2. ICID 2019. Sprinkler and Micro Irrigated Area. Available online: <http://www.icid.org/sprinklerandmicro.pdf> (accessed on 21 March 2019).
3. Bucks, D.A.; Nakayama, F.S.; Gilbert, R.G. Trickle irrigation water quality and preventive maintenance. *Agric. Water Manag.* **1979**, *2*, 149–162. [[CrossRef](#)]
4. WHO. *Guidelines for the Safe Use of Wastewater, Excreta and Greywater*; World Health Organization Press: Geneva, Switzerland, 2006; Volume 2.
5. Asano, T.; Burton, F.L.; Leverenz, H.L. *Water Reuse: Issues, Technologies and Applications*; McGraw Hill Inc.: New York, NY, USA, 2007.
6. Barragán, J.; Bralts, V.; Wu, I.P. Assessment of emission uniformity for microirrigation design. *Biosyst. Eng.* **2006**, *93*, 89–97. [[CrossRef](#)]
7. Wu, I.P.; Barragán, J.; Bralts, V. Field performance and evaluation. In *Microirrigation for Crop Production. Design, Operation and Management*; Lamm, F.R., Ayars, J.E., Nakayama, F.S., Eds.; Elsevier: Amsterdam, The Netherlands, 2007; pp. 357–388.
8. Ravina, I.; Paz, E.; Sofer, Z.; Marcu, A.; Shisha, A.; Sagi, G. Control of emitter clogging in drip irrigation with reclaimed wastewater. *Irrig. Sci.* **1992**, *13*, 129–139. [[CrossRef](#)]
9. Merriam, J.L.; Keller, J. *Farm Irrigation System Evaluation: A Guide for Management*; Department of Agricultural and Irrigation Engineering, USU: Logan, UT, USA, 1978.
10. Vermeiren, L.; Jobling, G.A. *Localized Irrigation*; Irrigation and Drainage Paper 36; FAO: Rome, Italy, 1986.
11. Juana, L.; Rodríguez-Sinobas, L.; Sánchez, R.; Losada, A. Evaluation of drip irrigation: Selection of emitters and hydraulic characterization of trapezoidal units. *Agric. Water Manag.* **2007**, *90*, 13–26. [[CrossRef](#)]
12. Trooien, T.P.; Lamm, F.R.; Stone, L.R.; Alam, M.; Rogers, D.H.; Clark, G.A.; Schlegel, A.J. Subsurface drip irrigation using livestock wastewater: Dripline flow rates. *Appl. Eng. Agric.* **2000**, *16*, 505–508. [[CrossRef](#)]
13. Puig-Bargués, J.; Arbat, G.; Elbana, M.; Duran-Ros, M.; Barragán, J.; Ramírez de Cartagena, F.; Lamm, F.R. Effect of flushing frequency on emitter clogging in microirrigation with effluents. *Agric. Water Manag.* **2010**, *97*, 883–891. [[CrossRef](#)]
14. Madramootoo, C.A.; Morrison, J. Advances and challenges with micro-irrigation. *Irrig. Drain.* **2013**, *62*, 255–261. [[CrossRef](#)]
15. Goldhamer, D.A.; Fereres, E. Irrigation scheduling of almond trees with trunk diameter sensors. *Irrig. Sci.* **2004**, *23*, 11–19. [[CrossRef](#)]
16. Casadesús, J.; Mata, M.; Marsal, J.; Girona, J. A general algorithm for automated scheduling of drip irrigation in tree crops. *Comput. Electron. Agric.* **2012**, *83*, 11–20. [[CrossRef](#)]
17. González-Perea, R.; Fernández García, I.; Martín Arroyo, M.; Rodríguez Díaz, J.A.; Camacho Poyato, E.; Montesinos, P. Multiplatform application for precision irrigation scheduling in strawberries. *Agric. Water Manag.* **2017**, *183*, 194–201. [[CrossRef](#)]
18. Morillo, J.G.; Martín, M.; Camacho, E.; Rodríguez Díaz, J.A.; Montesinos, P. Toward precision irrigation for intensive strawberry cultivation. *Agric. Water Manag.* **2015**, *151*, 43–51. [[CrossRef](#)]
19. Sivagami, A.; Hareeshvare, U.; Maheshwar, S.; Venkatachalapathy, V.S.K. Automated irrigation system for greenhouse monitoring. *J. Inst. Eng. Ser. A* **2018**, *99*, 183–191. [[CrossRef](#)]
20. Fernández-Pacheco, D.G.; Molina-Martínez, J.M.; Jiménez, M.; Pagán, F.J.; Ruiz-Canales, A. SCADA platform for regulated deficit irrigation management of almond trees. *J. Irrig. Drain. Eng.* **2014**, *140*, 04014008. [[CrossRef](#)]
21. Li, D.; Hendricks Franssen, H.-J.; Han, X.; Jiménez-Bello, M.A.; Martínez Alzamora, F.; Vereecken, H. Evaluation of an operational real-time irrigation scheduling scheme for drip irrigated citrus fields in Picassent, Spain. *Agric. Water Manag.* **2018**, *208*, 465–477. [[CrossRef](#)]
22. Rijo, M. Design and field tuning of an upstream controlled canal network SCADA. *Irrig. Drain.* **2008**, *57*, 123–137. [[CrossRef](#)]

23. Rijo, M.; Arranja, C. Supervision and water depth automatic control of an irrigation canal. *J. Irrig. Drain. Eng.* **2010**, *136*, 3–10. [[CrossRef](#)]
24. Bové, J.; Puig-Bargués, J.; Arbat, G.; Duran-Ros, M.; Pujol, T.; Pujol, J.; Ramírez de Cartagena, F. Development of a new underdrain for improving the efficiency of microirrigation sand media filters. *Agric. Water Manag.* **2017**, *179*, 296–305. [[CrossRef](#)]
25. Li, J.; Chen, L.; Li, Y.; Yin, J.; Zhang, H. Effects of chlorination schemes on clogging in drip emitters during application of sewage effluent. *Appl. Eng. Agric.* **2010**, *26*, 565–578. [[CrossRef](#)]
26. Duran-Ros, M.; Puig-Bargués, J.; Arbat, G.; Barragán, J.; Ramírez de Cartagena, F. Definition of a SCADA system for a microirrigation network with effluents. *Comput. Electron. Agric.* **2008**, *64*, 338–342. [[CrossRef](#)]
27. Bliesner, R.D. Field evaluation of trickle irrigation efficiency. In Proceedings of the ASCE Irrigation and Drainage Division Specialty Conference on Water Management for Irrigation and Drainage, Reno, NV, USA, 20–22 July 1977; pp. 382–393.



© 2019 by the authors. Licensee MDPI, Basel, Switzerland. This article is an open access article distributed under the terms and conditions of the Creative Commons Attribution (CC BY) license (<http://creativecommons.org/licenses/by/4.0/>).

6. GENERAL DISCUSSION

6. GENERAL DISCUSSION

6.1. FILTER PERFORMANCE

6.1.1. Pressure loss across the filters

Six pressure transducers placed across the filter allowed recording the pressure every minute using a SCADA system. One transducer was located at the filter inlet, three across the filter body in where filtration media were placed, one after the underdrain and the sixth one after the collector. The arm collector filter had the underdrain and the collector in only one piece, therefore only five pressure transducers were used with this filter, being the fourth one placed before the underdrain and the fifth after it.

With the pressure of two consecutive transducers, pressure loss in the different filter sections (Figure 6.1) was determined. Thus, head loss across Section 1 was caused by the diffuser, across Sections 2 and 3 by the filter media, across Section 4 by the underdrain, and across Section 5 by the collector. It should be pointed out that when a media height of 0.2 m was used, there were no filter media in Section 2.

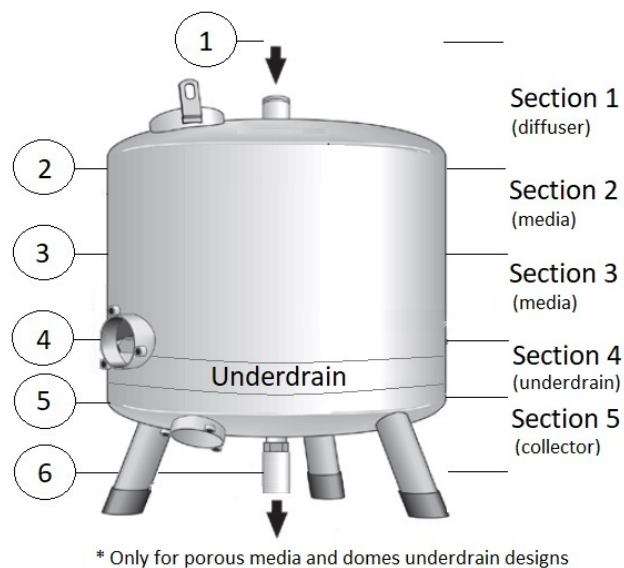


Figure 6.1. Pressure transducers (1-6) across the filters and head loss sections.

The discussion of pressure distribution across the filter will be limited to those filtration cycles that were considered effective (following the criteria explained in Chapter 3). Figure 6.2 shows the average pressure profiles along the filters for each tested condition. Differences between two consecutive transducers show pressure loss for each Section, which differed from one filter to another as well as among experimental conditions. When using 0.2 m media height, there was only one pressure loss measure for the media (Section 3), while with 0.3 m two measurements at Section 2 (first part of the media) and Section 3 (second part, before the underdrain) were available.

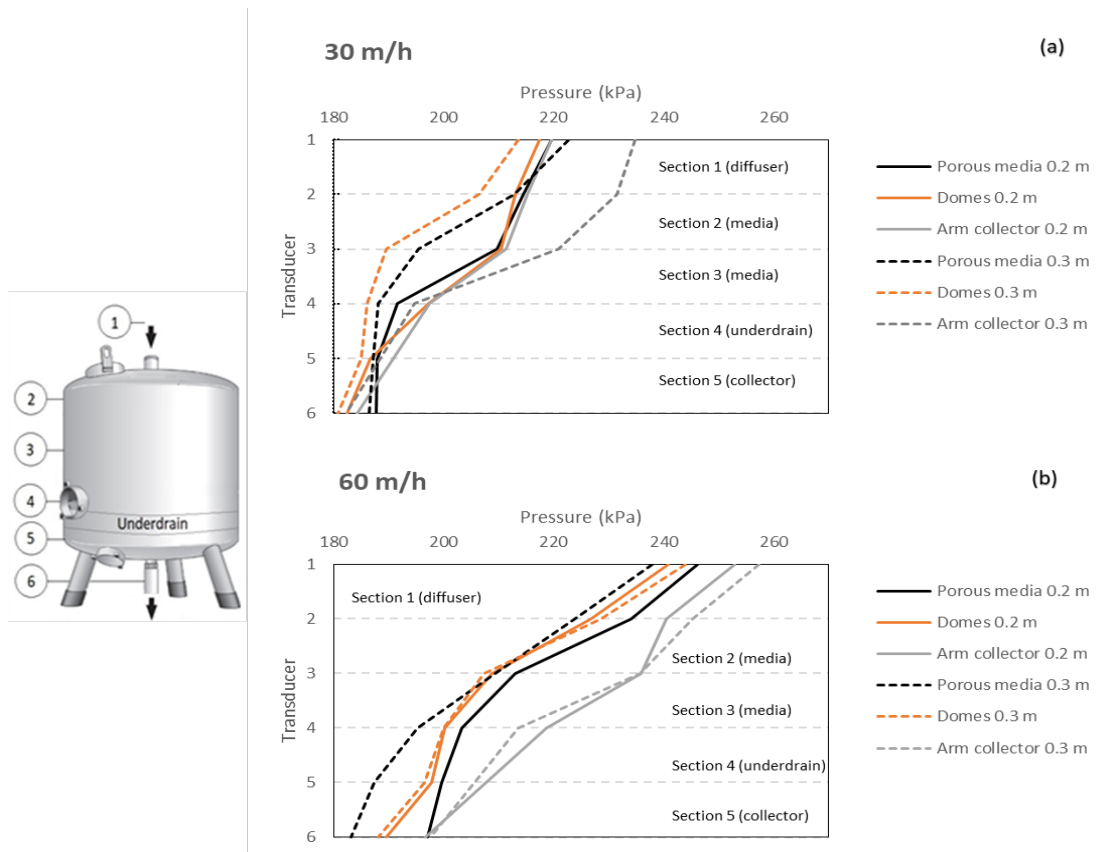


Figure 6.2. Pressure profiles throughout the vertical axis along the three different filter designs for the two media heights (0.2 and 0.3 m), at a filtration velocity of 30 m/h (a) and 60 m/h (b).

In general, pressure loss was higher in Sections 2 and 3 where media was placed than in the underdrain. Burt (2010) also found higher pressure losses across the media than at the underdrain working with commercial filters. Bové et al. (2015b), running a scaled filter with an inserted dome underdrain using tap water and filtration velocity and media similar to this experiment, but with a slightly higher media height (31.7 cm), found more pressure loss in the underdrain, being the head loss produced by both media bed and the underdrain 50% of the total. The differences in pressure loss across the different sections among studies could be explained by the use of reclaimed effluents, since their higher particle load clog the media faster producing therefore higher head loss.

Figure 6.3 represents the total filter pressure loss for different underdrain designs and conditions tested. Higher pressure losses were obtained using reclaimed effluents compared to studies which used tap water. Moreover, higher pressure losses were found with higher velocities (60 m/h) for each filter design, while this difference is not that clear if media heights are compared. These results agree with Mesquita et al. (2012) who pointed out that the pressure loss was significantly affected by the filtration velocity and proportional to its increase. However, de Deus et al. (2016) observed that for low filtration velocities (20 m/h), pressure loss is not affected by bed depth changes. It should be pointed out that in the other works previously cited tap water was used instead of effluent. Because of the variability of water quality of the effluent used, a water quality parameter (turbidity or dissolved oxygen) was considered as co-variable in this study since it affected filter performance and operational conditions, as the designs and operational conditions worked with different water characteristics.

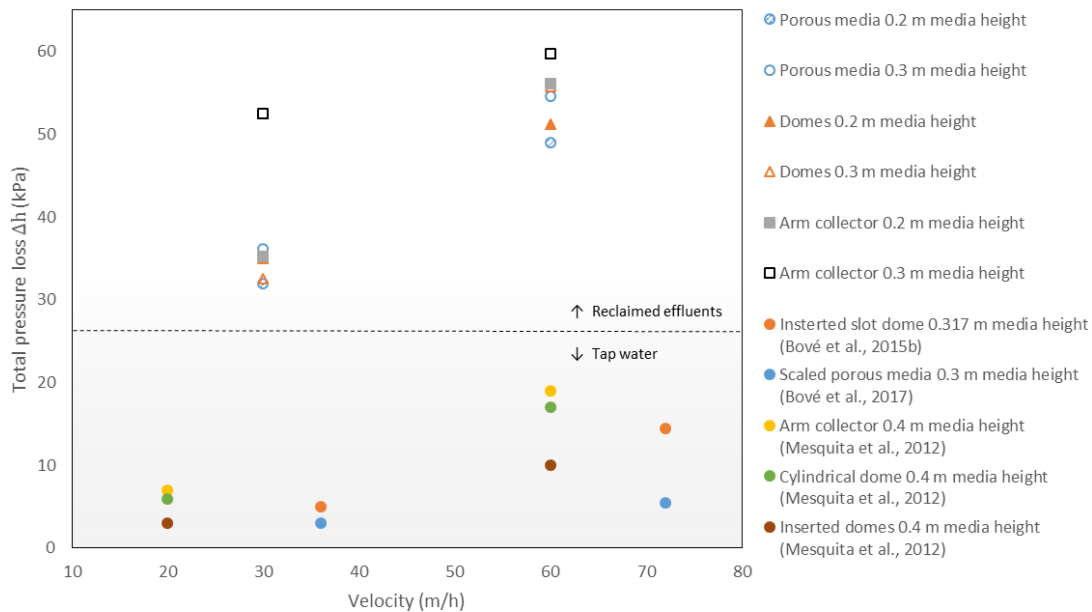


Figure 6.3. Average pressure loss across the whole filter regarding filtration velocity for different underdrain designs and conditions tested.

The aim of the new porous media underdrain design was to reduce pressure loss (Bové et al., 2017). However, this underdrain only showed less pressure loss than the arm collector design (in this case, considering the joint effect of the collector) at both velocities, and than the dome design, but only at 30 m/h. Thus, when comparing the porous media and dome underdrains, the results agree with those found by Bové et al. (2017) for filtration velocities below 36 m/h, since the porous media reduced the pressure loss by 20% but, conversely, do not match with those for filtration velocities above 72 m/h, where porous media reduced pressure loss by 45% more than dome underdrain.

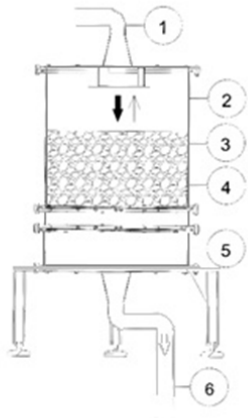
Mesquita et al. (2019) analyzed the head loss of a diffuser plate similar than that of porous media and arm collector designs using tap water, with filtration velocities between 3.6 and 18 m/h obtaining head losses between 0.24 and 4.78 kPa. At 30 m/h, porous media caused a head loss of 7.55 kPa and arm collector 3.84 kPa, while at 60 m/h, pressure drops were 13.22 and 13.31 kPa, respectively. Although they only calculated the pressure loss specifically for the diffuser plate and not for all the section, there is a linear relation between the increase of filtration velocity and diffuser plate head loss for both studies.

6.1.2. Pressure loss throughout sections and filtration cycles

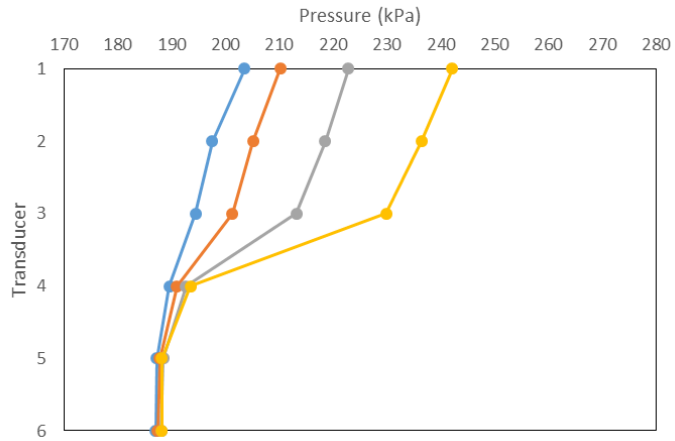
Pressure in each transducer varied along the filtration cycles. In order to have a representative value for the different filtration cycle phases, four different filtration times were established for each filter: at the beginning, at 1/3 and 2/3 of the time, and at the end of the cycle. For every period, an average value for each transducer was calculated taking the values obtained during the first 5 min for each period. Only at the beginning of the cycles a lag of 4 min before recording was used to allow the pressures in all transducers to stabilize after the backwashing.

Figures 6.4 (porous media), 6.5 (domes) and 6.6 (arm collector) show the average pressure values at different filtration times for the different operational conditions. Inlet pressures increased during filtration cycles and were higher with higher filtration velocities, while outlet pressures remained more or less the same because a default pressure value at the beginning of irrigation subunits was established (Chapter 4), meaning that head loss increased throughout cycles. This increase occurred mainly in the media, as a consequence of media clogging due to filtration, although pressure loss percentages in the different sections varied between them, the operational conditions and the time of the cycle (Table 6.1).

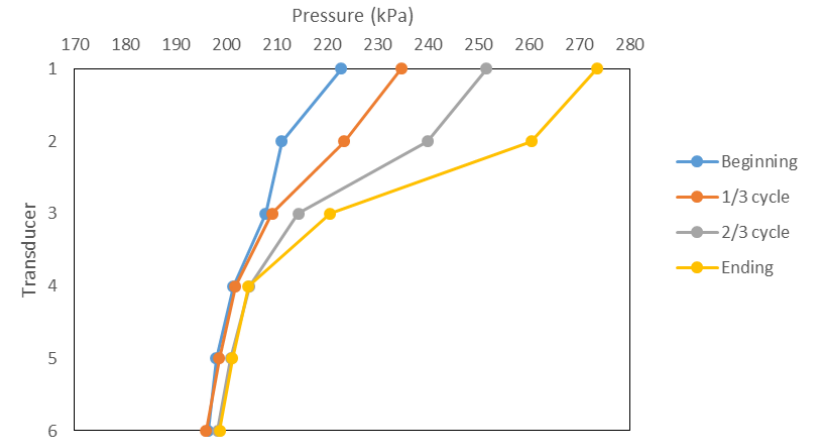
Porous media design



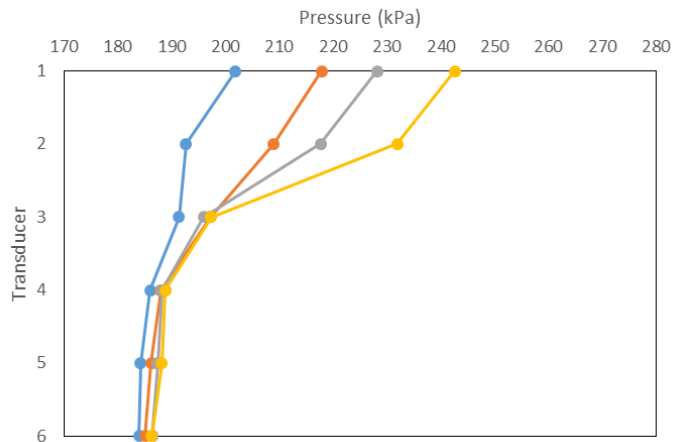
0.2 m - 30 m/h



0.2 m - 60 m/h



0.3 m - 30 m/h



0.3 m - 60 m/h

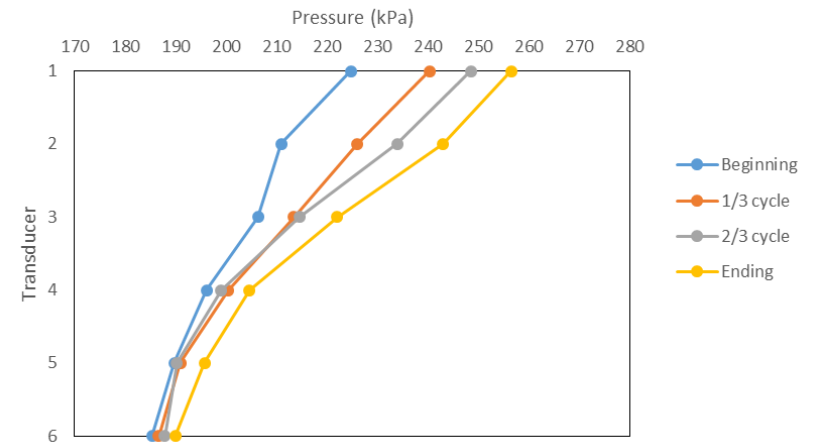


Figure 6.4. Average pressure (kPa) values for each operational condition of the different pressure transducers across the filter at the beginning, 1/3, 2/3 and at the end of the filtration cycles, for the porous media underdrain filter.

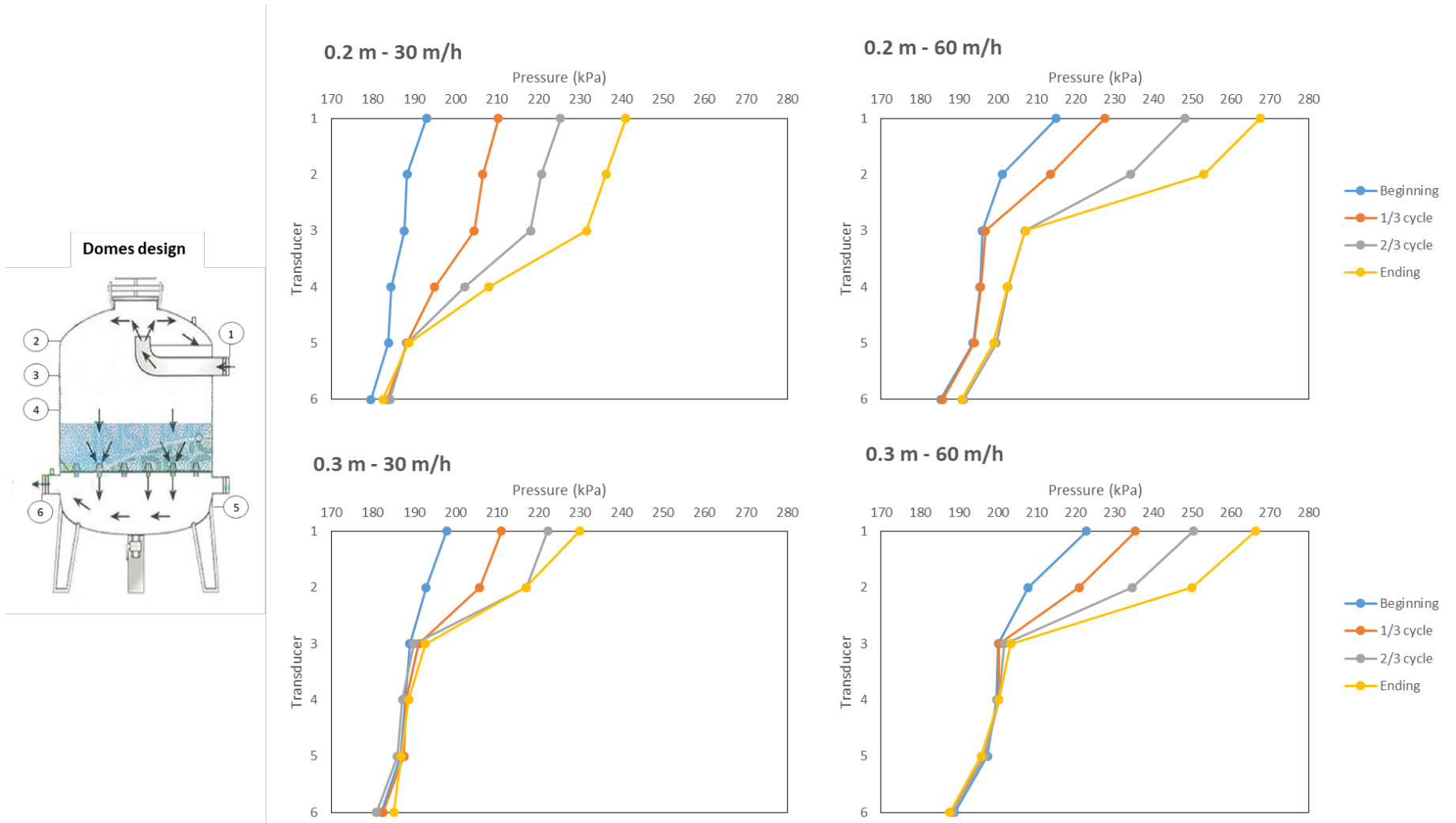


Figure 6.5. Average pressure (kPa) values for each operational condition of the different pressure transducers across the filter at the beginning, 1/3, 2/3 and at the end of the filtration cycles, for the domes underdrain filter.

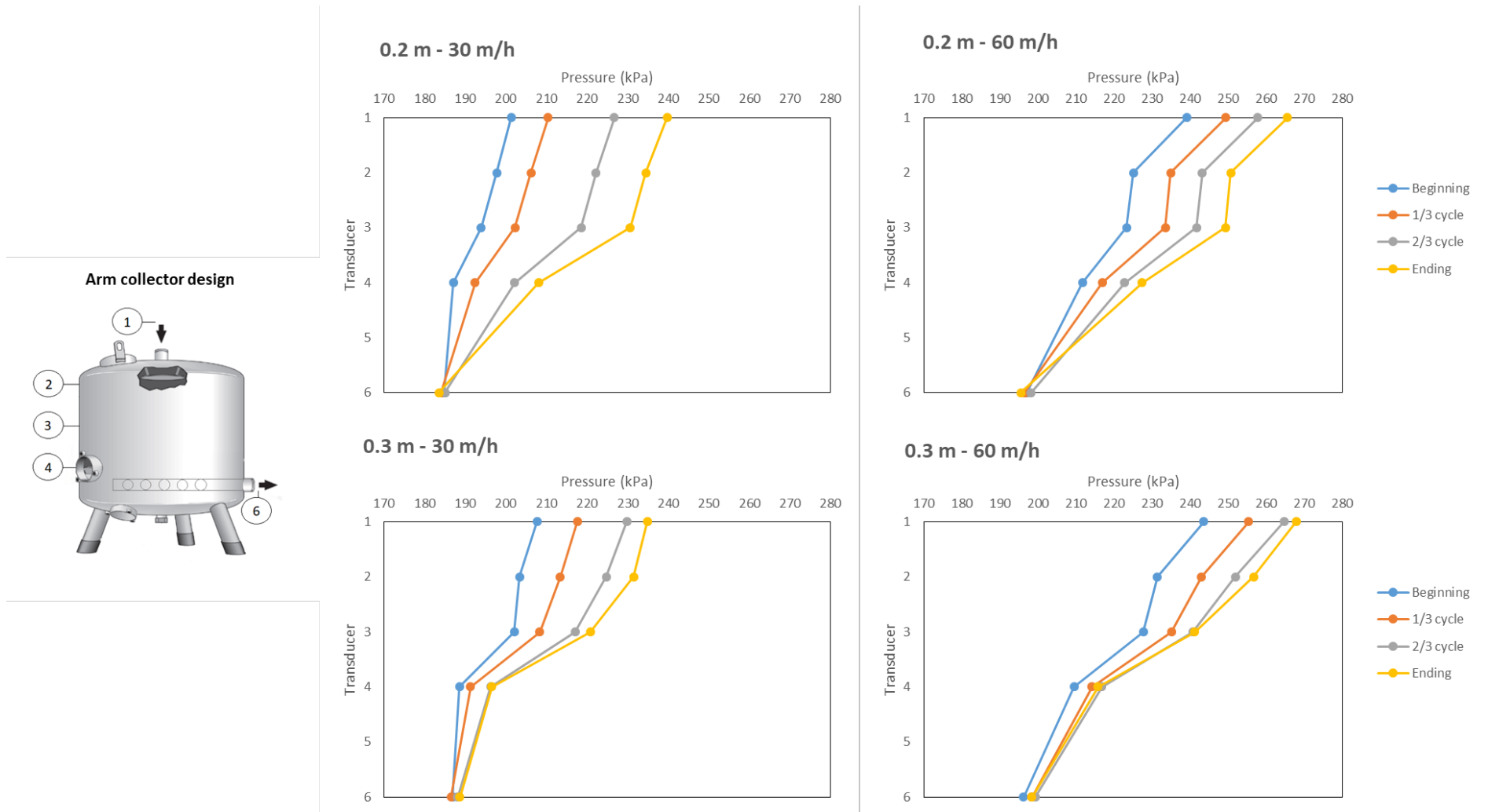


Figure 6.6. Average pressure (kPa) values for each operational condition of the different pressure transducers across the filter at the beginning, 1/3, 2/3 and at the end of the filtration cycles, for the arm collector underdrain filter.

Table 6.1. Pressure loss percentage (%) of the different filter designs for the different sections and operational conditions, at the beginning of the cycle, 1/3, 2/3, end of the cycle and mean value.

Porous media	Section 1 (diffuser)				Section 2 (media)				Section 3 (media)				Section 4 (underdrain)				Section 5 (collector)			
	0.2 m 30 m/h	0.2 m 60 m/h	0.3 m 30 m/h	0.3 m 60 m/h	0.2 m 30 m/h	0.2 m 60 m/h	0.3 m 30 m/h	0.3 m 60 m/h	0.2 m 30 m/h	0.2 m 60 m/h	0.3 m 30 m/h	0.3 m 60 m/h	0.2 m 30 m/h	0.2 m 60 m/h	0.3 m 30 m/h	0.3 m 60 m/h	0.2 m 30 m/h	0.2 m 60 m/h	0.3 m 30 m/h	0.3 m 60 m/h
Beginning	36.27	46.66	51.69	35.06	18.81	12.4	7.3	11.71	29.7	21.45	30.34	25.82	14.26	9.48	10.11	16.35	0.96	10.01	1.12	11.05
1/3 cycle	22.04	29.26	30.9	27.64	16.95	36.92	40.97	24.38	45.51	18.91	22.57	25.2	13.95	8.31	5.21	14.49	1.54	6.6	0.35	8.29
2/3 cycle	12.26	22.05	25.12	23.35	15.27	47.92	51.91	30.9	59.26	18.13	18.66	24.68	12.02	6.95	1.91	14.06	1.19	4.94	2.39	7.02
Ending	10.58	16.94	19.01	20.94	12.27	51.94	61.28	32.49	67.17	21.03	15.28	26.91	10.01	6.82	1.07	13.77	-0.04	3.26	3.37	5.82
Cycle mean	20.29	24.48	27.23	25.71	15.82	42.95	47.89	26.39	50.41	19.86	20.25	25.65	12.56	7.48	2.7	14.47	0.91	5.23	1.94	7.67

Domes	Section 1 (diffuser)				Section 2 (media)				Section 3 (media)				Section 4 (underdrain)				Section 5 (collector)			
	0.2 m 30 m/h	0.2 m 60 m/h	0.3 m 30 m/h	0.3 m 60 m/h	0.2 m 30 m/h	0.2 m 60 m/h	0.3 m 30 m/h	0.3 m 60 m/h	0.2 m 30 m/h	0.2 m 60 m/h	0.3 m 30 m/h	0.3 m 60 m/h	0.2 m 30 m/h	0.2 m 60 m/h	0.3 m 30 m/h	0.3 m 60 m/h	0.2 m 30 m/h	0.2 m 60 m/h	0.3 m 30 m/h	0.3 m 60 m/h
Beginning	35.05	46.81	31.33	44.08	4.75	1.81	25.47	22.54	24.16	17.24	7.23	1.22	4.51	6.12	6.88	7.14	31.52	28.02	29.09	25.02
1/3 cycle	13.72	33.49	18.42	30.62	7.85	2.81	58.48	43.44	35.98	40.11	4.78	0.36	25.15	3.98	0.68	7.84	17.3	19.61	17.64	17.74
2/3 cycle	11.04	24.75	12.49	25.23	6.46	0.64	70.5	54.87	38.69	54.69	1.64	0.72	33.88	5.18	3.07	5.62	9.92	14.73	12.3	13.56
Ending	8.12	18.98	24.33	20.65	7.95	0.89	47.3	63.26	40.44	64.94	13.15	0.07	36.23	4.51	8.9	5.68	7.25	10.68	6.31	10.33
Cycle mean	16.98	27.43	21.64	27.53	6.75	1.34	50.44	50.65	34.82	50.37	6.7	0.49	24.94	4.81	4.89	6.34	16.5	16.05	16.33	14.99

Arm collector	Section 1 (diffuser)				Section 2 (media)				Section 3 (media)				Sections 4 + 5 (underdrain + collector)			
	0.2 m 30 m/h	0.2 m 60 m/h	0.3 m 30 m/h	0.3 m 60 m/h	0.2 m 30 m/h	0.2 m 60 m/h	0.3 m 30 m/h	0.3 m 60 m/h	0.2 m 30 m/h	0.2 m 60 m/h	0.3 m 30 m/h	0.3 m 60 m/h	0.2 m 30 m/h	0.2 m 60 m/h	0.3 m 30 m/h	0.3 m 60 m/h
Beginning	21.3	33.24	20.67	25.82	23.64	4.29	6.55	7.77	41.32	27.62	64.63	38.42	13.74	34.86	8.15	27.98
1/3 cycle	16.11	27.4	13.6	21.8	14.92	2.69	16.24	13.8	37.44	31.4	54.77	36.68	31.54	38.52	15.39	27.72
2/3 cycle	10.75	24.47	12.06	19.57	8.88	2.52	18.48	17.09	39.21	31.7	50	36.54	41.17	41.32	19.46	26.79
Ending	9.33	21.17	6.25	16.02	6.91	2.09	20.3	22.36	40.09	31.23	49.43	36.52	43.67	45.52	23.45	24.9
Cycle mean	14.37	25.72	13.14	20.2	13.58	2.74	15.39	16.02	39.51	30.74	54.71	36.82	32.53	40.8	16.61	26.61

For the porous media underdrain design, the deflector section showed pressure losses of 20.29 – 27.23% of the total, depending on the operational conditions. Head loss percentage of Section 2 was 15.82 – 42.95% (without media) and 26.39 – 47.89% (with media). For Section 3 was 19.86 – 50.41%, for the underdrain was 2.70 – 14.47% and for the collector 0.91 – 7.67%. In general, the greatest pressure losses were produced across the media (Sections 2 and 3), having the collector the lowest values. The underdrain showed always less head loss percentage than Sections 2 and 3 in all conditions. However, higher percentages of pressure loss were found with higher inlet turbidity, which meant more effluent particle load and more media clogging, as it was discussed in Section 6.1.1. Pressure loss distribution of the porous media underdrain filter is different than that obtained by Bové et al. (2017) working with a scaled underdrain design in a laboratory experiment using a sand silica bed of 0.3 m with a grain size between 0.63 and 0.75 mm. Bové et al. (2017) found that the media caused the highest head loss percentage (52%), followed by the underdrain (39%), while the head loss was smaller in the collector and the diffuser plate (6 and 3% respectively).

For the dome underdrain design, the deflector accumulated pressure losses of 16.98 – 27.53%, Section 2, 1.34 – 6.75% (without media) and 50.44 – 50.63% (with media), Section 3, 0.49 – 50.37%, the underdrain of 4.81 – 24.94% and the collector 14.99 – 16.50%. For this filter, the greater head loss was produced at the first media layers, because they retain more particles than the rest of the media. This phenomenon was also found by Burt (2010) and de Deus et al. (2016) and it will be further discussed in Section 6.2. The dome underdrain had relative low pressure loss percentages, although they may be hidden by the high head losses observed across the media.

A similar scaled dome underdrain was tested with tap water under laboratory conditions (Bové et al., 2015b) with a silica sand bed of 0.3 m with a grain size between 0.63 and 0.75 mm, being the highest head loss percentage located at the underdrain (53%), followed by the media (36%), collector (8%) and diffuser (4%). The diffuser plate used by Bové et al. (2015b) had a flat structure and was different from the elbow pipe used in the filter used in the present experiment. This could explain the different percentages obtained. The diffuser plate design can affect to the incorrect direction of the water into the filter, increasing turbulence on the filtration surface (de Deus et al., 2016; Mesquita et al., 2019) and therefore moving media particles and affecting pressure losses inside the filter.

Finally, for the arm collector filter design, head losses were 13.14 – 25.72% for the deflector section, 2.74 – 13.58% (without media) and 15.39 – 16.02% (with media) for Section 2, 30.74 – 54.71% for filter media, 16.61 – 40.80% for both underdrain and collector. For all the operational conditions tested, the highest head losses were found inside the media (Section 3), followed by the underdrain and the collector (Section 4+5).

The head loss fluctuated depending on the period of the cycle (Table 6.2). For the porous media and dome designs, at the beginning of the cycle, the higher pressure loss was produced in the diffuser, followed by first media layer, while at the end of the cycle the major head loss was also located in the first media layer. For almost all operational conditions for these two designs, the percentage of head loss caused by the underdrain was the second lowest, after the water collector section. On the contrary, for the arm collector design at the beginning of the cycle, higher pressure loss was located in the media (Section 3), followed by the diffuser plate, while at the end, higher pressure loss was also located in the media (Section 3) but followed by the underdrain and collector (Sections 4+5). The head loss at the diffuser plate at the beginning of the cycle point out its importance of the uniform distribution flow and its kinetic energy (de

Deus et al. 2016). The underdrain played a small part in head loss reduction at the beginning (4.51 – 7.14%), while late at the end of the cycle the reduction percentage was bigger (4.51 – 36.23%).

Table 6.2. Graded sections depending on the percentage of head loss for different filtration operating conditions and time of the cycle for the three filters tested.

Conditions and timing	Filter design	Order of the filter sections regarding their head loss percentage				
0.2 m 30 m/h	Porous media	Section 3	Section 1	Section 2	Section 4	Section 5
	Domes	Section 3	Section 4	Section 1	Section 5	Section 2
	Arm collector	Section 3	Section 4	Section 1	Section 2	-
0.2 m 60 m/h	Porous media	Section 2	Section 1	Section 3	Section 4	Section 5
	Domes	Section 2	Section 1	Section 5	Section 4	Section 3
	Arm collector	Section 4	Section 3	Section 1	Section 2	-
0.3 m 30 m/h	Porous media	Section 2	Section 1	Section 3	Section 4	Section 5
	Domes	Section 2	Section 1	Section 5	Section 4	Section 3
	Arm collector	Section 3	Section 4	Section 1	Section 2	-
0.3 m 60 m/h	Porous media	Section 2	Section 1	Section 3	Section 4	Section 5
	Domes	Section 2	Section 1	Section 5	Section 4	Section 3
	Arm collector	Section 3	Section 4	Section 1	Section 2	-
Beginning	Porous media	Section 1	Section 3	Section 2	Section 4	Section 5
	Domes	Section 5	Section 1	Section 2	Section 3	Section 4
	Arm collector	Section 3	Section 1	Section 4	Section 2	-
1/3 cycle	Porous media	Section 3	Section 2	Section 1	Section 4	Section 5
	Domes	Section 2	Section 1	Section 5	Section 3	Section 4
	Arm collector	Section 3	Section 4	Section 1	Section 2	-
2/3 cycle	Porous media	Section 2	Section 3	Section 1	Section 4	Section 5
	Domes	Section 2	Section 1	Section 5	Section 4	Section 3
	Arm collector	Section 3	Section 4	Section 1	Section 2	-
Ending	Porous media	Section 2	Section 3	Section 1	Section 4	Section 5
	Domes	Section 2	Section 1	Section 4	Section 3	Section 5
	Arm collector	Section 3	Section 4	Section 1	Section 2	-

In most of the conditions tested for all the filters, the highest head loss was located in the first media layer (i.e. Section 2 and 3 with 0.3 and 0.2 m height, respectively), excluding arm collector with 0.3 m media height, for which was Section 3 (second layer), and porous media with 0.2 m and 60 m/h, for which was Section 2 (empty filter body). In this latter case, the turbulences of the water caused by higher velocities, probably generated by an unequal water distribution by the diffuser plate (Mesquita et al., 2019) could explain these values. These results confirm the idea that media head losses are higher than those produced by the underdrain. Only the arm collector underdrain at 0.2 m and 60 m/h had higher values of pressure loss than the first media layer, being this design the one which showed the highest underdrain head loss values.

In order to compare the pressure loss reductions among filtration operational conditions and cycle duration for the three different designs, Table 6.2 shows the order of the different filter sections for head loss for each condition and timing. Average values for both conditions and timing (for the four conditions) were taken. In general, throughout filtration cycles, media

followed by underdrain sections accumulate more head loss compared to other sections, such as the diffuser plate.

6.1.3. Pressure loss evolution regarding the filtered volume

The pressure loss regarding the filtered volume differed from each operational condition among filters, and within the same conditions for each filter.

Table 6.3 shows the number of valid cycles for each condition, the mean filtered volume for all the cycles, the filtered total volume for the longest and shortest cycles and the number of cycles regarding the filtered volume range. For 0.2 m media height and 30 m/h, there were less cycles because some filtered volumes were not recorded due to an issue with the acquisition data software. At 30 m/h, porous media filtered more volume than the other two filter designs, although at 60 m/h it was the arm collector the design that showed the highest values, especially with a 0.2 m height.

Table 6.3. Number of cycles, mean filtered volume per cycle (m³), maximum and minimum filtration volume per cycle (m³) and cycle distribution regarding the filtered volume for each filter design regarding operational conditions.

Operational conditions	Filter design	Number of effective cycles	Filtered volume per cycle (m ³)			Number of cycles regarding filtered volume (in m ³)				
			Mean ± standard error	Maximum	Minimum	<20	20 - 40	40 - 60	60 - 80	> 80
0.2 m 30 m/h	Porous media	14	31.04 ±4.84	60.37	4.07	5	5	4	0	0
	Domes	28	17.51 ±1.64	39.62	2.80	18	10	0	0	0
	Arm collector	47	15.73 ±1.02	28.95	3.81	33	14	0	0	0
0.2 m 60 m/h	Porous media	77	36.43 ±3.30	112.07	4.66	27	21	14	8	7
	Domes	42	54.19 ±5.26	135.62	3.89	4	15	7	6	10
	Arm collector	29	55.45 ±8.50	128.43	5.60	12	3	1	4	9
0.3 m 30 m/h	Porous media	10	92.12 ±21.53	216.50	3.30	1	1	1	1	6
	Domes	36	39.82 ±4.89	119.47	2.40	11	10	5	8	2
	Arm collector	35	37.14 ±3.95	74.72	2.20	11	11	9	4	0
0.3 m 60 m/h	Porous media	75	33.10 ±2.57	104.23	5.07	25	34	6	6	4
	Domes	111	24.22 ±1.40	63.43	5.60	54	41	14	2	0
	Arm collector	84	33.66 ±1.60	63.06	6.00	17	42	22	3	0

Figures 6.7 and 6.8 show the pressure loss regarding the filtered volume for each filter design. Because representing all the cycles for each condition was unfeasible due to their large number, for each range of filtered volume only a representative cycle is shown.

As it can be seen, in some cases pressure loss surpassed the 50 kPa established to activate backwashing. This was because SCADA system calculated automatically pressure loss every second, but only recorded it every minute. As the criterion for activate backwashing was surpassing head loss of 50 kPa for more than 1 min, if during that period head loss descended this value (e.g. for 2 s), then the system waited for the next 1 consecutive min for ordering a filter backwashing.

Inlet water quality varied among cycles, as discussed in Chapter 3, affecting its behaviour. In general, there was a pronounced head loss increase in all filters for all conditions for the shortest cycles (<20 m³). For most of the cycles above 40 m³, there was greater pressure loss increase above this volume (e.g. all filter designs for 0.3 m and 30 m/h, and dome for 0.3 m and 60 m/h) (Figures 6.7 and 6.8).

Short cycles (<20 m³) could be caused by previous ineffective backwashing. Elbana et al. (2012) obtained more number of inefficient backwashing after longer cycles in which more water was filtered, as more particles were trapped within the sand filter and were more difficult to be released after a backwashing. This effect could explain that a large number of short cycles (with a high initial head loss) happened after a long cycle. The underdrain design also affects backwashing efficiency, being the designs with more effective filtration area the ones with better performance (Mesquita, 2014).

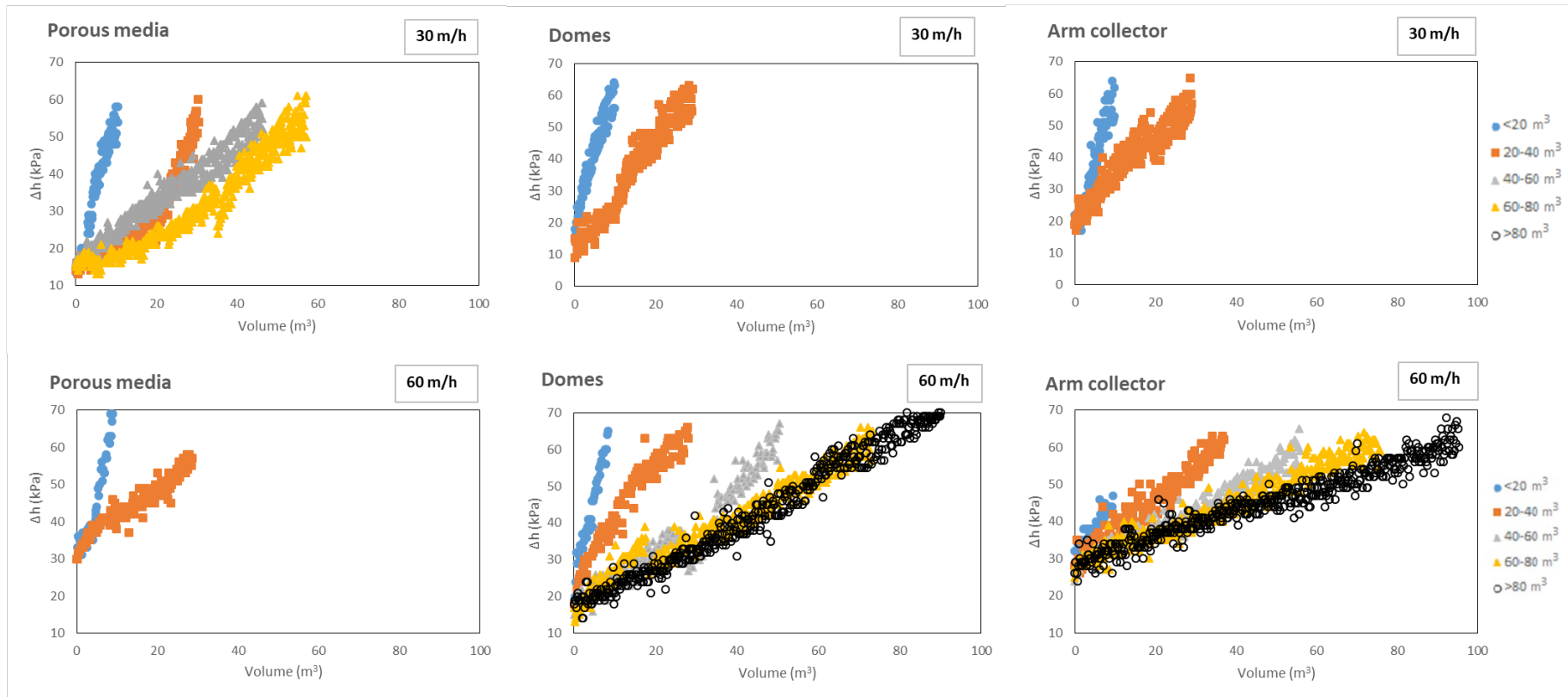


Figure 6.7. Head loss (kPa) regarding filtered volume (m³) for the three different filters designs and two filtration velocities under 0.2 m media height.

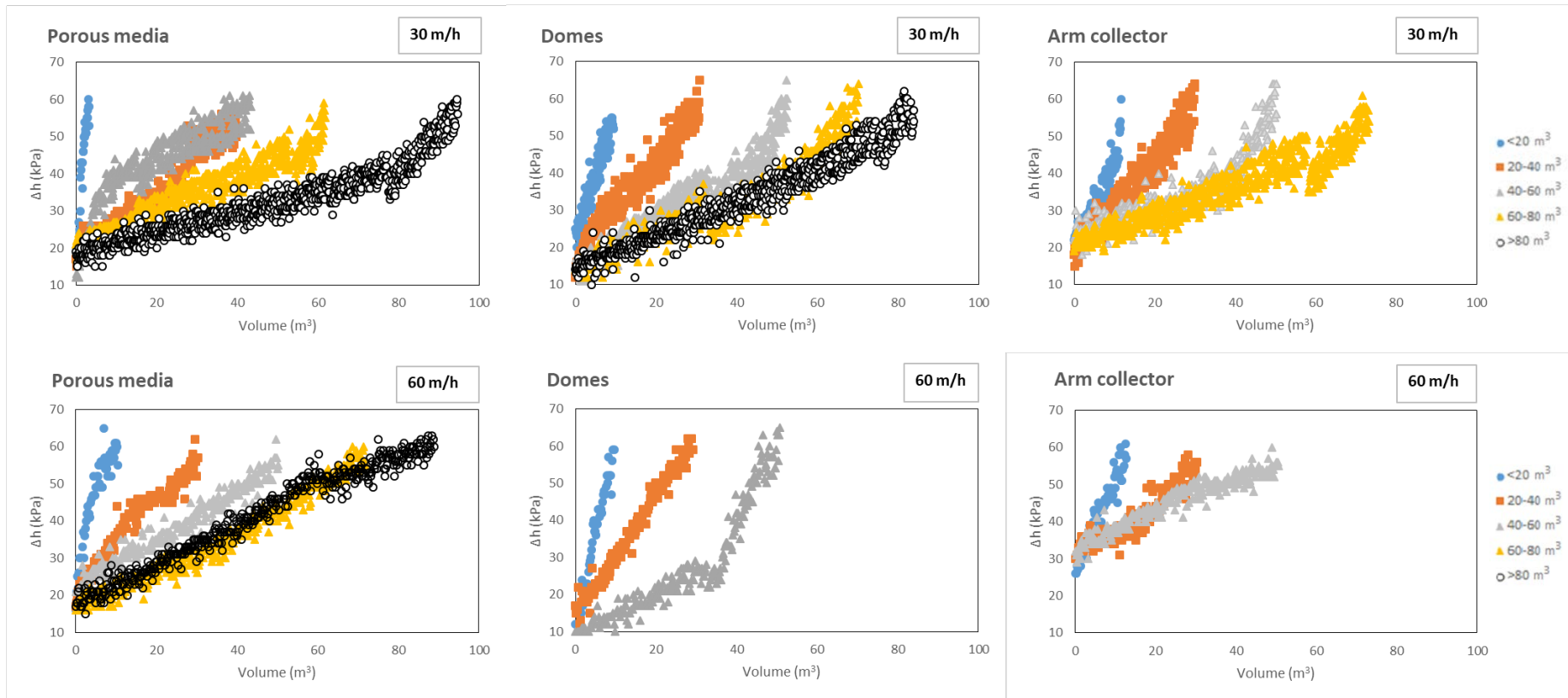


Figure 6.8. Head loss (kPa) regarding filtered volume (m^3) for the three different filters designs and two filtration velocities under 0.3 m media height.

6.1.4. Effect of filtration and operational conditions on effluent quality

As water samples were taken at both filter inlet and outlet, it was possible to study the effect of the three different designs and the four experimental conditions on effluent quality. The effluent characteristics were different across the experiment due to its variability, being the main values of the parameters recorded shown in Chapter 3.

Turbidity removal is related to the solid retention capacity of the filter, and therefore, to emitter clogging risk reduction. As explained in Chapter 3, there was a triple interaction between filter design, media height and filtration velocity on turbidity removals. Overall, porous media underdrain design presented higher turbidity removals than the other two underdrain designs in all the operative conditions tested, except for media height of 0.3 m and filtration velocity of 30 m/h, for which was the dome underdrain which achieved higher removals (47.74 vs. 39.19% of the porous media underdrain). This higher percentage could be related to the greater inlet turbidity value when the dome design was used in that condition in comparison to the other two, as it is more difficult to remove suspended solids with low inlet values, hence, removal percentage is lower.

For all the underdrain designs, 60 m/h filtration velocity presented less turbidity removals efficiencies, which concurs with the results obtained by Mesquita et al. (2012) and de Deus et al. (2016). However, there was not a clear pattern in media height variations on turbidity removal. Uncertain relation between media height and turbidity removal was also noticed by de Deus et al. (2016).

After each filtration period of the conditions tested, it was observed a fine line of debris in the first media layer, corresponding to higher amount of retained particles. As an example, Figure 6.9 shows the accumulated debris after 250 h with 0.3 m media height and 30 m/h filtration velocity for porous media design before backwashing. This phenomenon means that the higher percentage of particles are retained in the first media layers, as also Burt (2010) and de Deus et al. (2016) found. It was also in this section where the higher pressure losses were located, as explained in Section 6.1.2. Thus, low media height could be enough to remove turbidity and improve backwashing efficiency, as less amount of media would be cleaned.



Figure 6.9. Debris deposition in the firsts centimetres (dotted line) on the first media layer after 250 h of filtration with 0.3 m and 30 m/h for porous media design.

When the filter design factor was taken out of the statistical model, the media height had not a significant effect on turbidity removal at 30 m/h. However, at 60 m/h, media height was significant ($p < 0.05$), showing a better turbidity removal at 0.2 m. Therefore, it is recommended to use smaller media heights (0.2 m) since it also reduce environmental costs (Bové et al., 2018). To sum up, lower velocities provide higher turbidity removals (34.17% at 30 m/h vs. 11.27% at 60 m/h), as do also porous media design (26.28%) regarding dome (18.53%) and arm collector (13.44%) designs.

Different authors have studied how filtration affects water irrigation quality, considering the type of filter (media, disc or screen), the internal filter design as well as operational conditions. The most common parameters analysed are turbidity and oxygen removal. In order to have a general review of the latest results in effluent quality performance, Table 6.4 shows the general characteristics and the results of the most recent experiments.

The results of these studies are diverse and depend on different factors. Some authors have carried out experiments with a similar commercial dome underdrain used in this experiment, like Duran-Ros et al. (2009a) and Elbana et al. (2012), who worked using a 0.5 m media height and silica sand with similar effective diameter (d_e) (0.40 and 0.47 mm, respectively), obtaining higher turbidity removals (57 and 60%, respectively). In the present study, when using 30 m/h, turbidity reductions ranged from 16 to 47.7%, while de Deus et al. (2016) obtained lower turbidity removals (ranging from 5 to 16%) with filtration velocities of 20 and 40 m/h and slightly higher media height (0.35 m), using water with 5.20 mg/l of total suspended solids. Wu et al. (2015) found turbidity removals ranging from 11 to 48% with a media height of 0.4 m, although the inlet concentration of suspended solids varied substantially. On the other hand, when using high filtration velocities, turbidity removal tend to happen in the first filtration layers, as Burt (2010) noticed using an arm collector and pod underdrain design.

Turbidity removal is also higher with smaller d_e . Duran-Ros et al. (2009a) obtained reductions of 66% with d_e of 0.27 mm, Elbana et al. (2012) reductions of 60 % with d_e of 0.47 mm, Wu et al. (2015) between 48 and 34% with d_e of 0.41 and 0.45 mm, respectively. Nakhla and Farooq (2003) reported a 33 – 56% turbidity removal efficiency using coarse sand filters ($d_e = 0.50$ mm) and 40

– 62 % with finer media sand filters ($d_e=0.30$ mm) when using an effluent with inlet turbidity of 0.20 – 0.95 FNU.

Regarding filter design, in some experiments (Duran-Ros et al., 2009a; Elbana et al., 2012) dome underdrain design showed better turbidity removals than the porous media used in the present experiment, although these differences might be explained by the higher media bed used (0.5 m). In some cases (Elbana et al., 2012; Tripathi et al., 2014), inlet turbidity values are far higher than those of the present experiment, which may explain the greater removals obtained. Due to the heterogeneity of the different experiments, there is not a clear difference between domes and porous media design. A metadata analysis might be carried out, but there are important differences in procedures and result presentation in the published works.

Overall, porous media filter presented a good turbidity removal performance (26.29%) compared to other designs of other studies (Table 6.4), even though the diverse operational conditions and water characteristics used among all them. It has to be highlighted the lower media height used in the present experiment compared to other studies.

Finally, there should be further research in media filters hydraulic performance in order to make advances in their designs. Some authors have studied hydraulic performance of commercial underdrains, such as dome underdrain (Arbat et al., 2011; 2013; Bové et al., 2015b), other dome alternative designs (Arbat et al., 2011; Bové et al., 2015b; Pujol et al., 2016) and porous media underdrain (Bové et al., 2017), but not for arm collector design. Although all of these studies focus on hydraulic behaviour during filtration process, none of them focuses on backwashing, which has great influence in the filter performance (Enciso-Medina et al., 2011).

Table 6.4. General experiment conditions, filter designs and operational conditions and turbidity removal efficiencies in different published studies using sand filters with effluents.

Study	Experimental setup characteristics	Head loss for backwashing activation (kPa)	Operation schedule (h/day)	Total duration of the experiment	Underdrain design	Media height (m)	Filtration velocity (m/h)	d _e (mm)	U _{Cs}	Inlet water values (turbidity/suspended solids)	Turbidity removals (%)
Duran-Ros et al. (2009a)	Two sand filters in parallel	50	6 to 12	1000 h	Domes	0.5	-	0.40	2.41	6.76 ±2.34 FNU	57.0
								0.27	2.89	4.08 ±2.76 FNU	66.0
Burt (2010)	Different designs tested. Water with contaminants added instead of effluent.	-	8	15 days	Pods under disks	590 kg of media	-	0.60	1.42	46 mg TSS/l	1 - 4.9
					Arm collector					51 mg TSS/l	3.1 - 12.0
Elbana et al. (2012)	Two sand filters in parallel	50	6 to 12	1620 h	Domes	0.5	50-55	0.47	1.81	10.80 ±8.17 FNU	60.0
Tripathi et al. (2014)	One sand filter	-	-	1 year	Domes	-	-	-	-	55 FNU	51.0
Wu et al. (2015)	One sand filter followed by disc filter (130 µm)	100	-	300 h per condition	-	0.4	40 - 140	2.10	1.48	3 to 53.3 mg TSS/l	11.4
								1.41	1.56		16.7
								0.41	1.95		48.0
								0.55	3.31		31.1
								0.50	3.00		27.0
0.45	2.40	34.3									
de Deus et al. (2016)	Three sand filters in parallel	-	-	-	Domes	0.35	20 /40 / 60 /75 per each sand size	0.55	1.34	5.20 ±3.09 mg TSS/l	different values
								0.77	1.28		
								1.04	1.36		
Chapter 3	Three different underdrain designs working individually	50	4 to 6 per filter	1000 h	Domes	0.2	30	0.48	1.73	8.16 ±0.36 FNU	38.5
										5.82 ±0.21 FNU	33.6
										4.07 ±1.04 FNU	39.2
										6.29 ±0.23 FNU	14.8
										7.49 ±0.36 FNU	31.9
										2.84 ±0.17 FNU	1.0
					Arm collector	0.2	30	0.48	1.73	7.35 ±0.91 FNU	47.7
										5.77 ±0.17 FNU	10.5
										8.51 ±0.42 FNU	35.9
										3.50 ±0.30 FNU	-9.9
										5.91 ±0.31 FNU	16.0
										5.98 ±0.24 FNU	3.3

6.2. EMITTER PERFORMANCE

As it was explained in Chapter 4, emitter clogging is affected by the interaction between underdrain design and irrigation time, underdrain design and emitter location, and time and emitter location. A decrease of emitter discharge along time was observed, as many other authors (e.g. Ravina et al., 1992; Duran-Ros et al., 2009a; Tripathi et al., 2014; Pei et al., 2014; Wu et al., 2015; Zhou et al., 2015). Thus, emitter discharge dropped from 2.49 l/h at the beginning of the experiment (almost 2.50 l/h, which is the nominal emitter flow given by the manufacturer) to 2.22 l/h after 1000 h, which means an overall flow reduction of 10.8%. Moreover, it was at the end of the experiment when less emitter discharge and completely clogged emitters were found at the last dripline locations.

Regarding filter design, no differences on emitter discharge between filters were found at the beginning of the experiment, but after 1000 h, average discharge of the emitters protected by the arm collector filter was significantly higher (2.26 l/h) than those protected by dome and porous media designs (both 2.20 l/h). Less completely clogged emitters (6) were found with arm collector than with porous media (10) and dome (8) designs.

There was also an effect of the filter design and emitter location. Duran-Ros et al. (2009a) also found a significant effect of the interaction of filter (screen, disc and sand media) and emitter location with similar filter inlet turbidity values (from 4.1 to 6.8 FNU), obtaining for emitters placed after the sand filter an average flow rate of 76% of the initial at the end of the lateral compared to 48% in this study if the six last emitters of all subunits are taken into account. In the present work, the emitters of the last 1.2 m of the lateral had significantly lower discharges than the rest in those subunits protected by porous media and dome filters, while with arm collector it was only for the last 0.8 m.

To sum up, a filter design effect was observed among time and emitter location, causing the arm collector design higher emitter discharges at the end of the experiment and for the last locations. There were no significant differences on the inlet turbidity values between filter designs for the whole experiment (Chapter 4), so the risk of physical clogging was similar for all subunits. Conversely, porous media design showed significantly higher turbidity removal, so it was this design which retained more solid particles, although the reduction of physical clogging risk achieved by this filter did not imply less emitter clogging. There were some issues related to the experiment procedure that may explain this, as it will be discussed below.

The interactions between filter design and time and emitter location could be explained by biological clogging, which is the most common clogging type when using effluents (Green et al., 2018; Zhou et al., 2018). Two main reasons could justify biological clogging behaviour in this experiment. On one hand, biofilm growth was partially controlled by continuous chlorination. Concentration of chlorine was periodically tested at different emitter locations along the lateral for the three subunits being the results the same in all cases. Chlorine pump injected 2 ppm of chlorine at the filter outlet, but only concentrations of 1 ppm were found in the firsts emitters, meaning that half of the concentration reacted before, and no chlorine was found in the last locations, allowing biofilm to develop. Some authors recommend free residual chlorine of 0.5 ppm (Cararo et al., 2006), 1.5 ppm (Li et al., 2010) or 2 ppm (Dehghanisani et al., 2005), at the end of the laterals, although all of them used shorter laterals. To prevent biofilm formation, a proportional chlorine injection could be installed to inject higher concentration when the microorganisms load is higher in function of the inlet dissolved oxygen value or the free chlorine

level at the end of the laterals. Another solution could be an extra chlorine injection at the end of the laterals. Although in all the previous studies commented the concentration of chlorine at the end of the laterals was higher, it did not prevent the completely formation of biofilm. In our experiment, as no concentration of chlorine was found at the end of the laterals, biofilm growth could be the main responsible of emitter clogging, as it happened also in the last locations.

On the other hand, the arm collector irrigation subunits remained less time with effluent inside the laterals. As the filtration units could work separately, the experiment started with porous media design and its corresponding irrigation subunit in March 6th, 13th for domes and 26th for arm collector. Short breakdowns (caused, for instance, by stuck valves or broken pipes) also happened more often in the porous media filtration unit (with a total of 7 days more of operation stops), mainly in May. This meant that porous media irrigation subunits remained more days with effluent inside the pipes than arm collector design, which, due to template weather in March (effluent average temperature of 15.6°C) and in May (effluent average temperature of 20.3°C) could favour biofilm growth and explain higher emitter clogging. In addition, the arm collector irrigation subunit could have lower temperature because it was located at the most shadowed side of the experimental site. On the other hand, there was not a significant difference between filters in the percentage of completely clogged emitters. A new set of experiment that is currently in process should confirm or refute this explanation.

Therefore, there was a clear effect of emitter location on emitter clogging at the end of the experiment, being the last locations more prone to clogging, as many other studies have pointed out (Duran-Ros et al., 2009a; Puig-Bargués et al., 2010a) even when using shorter lateral distance, such as 8 m (Wu et al., 2015), 9 m (Tripathi et al., 2014), or 25 m (Pei et al., 2014). So, comparing results from different studies using effluents, it seems that emitter clogging does not depend so much on the total lateral length, but on relative location to the end (e.g. last 5% distance of the total lateral length). Studying emitter clogging with different lateral length using same filtration conditions should be of interest, as well as establishing a chlorine concentration in function of the lateral length.

Finally, there was also an interaction between irrigation time and emitter location. The reduction of emitter discharge for all subunits was higher in the first stage of the experiment (7.57% from 0 to 500 h, with 0.2 m media height) than in the last stage (3.09% from 500 to 1000h, with 0.3 m media height). No significant differences were found in inlet turbidity levels between the two stages, but turbidity removals were significantly higher in the first stage with 0.2 m media height (24.8%) than in the second stage with 0.3 m (14.8%), which also indicates that the main cause of emitter clogging might be biological rather than physical.

Figure 6.10 shows the interior view of some of the last emitters. Even though only visual observation was carried out, small solid particles clearly different than sand from media were found inside the emitters, as well as biofilm, meaning that these kind of particles are able to pass through sand filtration bed ($d_e=0.48$ mm) and settle at the end of the lateral and inside the channel. Wu et al. (2015) used different d_e ranging from 0.41 to 2.10 mm, also noticed significant emitter discharge reductions at the last locations after 300 h, although did not studied differences among sand d_e . It was also observed biological growth in the labyrinth channels, especially in the inlet and vortex zones of the emitter (emitter channel protected by dome filter in Figure 6.10). Ait-Mouheb et al. (2018) also detected biofilm growth in these areas, using an optical microscope with a transparent emitter prototype and a synthetic wastewater solution (Gamri et al., 2014).

On the other hand, emitter clogging of the last emitters could be explained by physical causes, due to the aggregation of small solid particles, such as clay, whose electric charges allow agglomeration in the presence of salts (Bounoua, 2010; Bounoua et al., 2016). In fact, as stated before, clay and silt particles were observed inside the emitters (Figure 6.10). In that sense, Bounoua et al. (2016), in an experiment with a similar setup to that of this work (100 m lateral length, 2 l/h emitter discharge emitters placed each 0.3 m and three 80 μm screen filters) but using river water instead of effluents, found that filtration process is not fully effective when there is presence of small particles in the water, since they agglomerate in larger aggregates. The concentration of salts in the water along with flow path strain can favor this agglomeration. This explanation would make sense in the current experiment, since using effluents, there were concentration of small solid particles and salts, although they were not classified or quantified.

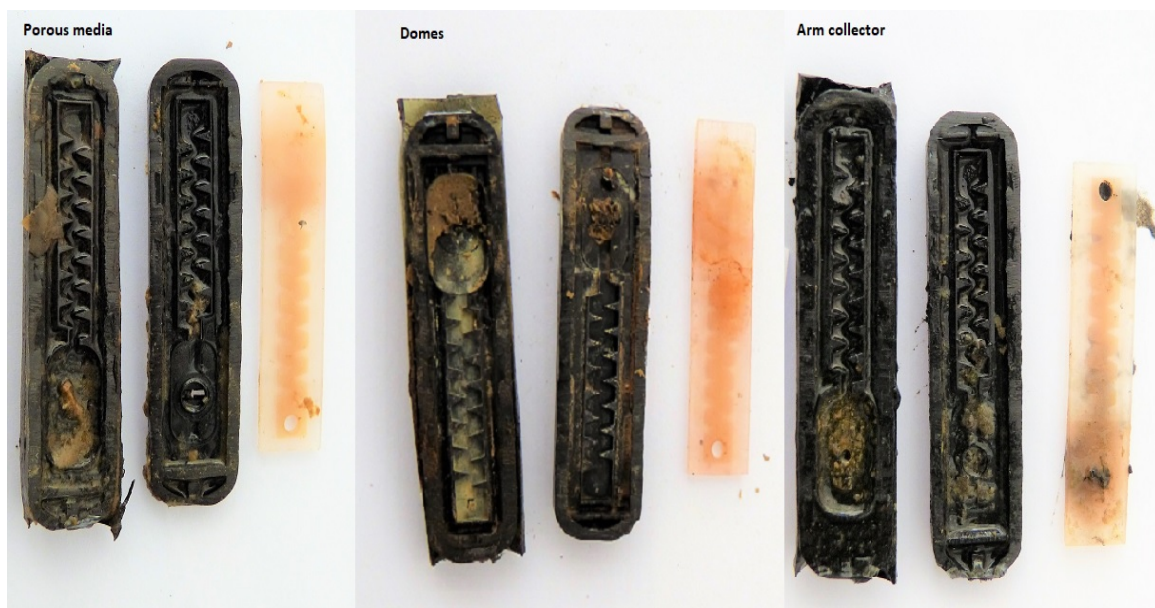


Figure 6.10. Inside views of last location emitters protected by the different filter designs at the end of the experiment.

6.3. IMPLICATIONS FOR IRRIGATION UNIFORMITY ASSESSMENT

As the flow discharge of all the emitters was measured at three different times, it was possible to compare the results of distribution uniformity assessment following different procedures, as well as emitter discharge distribution during the experiment. Water volume and pressure values along the lateral were also recorded continuously through an SCADA system (Chapter 5). Normality of the emitter discharge values was assessed with Kolmogorov-Smirnov and Shapiro-Wilk tests, and differences on DU_{iq} were assessed using the root mean square error (RMSE). As it was commented in Chapter 5, pressure distribution across laterals was always over 90%, meaning that it was uniform along the lateral for the whole experiment and discharge reductions could mainly be explained by emitter clogging, as the emitter manufacturing coefficient of variation was below 3%.

6.3.1. Emitter discharge distribution

Figure 6.11 shows the frequencies of the discharges of all emitters for the three irrigation subunits considered together for the three times sampled (0, 500 and 1000 h). According to both Kolmogorov-Smirnov and Shapiro-Wilk tests, emitter discharge did not follow a normal distribution in any of the uniformity assessment period. Normal distribution is expected in a microirrigation uniformity estimation (Bralts and Kesner, 1983), although Noory and Al Thamiery (2012) did not found it. With the increase of irrigation time, due to emitter clogging, the range of emitter discharges widened, increasing from 0.29% at 500 h to 0.96% at 1000 h, and, consequently, their distribution show more asymmetry and kurtosis.

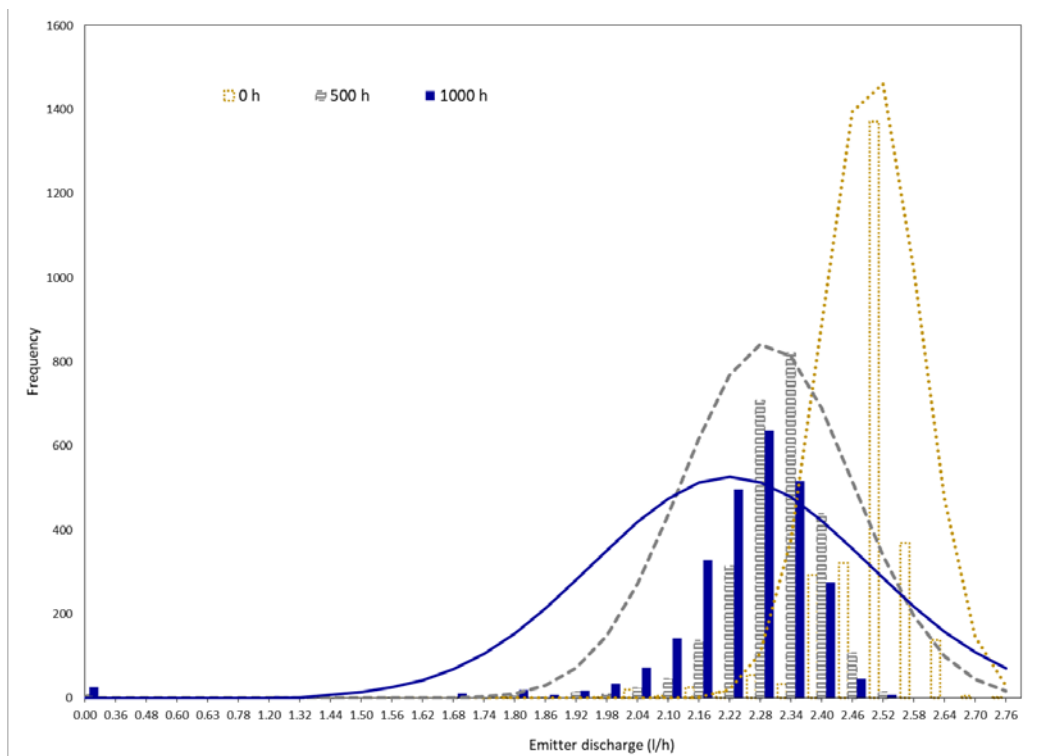


Figure 6.11. Frequency of the discharges of all the emitters for all irrigation subunits at different measuring times and normal plot adjustments.

6.3.2. Distribution uniformity assessment

Table 6.5 shows the values of DU_{iq} for the different methods during the three different measuring times for the three irrigation subunits. Values differ from one method to another as each method uses different locations to calculate DU_{iq} . Representativeness of selected emitters was the main objection that Juana et al. (2007) posed against Merriam and Keller (1978) procedure. In fact, as Merriam and Keller (1978) method uses the last two emitters in a dripline, it is easier to obtain lower distribution uniformity values with this method since it is more probable to find completely clogged emitters in these positions (Ravina et al. 1992; Trooien et al. 2000). As it can be seen in Table 6.5, DU_{iq} computed following Merriam and Keller (1978) showed the lowest values when those emitters located at the end of driplines began to become clogged, around 500 h. Burt (2004) method, which also uses emitters located at dripline end but in a higher number (28), showed smaller values (74.84%) when more completely clogged

emitters were found (1.22%) than DU_{iq} computed with all emitters (89.19%). DU_{iq} computed with SCADA system showed the lowest values at the beginning of the experiment (90.54%), and low values (76.92%) when more completely clogged emitter were found (1.22%), as it calculates the average emitter discharge for a lateral section. As locations suggested by Juana et al. (2007) were far away from distal positions, the DU_{iq} computed with this procedure showed globally the highest values.

Table 6.5. DU_{iq} computed with different emitter samples and number of completely clogged emitters for each irrigation subunit at the three different irrigation accumulated times.

Time (h)	Subunit	% Totally clogged emitters	DU_{iq} computed with emitter selection procedure				
			All emitters	Merriam and Keller (1978)	Burt (2004)	Juana et al. (2007)	SCADA
0	1	0	95.41	94.85	95.48	97.59	90.54
	2	0	93.97	96.06	95.48	96.01	91.71
	3	0	96.31	97.67	96.34	98.66	95.50
500	1	0.66	92.83	66.36	94.41	96.00	85.35
	2	0.22	93.07	82.13	95.48	98.47	88.93
	3	0	94.84	95.74	93.23	96.47	96.03
1000	1	1.22	89.18	46.57	74.84	92.39	79.26
	2	1	87.88	33.55	86.97	92.70	76.92
	3	0.66	91.44	60.89	89.17	95.21	94.66

Differences on DU_{iq} values were assessed computing the root mean square error (RMSE) between each method and the results obtained using the discharge of all the emitters in the field (Table 6.6). In the first emitter discharge assessment, carried out within the first 20 h of operation, RMSE was small, showing the SCADA system procedure the highest error, 3.15%, followed by Juana et al. (2017), 2.15%. After 500 h of operation, some completely clogged emitters appeared and RMSE values increased slightly for Burt (2004) (from 0.87 to 1.72%), Juana et al. (2007) (from 2.15 to 3.57%) and SCADA (from 3.15 to 5.24%), but noticeably for Merriam and Keller (1978) (from 1.44 to 16.80%) as some completely clogged emitters were found at those positions used for this procedure. Burt (2004) methodology uses also some of the distal emitters but only from one dripline and with a higher sample (28 emitters), while SCADA system uses all the emitters of the last section, meaning that the effect of clogged emitters with no discharge is minimized for both methods. After 1000 h of irrigation with reclaimed effluents, RMSE reached their maximum values, being dramatically high for Merriam and Keller (1978) procedure (43.92%) but reasonably low for Juana et al. (2007) (3.65%), followed by Burt (2004) (8.64%) and SCADA system (8.97%). If overall results are analyzed, lower RMSE were found for Juana et al. (2007) (3.16%), Burt (2004) (5.11%) and SCADA system (6.27%) than for Merriam and Keller (1978) (27.16%).

Table 6.6. Root mean square error (RMSE) between DU_{lq} obtained using all emitter discharges regarding DU_{lq} computed following the different procedures.

Sampling period	N	% Average completely clogged emitters	RMSE for DU_{lq} (%)			
			Merriam and Keller (1978)	Burt (2004)	Juana et al. (2007)	SCADA
0	3	0	1.44	0.87	2.15	3.15
500	3	0.29	16.8	1.72	3.47	5.24
1000	3	0.96	43.92	8.64	3.65	8.97
All data	9	0.42	27.16	5.11	3.16	6.27

As Juana et al. (2007) avoided selecting distal positions in a lateral, its methodology obtained low RMSE and a DU_{lq} closer to real DU_{lq} . When the last emitters in a dripline are selected, as it happens with Merriam and Keller (1978) procedure, DU_{lq} differs more from real DU_{lq} , although these last positions are probably the critical ones where clogging can be easily detected. However, with this method, if previous positions are selected its DU_{lq} is more close to real value.

Measuring emitter discharge with more emitters following Burt (2004) methodology or using a SCADA system did not yield a DU_{lq} as close as to its real value than the assessed by Juana et al. (2007) procedure when clogged emitters were found, because these methods also take into account last positions, although their overall RMSE was not high. However, SCADA system showed high correlations (Chapter 5) with real distribution uniformities (both for pressure and emitter discharges) and allowed monitoring the performance of the irrigation system in real time and without the need of field measurements, being an interesting tool for assessing DU_{lq} .

Finally, the experimental framework was the basic expression of a drip irrigation system (four laterals) with four measuring points per lateral. SCADA systems have already been used in drip irrigation systems but mostly for research purposes. It is worth studying whether the implementation of a SCADA system like the one proposed can be transferred to plot level for farmers. Given the measuring equipment, sensors and technology used, the initial economic cost is high for a farmer. In this sense, a SCADA system with the minimum number of sensors would be economically viable to calculate the desired parameters. Further research in that field would be of great interest.

7. CONCLUSIONS

7. CONCLUSIONS

The main conclusions derived from this thesis are:

1. Regarding water quality:
 - 1.1. Effluent turbidity removal was affected by the combined effect of underdrain design, media height and filtration velocity.
 - 1.2. The porous media design achieved higher turbidity removals for all operational conditions except for 0.3 m height and 30 m/h.
 - 1.3. The filtration velocity of 30 m/h showed higher turbidity removal efficiency for all filter designs.
2. Regarding pressure loss, filtered volume and energy consumption:
 - 2.1. Media bed presented higher pressure losses than other sections (such as the diffuser plate or the underdrain) in all cases for all filter designs.
 - 2.2. Higher filtration velocities presented higher pressure losses for all operational conditions and filter designs, except for the case of arm collector with 0.3 m bed height and 30 m/h.
 - 2.3. Porous media design filtered significantly more water volume at 30 m/h than the other two designs.
 - 2.4. Regarding media height, there was more filtered water volume per energy unit with a media height of 0.2 m than 0.3 m for both filtration velocities, and with 0.3 m, filtration velocity of 30 m/h filtered more water volume per energy unit than 60 m/h. The porous media design also showed greater ratios of filtered water per energy unit than the other two designs at both filtration velocities.
3. Regarding the emitter performance:
 - 3.1. Emitter clogging was affected by the double interactions of underdrain design and time, underdrain design and emitter location, and time and emitter location.
 - 3.2. The emitters protected by the arm collector filter showed higher emitter discharge than those that had the other two filter designs at the end of the experiment. With the arm collector filter, the percentage of completely clogged emitters was smaller, although no significant differences among filters were found.

3.3. The emitter location had a significant effect on emitter discharge in the three last emitters after 500 h, and the four after 1000 h. The last locations presented less emitter discharge in all irrigation subunits.

4. Regarding the different methodologies for assessing irrigation uniformity distribution:

4.1. The methodology for assessing flow distribution uniformity (DU_{iq}) suggested by Juana et al (2007) showed a better agreement with the real DU_{iq} using all the emitters for all the time measurements carried out.

4.2. There was a good correlation between distribution uniformity assessed by the SCADA system and the real one. Therefore, SCADA system is a good tool to assess DU_{iq} in real time.

7.1. FUTURE PROSPECTIONS

At the time of writing this doctoral thesis, more experiments are being carried out with the same setup and operational conditions, using crushed recycled glass instead of silica sand for filtration media. These experiments will provide more data of the operational conditions and consumptions of the three tested filters working with another filtration media. The experiment will also allow the study of emitter clogging and distribution uniformity assessment, contrasting the results of the present thesis.

Future research will also allow the evaluation of filtering drip irrigation systems to reduce energy consumption and being eco-efficient, carrying out a Life cycle assessment (LCA). Finally, it would be of interest the evaluation of SCADA systems for farmers using reclaimed water.

On the other hand, a series of experiments have been carried out to analyze and determine particle retention in filtration media using Optical Coherence Tomography (OCT) technique and image analysis. The results are promising and show the feasibility of OCT technique to determine and study particle retention in filtration media, and it is expected to carry out the experiments for further analysis in future.

Moreover, the next step would also include the study of filter hydraulic performance using tools such as Computational Fluid Dynamics (CFD) for developing a model to predict filter and emitter clogging using reclaimed effluents with different operational conditions, as well as the study of backwashing in detail, in order to further justify the results obtained.

8. REFERENCES

8. REFERENCES

- Abbott, J.S., 1985. Emitter clogging-causes and prevention. *ICID Bulletin*, 34 (2), 11-20.
- ACA, 2018. Evolució anual del volum d'aigua reutilitzat per usos (hm³). Agència Catalana de l'Aigua, Departament de Territori i Sostenibilitat, Generalitat de Catalunya. Departament de Territori i Sostenibilitat, Barcelona.
- Adin, A., Sacks, M., 1987. Water quality and emitter clogging relationship in wastewater irrigation. Proceedings of Water Reuse Symposium IV, Denver, Colorado, 517-530.
- Adin, A., Sacks, M., 1991. Dripper-clogging factors in wastewater irrigation. *Journal of Irrigation and Drainage Engineering*, 117 (6), 813-826.
- Adin, A., 2002. Water treatment and filtration for drip/micro irrigation. International meeting on advances in drip/micro irrigation, Puerto de la Cruz, 221-237.
- Ait-Mouheb, N., Bahri, A., Ben Thayer, B., Benyahia, B., Bourrié, G., Cherki, B., Condom, N., Declerq, R., Gunes, A., Héran, M., Kitir, N., Molle, B., Patureau, D., Pollice, A., Rapaport, A., Renault, P., Riahi, K., Romagny, B., Sar, T., Sinfort, C., Steyer, J.P., Talozzi, S., Topcuoglu, B., Turan, M., Wéry, N., Yildirim, E., Harmand, J., 2018. The reuse of reclaimed water for irrigation around the Mediterranean Rim: a step towards a more virtuous cycle? *Regional Environmental Change*, 18, 693-705.
- Ait-Mouheb, N., Schillings, J., Al-Muhammad, J., Bendoula, R., Tomas, S., Amielh, M., Anselmet, F., 2019. Impact of hydrodynamics on clay particle deposition and biofilm development in a labyrinth-channel dripper. *Irrigation Science*, 37, 1-10.
- Al-Muhammad, Tomas, S., Ait-Mouheb, N., Amielh, M., Anselmet, F., 2018. Micro-PIV characterization of the flow in a milli-labyrinth-channel used in drip irrigation. *Experiments in Fluids*, 59 (12), 181.
- Amburgey, J.E., Amirtharajah, A., 2005. Strategic filter backwashing techniques and resulting particle passage. *Journal of Environment Engineering*, 131 (4), 535-547.
- Amirtharajah, A., 1985. The interface between filtration and backwashing. *Water Research*, 19 (5), 581-588.
- Arbat, G., Pujol, T., Puig-Bargués, J., Duran-Ros, M., Barragán, J., Montoro, L., Ramírez de Cartagena, F., 2011. Using computational fluid dynamics to predict head losses in the auxiliary elements of a microirrigation sand filter. *Transactions of the ASABE*, 54 (4), 1367-1376.
- Arbat, G., Pujol, T., Puig-Bargués, J., Duran-Ros, M., Montoro, L., Barragán, J., 2013. An experimental and analytical study to analyse hydraulic behaviour of nozzle-type underdrains in porous media filters. *Agricultural Water Management*, 126, 64-74.

- Aronino, R., Dlugy, C., Arkhangelsky, E., Shandalov, S., Oron, G., Brenner, A., Gitis, V., 2009. Removal of viruses from surface water and secondary effluents by sand filtration. *Water Research*, 43 (1), 87-96.
- ASAE. 2003. ASAE Standards. EP405.1. Design and Installation of Micro-Irrigation Systems. St. Joseph, Michigan.
- Ayars, J. E., Bucks, D. A., Lamm, F. R., Nakayama, F. S., 2007. Introduction. In: Lamm, F.R., Ayars, J.E., Nakayama, F.S. (Eds), *Microirrigation for crop production: Design, Operation and management*. Developments in Agricultural Engineering, vol. 13. Elsevier, Amsterdam, 1-26.
- Ayars, J.E., Phene, C.J., 2007. Automation. In: Lamm, F.R., Ayars, J.E., Nakayama, F.S. (Eds.), *Microirrigation for Crop Production: Design, Operation and Management*. Developments in Agricultural Engineering, vol. 13. Elsevier, Amsterdam, 259-284.
- Bahri, A., 2009. Managing the other side of the water cycle: making wastewater an asset, Background paper nº 13. Global Water Partnership, Stockholm.
- Barragán, J., Bralts, V., Wu, I.P., 2006. Assessment of emission uniformity for microirrigation design. *Biosystems Engineering*, 93 (1), 89-97.
- Belaud, G., Mateos, L., Aliod, R., Buisson, M.C., Faci, E., Gendre, S., Ghinassi, G., Gonzales-Perea, R., Lejars, C., Maruejols, F., Zapata, N., 2019. Irrigation and Energy: issues and challenges. *Irrigation and Drainage*, DOI: 10.1002/ird.2343.
- Bounoua, S., 2010. Étude du colmatage des systèmes d'irrigation localisée. PhD dissertation. Université de Provence, Aix-Marseille.
- Bounoua, S., Tomas, S., Labille, J., Molle, B., Granier, J., Haldenwang, P., Izzati, S., 2016. Understanding physical clogging in drip irrigation: in situ, in-lab and numerical approaches. *Irrigation Science*, 34, 327-342.
- Bové, J., 2018. Optimización del diseño de los filtros de arena utilizados en sistemas de riego por goteo. PhD dissertation. Universitat de Girona, Girona.
- Bové, J., Arbat, G., Duran-Ros, M., Pujol, T., Velayos, J., Ramírez de Cartagena, F., Puig-Bargués, J. 2015a. Pressure drop across sand and recycled glass media used in micro irrigation filters. *Biosystems Engineering*, 137, 55-63.
- Bové, J., Arbat, G., Duran-Ros, M., Pujol, T., Velayos, J., Ramírez de Cartagena, F., Puig-Bargués, J. 2015b. Reducing energy requirements for sand filtration in microirrigation: Improving the underdrain and packing. *Biosystems Engineering*, 140, 67-78.
- Bové, J., Arbat, G., Duran-Ros, M., Pujol, T., Ramírez de Cartagena, F., Pujol, J., 2015c. Filtro de matriz granular. Spanish utility model U201530629.
- Bové, J., Puig-Bargués, J., Arbat, G., Duran-Ros, M., Pujol, T., Pujol, J., Ramírez de Cartagena, F., 2017. Development of a new underdrain for improving the efficiency of microirrigation sand media filters. *Agricultural Water Management*, 179, 296-305.

- Bové, J., Pujol, J., Arbat, G., Duran-Ros, M., Ramírez de Cartagena, F., Puig-Bargués, J., 2018. Environmental assessment of underdrain designs for a sand media filter. *Biosystems Engineering*, 167, 126-136.
- Bralts, V.F., Kesner, D., 1983. Drip irrigation field uniformity estimation. *Transactions of the ASAE*, 26 (5), 1369-1374.
- Bucks, D.A., Nakayama, F.S., Gilbert, R.G., 1979. Trickle irrigation water quality and preventive maintenance. *Agricultural Water Management*, 2 (2), 149-162.
- Burt, C., 2004. Rapid field evaluation of drip and microspray distribution uniformity. *Irrigation and Drainage Systems*, 18, 275-297.
- Burt, C., 2005. Overview of supervisory control and data acquisition (SCADA). In: Burt, C.M., Anderson, S.S. (Eds.), *SCADA and Related Technologies for Irrigation District Modernization*. USCID, Denver, Colorado.
- Burt, C., 2010. Hydraulics of commercial sand media filter tank used for agricultural drip irrigation. *Irrigation and Drainage Systems*. Report N° R 10001. San Luis Obispo, California.
- Burt, C., Howes, D. J., Freeman, B., 2011. Public Interest Energy Research (PIER) Program. Final Project Report, Agriculture Water Energy Efficiency. California Energy Commission and Irrigation Training and Research Center (ITCR), San Luis Obispo, California, 262-263.
- Burt, C., Styles, S.W., 2000. Riego por goteo y por microaspersión para árboles, vides y cultivos anuales. Irrigation Training and Research Center (ITRC), California Polytechnic State University, San Luis Obispo, California.
- Burt, C., Styles, S.W., 2007. Drip and Micro Irrigation Design and Management. Irrigation Training and Research Center (ITCR), San Luis Obispo, California.
- Canna-Michaelidou, S., Christodoulidou, M., 2008. Development and implementation of indices for the quality of treated effluent. *International Journal of Environment and Pollution*, 33 (1), 72-81.
- Capra, A., Scicolone, B., 2004. Emitter and filter tests for wastewater reuse by drip irrigation. *Agricultural Water Management*, 68 (2), 1529-1534.
- Capra, A., Scicolone, B., 2007. Recycling of poor quality urban wastewater by drip irrigation systems. *Journal of Cleaner Production*, 15 (16), 1529-1534.
- Cararo, D.C., Botrel, T.A., Hills, D.J., Leverenz, H.L., 2006. Analysis of clogging in drip emitters during wastewater irrigation. *Applied Engineering in Agriculture*, 22 (2), 251-257.
- Carrillo-Cobo, M.T., Camacho-Poyato, E., Montesinos, P., Rodríguez-Díaz, J.A., 2014. Assessing the potential of solar energy in pressurized irrigation networks. The case of Bembézar MI irrigation district (Spain). *Spanish Journal of Agricultural Research*, 12 (3), 838-849.
- Casadesús, J., Mata, M., Marsal, J., Girona, J., 2012. A general algorithm for automated scheduling of drip irrigation in tree crops. *Computers and Electronics in Agriculture*, 83, 11-20.

- Chandel, S.S., Nagaraju Naik, M., Chandel, R., 2015. Review of solar photovoltaic water pumping system technologies for irrigation and community drinking water supplies. *Renewable and Sustainable Energy*, 29, 1084-1099.
- Cirelli, G.L., Consoli, S., Licciardello, F., Aiello, R., Giuffrida, F., Leonardi, C., 2012. Treated municipal wastewater reuse in vegetable production. *Agricultural Water Management*, 104, 163-170.
- Corominas, J., 2010. Agua y energía en el riego en la época de la sostenibilidad. *Ingeniería del Agua*, 17 (3), 219-233.
- Cortesi, N., Gonzalez-Hidalgo, J.C., Brunetti, M., Martin-Vide, J., 2012. Daily precipitation concentration across Europe 1971-2010. *Natural Hazards and Earth System Sciences*, 12, 2799-2810.
- Cramer, W., Guiot, J., Fader, M., Garrabou, J., Gattuso, J.P., Iglesias, A., Lange, M.A., Lionello, P., Llasat, M.C., Paz, S., Peñuelas, J., Snoussi, M., Toreti, A., Tsimplis, M.N., Xoplaki, E., 2018. Climate change and interconnected risks to sustainable development in the Mediterranean. *Nature Climate Change*, 8, 972-980.
- Daccache, A., Ciurana, J.S., Rodriguez-Diaz, J.A., Knox, J.W., 2014. Water and energy footprint of irrigated agriculture in the Mediterranean region. *Environmental Research Letters*, 9 (12), 1-12.
- Darby, J.L., Lawler, D.F., 1990. Ripening in depth filtration. *Environmental Science and Technology*, 24 (7), 1069-1079.
- De Deus, F.P., Testezlaf, R., Mesquita, M., 2016. Assessment methodology of backwashing in pressurized sand filters. *Revista Brasileira de Engenharia Agrícola e Ambiental*, 20 (7), 600-605.
- Dehghanisani, H., Yamamoto, T., Rasiyah, V., Utsunomiya, J., Inoue, M., 2004. Impact of biological clogging agents on filter and emitter discharge characteristics of microirrigation systems. *Irrigation and Drainage*, 53 (4), 363-373.
- Dehghanisani, H., Yamamoto, T., Ould Ahmad, B., Fujiyama, H.Y., Miyamoto, K., 2005. The effect of chlorine on emitter clogging induced by algae and protozoa and the performance of drip irrigation. *Transactions of the ASAE*, 48 (2), 519-527.
- Diotto, A. V., Folegatti, M. V., Duarte, S. N., Romanelli, T. L., 2014. Embodied energy associated with the materials used in irrigation systems: drip and centre pivot. *Biosystems Engineering*, 121, 38-45.
- Domingo, J., Gámiz, J., Grau, A., Martínez, H. 2003. Diseño y aplicaciones con autómatas programables. Editorial UOC, Barcelona.
- Dos Santos, M. B., Mesquita, M., Testezlaf, R., 2013. Application of a vertical wind tunnel to evaluate flow lines generated by sand filters underdrains. *Engenharia Agrícola*, 33 (3), 548-559.

- Duran-Ros, M., Puig-Bargués, J., Arbat, G., Barragán, J., Ramírez de Cartagena, F., 2008. Definition of a SCADA system for a microirrigation network with effluents. *Computers and Electronics in Agriculture*, 64 (2), 338-342.
- Duran-Ros, M., Puig-Bargués, J., Arbat, G., Barragán, J., Ramírez de Cartagena, F., 2009a. Effect of filter, emitter and location on clogging when using effluents. *Agricultural Water Management*, 96 (10), 67-79.
- Duran-Ros, M., Puig-Bargués, J., Arbat, G., Barragán, J., Ramírez de Cartagena, F., 2009b. Performance and backwashing efficiency of disc and screen filters in microirrigation systems. *Biosystems Engineering*, 103 (1), 35-42.
- Enciso-Medina, J., Multer, W.L., Lamm, F.R., 2011. Management, maintenance and water quality effects on the long-term performance of subsurface drip irrigation systems. *Applied Engineering and Agriculture*, 27 (6), 969-978.
- Elbana, M., Ramírez de Cartagena, J., Puig-Bargués, J., 2012. Effectiveness of sand media filters for removing turbidity and recovering dissolved oxygen from a reclaimed effluent used for micro-irrigation. *Agricultural Water Management*, 111, 27-33.
- El-Berry, A.M., Bakeer, G.A., and Al-Weshali, A.M., 2003. The effect of water quality and aperture size on clogging of emitters. International Workshop on Improved Irrigation Technologies and Methods: research, development and testing, Montpellier.
- European Commission. 2019. Water reuse. <https://ec.europa.eu/environment/water/reuse.htm> (date of access: 10 – 09 – 19).
- FAO. 2019a. AQUASTAT website. <http://www.fao.org/nr/water/aquastat/main/index.stm> (date of access: 04 – 15 – 19).
- FAO. 2019b. FAOSTAT Online Statistical Service, Food and Agriculture Organization, Rome. <http://www.fao.org/statistics/en> (date of access: 05 – 07 – 2019).
- Feng, J., Li, Y., Wang, W., Xue, S., 2018. Effect of optimization forms of flow path on emitter hydraulic and anti-clogging performance in drip irrigation system. *Irrigation Science*, 36 (1), 37-47.
- Feng, D., Kang, Y., Wan, S., Liu, S., 2017. Lateral flushing regime for managing emitter clogging under drip irrigation with saline groundwater. *Irrigation Science*, 35 (3), 217-225.
- Fernández-García, I., Rodríguez-Díaz, J.A., Camacho-Poyato, E., Montesinos, P., Berbel, J. 2014. Effects of modernization and medium term perspectives on water and energy use in irrigation districts. *Agricultural Systems*, 131, 56-63.
- Fernández-Pacheco, D.G., Molina-Martínez, J.M., Jiménez, M., Pagán, F.J., Ruiz-Canales, A., 2014. SCADA platform for regulated deficit irrigation management of almond trees. *Journal of Irrigation and Drainage Engineering*, 140 (5), 04014008.
- Gamri, S., Soric, A., Tomas, S., Molle, B., Roche, N., 2014. Biofilm development in micro-irrigation emitters for wastewater reuse. *Irrigation Science*, 32 (1), 77-85.

- García de Rentería, P., Pérez, A., Ballesteros, M., 2018. El agua en la economía circular: un análisis del estado de la cuestión a partir de indicadores. Congreso Nacional de Medio Ambiente, Madrid.
- Goldhamer, D.A., Fereres, E., 2004. Irrigation scheduling of almond trees with trunk diameter sensors. *Irrigation Science*, 23 (1), 11-19.
- Gonçalves, R.A.B., Folegatti, M.V., Gloaguen, T.V., Libardi, P.L., Montes, C.R., Lucas, Y., Dias, C.T.S., Melfi, A.J., 2007. Hydraulic conductivity of soil irrigated with treated sewage effluent. *Geoderma*, 139 (1-4), 24-248.
- González-Díaz, J.A., Celaya, R., Fernández-García, F., Osoro, K., Rosa-García, R., 2019. Dynamics of rural landscapes in marginal areas of northern Spain: Past, present and future. *Land, Degradation and Development*, 30 (2), 141-150.
- González-Perea, R., Fernández-García, I., Martín-Arroyo, M., Rodríguez-Díaz, J.A., Camacho-Poyato, E., Montesinos, P., 2017. Multiplatform application for precision irrigation scheduling in strawberries. *Agricultural Water Management*, 183, 194-201.
- Green, O., Katz, S., Tarchitzky, J., Chen, Y., 2018. Formation and prevention of biofilm and mineral precipitate clogging in drip irrigation systems applying treated wastewater. *Irrigation Science*, 36 (4-5), 257-270.
- Greve, P., Gudmundsson, L., Seneviratne, S.I., 2018. Regional scaling of annual mean precipitation and water availability with global temperature change. *Earth System Dynamics Discussion*, 9, 227-240.
- Gushiken, E.C., 1995. Irrigate with reclaimed water through permanent subsurface drip irrigation system. Proceedings of the Fifth International Microirrigation Congress, Orlando, Florida, 269 – 274.
- Haman, D.Z., Smajstrla, A.G., and Zazueta, F.S, 1994. Media filters for trickle irrigation in Florida. Institute of Food and Agriculture Science, University of Florida, Gainesville, Florida.
- Hamilton, A.J., Stagnitti, F., Xiong, X., Kreidl, S.L., Benke, K.K., Maher, P., 2007. Wastewater irrigation: the state of play. *Vadose Zone Journal*, 6 (4), 823-840.
- Hao, F.Z., Li, J., Wang, Z., Li, Y.F., 2018. Effect of chlorination and acidification on clogging and biofilm formation in drip emitters applying secondary sewage effluent. *Transactions of the ASABE*, 61 (4), 1351-1363.
- Hardy, L., Garrido, A., 2012. Water, agriculture and the environment in Spain: can we square the circle. Challenges and opportunities related to the Spanish Water-Energy Nexus, chapter 14. CRC Press, Leiden, 177-189.
- Haruta, S., Chen, W., Gan, J., Simunek, J., Chang, A.C., and Wu, L., 2008. Leaching risk of N-nitromethyleamine (NDMA) in soil receiving reclaimed wastewater. *Ecotoxicology and Environmental Safety*, 69, 374-380.
- Hills, D.J., Brenes, M.J., 2001. Microirrigation of wastewater effluent using drip tape. *Applied Engineering in Agriculture*, 17 (3), 303-308.

- Horan, N., Lowe, M., 2007. Full-scale trials of recycled glass as tertiary filter medium for wastewater treatment. *Water Research*, 41 (1), 253-259.
- Hu, Z., Gagnon, G. A., 2006. Impact of filter media on the performance of full-scale recirculating biofilters for treating multi-residential wastewater. *Water Research*, 40 (7), 1474-1480.
- ICID. 2013. Sustainable Intensification of Agriculture. International Commission on Irrigation and Drainage. Annual Report 2012-2013. ICID, New Delhi.
- ICID. 2019. Agricultural Water Management for Sustainable Rural Development. International Commission on Irrigation and Drainage. Annual Report 2018-2019. ICID, New Delhi.
- Jackson, R.B., Carpenter, S.R., Dahm, C.N., McKnight, D.M., Naiman, R.J., Postel, S.L., Running, S.W., 2001. Water in a changing world. *Ecological Applications*, 11 (4), 1027-1045.
- Jiménez-Bello, M.A., Martínez, F., Bou, V., Bartolí, H.J., 2010. Methodology for grouping intakes of pressurized irrigation networks into sectors to minimize energy consumption. *Biosystems Engineering*, 105, 429-438.
- Jiménez-Bello, M.A., Royuela, A., Manzano, J., García Prats, A., Martínez-Alzamora, F., 2015. Methodology to improve water and energy use by proper irrigation scheduling in pressurized networks. *Agricultural Water Management*, 149, 91-101.
- Juana, L., Rodríguez-Sinobas, L., Sánchez, R., Losada, A., 2007. Evaluation of drip irrigation: Selection of emitters and hydraulic characterization of trapezoidal units. *Agricultural Water Management*, 90, 13-26.
- Kansas State University, 2019. K-State Research Extension, Drawings of Microirrigation Components. <https://www.ksre.k-state.edu/sdi/photos/dmc.html> (date of access: 09-22-2019).
- Katz, S., Dosoretz, C., Chen, Y., Tarchitzky, J., 2014. Fouling formation and chemical control in drip irrigation systems using treated wastewater. *Irrigation Science*, 32 (6), 459-469.
- Kiziloglu, F.M., Turan, M., Sahin, U., Kuslu, Y., Dursun, A., 2008. Effects of untreated and treated wastewater irrigation on some chemical properties of cauliflower (*Brassica oleracea* L. var. botrytis) and red cabbage (*Brassica oleracea* L. var. rubra) grown on calcareous soil in Turkey. *Agricultural Water Management*, 95 (6), 716-724.
- Kouamé, P.K., Nguyen-Viet, H., Dongo, K., Biémi, J., Bonfoh, B., 2017. Microbiological risk infection assessment using QMRA in agriculture systems in Côte d'Ivoire, West Africa. *Environmental Monitoring and Assessment*, 189 (11), 587.
- Lavanholi, R., Oliveira, F.C., de Camargo, A.P., Frizzione, J.A., Molle, B., Ait-Mouheeb, N., Tomas, S., 2018. Methodology to evaluate dripper sensitivity to clogging due to solid particles: an assessment. *The Scientific World Journal*, 2018, 7697458.
- Lazarova, V., Emsellem, Y., Paille, J., Glucina, K., Gislette, P., 2011. Water quality management aquifer recharge using advanced tools. *Water Science and Technology*, 64 (5), 1161-1168.

- Lequette, K., Ait-Mouheb, N., Wery, N., 2019. Drip irrigation with treated wastewater: sanitary issues of biofouling. 20th International Symposium on Health Related Water Microbiology, Vienna.
- Li, J., Chen, L., Li, Y., Yin, J., Zhang, H., 2010. Effects of chlorination schemes on clogging in drip emitters during application of sewage effluent. *Applied Engineering in Agriculture*, 26 (4), 565-578.
- Li, D., Hendricks-Franssen, H.J., Han, X., Jiménez-Bello, M.A., Martínez-Alzamora, F., Vereecken, H., 2018b. Evaluation of an operational real-time irrigation scheduling scheme for drip irrigated citrus fields in Picassent, Spain. *Agricultural Water Management*, 208, 465-477.
- Li, N., Kang, Y., Li, X., Wan, S., Zhang, C., Wang, X., 2019b. Lateral flushing with fresh water reduced emitter clogging in drip irrigation with treated effluent. *Irrigation Science*, 37 (5), 627-635.
- Li, G.B., Li, Y.K., Xu T.W., Liu Y.Z., Jin, H., Yang, P.L., Yan, D.Z., Ren, S.M., 2012. Effects of average velocity on the growth and surface topography of biofilms attached on the reclaimed wastewater drip irrigation system laterals. *Irrigation Science*, 30 (2), 103-113.
- Li, Y., Song, P., Pei, Y., Feng, J., 2015. Effects of lateral flushing on emitter clogging and biofilm components in drip irrigation systems with reclaimed water. *Irrigation Science*, 33 (3), 235-245.
- Li, A., Stokal, M., Bai, Z., Kroeze, C., Ma, L., 2019a. How to avoid coastal eutrophication - a back-casting study for the North China Plain. *Science of the Total Environment*, 692, 676-690.
- Li, Z., Yu, L., Li, N., Chang, L., Cui, N., 2018a. Influence of flushing velocity and flushing frequency on the service life of labyrinth-channel emitters. *Water*, 10 (11), 1630.
- Madramootoo, C.A., Morrison, J., 2013. Advances and challenges with micro-irrigation. *Irrigation and Drainage*, 62 (3), 255-261.
- Magesan, G.N., 2001. Changes in soil physical properties after irrigation of two forested soils with municipal wastewater. *New Zealand Journal of Forestry Science*, 31 (2), 188-195.
- Magesan, G.N., Williamson, J.C., Yeates, G.W., Lloyd-Jones, A.R.H., 2000. Wastewater C/N ratio effects on soil hydraulic conductivity and potential mechanisms for recovery. *Bioresource Technology*, 71 (1), 21-27.
- MAPAMA. 2018. Encuesta sobre superficies y rendimientos de cultivos. Informe sobre el riego en España. Ministerio de Agricultura, Alimentación y Medio Ambiente de España, Madrid.
- Mareels, I., Weyer, E., Ooi, S.K., Cantoni, M., Li, Y., Nair, G., 2005. System engineering for irrigation system: Successes and challenges. *Annual Review in Automatic Programming*, 29 (2), 191-204.
- Martin-Vide, J., 2004. Spatial distribution of a daily precipitation concentration index in peninsular Spain. *International Journal of Climatology*, 24, 959-971.
- Mérida-García, A., Gallagher, J., McNabola, A., Camacho-Potayo, E., Montesinos, P., Rodríguez-Díaz, J.A., 2019. Comparing the environmental and economic impacts of on- or off-grid

solar photovoltaics with traditional energy sources for rural irrigation systems. *Renewable Energy*, 140, 895-904.

Merriam, J.L., Keller, J., 1978. *Farm Irrigation System Evaluation: A Guide for Management*. Utah State University, Logan, Utah.

Mesquita, M., 2014. *Desenvolvimento tecnológico de um filtro de areia para irrigação localizada*. PhD dissertation. Universidade Estadual de Campinas, Campinas.

Mesquita, M., Testezlaf, R., de Deus, F.P., da Rosa, L., 2017. Characterization of flow lines generated by pressurized sand filter underdrains. *Chemical Engineering Transactions*, 53, 715-720.

Mesquita, M., de Deus, F., Testezlaf, R., da Rosa, L., Diotto, A., 2019. Design and hydrodynamic performance testing of a new pressure sand filter diffuser plate using numerical simulation. *Biosystems Engineering*, 183, 59-69.

Mesquita, M., Testezlaf, R., Ramirez, J., 2012. The effect of media bed characteristics and internal auxiliary elements on sand filter head loss. *Agricultural Water Management*, 115, 178-185.

Molle, B., Brelle, F., Bessy, J., Gantel, D., 2012. Which water quality for which uses? Overcoming overzealous use of the precautionary principle to reclaim waste water for appropriate irrigation uses. *Irrigation and Drainage*, 61, 87-94.

Molle, B., Tomas, S., Huet, L., Audouard, M., Olivier, Y., Granier, J., 2016. Experimental approach to assessing aerosol dispersion of treated wastewater distributed via sprinkler irrigation. *Journal of Irrigation and Drainage Engineering*, 142 (9), 04016031.

Moreno, M.A., Ortega, J. F., Córcoles, J. I., Martínez, A., Tarjuelo, J. M., 2010. Energy analysis of irrigation delivery systems: monitoring and evaluation of proposed measures for improving energy efficiency. *Irrigation Science*, 28 (5), 445-460.

Morillo, J.G., Martín, M., Camacho, E., Rodríguez Díaz, J.A., Montesinos, P., 2015. Toward precision irrigation for intensive strawberry cultivation. *Agricultural Water Management*, 151, 43-51.

Müller, K., Magesan, G.N., Bolan, N.S., 2007. A critical review of the influence of effluent irrigation on the fate of pesticides in soil. *Agriculture, Ecosystems and Environment*, 120(2-4), 93-116.

Nakayama, F.S., Gilbert, R.G., Bucks, D.A., 1978. Water treatments in trickle irrigation systems. *Journal of the Irrigation and Drainage Division*, 104 (1), 23-25.

Nakayama, F.S., Boman, B.J., Pitts, D.J., 2007. Maintenance. In: Lamm, F.R., Ayars, J.E., Nakayama, F.S. (Eds.), *Microirrigation for Crop Production. Design, Operation, and Management*. Developments in Agricultural Engineering, vol. 13. Elsevier, Amsterdam, 389-430.

Nakhla, G., Farooq, S., 2003. Simultaneous nitrification–denitrification in slow sand filters. *Journal of Hazardous Materials*, 96 (2–3), 291-303.

- Nejatijahromi, Z., Nassery, H.R., Hosono, T., Nakhaei, M., Alijani, F., Okumura, A., 2019. Groundwater nitrate contamination in an area using urban wastewaters for agricultural irrigation under arid climate condition, southeast of Tehran, Iran. *Agricultural Water Management*, 221, 397-414.
- Niu, W., Liu, L., Chen, X., 2013. Influence of fine particle size and concentration on the clogging of labyrinth emitters. *Irrigation Science*, 31 (4), 545-555.
- Noori, J.S., Al Thamiry, H.A., 2012. Hydraulic and statistical analyses of design emission uniformity of trickle irrigation systems. *Journal of Irrigation and Drainage Engineering*, 138 (9), 791-798.
- Ojha, C.S.P., Graham, N.J.D., 1994. Computer-aided simulation of slow sand filter performance. *Water Research*, 28 (5), 1025-1030.
- Oliver, M.M.H., Hewa, G.A., Pezzaniti, D., 2014. Bio-fouling of subsurface type drip emitters applying reclaimed water under medium soil thermal variation. *Agricultural Water Management*, 133, 12-23.
- Pardo, M.A., Manzano, J., Cabrera, E., García-Serra, J., 2013. Energy audit of irrigation networks. *Biosystems Engineering*, 115 (1), 89-101.
- Pei, Y.T., Li, Y.K., Liu, Y.Z., Zhou, B., Shi, Z., Jiang, Y.G., 2014. Eight emitters clogging characteristics and its suitability evaluation under on-site reclaimed water drip irrigation. *Irrigation Science*, 32(2), 141-157.
- Pereira, L.S., Oweis, S.T., Zairi, A., 2002. Irrigation management under water scarcity. *Agricultural Water Management*, 57 (3), 175-206.
- Petrucci, R., 2007. *General Chemistry: Principles and Modern Applications*. Ed. Prentice Hall, New Jersey.
- Picazo, M.A.P., Juárez, J.M., García-Márquez, D., 2018. Energy consumption optimization in irrigation networks supplied by a standalone direct pumping photovoltaic system. *Sustainability*, 10 (11), 4203.
- Picó, Y., Alvarez-Ruiz, R., Alfarhan, A.H., El-Sheikh, M.A., Alobaid, S.M., Barceló, D., 2019. Uptake and accumulation of emerging contaminants in soil and plant treated with wastewater under real-world environmental conditions in the Al Hayer area (Saudi Arabia). *Science of the Total Environment*, 652, 562-572.
- Pitts, D.J., Haman, D.Z., Smajstrla, A.G., 1990. Causes and prevention of emitter plugging in microirrigation system. Bulletin 258. Institute of Food and Agriculture Science, University of Florida, Gainesville, Florida.
- Pizarro, F., 1987. *Riegos localizados de Alta Frecuencia*. Ediciones Mundi Prensa, Madrid.
- Postel, S., 1992. *The last oasis: facing water scarcity*. Worldwatch Institute, Washington D.C.
- Puig-Bargués, J., 2003. *Utilización de aguas residuales en los sistemas de riego localizado: embozamiento y filtración*. PhD dissertation. Universitat de Lleida, Lleida.

- Puig-Bargués, J., Arbat, G., Barragán, J., Ramírez de Cartagena, F., 2005b. Hydraulic performance of drip irrigation subunits using WWTP effluents. *Agricultural Water Management*, 77 (1-3), 249-262.
- Puig-Bargués, J., Arbat, G., Elbana, M., Duran-Ros, M., Barragán, J., Ramírez de Cartagena, F., Lamm, F.R., 2010a. Effect of flushing frequency on emitter clogging in microirrigation with effluents. *Agricultural Water Management*, 97 (6), 883-891.
- Puig-Bargués, J., Barragán, J., Ramírez de Cartagena, F., 2005a. Filtration of effluents for microirrigation systems. *Transactions of the ASAE*, 48 (3), 969-978.
- Puig-Bargués, J., Lamm, F.R., Trooien, T.P., Clark, G.A., 2010b. Effect of dripline flushing on subsurface drip irrigation systems. *Transactions of the ASABE*, 53 (1), 147-155.
- Pujol, J., Duran-Ros, M., Arbat, G., Ramírez de Cartagena, F., Puig-Bargués, J., 2011. Private microirrigation costs using reclaimed water. *Spanish Journal of Agricultural Research*, 9 (4), 1120-1129.
- Pujol, T., Arbat, G., Bové, J., Puig-Bargués, J., Duran-Ros, M., Velayos, J., Ramírez de Cartagena, F., 2016. Effects of the underdrain design on the pressure drop in sand filters. *Biosystems Engineering*, 150, 1-9.
- Ravina, I., 2002. Drip irrigation with treated sewage effluent. International Meeting on Advances in Drip/Microirrigation, Puerto de la Cruz, 241-252.
- Ravina, I., Paz, E., Sofer, Z., Marcu, A., Shisha, A., Sagi, G., 1992. Control of emitter clogging in drip irrigation with reclaimed wastewater. *Irrigation Science*, 13 (3), 129-139.
- Ravina, I., Paz, E., Sofer, Z., Marcu, A., Shisha, A., Sagi, G., Yechiely, Z., 1997. Control of clogging in drip irrigation with stored treated municipal sewage effluent. *Agricultural Water Management*, 33, (2-3), 127-137.
- Real Decreto 1620/2007, de 7 de diciembre, por el que se establece el régimen jurídico de la reutilización de las aguas depuradas. Ministerio de la Presidencia «BOE» núm. 294, Madrid.
- Reca, J., Torrente, C., López-Luque, R., Martínez, J., 2016. Feasibility analysis of a standalone direct pumping photovoltaic system for irrigation in Mediterranean greenhouses. *Renewable Energy*, 85, 1143-1154.
- Rijo, M., 2008. Design and field tuning of an upstream controlled canal network SCADA. *Irrigation and Drainage*, 57 (2), 123-137.
- Rijo, M., Arranja, C., 2010. Supervision and water depth automatic control of an irrigation canal. *Journal of Irrigation and Drainage Engineering*, 136 (1), 3-10.
- Rodríguez-Díaz, J.A.; López, R.; Carrillo, M.T.; Montesinos, P.; Camacho, E., 2009. Exploring energy saving scenarios for on-demand pressurized irrigation networks. *Biosystems Engineering*, 104, 552-561.

- Rodrigo, J., Hernández, J.M., Pérez, A., González, J.F., 1997. Riego localizado. Ediciones Mundi-Prensa and MAPA-IRYDA, Madrid.
- Rowan, M.A., 2004. The utility of drip irrigation for the distribution of on-site wastewater effluent. PhD dissertation. The Ohio State University, Columbus, Ohio.
- Rutledge, S. O., Gagnon, G. A., 2002. Comparing crushed recycled glass to silica sand for dual media filtration. *Journal of Environmental Engineering and Science*, 1 (5), 349-358.
- Sala, L., Mujeriego, R., 2001. Cultural eutrophication control through water reuse. *Water Science and Technology*, 43 (10), 109-116.
- Sala, L., Serra, M., 2004. Towards sustainability in water recycling. *Water Science and Technology*, 50, (2), 1-7.
- Saladié, O., Oliveras, J., 2010. Desenvolupament sostenible. Càtedra DOW/URV de Desenvolupament Sostenible. Publicacions URV, Tarragona.
- Sallach, J.B., Bartelt-Hunt, S.L., Snow, D.D., Li, X., Hodges, L., 2018. Uptake of antibiotics and their toxicity to lettuce following routine irrigation with contaminated water in different soil types. *Environmental Engineering Science*, 35 (8), 887-896.
- Sánchez, J.J., 2008. El crecimiento de la población: implicaciones socioeconómicas, ecológicas y éticas. Ed. Tirant lo Blanc, València.
- Sawa, A.P., and Frenken, K., 2002. Irrigation manual: planning, development, monitoring and evaluation of irrigated agriculture with farmer participation. Food and Agriculture Organization of the United Nations (FAO), Sub-Regional Office for East and Southern Africa (SAFR), Harare.
- Senol, R., 2012. An analysis of solar energy and irrigation systems in Turkey. *Energy Policy*, 47, 478-486.
- Shannon, W.M., James, L.G., Basset, D.L., Mih, W.C., 1982. Sediment transport and deposition in trickle irrigation laterals. *Transactions of the ASABE*, 25 (1), 160-164.
- Schischa, A., Ravina, I., Sage, G., Paz, E., Yechiely, Z., Alkon, A., Scharamm, G., Sofer, Z., Marcu, A., Lev, Y., 1997. Drip irrigation with reclaimed effluents – the clogging problem. *International Water and Irrigation Review*, 17 (3), 8-12.
- Song, P., Li, Y., Zhou, B., Zhang, Z., Li, J., 2017. Controlling mechanism of chlorination on emitter bio-clogging for drip irrigation using reclaimed water. *Agricultural Water Management*, 184, 36-45.
- Soto-García, M., Martín-Gorriz, B., García-Bastida, P.A., Alcon, F., Martínez-Alvarez, V., 2013. Energy consumption for crop irrigation in a semiarid climate (south-eastern Spain). *Energy*, 55, 1084-1093.
- Soyer, E., Akgiray, O., Eldem, N., & Saatçr, A., 2010. Crushed recycled glass as a filter medium and comparison with silica sand. *Clean-Soil, Air, Water*, 38 (10), 927-935.

- Tajrishy, M.A., Hills, D.J., Tchobanoglous, G., 1994. Pretreatment of secondary effluent for drip irrigation. *Journal of the Irrigation and Drainage Engineering*, 120 (4), 716-731.
- Tarchitzky, J., Rimon, A., Kenig, E., Dosoretz, C.G., Chen, Y., 2013. Biological and chemical fouling in drip irrigation systems utilizing treated wastewater. *Irrigation Science*, 31 (6), 1277-1288.
- Tarjuelo, J.M., Rodríguez-Díaz, J.A., Abadía, R., Camacho, E., Rocamora, C., Moreno, M.A., 2015. Efficient water and energy use in irrigation modernization: lessons from Spanish case studies. *Agricultural Water Management*, 162, 67-77.
- Taylor, H.D., Bastos, R.K.X., Pearson, H.W., Mara, D.D., 1995. Drip irrigation with waste stabilization pond effluents: solving the problem of emitter fouling. *Water Science and Technology*, 31 (12), 417-424.
- Tripathi, V.K., Rajput, T.B.S., Patel, N., 2014. Performance of different filter combinations with surface and subsurface drip irrigation systems for utilizing municipal wastewater. *Irrigation Science*, 32, 379-391.
- Tripathi, V.K., Rajput, T.B.S., Patel, N., 2016. Effects on growth and yield of eggplant (*Solanum melongema* L.) under placement of drip laterals and using municipal wastewater. *Irrigation and Drainage*, 65 (4), 480-490.
- Trooien, T.P., Lamm, F.R., Stone, L.R., Alam, M., Rogers, D.H., Clark, G.A., Schlegel, A.J., 2000. Subsurface drip irrigation using livestock wastewater: dripline flow rates. *Applied Engineering in Agriculture*, 16 (5), 505-508.
- Trooien, T.P., Hills, D.J., 2007. Application of biological effluent. In: Lamm, F.R., Ayars, J.E., Nakayama, F.S. (Eds.), *Microirrigation for Crop Production. Design, Operation, and Management*. Elsevier, Amsterdam, 329-356.
- Tomas, S., Molle, B., Chevarin, C., Serra-Wittling, C. 2019. Transport Modelling in Sprinkler Irrigation. *Journal of Irrigation and Drainage Engineering*, 145 (8), 04019014.
- UNESCO. 2017. Wastewater: the untapped resource. The United Nations World Water Development Report 2017. United Nations Educational, Scientific and Cultural Organization, Paris.
- UNESCO. 2018. The United Nations World Water Development Report 2018. United Nations Educational, Scientific and Cultural Organization, Paris.
- United Nations. 2017. World Population Prospects, Key findings and advance tables. The 2017 Revision. Department of Economic and Social Affairs. Population Division, United Nations, New York.
- Valdés, J.R., Santamaria, C., 2007. Particle transport in a nonuniform flow field: Retardation and clogging. *Applied Physics Letters*, 90 (24), 244101.
- Vigneswaran, S., Kwon, D.Y., 2015. Effect of ionic strength and permeate flux on membrane fouling: Analysis of forces acting on particle deposit and cake formation. *KSCE Journal of Civil Engineering*, 19 (6), 1604-1611.

- Viñas, C.D., 2019. Depopulation processes in European Rural Areas: A case study of Cantabria (Spain). *European Countryside*, 11 (3), 341-369.
- Wettstein, S., Muir, K., Scharfy, D., Stucki, M., 2017. The environmental mitigation potential of photovoltaic-powered irrigation in the production of South African Maize. *Sustainability*, 9, 1772.
- Wilén, B.M., Cimbritz, M., Pettersson, T., Mattsson, A., 2016. Large scale tertiary filtration – results and experiences from the discfilter plant at the Rya WWTP in Sweden. *Water Practice and Technology*, 11 (3), 547-555.
- Wu, I.P., Barragán, J., Bralts, V., 2007. Field performance and evaluation. In: Lamm, F.R., Ayars, J.E., Nakayama, F.S. (Eds.) *Microirrigation for crop production. Design, Operation and Management. Developments in Agricultural Engineering*, vol. 13. Elsevier, Amsterdam, 357-388.
- Wu, W.Y., Huang, Y., Liu, H.L., Yin, S.Y., Niu, Y., 2015. Reclaimed water filtration efficiency and drip irrigation emitter performance with different combinations of sand and disc filters. *Irrigation and Drainage*, 64, 362-369.
- Van Puijenbroek, P.J.T.M., Bouwman, A.F., Beusen, A.H.W., Lucas, P.L., 2015. Global implementation of two shared socioeconomic pathways for future sanitation and wastewater flows. *Water Science and Technology*, 71 (2), 227-233.
- Vermeiren, L., Jobling, G.A., 1986. Localized irrigation. Irrigation and Drainage Paper 36, FAO, Rome.
- Yavuz, Y., Demirel, K., Erken, O., Bahar, E., Etoz, M., 2010. Emitter clogging and effects on drip irrigation systems performances. *African Journal of Agriculture Research*, 5 (7), 532-538.
- Zhou, B., Li, Y.K., Yaoza, L., Feipeng, X., 2015. Effect of drip irrigation frequency on emitter clogging using reclaimed water. *Irrigation Science*, 33 (3), 221-234.
- Zhou, B., Wang, D., Wang, T.Z., Li, Y.K., 2018. Chemical clogging behavior in drip irrigation systems using reclaimed water. *Transactions of the ASABE*, 61 (5), 1667-1675.